University of the Western Cape

Extraction, fractionation, nanoparticles formulation, and antimicrobial activity of lipids from black soldier fly larvae

By

Raissa Andong Omores

Master of Technology (MTech): Chemistry (cum laude) – Cape Peninsula University of Technology

Bachelor of Technology (BTech): Chemistry – Cape Peninsula University of Technology

A thesis submitted in fulfilment of the requirements for the degree of

Doctor of Philosophy in Chemistry

In the

Department of Chemistry

University of the Western Cape

Supervisor: Prof. Leslie F. Petrik

Co-Supervisor: Prof W T Mabusela

October 2021

DECLARATION OF AUTHORSHIP

By submitting this thesis, I declare that "Fractionation, nanoparticles formulation and antimicrobial activity of lipids from black soldier fly larvae" is my original work and that it has not been submitted for any degree or examination in any other university and that all the sources I used or quoted have been indicated and acknowledged by appropriate references

Raissa Andong Omores

Signature: Date: 01/10/2021

UNIVERSITY *of the*
WESTERN CAPE

KEYWORDS

Nanoparticles

Antimicrobial activity

Lipids

Black soldier fly larvae

Electrospraying

Chitosan

Extraction

Triglycerides

Diglycerides

Monoglycerides

Fatty acids

Micrococcus luteus

Pseudomonas aeruginosa

Soxhlet extraction

Column chromatograph

Thin layer chromatography

ABSTRACT

Hermetia illucens (Diptera: Stratiomyidae) known as the black soldier fly (BSF) is an efficient ecological organic waste decomposer. Its larvae grow through six larval instars on a variety of decomposing organic substrates inhabited by a variety of microorganisms, including pathogenic ones. Survival in these environments requires a good functioning immune system to protect them from pathogen invasion, hence it can be expected that the BSF larvae possess antimicrobial substances. BSF larvae farming has recently gained popularity as a new source of protein and lipid. The lipid is highly sourced due to its applications in a variety of areas which span across food and pharmaceutical industries. Different extraction methods have been used to extract lipid from different sources. However, its effective extraction depends on the extraction method and the extraction parameters (solvent type, temperature, time, etc.). Furthermore, the lipids are often fractionated into individual lipid classes and can be tested for various potential applications. But little or no reports show the extraction, the conditions of extraction for better yield, and fractionation of lipid from black soldier fly (BSF) larvae. Substances are known to perform better in their nano scale. Hence, attention has also been drawn towards the development of nanoparticles of lipid for pharmaceutical applications.

To effectively maximise the potential of lipid from BSF larvae, this research aimed at extracting lipid from BSF larvae, compared different extraction for maximum yield, fractionated, and further characterised each lipid fraction. The preparation of lipid nanoparticles from BSF larvae using the electrospraying method is also investigated in this study. To achieve that, the lipid fractions (triglycerides, diglycerides, monoglycerides, and free fatty acids) isolated from BSF larvae were individually mixed with commercial chitosan to form lipid-chitosan hybrid nanoparticles, which were then electrosprayed. The antibacterial activities of isolated lipid fractions (triglycerides, free fatty acids, diglycerides, and monoglycerides) from BSF larvae, as well as their nanoparticles, were then tested against *Micrococcus luteus and Pseudomonas aeruginosa*.

Three extraction methods (Soxhlet extraction, ultrasonic-assisted extraction, and maceration extraction) were investigated for their lipid yield and fatty acid composition. The lipid extracted from the BSF larvae was then fractionated into lipid classes with silica gel column chromatography and the separation was checked using thin layer chromatography (TLC). Gas

chromatography flame ionisation (GC-FID), Fourier-transform infrared spectroscopy (FTIR), and nuclear magnetic resonance (NMR) spectroscopy were used to characterise the lipid fractions. NMR studies were made with ^{1}H-NMR and ^{13}C-NMR. For the production of the lipid nanoparticles, the electrospraying method was employed. Due to the difficulty of producing solid lipid nanoparticles without oil droplets during electrospraying, commercial chitosan was mixed with individual lipid fractions (triglycerides, diglycerides monoglycerides, and fatty acids) to produce a chitosan-lipid mixture. Chitosan was chosen for the advantage of its antimicrobial properties, its non-toxicity, and biocompatibility, mechanical and thermal stability. Before mixing the chitosan with the lipid fractions, the effects of the chitosan concentration (0.5, 1, 2, 3, and 4 wt %) and stirring time (12, 24, and 48 h,) on the formation of the chitosan nanoparticles were investigated to bring chitosan to the state possible for it to form an effective hybrid with the lipids. Then, to obtain the best formulation of the chitosan-lipid nanoparticles, the effect of chitosan-lipid concentration was investigated at three different concentrations of 0.02, 0.03, and 0.04 g/mL by dissolving 0.2, 0.3, and 0.4 g of the lipid fractions in liquid form in 1 wt % (0.1g of chitosan in 10 mL of 90 % acetic acid) of the chitosan solution. 0.01g/mL which is 0.1 g of the lipid in 1wt % chitosan. The chitosan-lipid nanoparticles were characterised in terms of their molecular structures using Fourier transform infrared spectroscopy (FTIR) and morphological using scanning electron microscopy (SEM). The antibacterial activities of the isolated lipids fractions (triglycerides, fatty acids, diglycerides, and monoglycerides) and their nanoparticle hybrid against *Micrococcus luteus* and *Pseudomonas aeruginosa* were investigated using agar disc diffusion method.

The extraction result showed that Soxhlet extraction was the appropriate method for BSF larvae lipid extraction due to its high lipid yield (40.68 %) and good fatty acids profile with the optimum extraction condition of petroleum ether at 70°C, a solvent to solid ratio of 0.03 g/mL and an extraction time of 4 h. Gas chromatography flame ionisation detection (GC-FID) revealed that the lipid extracted from the BSF larvae using Soxhlet extraction was a rich source of saturated fatty acids (68.64 %) with lauric acid being the most abundant fatty acid (31.99 %). Monounsaturated and polyunsaturated fatty acids were found at the percentage of 2.12 and 3.56 % respectively. On the fractionation methods investigated, column chromatography resulted in the complete separation of six different lipid classes including cholesterol esters, triglycerides, cholesterol, fatty acids, diglycerides, and monoglycerides. Triglyceride (30 %) was the main component of BSF larvae lipid while cholesterol esters (1.6 %) and cholesterol (0.6 %) were the least abundant lipid fractions. The composition of the triglycerides, diglycerides, monoglycerides, and fatty acids subcomponents were further determined using

GC-FID and the results showed that lauric acid (27.65 %), trilaurin (27.32 %), dilaurin (29.26 %), and monolaurin (14.50 %) were the main subcomponent of the fatty acids, triglycerides, diglycerides, and monoglycerides fractions, respectively.

The production of chitosan-lipid nanoparticles (chitosan-triglyceride, chitosan-diglyceride, chitosan-monoglyceride, and chitosan-fatty acids nanoparticles) was successfully done using the electrospray method. The optimum concentration and stirring time of the chitosan solution were 1 wt % and 48 h respectively. The chitosan-lipids solutions prepared at 3 different concentrations (0.02, 0.03, and 0.04 g/mL) showed that the optimum chitosan-lipids concentration was 0.02 g/mL.

The antimicrobial activity of the lipid fraction and chitosan-lipids nanoparticles against *Micrococcus luteus* and *Pseudomonas aeruginosa* showed that the lipid fractions by themself were effective in inhibiting *Micrococcus luteus* growth but not *Pseudomonas aeruginosa*. While the individual chitosan-lipid nanoparticles (chitosan-triglyceride, chitosan-diglyceride, chitosan-monoglyceride, and chitosan-fatty acids nanoparticles) were strongly active against both *Micrococcus luteus* and *Pseudomonas aeruginosa*.
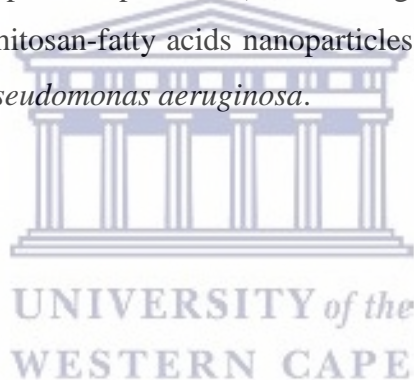
RESEARCH OUTPUT

Drafted manuscripts

- Andong Omores, R., Petrik, L.F., Mabusela, W.T. (2021). The Effect of solvent polarity on lipid yields and fatty acid composition of black soldier fly larvae, *Journal of Oleo Science* (manuscript).

- Andong Omores, R., Petrik, L.F., Mabusela, W.T. (2021). Influence of extraction time and solid to solvent ratio on yield and composition of lipids extracted from black soldier fly larvae, *Journal of Oleo Science* (manuscript).

- Andong Omores, R., Petrik, L.F., Mabusela, W.T. (2021). A comparative analysis of Soxhlet, maceration, and ultrasonic assisted extraction of lipid from black soldier fly larvae, *European Journal of Lipid Science and Technology* (manuscript).

- Andong Omores, R., Petrik, L.F., Mabusela, W.T. (2021). Fractionation and analysis of lipids extracted from the black soldier fly larvae by chromatographic methods, *European Journal of Lipid Science and Technology* (manuscript).

- Andong Omores, R., Petrik, L.F., Mabusela, W.T. (2021). Antibacterial activity of the fatty acids from black soldier fly larvae against selected bacteria, *Biotechnology Advances* (manuscript).

- Andong Omores, R., Petrik, L.F., Mabusela, W.T. (2021). Antibacterial activity of the triglycerides, diglycerides, monoglycerides, and fatty acids from black soldier fly larvae against *Micrococcus luteus*, *Microorganisms* (manuscript).

- Andong Omores, R., Petrik, L.F., Mabusela, W.T. (2021). Electrospraying method for fabrication of triglycerides, diglycerides, monoglycerides, and fatty acids from black soldier fly larvae and antimicrobial properties, *Journal of Nanoparticle Research* (manuscript).

DEDICATION

This thesis is dedicated to my:

Parents

Mr. Bruno Omores

Mrs. Blandine Obiang

Mr. Dieudonne Nkassa Emane

And

My wonderful husband

Uchenna Ogemdi Okwuosa

ACKNOWLEDGMENT

Dr. Chris Bode-Aluko, Dr. Oluseyi Omoniyi, Dr. Mero-Lee Cornelius, Dr. Kassim Badmus, Dr. Omoniyi Pereao, Dr. Cosmas Uche, Dr. Emile Massima, Emmanuel Omoniyi, Abegunde, Dr. Cecilia Sanusi Jean-Luc Mukhaba, for their all their help and advice.

- I would like to offer my special thanks to Masande Yalo and Masixole Makhaba from the organic chemistry lab for their training in thin layer chromatography and column chromatography.

- I would like to express my heartfelt gratitude to my darling spouse for his patience, love, encouragement, and support throughout my studies, as well as for enduring this long journey with me.

- Finally, I would like to thank my family (Theresa Okwuosa, Marie Andong, Bruno Omores, Blandine Obiang, Dieudonne Nkassa Emane, Sylvie Nkassa, Yvette, Cally, Eridis, Chancia, Gerfenia, Brunel, Kevin, Dao, Aristide, Laury, Gessica, Francis, Liza, Deguy, Akim, Stephanie and Lea). It would have been difficult for me to finish my studies without their wonderful understanding and encouragement throughout the last few years.

TABLE OF CONTENTS

LIST OF FIGURES

LIST OF TABLES

LIST OF EQUATIONS

xxii

UNIVERSITY *of the* WESTERN CAPE

http://etd.uwc.ac.za/

LIST OF ABBREVIATIONS

AMPs	Antimicrobial peptides
BSF	Black soldier fly
CH	Chitosan
DG	Diglycerides
DLPs	Defensin-like peptides
FDA	Food and Drug Administration
FA	Fatty acids
FTIR	Fourier transform infrared spectroscopy
GC-FID	Gas chromatography flame ionisation detection
GC-MS	Gas chromatography mass spectrometry
GLC	Gas-liquid chromatography
HPLC	High-performance liquid chromatography
HP-TLC	High-performance thin-layer chromatography
LLE	Liquid-liquid extraction
ME	Maceration extraction
MG	Monoglycerides
MUFAs	Monounsaturated fatty acids
NMR	Nuclear magnetic resonance spectroscopy
PUFAs	Polyunsaturated fatty acids
SE	Soxhlet extraction
SEM	Scanning electron microscopy
SFAs	Saturated fatty acids
SFE	Supercritical fluid extraction
SLNs	Solid lipid nanoparticles
TGA	Triglycerides
TLC	Thin-layer chromatography
UAE	Ultrasonic-assisted extraction
UPLC	Ultra-performance liquid chromatography

CHAPTER 1: GENERAL INTRODUCTION

1.1   Introduction

Some scientists claim that insects are remedies for global problems. The use of insects in addressing global issues, including renewable fuel, nutrition, and environmental mitigation is increasingly promoted. Among a variety of insects, *Hermetia illucens* (Diptera: *Stratiomyidae*) commonly known as black soldier fly (BSF) is a fascinating species that have captured the interest of scientists. The black soldier fly is a non-pest insect that is distributed worldwide throughout the tropics and warm temperate regions (Banks, 2014). The insect's life cycle consists of five stages: egg, larva, prepupal, pupa, and adult stage. The BSF has been seen to play a significant role in relieving much of the world's problems. Hence, it is often referred to as the "golden insect" or 'crown jewel' (Tomberlin & van Huis, 2020). For instance, to address waste management problems, Cickova et al. (2015) proposed the use of black soldier fly (BSF) larvae as an alternative waste management strategy. Aside from waste control, BSF larvae are an effective source of renewable energy (Feng et al., 2018; Ishak & Kamari, 2019). Cullere et al. (2018), Barragan-Fonseca et al. (2019) and Stahls et al. (2020) showed that BSF larvae can be used as a possible alternative main protein source for livestock and human consumption because it has a high protein (42%) and lipid (35%) content, including essential amino acids and fatty acids. When compared to other insects species, such as house fly (*Musca domestica L.*), watermelon bugs (*Aspongopus viduatus*), oriental latrine fly larvae (*Chrysomya megacephala*) and darkling beetle larvae (*Zophobas morio*), *Hermetia illucens* has often been selected over the aforementioned insects because it is a non-pest and non-vector insect, and also due to its high lipid content (Cickova et al., 2015; Rabani et al., 2019).

As published by Research and Markets on February 14, 2020, the world demand for BSF is expected to hit $2.57 billion by 2030 with a compound annual growth rate (CAGR) of 33.3 %. The most popular companies operating in the BSF market are BioflyTech (Spain), Protix (Netherlands), Hermetia GmbH (Germany), EnviroFlight (U.S.), SFly (France), Hexafly (Ireland), F4F (Chile), InnovaFeed (France), and Entofood (Malaysia) (Meticulous, 2014). These companies' common mission is to mitigate the environmental and financial effects of animal production. They do this by producing high-quality feeds that will stand the test of time

for livestock, humans, and plants. Interestingly, BSF insect has the potential for medical use as a source of antimicrobial compounds, which could be especially useful for microbial infections that are difficult to treat. Hence there is a need to study the characteristics of the novel bioactive compounds in the BSF larvae lipid.

1.2 Background

Antibiotic resistance, which is one of the most severe health issues, forms one of the reasons for this study. The growing number of diseases that are becoming more difficult to treat is caused by the fact that the antibiotics used to treat them turn out to be less effective (Thormar et al., 2013; Kahsay & Muthupandian, 2016; Cansizoglu & Toprak, 2017; Browne et al., 2020). Antibiotic resistance happens when bacteria adjust in ways that make antibiotics ineffective against them. Some of the causes of antibiotic resistance have been attributed to over-prescription of antibiotics, patients not completing the full antibiotic course, overuse of antibiotics in livestock and fish farming, inadequate infection control in health care settings, and inadequate sanitation and hygiene. Six highly virulent and antibiotic resistant bacterial pathogens (abbreviated as ESKAPE), which include *Enterococcus faecium, Staphylococcus aureus, Klebsiella pneumoniae, Acinetobacter baumannii, Pseudomonas aeruginosa, and Enterobacter* (facultatively anaerobic Gram-negative bacilli) and which have antibiotic resistant, are evidenced to possess a threat to humans (Sattarahmady et al., 2017; Mbelle et al., 2020). It is well known that black soldier fly (BSF) larvae can live in extremely harsh conditions, such as manure and compost, populated by an extremely wide range of potentially harmful microorganisms (bacteria, viruses, and protozoa) (Moula et al., 2018; Mirand et al., 2020 ; Marco et al., 2021; Indri et al., 2021; Liu et al., 2022). This indicates that the larvae have a potent immune response against harmful invaders (Vogel et al., 2018; Bruno et al., 2021; Thrastardottir et al., 2021; von Bredow et al., 2021). The biodefence mechanism of BSF larvae has gained research attention in recent times. However, this effort to scrutinize its bioactive substances is still at the infant stage with little work in the public domain. Research has shown that BSF larvae contain compounds having antimicrobial properties (Dabbou et al., 2021; Mohamed et al., 2021). For instance, lipids such as fatty acids and monoglycerides that are primarily present in BSF larvae have been reported to possess antimicrobial properties (Park et al., 2015; Zdybicka-Barabas et al., 2017). Lipids exhibit several promising features that make them desirable for antibacterial use. This includes a wide range of activities against microbes and a lack of classical resistance mechanisms to the action of these compounds. Lipids such as

fatty acids (amphiphilic acids consisting of saturated or unsaturated hydrocarbon chains bound to a carboxyl group) and monoglycerides (esterified adducts of a fatty acid and glycerol molecule) from various animals and plants have been highlighted. Studies conducted on different types of fatty acids has shown that lauric acid (C12:0) has the most potent antimicrobial properties when exposed to Gram-positive and Gram-negative bacteria compared to other fatty acids (Desbois & Lawlor, 2013; Abbas et al., 2017; Silalahi & Putra, 2018). It should be highlighted that lauric acid is the most abundant fatty acid present in BSF larvae, comparable to the lauric acid found in coconut o (Kim et al., 2020). Researchers strongly believe that antimicrobial fatty acids and monoglycerides can be candidates to overcome the alarming problem of acquired bacterial drug resistance (Thormar et al., 2013; Jumina et al., 2018). The analysis of lipids from the biological system requires two key steps, the extraction, and identification stage. Several extraction techniques are well known to remove the lipid from biological system. These techniques can be classified into distinct categories, namely solvent extraction (Soxhlet extraction, maceration, ultrasonication, Goldfish, Majonnier) and non-solvent extraction (Babcock, Gerber, detergent methods) (Nielsen and Carpenter, 2017).

The physical and chemical properties of lipids can be improved in terms of their antimicrobial activity by developing a new system, namely lipid nanoparticles (Saporito et al., 2018; Thorn et al., 2021). Nanoparticles are extremely small particles (from 1 to 100 nm) (Mai et al., 2018; Evers et al., 2018; Fan et al., 2021). The use of materials in the nanoscale offers many advantages in assisting humanity in all aspects of life (Trucillo et al., 2019; Dhiman et al., 2021; Fisher et al., 2021). Furthermore, the use of nanoparticles inspires great optimism for future scientific revolutions in fields such as physics, chemistry, biology, and engineering (Nasrollahzadeh et al., 2019; Raghav et al., 2020; Prasade et al., 2021; Zain et al., 2022). In medicine, nanoparticles are the new way by which scientists can deliver drugs into the body cells by minimising any side effect as opposed to the use of large- sized molecules in drug delivery having several negative consequences (poor bioavailability, cannot be absorbed effectively, less solubility, less stability, etc.) (Naskar et al., 2019; Fam et al., 2020). In synthesizing nanoparticles, depending on the application and the final product, several methods are employed (Rane et al., 2018; Duan et al., 2020; Hou et al., 2020). Among the methods (high-pressure homogenization, ultrasonication, electrospraying, supercritical fluid, microemulsion, spray drying, reverse micellar method, etc.). The electrospraying (electrohydrodynamic spraying) method has been widely used due to its low cost, its simplicity, and the fact that it does not require the use of harmful organic substances (surfactants) (Singh

et al., 2019; Duan et al., 2020). Despite these advantages, relatively few studies have addressed the electrospraying of lipids isolated from the BSF larvae. Lipids might not be easy to synthesise into powder form due to their oily nature, hence they need to be transformed into hybrid substances for structural and mechanical purposes.

1.3   Problem statement

Antimicrobial resistance is a worldwide top priority problem that urgently needs to be addressed. It is estimated that 700,000 deaths are caused every year globally by drug resistance (Tadesse et al., 2017). If the current trend persists, Yougbare et al. (2019) and other previous scientists (Berglund, 2015; Zhang et al., 2016) have predicted that the primary cause of death in 2050 would be associated with antimicrobial resistance, with around 10 million deaths annually. Antimicrobial resistance is a serious challenge in the United States, where at least 2. 8 million patients suffer from a serious infection that is resistant to antibiotics and results in an estimated 35,000 deaths. Data from a study conducted in 2007 reported that about 400,000 patients experience side effects due to antibiotic-resistant bacteria yearly, causing 25,000 deaths in Europe Ekwanzala et al., 2018). The resistance to antibiotics leads to 38,000 deaths a year in Thailand (Berglund, 2015; Zhang et al., 2016). India has recorded more than 58,000 deaths of infants from an antibiotic- resistant infection contracted from their mothers (Soll & Edwards, 2015). Practically, in every region of Africa, antimicrobial resistance remains one of the most severe health problems. South Africa is not an exception in infectious diseases, with tuberculosis being the most prominent. It was reported that 80 % of South Africa's population is believed to be infected with tuberculosis bacteria, most of which have tuberculosis latent rather than active tuberculosis infection (McNeish, 2018). Tuberculosis is caused by various gram-negative bacterium strains (Mycobacteria), among which the *Mycobacterium tuberculosis* strain has developed resistance to the majority of known antibiotics such as fluoroquinolones and rifampicin (McBryde et al., 2017; Ruddaraju et al., 2020). It should be remembered that antibiotics have played a crucial role in preventing illness and death in animals and humans worldwide. However, Tadesse et al. (2012) had it on record that misuse and overuse of antimicrobial pharmaceutical products is the key force behind the rise in antibiotic resistance. In South Africa, for example, some antibiotics are still used for animal husbandry despite their prohibition, which makes it difficult for antimicrobial resistance management to be controlled (Tatsing Foka et al., 2018). According to researchers, two main approaches can be used to address this antimicrobial drug resistance problem: either to create

new antimicrobial agents or to look for smart approaches to restore or maintain the effectiveness of existing antimicrobial agents (Garces et al., 2018; Mishra et al., 2018; Saporito et al., 2018).

Scientists have focused on the discovery of novel and alternative sources of antibiotics in natural products such as plants (Subramani et al., 2017; Naß & Efferth, 2018; Martini et al., 2020), various algae (Jahan et al., 2017; Ilekuttige et al., 2019), fungi (Belyagoubi et al., 2018) and metals (Khan et al., 2016; Fan et al., 2017; Chudasama & Bhupendra, 2018). Unfortunately, one of the most abundant and cheap sources of bioactive compounds is yet to be explored with full attention. The products derived from insects are yet to become as popular as products derived from plants and metals. Indeed, if given the proper attention, insect-derived substances hold great promise for the future of natural product drug discovery.

1.4   Motivation of the study

Considering the challenges faced by traditional antibiotics in which the active compounds emanate from plants, new and alternative strategies to overcome antibiotic resistance need to be developed. According to researchers, antimicrobial lipids from the black soldier fly (BSF) larvae could be a model for the creation of an improved class of antibiotics (Jackman et al., 2016; Jumina et al., 2018). The reason is that such lipids exhibit several promising features that make them attractive options for antimicrobial uses. Their advantages over other sources of lipids include low cost, a broad spectrum of activity, and a lack of classical resistance mechanisms against the actions of these compounds. Black soldier fly larvae produce bioactive compounds that can meet human and animal protection purposes. BSF larvae have a powerful microorganism defence that enables them to feed on various decomposing organic substrates infested with pathogenic microorganisms. Interest is particularly in the potent antimicrobial lipids found in the black soldier larvae that should be intensively explored. In the face of multidrug-resistant bacteria, many antibiotics are losing effectiveness and drug-resistant bacteria continue to rise persistently. Studies on the use of antimicrobial lipids from the BSF larvae as a way to avoid antimicrobial resistance are lacking. Tapping into the abundant, cheap, and bioactive substances of BSF larvae this study explored the potential use of antimicrobial fatty acids, monoglycerides, diglycerides, and triglycerides extracted from the BSF larvae and tested their ability to inhibit *Micrococcus luteus* and *Pseudomonas aeruginosa*.

1.5   Aims and objectives

This work aimed to extract antimicrobial lipids from black soldier (BSF) larvae and apply them as potent antimicrobial agents as well as to identify their potential formulations in the form of nanoparticles. To achieve this, the objectives presented below were undertaken

- To compare three extraction methods (Soxhlet extraction, ultrasonic-assisted extraction, and maceration extraction) of the lipid from black soldier fly larvae.
- To determine the optimal extraction conditions of the lipid from black soldier fly larvae using Soxhlet extraction.
- To fractionate the extracted lipids from black soldier fly larvae into lipid classes using column chromatography and thin-layer chromatography.
- To characterise the lipid fractions from the black soldier fly larvae lipid using FTIR and NMR.
- To synthesise chitosan-lipid nanoparticles and to characterise them using SEM and FTIR
- To test antibacterial activities of the isolated lipids fractions on *Micrococcus luteus* and *Pseudomonas aeruginosa* using disc diffusion method.
- To test antibacterial activities of the chitosan - lipid nanoparticles on *Micrococcus luteus* and *Pseudomonas aeruginosa* using disc diffusion method.

1.6   Research questions

This study aims to find answers to the following research questions to achieve the aim and objectives listed in section 1.5:

- What is the percentage recovery of lipid extracted from black soldier fly larvae using different extraction methods?
- What is the influence of the extraction methods on the fatty acids composition of the black soldier fly larvae lipid
- What are the optimal extraction conditions of the lipid from black soldier fly larvae using Soxhlet extraction?
- Can column chromatography be suitable for the fractionation of the lipid from black soldier fly larvae?
- Can the lipids be formulated as nanoparticles?
- Are lipid fractions able to inhibit the growth of *Micrococcus luteus* and *Pseudomonas aeruginosa*?

- Are chitosan-lipid nanoparticles formulated more effective in inhibiting the growth of *Micrococcus luteus* and *Pseudomonas aeruginosa* compared to their free form?

1.7 Hypothesis

Lipids isolated from black soldier fly (BSF) larvae have the potential for inhibiting the growth of some selected microorganisms with enhanced potency in the form of nanoparticles.

1.8 Experimental research approach

To achieve the experimental aspect of this study, the lipid of the black soldier (BSF) larvae was first extracted using different three types of extraction procedures which included maceration, Soxhlet extraction, and ultrasonic-assisted extraction. For the sample preparation the BSF larvae sample was wash with distilled water, freeze dried, ground and sieved before the extractions. This first test enabled the lipid percentage recovery to be calculated when using the aforementioned methods. All three methods had their advantages and disadvantages. However, the main goal was to select the method having a high lipid yield percentage. BSF larvae lipid contained different classes of lipid, hence the BSF larvae lipid was fractionated into lipid classes. The fractionation was achieved using column chromatography packed with silica gel as a stationary phase and thin-layer chromatography. The separation into individual fractions was achieved by serial elution with a mixture of two solvents: hexane, and diethyl ether at different ratios. The purity of the eluted fractions was checked by the use of thin-layer chromatography. The characterization of the lipid fractions was performed on the GC system, with a flame ionisation detection (FID) and capillary column. Fourier-transform infrared spectroscopy (FTIR), and nuclear magnetic resonance (NMR) which were 1H and 13C-NMR were valuable techniques to identify the functional groups of the lipid samples. The antibacterial activity tests were performed on the lipid fractions to assess their potential inhibition of selected gram-positive and gram-negative bacteria. Another important experimental step was to synthesised nanoparticles from the isolated lipids. This was achieved by mixing the lipid fractions with commercial chitosan and forming nanoparticles using the electrospraying technique. The electrospraying technique uses a high voltage that is applied between a steel needle in a 10 mL syringe filled with the sample and an infusion pump. A droplet forms at the end of the needle is pumped through a syringe at a steady rate. The nanoparticles are expelled in a jet shape, traveling toward a collector. The morphology of the nanoparticle was characterised using scanning electron microscopy (SEM). The synthesised

nanoparticles were tested for antimicrobial activity. The following schematic experimental protocol illustrated in Figure 1.1 showed the different steps use to achieve the aims and objectives of this study.

8
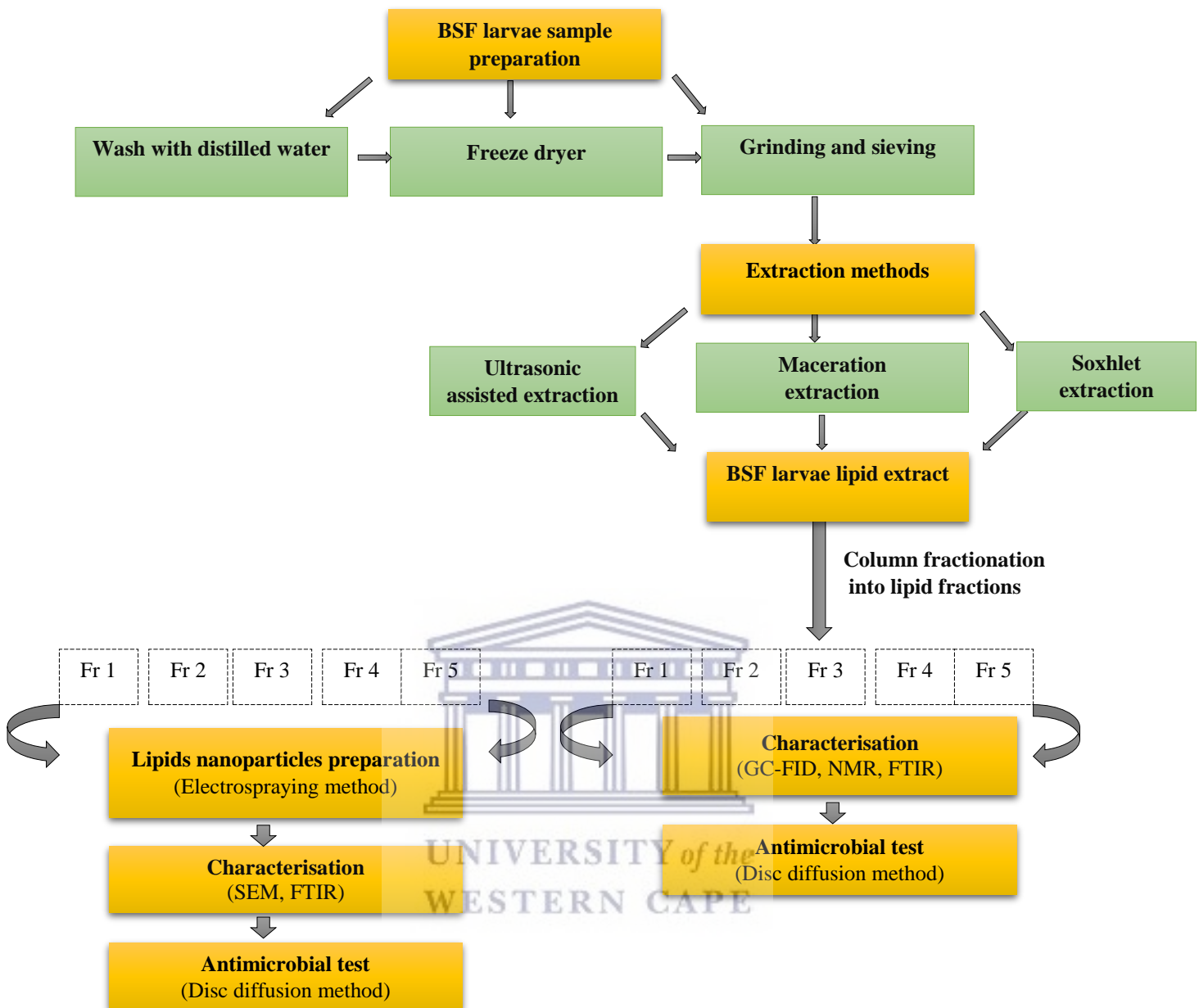
Figure 1.1: Schematic illustration of the experimental protocol

1.9   Scope and delimitations of the study

The key focus of this research is on the extraction, isolation, purification, and antimicrobial properties of lipids from black soldier (BSF) larvae. The protein and chitin components of the BSF were not investigated. Also, this study did not investigate the biodiesel from the lipid of the BSF larvae. The only insect of interest was the BSF, no other insects were examined.

1.10   Thesis outline

Chapter 1: General introduction

The conceptual basis of the present study is described in this chapter. It contains the context of the study, which offers general research information and explains why it is important to perform the research. Besides, it provides what progress is being made concerning the current state of the art. Also, this chapter contains the study's description of the issue, aim, objectives, research questions, hypothesis, research methodology, scope, and delimitations.

Chapter 2: Literature review

This chapter contains literary analyses of previous research articles containing significant findings and observations as well as theoretical and methodological contributions. The significance and role of black soldier (BSF) larvae as a biological resource in our society were further discussed. Furthermore, chapter two addressed the nutritional value and the bioactive compounds found in the BSF insects that can be used for various applications. Besides, this chapter describes various methods of extracting the above bioactive substances. Different characterisation methods are also illustrated. Also, a review of processes for producing nanoparticles using different techniques is discussed.

Chapter 3: Research concepts and procedures

This chapter describes the experimental methods to achieve the goals mentioned above. It includes the list of chemicals and materials used in this study. The various sample preparation methods are presented as well as the extraction methods. The different characterisation methods are described. The protocol for the synthesis of the lipid nanoparticles is also described. Finally, the antimicrobial test protocol for the lipid fraction and nanoparticles formulated is also given.

Chapter 4: A comparative analysis of different methods to extract lipid from black soldier fly larvae

This chapter presents the results of different extraction approaches to extract the lipid from the black soldier (BSF) larvae, which are: The maceration technique in which the sample is soaked in an organic solvent at room temperature, the ultrasonic-assisted extraction that uses ultrasound to penetrate the solvent in contact with the solid matrix to extract the content from the sample solution and lastly, the Soxhlet extraction which is based on solid-liquid extraction.

Chapter 5: Black soldier fly larvae lipid fractionation and characterisation

This chapter presents the results of separating and purifying lipids from black soldier (BSF) larvae lipid into different groups. The fractionation and purification are accomplished by employing two chromatographic methods: column chromatography (CC) and thin-layer chromatography (TLC). The targeted lipids are cholesterol esters, triglycerides, fatty acids, cholesterols, diglycerides, or monoglycerides. The results of the Gas chromatography (GC-FID), Fourier-transform infrared spectroscopy (FTIR), and nuclear magnetic resonance (NMR) spectroscopy for characterising the extracted lipids are discussed in this chapter. NMR and FTIR were used to confirm the purity and structure of the lipids.

Chapter 6: Synthesis of chitosan-lipid hybrid nanoparticles

This chapter presents the results of the production of chitosan-lipid hybrid nanoparticles using electrohydrodynamic atomisation (electrospraying). The effects of the chitosan concentration and stirring time on the formation of the nanoparticles are also discussed.

Chapter 7: Antibacterial activity of the lipids and chitosan-lipid hybrid nanoparticles from black soldier fly larvae against *Micrococcus luteus* and *Pseudomonas aeruginosa*

This chapter presents the results of the evaluation of the antimicrobial ability of isolated lipid fractions by using agar discs methods. Triglycerides, fatty acids, monoglycerides, and diglycerides were tested against *Micrococcus luteus* and *Pseudomonas aeruginosa*. This chapter also presents the results of the antimicrobial activity of chitosan-lipid hybrid nanoparticles from the lipid of the black soldier (BSF) larvae.

Chapter 8: Conclusions, novelty, and recommendations

This chapter provides the general conclusion, novelty, and recommendations for future research.

CHAPTER 2: LITERATURE REVIEW

2.1 Introduction

One of the purposes of this chapter was to first describe the biology of the black soldier fly (BSF), then discuss the various benefit of the insect larvae, such as its importance in organic waste management, its role as a potential source of sustainable energy as well as a source of protein and lipid. This chapter also explores the use of the BSF larvae lipids as a new generation of potent antibacterial agents. In this respect, bioactive substances derived from insect larvae such as fatty acids, and esters formed from glycerol and fatty acids (monoglycerides, diglycerides, triglycerides), and antimicrobial peptides are discussed. Also, detailed information on the various extraction methods of the lipids from the BSF larvae is presented. The different chromatographic separations and analysis of the lipids are compared and discussed. Lastly, antimicrobial lipids have demonstrated effectiveness against various drug-resistant bacteria that could be very useful in many applications beneficial to the health and wellbeing of humans (Kim et al., 2018; Lauritano et al., 2020). Despite their promising antibacterial features, some limitations such as poor solubility (Jackman et al., 2016) can hinder their performance. Because of that limitation, the last section of this chapter discussed some formulations such as liposomes, solid lipid nanoparticles to overcome the above-mentioned challenge.

2.2 Biology of black soldier fly (*Hermetia illucens*)

2.2.1 Distribution of black soldier fly

The earliest study, undertaken 200 years ago by Carl Linnaeus, classified *Hermetia illucens* known as black soldier fly (BSF), to belong to the order of Dipterans, *Stratiomyidae* family, and sub-family of *Hermetiinae* (Oliveira et al., 2016). In recent times, Surendra et al. (2016), Feng et al. (2018), and Belghit et al. (2019) reported that the insect has gained popularity as an efficient system for the bioconversion of organic wastes (manure) into useful products (protein). Kamau et al. (2018) identified that BSF is a widespread species from North America, South America, and Australia. Over time, due to climate change and industrialisation, the BSF can now be found in many continents such as Europe, Africa, and Asia (Park, 2016). The

importance and benefit of BSF have led to its commercial farming. For instance, in Africa, South Africa is the first country that has commercialized BSF farming in the world. Thereafter other countries, such as the Netherlands, Spain, Malaysia, France, and Ireland have established similar/corresponding industrial production plants (Cickova et al., 2015). Other African countries such as Guinea, Kenya, and Ghana more recently have come on board to farm and commercialise BSF (Quilliam et al., 2020).

2.2.2 Morphology of black soldier fly

Based on its morphological characteristics there is often confusion between adult black soldier fly (BSF) and wasps. They both have antennae and a translucent area on the basal abdominal segment. What distinguishes them is the absence of a stinger for the BSF, making the insect harmless (Oliveira et al., 2016). Authors such as Diener et al. (2011) observed that the insect is not a biological vector for diseases, unlike mosquitoes. This has also been confirmed in a recent study undertaken by Hasnol et al. (2020). Even though the BSF is not seen as a biological vector for diseases, Gujarathi & Pejaver (2013) have provided evidence that the fly can be a potential mechanical vector of various microorganisms capable of causing diseases. Adult BSF (Figure 2.1) is measured to be 15 to 20 mm in length. The insect has two long, black, straight antennas, and one pair of wings (Oliveira et al., 2016).

Figure 2.1: Black soldier fly at the adult stage (Kidadl, 2021)

Gender-wise, the female is bigger and has a reddish-coloured abdomen, while the male abdomen has more bronze (Park, 2016). Also, the female black soldier fly's tail ends with a scissor-shaped structure which is their sexual organ for mating and ovipositioning while the male black soldier fly's tail ends with a plate-like structure (Tomberlin & Sheppard, 2002).

2.2.3 Description and life cycle

The black soldier fly (BSF)'s life cycle consists of five stages; egg, larva, pre-pupal, pupal, and adult stage (Figure 2.2)
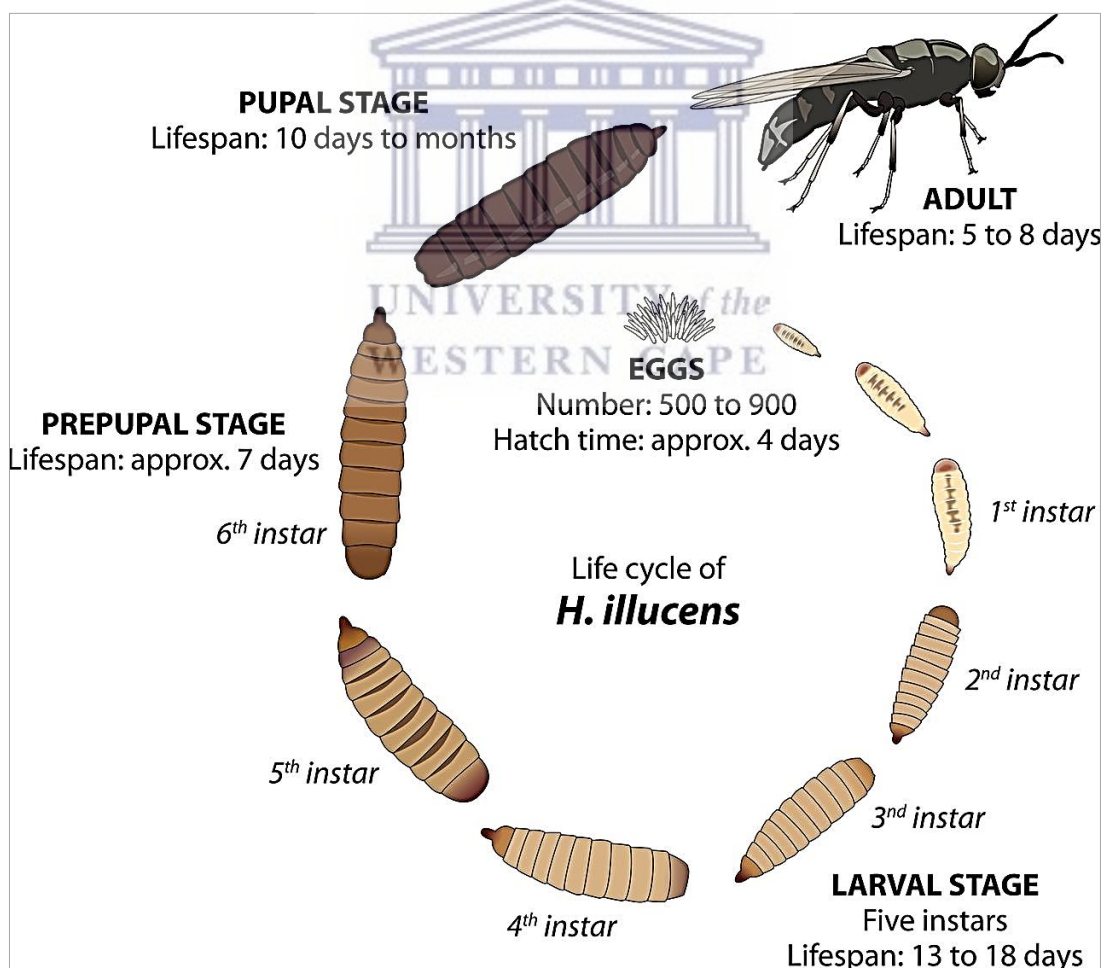
Figure 2.2: The life cycle of black soldier fly (De Smet et al., 2018)

Under normal conditions, reproduction usually occurs in the tropics throughout the year (Tomberlin & Sheppard, 2001). Over the years, studies showed that the insects lay approximately between 200 and 500 eggs (1 mm long) in decaying organic matter, garbage, feces, and animal manure. The eggs remain at this stage for around 4.5 days. When the eggs hatch, the larvae are approximately 1 mm long and begin to consume any organic waste they come across (Hoc et al., 2019). BSF larvae are creamy-white with a small yellowish to black head containing their mouthparts. The larva develops in six instars, the last being reddish-brown and it takes about fourteen days for this stage to complete. After the development, the larvae (Figure 2.3) disperse into dry sheltered places, leaving the feeding place for pupation. At that last stage, the larvae can reach 27 mm in length, 6 mm in width, and weigh up to 220 mg (Makkar et al., 2014a).

Figure 2.3: Black soldier fly larvae (Müller et al., 2017a)

When it comes to artificial breeding, a series of recent studies have indicated that environmental conditions such as light sources, humidity, and temperature were essential for mating and oviposition. For instance, Nakamura et al. (2016) showed that mating was not possible when BSF was exposed to rare earth light (fluorescent tube light). Similarly, a previous study conducted by Zhang et al. (2010) revealed that a 61 % mating rate was observed when BSF was exposed to illumination from a quartz iodine lamp in comparison with those bred in the sunlight. Thereafter, Heussler et al. (2019) verified that the best light source for mating was LED light when compared to fluorescent and halogen light. Oviposition on the other hand

has been influenced by temperature and humidity (Tomberlin & Sheppard, 2002; Tomberlin et al., 2009; Hoc et al., 2019). These investigations have underlined the importance of improving breeding methods for maximising fly reproduction.

2.3 Benefits of black soldier fly larvae

2.3.1 Black soldier fly larvae as recyclers of waste

With current urbanisation and population growth, organic wastes are receiving growing attention due to their negative environmental, social, and economic impacts (Adhikari et al., 2006b; Nguyen et al., 2015; Lalander et al., 2019). Singapore, for instance, is facing a waste crisis. Some authors including Bundhoo. (2018) have predicted that the city will run out of space in its landfill by 2035. The United States of America (USA) is battling with waste management too. Perednia et al. (2017) mentioned that the country alone produces roughly 66.5 million tons of food waste and over 1 billion tons of animal manure annually. The management of organic wastes such as faecal sludge is a big challenge in Africa. Researchers like Nguyen-Viet et al. (2009) have assumed that the huge waste amount leads to the spreading of diseases such as diarrhoea. More than 60 % of the population has no access to adequate sanitation in Africa. This is the case in South Africa too, where more than 50% of the population does not have access to adequate sanitation (Nguyen-Viet et al., 2009).

In the past decade, municipalities have stepped up their efforts to find sustainable solutions to the management of organic waste. In developing countries, some of the standard methods of disposal of waste described by Singh et al. (2011) can be classified as chemical (biochemical conversions), biological (aerobic and anaerobic), thermal and physical (landfilling) methods. Such various approaches as reported by Bojor, (2008) have their disadvantages concerning the effects of global warming, emissions (soil, air, and water), and economic costs. Landfill continues to be the most common final disposal for solid waste. According to the Department of Water and Forestry, about 95 % of the waste produced in South Africa ends up in landfills and only 10 % of waste is recycled (Department of Environmental Affairs, 2018). Incineration and landfilling remain the least desirable waste management option since waste disposal should be aimed not only at reducing waste but to make the waste a resource that can be utilised.

Worldwide researchers have proposed the use of BSF larvae as an effective and alternative waste management tool for processing organic waste. The BSF larvae can convert a large number of organic wastes such as feces sludge (Lalander et al., 2013; Banks et al., 2014),

household kitchen waste (Arthur et al., 2019), coconut waste (Lim et al., 2019), livestock manure (Doyle & Erickson, 2006; Salomone et al., 2017b) such as dairy (Liu et al., 2008), and poultry (Rehman et al., 2019). The BSF larvae can survive in manure which is usually full of bacteria because they can synthesise antimicrobial substances to protect themselves from microbial infections (Veldkamp & Bosch, 2015).

 Several studies have assessed the consumption and reduction capacity of BSF larvae. Nguyen et al. (2015) showed that during the larval stage, BSF larvae were able to reduce fruit and vegetable waste by 99 % and kitchen waste by 74 %. Lalander et al. (2019) reported a reduction of 85 % in poultry manure. Rehman et al. (2017) observed a reduction of 63 % and 74 % for dairy and soybean wastes, respectively. Interesting studies showed that BSF larvae can be selective when it comes to consuming organic wastes (Nguyen et al., 2015; Oonincx et al., 2016; Jucker et al., 2020). In their study, Nguyen et al. (2015) revealed that BSF larvae will avoid foods with heavy metal contaminations when given a choice, on the contrary, they will consume less as compared with diets with no heavy metals. They also found that BSF larvae had a preference for high-fat and energy-rich organic waste to build the fat body required for their development and their survival as adults.

Another benefit of BSF larvae is the reduction of volatile organic compound emissions generated during the decomposition process of manures. Examples of those volatile organic compound gases are organic sulphides, indoles, alcohols, and phenols. Hales et al. (2012) found that 67. 3 % of noxious odour production was caused by 4-methyl phenol from dairy manure. Kalus et al. (2017) mentioned that poultry manure releases ammonia and hydrogen sulfide. The aforementioned volatile organic compounds (VOCs) can affect the health of those living around animal farms. The capacity to eliminate those compounds in manure by using BSF larvae has been investigated by various researchers. For instance, Beskin et al. (2018) reported that BSF larvae reduced emissions of volatile organic compounds such as phenol, 4-methyl phenol, indole, volatile fatty acids by 95 % in poultry manure. Similarly, Liu et al. (2019) reported the reduction of volatile fatty acids by 25.58 – 80.08 % in livestock manures. Silva & Hesselberg. (2020) reported that temperature and humidity were two factors influencing the capacity of the BSF larvae to reduce microorganisms in the manure during the feeding process. Similarly, Liu et al. (2008) found that BSF larvae were able to significantly reduce *Escherichia coli* in dairy manure at 23, 27, and 31 °C, with the greatest suppression at 27 °C. Lalander et al. (2013) found that insect larvae deactivated *Salmonella* in human feces in eight days at a temperature of 20 to 25 °C. The above-mentioned studies have shown the advantages of using

BSF larvae as a tool for manure management, odour pollution, and pathogenic bacteria reduction.

2.3.2   Black soldier fly larvae contribution towards sustainable energy security

Black soldier fly (BSF) larvae is an effective source of renewable energy aside from waste control (Feng et al., 2018; Ishak & Kamari, 2019). Liu, (2019) mentioned that the world was gradually headed towards an energy crisis caused by overpopulation and the low popularity of renewable energy. Scientists have reported that conventional energies (fossil fuels and nuclear materials), which are non-renewable energy resources, are slowly being depleted and expected to be exhausted soon. (Guglielmo, 2012; Arutyunov & Lisichkin, 2017). In that regard, extensive work has been undertaken to reduce the burden on conventional energy resources. Biodiesel, for example, a biodegradable, non-toxic, and renewable energy option, has caught public attention in most countries (Sajjadi et al., 2016). According to Ahmad et al. (2011), the high cost of biodiesel feedstuffs, mainly from edible plants (sunflower, palm, coconut, soybean, and canola lipid) and non-edible plants (tobacco, Karanja tree, rubber tree) are, sadly, causing an economic and ethical competition between food, land and fuel industries. To address this concern, the use of different kinds of insects as an alternative raw material for the production of biodiesel was and is still being explored. A biochemical process to convert organic wastes into biodiesel by BSF larvae had been developed. The method of converting lipid into biodiesel is called transesterification, which is the reaction of triglyceride (lipid) with an alcohol to form esters and glycerol (Li et al., 2011; Rehman et al., 2017). In comparison to other insect species, Surendra et al. (2016) reported that BSF larvae have often been selected due to their high lipid content, rapid reproduction rate, and short life cycle. Li et al. (2011) found that BSF larvae fed with chicken manure were the best solution for achieving maximum BSF larvae biomass with high protein and lipid content, compared to cattle and pig manure. They also found that biodiesel properties (density, viscosity, cetane number) from BSF larvae were comparable to those from rapeseed lipid-based biodiesel.

2.4   Nutritional aspects of black soldier fly larvae

Because of the increasing world population insects were proposed as a high-quality, effective, and sustainable alternative source of protein. The use of insects as a source of protein can contribute to minimising food competition and reducing excessive livestock production to meet the demand for protein. Among the protein used for animal feed, soybean is the main dietary

ingredient used both as a protein and lipid source for animal and human food (Cullere et al., 2018). Such protein sources, however, are costly and their massive production poses serious environmental consequences such as deforestation, soil erosion, and extensive use of pesticides (Khan, 2018). To address that issue, black soldier fly (BSF) larvae based diets have been proposed as an alternative to soybean and fish meals due to their nutritive and chemical composition. Makkar et al. (2014) presented that BSF larvae are composed of 30 to 40 % lipid, 40 to 60 % of protein, and minerals which are similar to soybean and fish meal's nutritional value. Proximate analysis of BSF larvae which is the determination of the level of substances within a material was assessed by many scientists. For instance, the percentage of crude protein, crude fiber, ash, crude lipid, and gross energy was reported by Renna et al. (2017) as 55.34, 7.0, 7.12, 17.97 %, and 24.37 MJ/kg, respectively. A similar result was reported by Caligiani et al. (2018). However, the value of the crude fat (37.10 %) was higher compared to the crude lipid value reported by Renna et al. (2017). BSF larvae are also rich in calcium (5 to 8%) and phosphorus (0.6 to 1.5 %) (Makkar et al., 2014a; Spranghers et al., 2017). The content of other minerals such as potassium and sodium is usually found in lower levels. BSF larvae lipid is rich in medium-chain fatty acids such as lauric acid (21.4 - 49.3 %) which is the most abundant fatty acid. Lauric acid is known for its antimicrobial properties against gram-positive bacteria. Meneguz et al. (2018) found that lauric acid from BSF larvae could improve the growth, performance, and gut health of broiler chickens. A similar result on the benefit of lauric acid was reported by Spranghers et al. (2018) on weaned piglets. St-Hilaire et al. (2007) have reported that omega-3 fatty acids (alpha-linolenic acid, eicosapentaenoic acid, and docosahexaenoic acid) which are essential fats with numerous health benefits can be improved and manipulated by feeding the larvae with fish waste.

Apart from being a good source of fatty acids, BSF larvae are also a source of amino acids. Cullere et al. (2016) found that the two most abundant essential amino acids were valine (35.8 g/kg) and leucine (33 g/kg). Spranghers et al. (2017) have it that the value of the essential and non-essential amino acids is much lower. BSF larvae's protein and lipid compounds are affected by what they are fed, how much they eat, and when they are harvested. If fed with an appropriate diet, they can thus be used as an accumulator and recycler of fatty acids that cannot be synthesised by the human body. Currently, there are large-scale facilities farming BSF to produce animal feed protein and lipid worldwide. It is critical for insect-breeding companies to constantly explore ways to increase production effectiveness to lower current insect costs and compete with traditional protein sources. Based on the Bloomberg news published on May

22th 2020, South Africa is planning on producing high-quality protein powder from BSF larvae to be used in food and sports.

2.5 Black soldier fly larvae as a source of bioactive substances

2.5.1 History

Over the centuries, the use of insect larvae as wound treatment has been well documented. The beneficial effect of using insect larvae to inhibit the growth of bacteria in infected wounds was first noticed in 1557 by Ambrose Paré, a pioneer in surgical techniques (Choudhary et al., 2016). More recently, Zacharias and Jones were the first people to apply maggot therapy techniques during the American civil war (Chan et al., 2007). William Baer subsequently refined this process by using sterile maggots to inhibit the growth of bacteria in infected wounds (Chan et al., 2007). The mechanisms by which larvae destroy bacteria in wounds are not fully established, but there was evidence that the larvae produce bioactive substances which are key elements of the innate immunity against harmful microorganisms (Prete, 1997; Choudhary et al., 2016; Rabani et al., 2019). Despite the considerable promise and demonstrated results, the use of maggots as a clinical application declined in the late 1940s with the widespread clinical use of antibiotics such as penicillin, the world's first antibiotic that became the main therapeutic approach for treating bacterial infections, and as a preventive measure for controlling suspected infections, as well as enhancing surgical procedures. However, as time progresses, antibiotics lose their potency to efficiently inhibit bacteria growth due to antimicrobial resistance. Therefore, it is desirable to create a new class of antibacterial agents. To tackle this issue, renewed focus has been given to antimicrobial compounds from maggots as an alternative to antibiotics to become next-generation antibacterial agents for the management of bacterial infections.

2.5.2 Antimicrobial efficacy of black soldier fly larvae lipids

Lipids are hydrophobic or amphiphilic biomolecules present in biological systems that are purposely used primarily for energy storage and structural components of the cell membranes (Baillet et al., 2018; Wang et al., 2019). Lipids can be divided into eight categories: fatty acids, glycerolipids, glycerophospholipids, sphingolipids, sterols, prenol lipids, glycolipids (triglyceride, diglyceride, monoglyceride), and polyketides. Pioneering work done by Robert Koch in the late 19 th century found that antimicrobial lipids inhibited the development of anthrax which is an infection caused by gram-positive *Bacillus anthracis* (Yoon et al., 2018).

Over the next decades, Burtenshaw and colleagues also reported that antimicrobial lipids are acting as a natural disinfectant to control the microbiome of the skin (Jackman et al., 2016). Several studies revealed that the maggots of black soldier fly (BSF) was extremely rich in antimicrobial lipids such as fatty acid, mono, di, and triglyceride that are effective against resistant bacterial strains (Chu et al., 2014; Park et al., 2014; Jiang et al., 2019; Veldkamp et al., 2021). It was pointed out that antimicrobial lipids exhibit some promising features that make them attractive options for antibacterial uses, including low cost, a broad spectrum of activity, and lack of classical resistance mechanism against the actions of these compounds (Jackman et al., 2016; Jumina et al., 2018). Particular attention is drawn toward two classes of antimicrobial lipid, the fatty acids, and their derivatives

2.5.2.1 Fatty acids

Fatty acids are the simplest form of lipids consisting of a hydrocarbon chain with a terminal reactive carboxylic acid group and a methyl group at the other end. Fatty acids chain lengths vary from 2 to 30 or more carbons. They are classified into two categories, which are saturated fatty acids (no double bonds) and unsaturated fatty acids (one or more double bonds). The unsaturated fatty acids can be subdivided into monounsaturated fatty acids (one double bond) and polyunsaturated fatty acids (multiple double bonds). Unsaturated fatty acids may also be categorized into cis (hydrogen atoms on the same side) or trans (hydrogen atoms on the opposite side) fatty acids based on the arrangement of hydrogen atoms for double bonds.

The physical and chemical properties of the fatty acids are affected by their chain length, degree of saturation, and unsaturation (Desbois & Smith, 2010; Abbas et al., 2017). As an example, short hydrocarbon chain fatty acids will have a lower melting point compared to long-chain hydrocarbon fatty acids. Similarly, unsaturated fatty acids will have a lower melting point when compared to saturated fatty acids with the same number of carbon. Figure 2.4 shows the structure of fatty acids commonly found in BSF larvae.
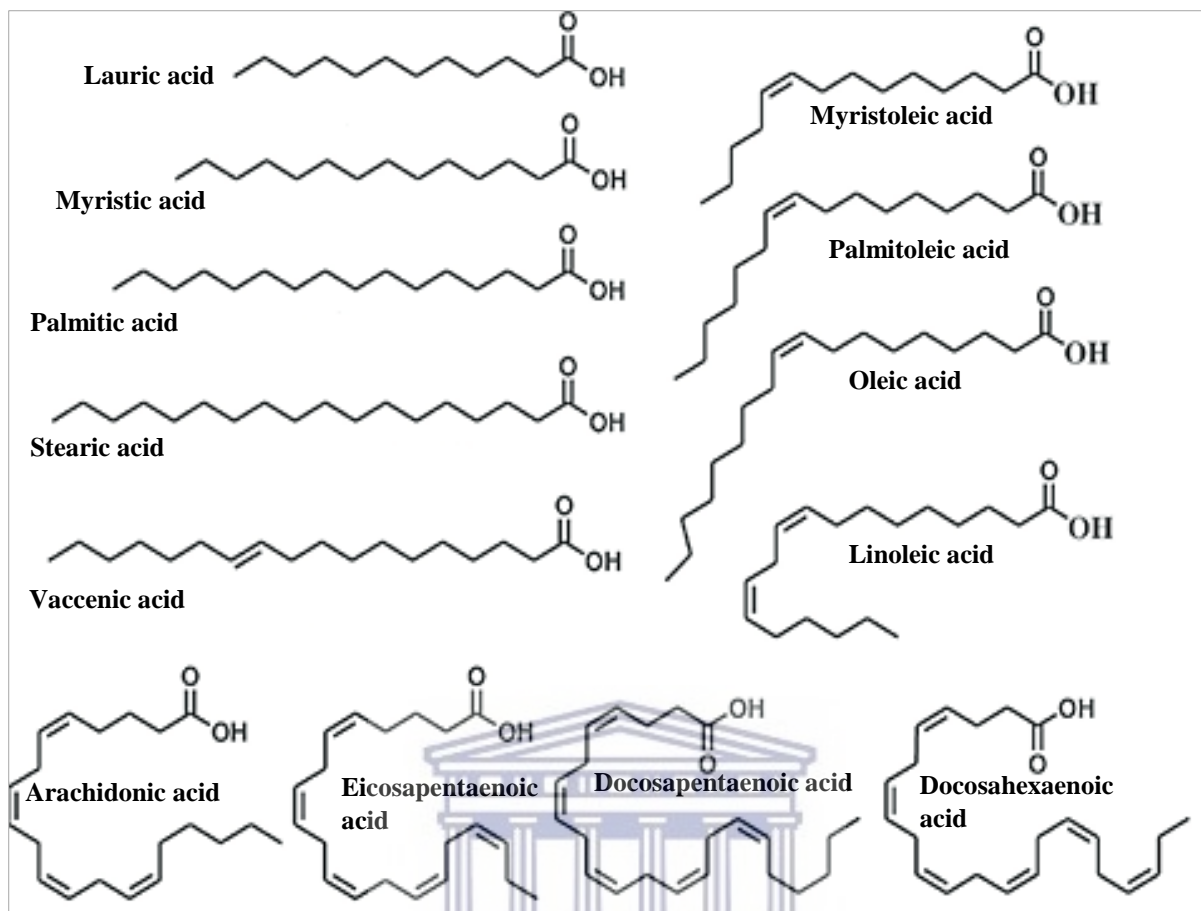
Figure 2.4: Chemical structure of the fatty acids (Dissanayake et al., 2016)

Table 2.1 shows the physical and chemical properties of fatty acids commonly found in BSF larvae.

Table 2.1: Physical and chemical properties of fatty acids

Name	Boiling point (°C)	Melting point (°C)	Molar mass (g/mol)	Appearance/Odour
Caprylic acid (C8:0)	239.7	16.7	144.2	Oily, colourless Faint, fruity odour
Capric acid (C10:0)	268.7	36.6	172.3	White crystals unpleasant odour
Lauric acid (C12:0)	298.9	45.0	200.3	Slight odour of bay lipid
Myristic acid (C14:0)	326.2	55.0	228.4	white solid
Palmitic acid (C16:0	271.5	62.9	256.4	White crystals
Stearic acid (C18:0)	232.0	69.0	284.5	white solid pungent, oily
Arachidic acid (C20:0)	328.0	76.0	312.5	White crystalline solid
Palmitoleic acid (C16:1)	162.0	0.5	254.4	Clear
Oleic acid (C18:1)	360.0	13.0	282.5	Brownish yellow oily with lard-like odor
Linoleic acid (C18:2)	230.0	-5.0	280.4	Colourless lipid
Arachidonic acid (C20:4)	169.0	-49.0	304.5	White to yellow powder
Eicosapentaenoic acid (C20:5)	439.3	-54.0	302.4	White fine powder
Docosapentaenoic acid (C22:5)	236.0	-78.0	330.5	-
Docosahexaenoic acid (C22:6)	446.7	-44.0	328.4	White fine powder

Fatty acids generate value as potential antimicrobial therapeutic agents due to their effectiveness, their safety, wide spectrum of action as well as lack of traditional resistance mechanisms (Sado-Kamdem et al., 2009; Choi et al., 2013; Matuszewska et al., 2018). Muniyan & Jayaraman, (2016) discovered that the structure and shape of fatty acids would influence their antibacterial properties. To give a brief example, several authors found that

medium (6 to 12 carbons) and long (13 to 21 carbons) chain unsaturated fatty acids from vegetable lipids are usually more active against gram-positive than gram-negative bacteria. The polyunsaturated fatty acids omega-3 fatty acids (docosahexaenoic acid and eicosapentaenoic acid) and omega -6 fatty acids (γ-linolenic acid and dihomo-γ-linolenic acid) were potent against a broad range of bacteria. Those include *Staphylococcus aureus*, (Kim et al., 2018; Lauritano et al., 2020), *Streptococcus mutans* (Sun et al., 2017), *Pseudomonas aeruginosa* (Belattmania et al., 2016), *Streptococcus agalactiae* (Dhouioui et al., 2016), *Helicobacter pylori* (Jung & Lee, 2016) and *Escherichia coli* (Dey et al., 2017). Concerning monounsaturated fatty acids, those having 14 or 16 carbon atoms such as myristoleic acid (C14:1) and palmitoleic acid (C16:1) were reported to be the most active against gram-positive and gram-negative bacteria when compared to other monosaturated fatty acids (Dhouioui et al., 2016; Yoon et al., 2018).

The relationship between the configuration (*trans*-oriented and *cis*-oriented double bonds) and the number of double bonds on the fatty acids carbon chain in connection to their bactericidal activity was discussed in several studies (Kalhapure et al., 2014; Gao et al., 2016). The aforementioned authors found the orientation of the hydrogen on the double bond can affect the efficiency and spectrum of the antibacterial action. For instance, a cis-oriented double bond that occurred naturally in fatty acids will be more potent than the fatty acids with *trans*-oriented double bonds. As for the number of bonds in fatty acids, Raychowdhury et al. (1985) in their pioneering work found that antimicrobial activity of the unsaturated fatty acid increases with the number of double bonds. However, studies done by Kalhapure et al. (2014), reported that commercial linoleic acid (two C = C), exhibited the highest antibacterial activity toward methicillin-resistant *Staphylococcus aureus* (MRSA) while the other commercial fatty acids such as arachidonic acid (four C = C bonds), linolenic acid (three C = C bonds), oleic acid and palmitoleic acid (one C = C bond) were less active. It must be noted that an addition of a second double bond was found to enhance the compound's toxicity to gram-positive bacteria. However, the fatty acids with three double bonds were not as effective as those with two double bonds. Thus, while there was some uncertainty as to whether a third double bond provides more or less activity, some general trends, however, do emerge on the following: C18:0 < oleic acid, C18:1 < linoleic acid, C18:2 > linolenic acid, C18:3 (Kalhapure et al., 2014; Penta, 2016; Gao et al., 2016).

As for the saturated fatty acids, several studies have reported that saturated fatty acids were less potent than unsaturated fatty acids of the same length of the carbon chain (Feldlaufer et

al., 1993; Kalhapure et al., 2014; Penta, 2016). Saturated fatty acid's antibacterial efficacy tends to increase with carbon chain length. Huang et al. (2014) investigated the effect of saturated medium-chain fatty acids of caproic acid (C6:0), caprylic acid (C8:0), capric acid (C10:0), and lauric acid (C12:0) on gram-positive bacteria. They found that lauric acid was the most active among the saturated fatty acids. Previous and current studies on the antimicrobial activity of lauric acid confirmed that it is the most potent among other fatty acids (Osman et al., 2018). Lauric acid is active in the prevention and treatment of a wide range of sexually transmitted infections (HIV, gonorrhea, chlamydia, genital herpes, human papillomavirus genital warts), foodborne infections (*Salmonella enteritidis, Listeria monocytogenes, Escherichia coli*), respiratory infections (swine flu, avian flu, common cold, and fever blisters) (Thormar et al., 2013). Lauric acid and capric acid in coconut lipid have been developed into pharmaceutical formulations as mouth and throat rinse, nose and throat spray, or nasal drops suitable for the treatment of respiratory syncytial virus (RSV) (Ramesh et al., 2020).

2.5.2.2 Monoglycerides, diglycerides, and triglycerides

Monoglycerides, diglycerides, and triglycerides are classes of lipids composed of a molecule of glycerol linked to one, two, and three fatty acids via an ester bond, respectively (Figure 2.5).

Monoglycerides
(One fatty acid bonded to glycerol)

Monolaurin

Diglycerides
(Two fatty acids bonded to glycerol)

Dilaurin

Triglycerides
(Three fatty acids bonded to glycerol)

Trilaurin
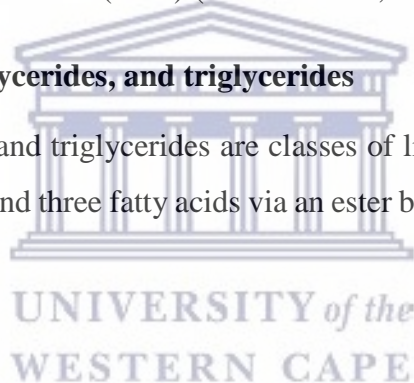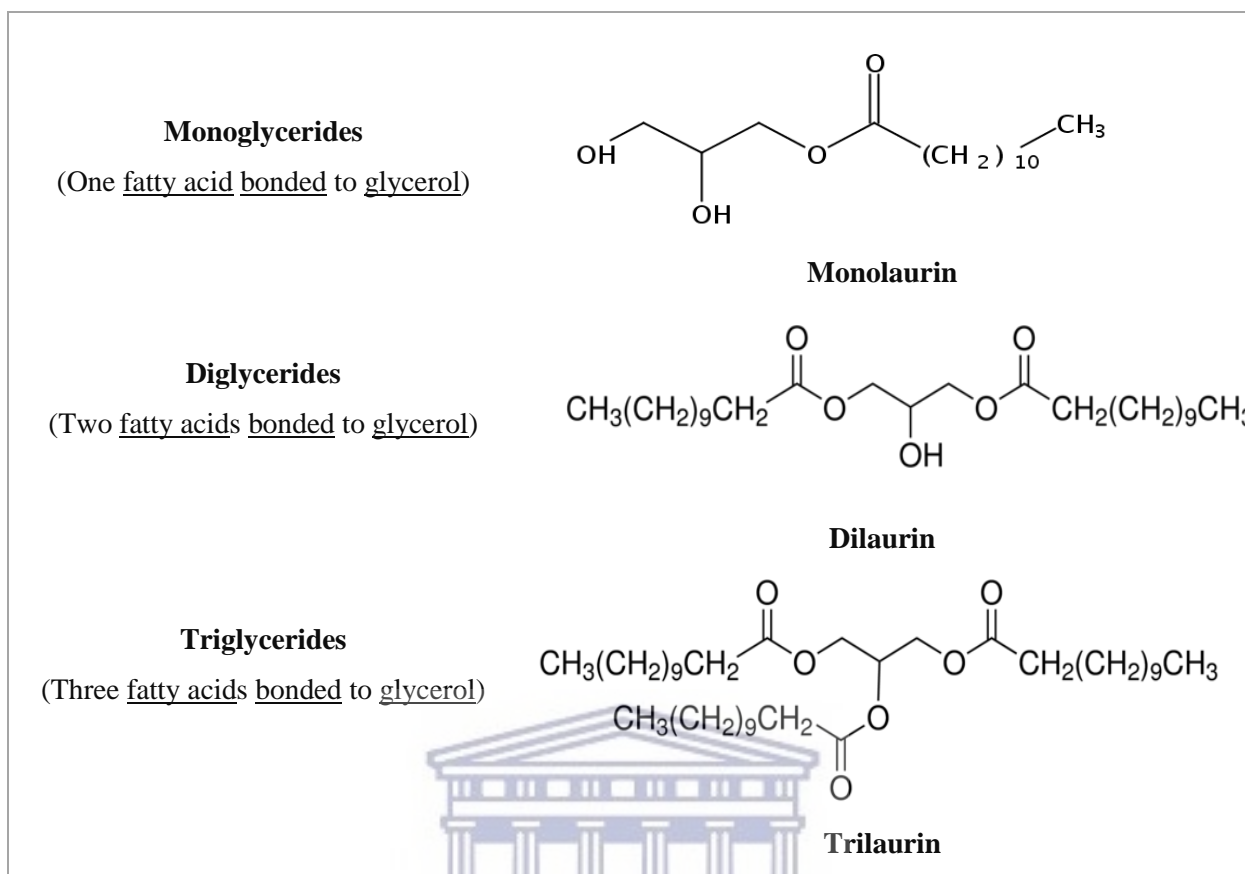
Figure 2.5: Structure of mono, di, and triglyceride

Table 2.2 shows the physical and chemical properties of triglycerides, diglycerides, and monoglycerides subcomponents commonly found in BSF larvae.

25

Table 2.2: Physical and chemical properties of lipid subcomponents (https://www.chembk.com/en/chem/Trilaurin)

Name	Boiling point (°C)	Melting point (°C)	Molar mass (g/mol)
Triglyceride subcomponents			
Trilaurin	591	46	639
Tristearin	260	72	891
Tripalmitin	310	66	807
Triolein	554	5	885
Trilinolenin	814	-23	814
Trilinolein	816	-5	879
Diglyceride subcomponents			
Dipalmitin	628	74	568
1,3 Distearin	669	71	625
Dilaurin	531	55	456
Monoglyceride subcomponents			
Monolaurin	397	63	274
Monopalmitin	451	65	330
Monomyristin	424	68	302

Various studies reported that among the three glyceride compounds, monoglycerides were the most potent compound against bacteria (Penta, 2016). This was shown by Batovska et al. (2009) who investigated the antibacterial action of the commercial medium-chain fatty acids (myristic, caprylic, lauric, and capric acids) and their corresponding monoglycerides (monomyristine, monocapryline monolaurin, and monocaprine) towards different gram-positive bacteria. The authors reported that the monoglycerides were more active than their precursor fatty acids. Besides, they found that among the monoglycerides, monolaurin displayed the greatest antibacterial action towards gram-positive bacteria. Recognition of the antimicrobial activity of the monoglyceride of lauric acid (monolaurin) has been documented since 1966 (Seleem et al., 2016; Nitbani et al., 2018). Kabara pioneered the research in the discovery of monolaurin in mother's milk in the 1960s and focused his work on the virucidal effects of monolaurin on enveloped RNA and DNA viruses. To date, monolaurin continues to be investigated by numerous researchers due to its high antiviral, antibacterial, antifungal, anti-yeast, and antiprotozoal activity (Seleem et al., 2016; Ezigbo & Mbaegbu 2017; Nitbani et al.,

2018). Monolaurin is generally recognized as a safe natural compound by the Food and Drug Administration (FDA) and can safely be combined with antibiotics, which might prove useful in the prevention or cure of bacteria resistant to traditional antibiotics (Batovska et al., 2009; Nitbani et al., 2018). Monolaurin has successfully exhibited antibacterial activity against a wide range of drug-resistant gram-positive bacteria including, *Candida albicans* and *Staphylococcus aureus, Listeria monocytogenes* (Seleem et al., 2018; Nitbani et al., 2018). However, it is generally less effective in the treatment of gram-negative bacteria such as *Escherichia coli* and *Klebsiella pneumonia* (Schlievert & Peterson, 2012). The enhancement of the compound's antimicrobial activity was investigated by various researchers. For instance, Batovska et al. (2009) found that the spectrum of activity of monolaurin can be broadened by combining it with other substances such as a cation chelator ethylenediaminetetraacetic acid (EDTA) or citrate. Branen & Davidson. (2004) reported that commercial monolaurin in combination with lactoferrin inhibited the growth of *Escherichia coli* (O157: H7) but not *Escherichia coli* (O104: H21). According to Subroto & Indiarto. (2020) monolaurin may be able to protect against SARS-CoV-2, the virus that caused the COVID-19 which became a pandemic in the world. However, clinical trials are needed to determine the efficacy and effectiveness of the monolaurin in fighting COVID-19 because no studies on the effectiveness of any monoglycerides in COVID-19 patients have been conducted (Aldridge, 2020).

For diglycerides and triglycerides, only a little work had been conducted in terms of the antimicrobial action of the diglycerides. It must be noted that a large proportion of animal and plant lipids are made up of triglycerides and it was observed that long-chain triglycerides are predominant. Coconut lipid is outstanding because it is mainly composed of medium-chain triglycerides (glyceride with fatty acids of 6 and 12 carbons) which were reported to possess healing properties (Dayrit, 2014; López-Colom et al., 2019; Chatterjee et al., 2020). Due to that a vast majority of all medium-chain triglycerides used by various researchers for medicinal purposes mostly come from coconut lipid. In this present work, it will be interesting to find out whether the black soldier fly larvae is rich in medium-chain triglycerides. Another interesting discovery made by Batovska et al (2009) is that glyceride compounds can be manipulated to enhance their potency in killing bacteria. This study was inspired by Kabara et al (1977) who did some pioneering works on fatty acids and derivatives as antimicrobial agents. In their work, they found that glyceride compounds of mixed chain length of fatty acids tend to be more active than the glyceride composed of the same fatty acids. The medium-chain triglycerides have also been found to eradicate unfriendly bacteria in the intestine (Rial et al., 2016). Intestinal dysbiosis refers to a condition in which the microorganisms in the intestine

become imbalanced. At this point, helpful microbes become dominated by unfavourable microbes which can then spread to multiple sites in the body (Gunsalus et al., 2015; Rial et al., 2016). *Candida albicans*, the most common human fungal pathogen was investigated by Arsenault et al. (2019) and their studies show that a diet containing medium-chain triglycerides could reduce Candida colonization in preterm infants and adults.

2.5.3   Antimicrobial peptides

Antimicrobial peptides (AMPs) also called host defence peptides (HDPs) are small cationic molecules containing 2 to 100 amino acids and residues exhibiting amphipathic characteristics (Guilhelmelli et al., 2013; Elhag et al., 2017) Antimicrobial peptides are synthesised predominantly in the fat bodies and certain blood cells of insects before being released into the body fluid where they act synergistically against microorganisms (Park & Yoe, 2017). Antimicrobial peptides have gotten increasing attention as potential therapeutic agents. They are shown to be promising for overcoming the growing problem of antibiotic resistance. This is made possible through several features such as broad-spectrum activity (antibacterial, antiviral, and antifungal), fast killing, selectivity, and no resistance development. According to the antimicrobial peptide database, more than 2000 AMPs have been identified in both prokaryotic and eukaryotic organisms and are classified into four families: magainin, cecropin, cathelicidin, and defensin family (Nakatsuji & Gallo, 2012). Among the four families of the antimicrobial peptides, two well-known antibacterial peptides; cecropins and defensins have been isolated and characterised in black soldier fly larvae in various studies (Park et al., 2015; Elhag et al., 2017). Cecropins were found to act on gram-positive and gram-negative bacteria while defensin-like peptides (DLPs) were found to act only on gram-positive bacteria (Wei et al., 2015). Even though AMP could be a possible novel class of antibiotics that could be used against a drug-resistant microbe, the cost of producing membrane-active peptides is high, hence making its use not feasible. Also, poor performance during physiological salt conditions was found to be a common issue with the membrane-active peptides, limiting their use. Furthermore, because of their cationic nature, they can be harmful to human cells (Nakatsuji & Gallo, 2012). Antimicrobial lipids, on the other hand, are abundant and cheap and show a better broad-spectrum and strong anti-microbial activity (Jackman et al., 2016).

2.5.4   Chitin and Chitosan

Chitin and chitosan are naturally renewable resources and the second most abundant biopolymer after cellulose (Song et al., 2018). They are found in marine animals (crabs,

prawns), mushrooms, insects, and the cell wall of fungi. Chitin consists of n-acetyl-d-glucosamine and a small amount of -d-glucosamine (Gachhi & Hungund, 2018). Chitosan is obtained through partial alkaline deacetylation of chitin to form n-acetyl-d-glucosamine and -d-glucosamine units connected by β-1,4-glycosidic linkages (Gachhi & Hungund, 2018) (Figure 2.6).
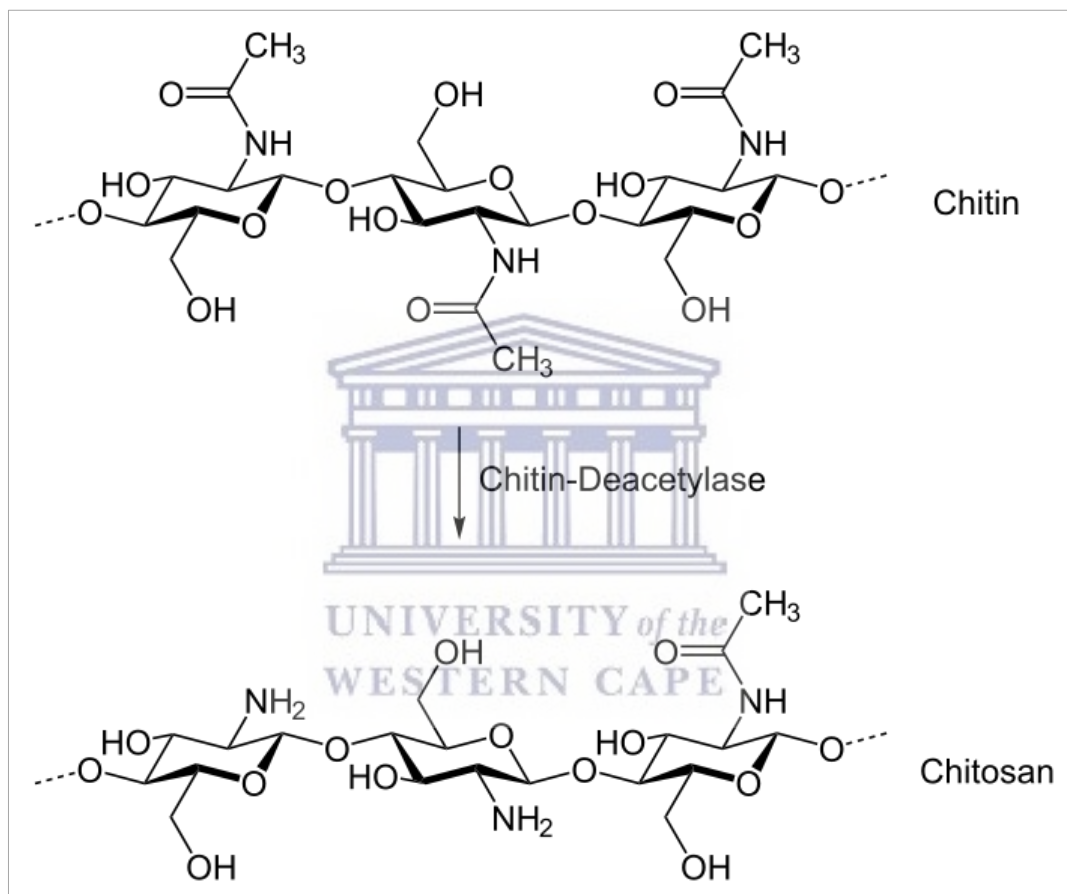
Figure 2.6: Schematic representation of chitin and chitosan (Goy et al., 2009)

Chitosan and chitin are of commercial interest because of their unique properties, such as non-toxicity, antimicrobial activity, and biodegradability, as well as their high nitrogen content compared to synthetically substituted cellulose, which makes them an effective chelating agent for medical products (Diener et al., 2011). Antimicrobial properties of chitin and chitosan have been studied against a wide range of microorganisms, including algae, bacteria, yeasts, and fungi (Song et al., 2018; Wardani et al., 2018; H. Zaghloul & H.A. Ibrahim, 2019). Chitin and chitosan are also used in the food and beverage industry, as well as wastewater treatment and

agrochemicals. Because of its use in healthcare and wastewater treatment, the chitin and chitosan market is expected to grow 3.3 times by 2027. (Soetemans et al., 2020). Crustaceans and mushrooms are currently the primary sources of commercialised chitin and chitosan (Ghormade et al., 2017). There is a search for more and new chitin sources to meet this demand. Scientists must consider the economic feasibility of extracting chitin from BSF larvae to do so.

2.6   Method of extraction of lipids from black soldier fly larvae

Several methods of extractions have been developed to extract lipids from a biological system (Danlami et al., 2014; Hernández-Santos et al., 2016; Al-sumri et al., 2017; Smets, Verbinnen, et al., 2020). Methods developed by Bligh and Dyer (1959) and Folch et al. (1957) had contributed immensely to lipid profiling, and to date, their method is still widely used (Wang et al., 2017a; Ravi et al., 2019; Smets, Verbinnen, et al., 2020). Their method involves a mixture of solvents (chloroform and methanol) in varying proportions. Methanol is integrated into an aqueous phase to break the hydrogen bonding between lipids and proteins (Iverson et al., 2001; Dabbou et al., 2021). Literature has demonstrated that in the extraction of lipids, solvent mixtures of acetonitrile and chloroform are not as effective as methanol and chloroform (Ulmer et al., 2018). The primary dissimilarities between Folch and Bligh and Dyer's procedures concern the quantities and the ratios of the solvents required during the extraction as well as the presence or absence of KCl in the water fraction. The effectiveness of extraction is dependent on the solvents selected; phospholipids are polar molecules hence are more soluble in polar solvents than in non-polar solvents. Zhao & Xu (2010) who applied Folch and Bligh and Dyer's techniques extracted phospholipids but not hydrophilic lipids such as phosphatidic acid phosphatidylcholine, phosphatidylethanolamine, and phosphatidylserine. (Byeon et al. (2012) improved on Folch et al. (1957) technique by comparing four different extraction methods; $CHCl_3$, MTBE, CH_3OH, and a combination of MTBE and CH_3OH. Their work shows that the combination of MTBE and CH_3OH is efficient in extracting most phospholipids. Zhao and Xu (2010) went further to experiment with the use of methanol to extract lysophospholipids and phospholipids from human plasma or serum without the generation of an artifact. Nagappan et al. (2019) optimised the existing technique developed by Folch et al. (1957) by replacing methanol with butanol.

To increase the extractability of the lipids, different cell disruption methods (chemical, mechanical, and biological methods) have been reported by various researchers. Chen et al. (2013)created a technique based on methyl-tert-butyl ether (MTBE). Their method facilitates

the faster removal of the most significant lipid classes. Lee et al. (2012) reported that among all disruptive techniques studied, the microwave extraction method is more effective for lipid extraction from green microalgae. In this field, some other techniques have proven to be effective in the extraction of lipids. Among them all, the Soxhlet extractor has found extensive use for this purpose. The simplicity and low cost of this method gained the interest of many scientists and researchers. Many improved versions (e.g. Soxtec) of this equipment have been manufactured, as the earliest version requires a large volume of solvent and lengthy extraction time Mubarak et al. (2015).

In the quest to achieve a safer and more efficient lipid extraction process, the supercritical fluid extraction (SFE) approach was developed and used to measure non-isolated lipids (Shinde & Mahadik, 2019). In place of harmful organic solvents, carbon dioxide is used as an extraction fluid (Molino et al., 2019). The high cost and environmental problems associated with the use and disposal of organic solvents motivate for use of supercritical techniques. The process of separation involves heating pressurised CO_2 above a critical temperature to become a supercritical fluid possessing gas and liquid characteristics. The gaseous properties of the CO_2 enable it to diffuse through the sample hence extracting the lipids in the process. The liquid properties imply that a high amount of lipids (particularly at greater pressures) will be dissolved (Bendif et al., 2018; Ouédraogo et al., 2018).

After the extraction stage, the sample must be purified or cleaned up before the instrumental analysis. This step allows the removal of matrix interferences and effectively raises the concentration of the lipid for easy detection during the analytical process. Lipid extracts from tissues usually contain substantial quantities of non-lipid contaminants (sugars, amino acids) that must be removed before analysis. Bligh and Dyer. (1959) and Folch et al. (1957) washing procedure can be used to removed non-lipid contaminants before analysis. To do so, a mixture of the chloroform-methanol extract is shaken and equilibrated. During the process, the mixture will separate into two layers; the upper layer contains the impurities while the lower layer consists of the analyte of interest. The time and quantity of solvent involved in the aforementioned methods led to the development of solid-phase extraction (SPE), an alternative method with outstanding advantages. This technique combines the three processes; sample extraction, pre-concentration, and clean-up. The sample extract is applied to sorbent phases (nonpolar, polar, ion) and analytes are retained and then selectively removed. The SPE promotes the elimination of the problems associated with the liquid-liquid extraction method. SPE surpasses liquid-liquid extraction (LLE) because it enhanced the removal of interferences,

improved selectivity, and specificity, higher recoveries rate, lower solvent consumption, reduced man- labour, allowed multiple samples analysis, and its automation is possible.

2.7 Chromatographic separation of lipid classes

Chromatography is a commonly used method for separating analyte mixtures based on polarity differences. Several studies using the chromatographic approach for the isolation and fractionation of lipids into groups have been reported (Ruiz-Gutiérrez & Pérez-Camino, 2000; Sajilata et al., 2008; Bui et al., 2016). Among traditional chromatographic separation techniques, liquid chromatography and gas chromatography is widely used for the separation of different classes of lipids from various matrices.

2.7.1 Liquid chromatography

2.7.1.1 Column chromatography

Low-pressure column chromatography has been widely used for the fractionation and purification of larger amounts of lipids (Warren, 2019). The adsorption technique is based on the distribution of the lipid between the stationary and the mobile phases. The stationary phase, as its name suggests, does not move; rather, the compounds travel through it at different rates depending on their polarity. The most common adsorbents used as stationary phases are silica, alumina, and magnesia. The rate at which the different lipid classes move through the absorbents is highly dependent on the activity of the adsorbent and the polarity of the solvent. As an example, if the activity of the adsorbent is very high and the polarity of the solvent is very low, then the separation will be very slow and a good resolution will be achieved. In the same manner, if the activity of the adsorbent is low and the polarity of the solvent is high this will lead to a rapid separation with a poor resolution of the compounds. The mobile phase (eluents) consists of organic solvents of different polarities that move through the stationary phase to separate compounds. Usually, the more polar the eluent, the faster all compounds run through the stationary phase. Therefore a nonpolar solvent such as hexane for instance is used to first remove the least polar compounds, then solvents of increasing polarity are used until the most polar compound is removed from the stationary phase.

In their study, Sajilata et al. (2008) successfully separated neutral lipids (mono and diacylglycerols and hydrocarbons), glycolipids, and phospholipids from *Spirulina platensis*, a good source of linolenic acid by silica gel column chromatography. The authors reported that the glycolipids fraction contained about 94 % of the total linolenic acid. In the late 1970s small,

commercial prepacked columns with a variety of solid stationary phases were introduced for the fractionation of small quantities of sample. The method was found to be easy to use, fast, cost-effective, and reduced solvent usage (Anna et al., 2017). Kaluzny et al. (1985), were able to fractionate lipid samples into cholesterol ester, triglycerides, diglycerides, monoglycerides, cholesterol, fatty acids, and phospholipids using SPE bonded aminopropyl. A few years later, Agren et al. (1992) proposed a simplified method to improve Kaluzny and co-workers' methods. Their method separated the lipids into groups with a single SPE bonded aminopropyl column which resulted in the reduction of the number of steps and less contamination. Besides the method of the aforementioned authors, a third method was developed by Neff et al. (1992). They used the SPE column prepacked with silica to isolate the lipid classes. Recently a more advanced version of their method has been published by Traversier et al. (2018); Warren, (2019); Alves et al. (2020); and Rach et al. (2020) in which the SPE column prepacked with a combination of silica and aminopropyl (aminopropyl silica) was used. Their method showed a better separation of the lipid classes.

2.7.1.2   Thin-layer chromatography

Thin-layer chromatography (TLC) is a popular separation technique widely used in modern analytical chemistry for the fractionation and identification of lipids. As mentioned for column chromatography, TLC also is based on the principle of adsorption and uses various stationary phases including silica gel, cellulose, and alumina. The TLC separation can improve the resolution of different classes of lipids by modifying the stationary phase with impregnating agents that will be incorporated in the stationary phase. The two widely used impregnating agents include silver (Ag) and boric acid (H_3BO_3). Silver is mainly used for the separation of unsaturated lipids according to their configuration, the position of the double bond, and the chain length (Momchilova & Nikolova-, 2016). On the other hand, H_3BO_3 is used for the detection of various isomers of diglycerides and phospholipids. Additional impregnating agents such as EDTA, have been used to achieve the most complex separation.

High-performance liquid chromatography (HPLC) or its recent version ultra-performance liquid chromatography (UPLC) is undeniably a superior separation technique due to higher performance and automatization. However, Ciura et al. (2017) enumerated several advantages that still make TLC competitive today. These are low cost, simplicity, effectiveness, and low solvent consumption with rapid separation of a large number of samples simultaneously. High-performance thin-layer chromatography (HP-TLC) which is a refined version of the classical

TLC technique, has been developed to increase the separation, resolution, reproducibility, and analysis speed (Fuchs et al., 2011). The main difference between the two methods is the characteristic of the stationary phase. HP-TLC plates are made of a sorbent with smaller particle sizes compared to traditional TLC. Moreover, it requires a smaller amount of mobile phase and accommodates a wide range of sorbents. It also uses an autosampler for sample spotting.

2.7.2   Gas chromatography

Gas chromatography (GC) also known as Gas-Liquid Chromatography (GLC) is a technique used to separate, identify, and quantify compounds. It is a type of chromatographic partition in which the mobile phase is an inert gas (helium, nitrogen, hydrogen), and the stationary phase is in liquid form. Based on the recommendation of several lipid analysts, it is often beneficial to use adsorption chromatography techniques (TLC, HPLC, or SPE) to conduct a preliminary fractionation of lipids into simpler groups before GC analysis. In the separation process, the sample is injected as a liquid into the GC injection port and vaporised at a higher temperature. The gaseous sample is then carried through the column by the mobile phase where it interacts with the stationary phase and is separated based on the polarity and volatility of the components. Compounds with less affinity for the stationary phase reach the detector quicker. Gas chromatography is usually used in combination with a specific detector such as mass spectrometry (MS) and flame ionisation detection (FID). The latter is widely used by lipid analysts. Niemi et al. (2019) compared their performances and they found that the choice of a detector type has little consequence on the lipids profile. However, the lack of any selectivity from GC-FID can limit its usefulness when applied to complex samples (Dodds et al., 2005). Despite the potential advantages of GC-MS in lipid analysis, GC-FID continues to be favourably used in many laboratories, especially by lipid experts (Danish & Nizami, 2019; Rydlewski et al., 2019; Francescangeli et al., 2020; Scortichini et al., 2020).

In the existing literature, fatty acid analysis usually requires derivatisation steps before GC analysis to increases analyte volatility of compounds that are difficult to evaporate and can lead to low detector sensitivity and response. However, the disadvantage associated with the derivatisation step includes a laborious and time consuming process. Even though the derivatisation step has still been used by various researchers until today, some researchers have carried out the direct determination of fatty acids without the derivatisation steps. For example, Meng et al. (2007) and Zhang et al. (2015) developed a derivatisation-free GC method using

fast temperature programming and a special capillary column. They were able to separate several fatty acids with satisfactory recoveries and reproducibility. Al-bukhaiti et al. (2017) identified certain benefits to GC, such as good resolution, high precision and accuracy, high repeatability and reproducibility that make it method of choice for the separation of fatty acids component of the lipids.

2.8   Nanotechnology formulations for antibacterial lipids

Although fatty acid, mono, di, and triglycerides have shown promising antibacterial features, the effectiveness of those compounds in the free form inside the organism is hampered by some technical challenges such as poor solubility which is further decreased after oral administration due to carboxyl protonation under gastric pH (Jackman et al., 2016). Moreover, oxidation, esterification, and complexation of lipid proteins decrease their bactericidal activity in vivo (Thamphiwatana et al., 2014; Jung et al., 2015). The aforementioned challenges can be overcome by using nanostructure formulations of those compounds. Nanoparticles are of interest because of their enhanced physical and chemical properties compared with larger particles of the same materials. There are several types of nanostructure formulations that are worth exploring and discussing but this section focuses mainly on lipid-based nanoparticles. Those are liposome, emulsion, and solid lipid nanoparticles. Lipid-based nanoparticles are extremely small particles ranging from 10 to 1000 nm (Li et al., 2017). They were discovered in the early nineties by Gasco (1993) followed by Müller and Lucks (1996). Today, although there have been increased numbers of studies done on lipid-based nanoparticles, the above-mentioned pioneers remain the leaders in this field and their works are still referenced when it has to do with the nanostructure. Solid-based nanoparticles promote and enhance the solubility, stability, and bioavailability of antimicrobial lipids.

2.8.1   Liposomes

The name liposome comes from the Greek word Lipos (fat), and Soma (body) (Mansoori et al., 2012; Akbarzadeh et al., 2013). Banerjee et al. (2015) have described them to be small, artificial, bilayered vesicles (20 - 100 nm) consisting mainly of cholesterol, fatty acid, and phospholipids. Liposome depicted in Figure 2.7 has a spherical shape with an aqueous solution core enclosed by a hydrophobic membrane. They are used as a means of nutrient and pharmaceutical administration (Mukherjee, 2017).
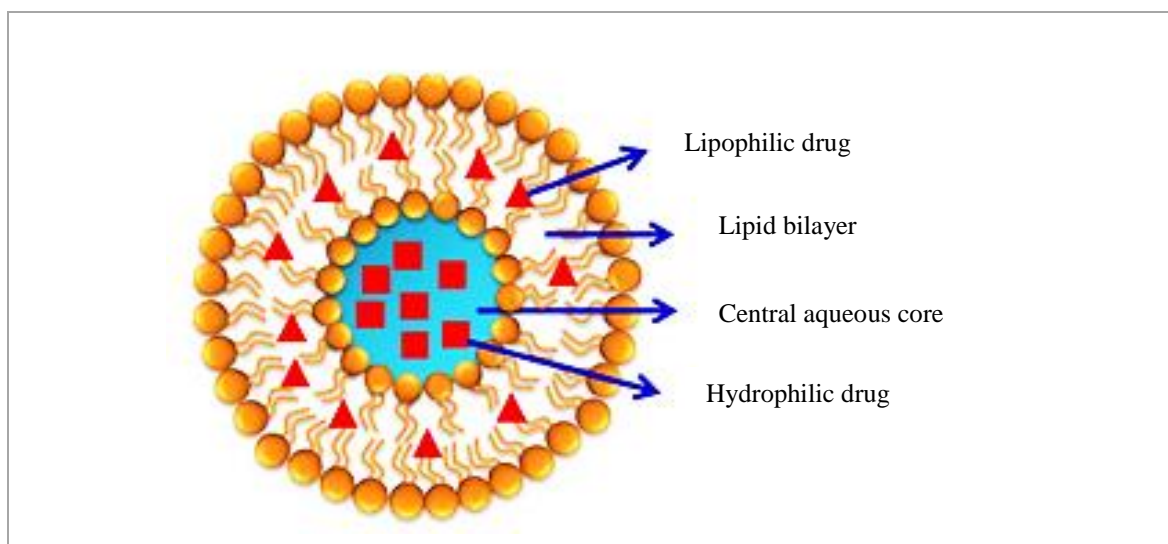
Figure 2.7: Structure of liposome (Din et al., 2017)

Liposomal nanoformulation of fatty acids had shown promising results based on several studies. The amphiphilic nature of fatty acids gives them the ability to be directly integrated into the hydrophobic membranes with large load output during liposome formation. Jung et al. (2015) have developed a liposomal nanoformulation of linolenic acid and oleic acid and evaluated their bactericidal activity against drug-resistant, *Helicobacter pylori, and Propionibacterium acnes*, respectively. The authors reported the fatty acids loaded into liposomes were effective in killing the aforementioned bacteria. Furthermore, Obonyoa et al. (2012) demonstrated the bactericidal activities of liposomal linolenic acid and free linolenic acid in treating *Helicobacter pylori* infection. They found *Helicobacter pylori* did not develop drug resistance when cultured in various sub-bactericidal concentrations with liposomal linolenic acid. Surprisingly, all the liposomal studies that have been conducted have focused exclusively on fatty acids. Due to the large industrial use of monoglycerides, diglyceride and triglyceride the development of liposomal formulations for the aforementioned lipids has considerable potential. It requires further investigation to ascertain if encapsulation of liposomes can also enhance the antimicrobial benefits of those mentioned lipids. This shows that there is room for further research on the antimicrobial lipids liposomal formulations.

2.8.2 Solid lipid nanoparticles

Solid lipid nanoparticles (SLNs), depicted in Figure 2.8 are nanometer-sized particles (50 to 1000 nm) with a solid lipid matrix.
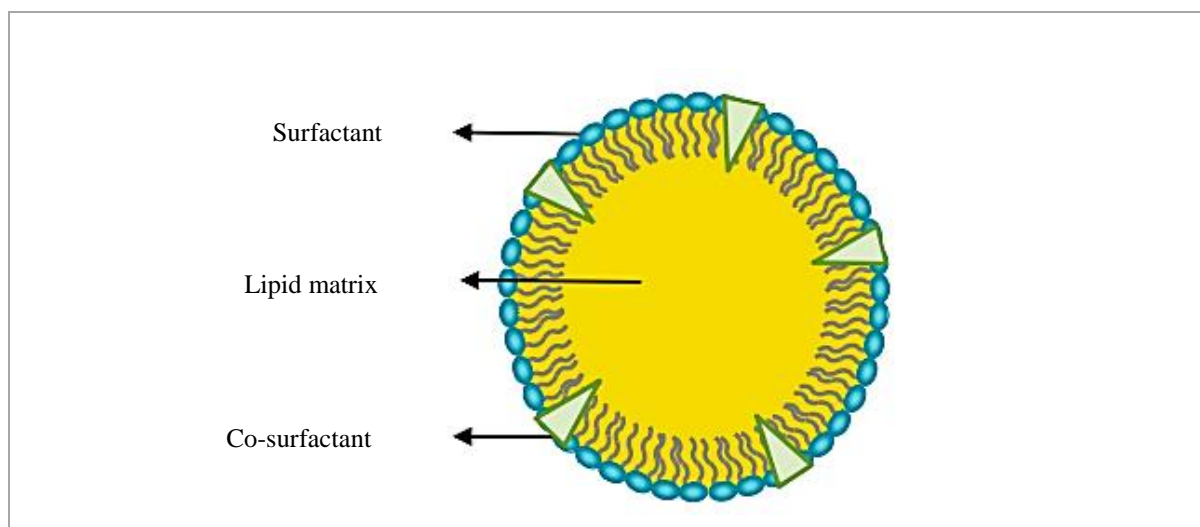
Figure 2.8: Schematic representation of solid lipid nanoparticle structure (Bayón-Cordero et al., 2019)

Solid lipid nanoparticles are the most promising nanoparticulate systems developed in the early 1990s for drug delivery. Based on several published studies, these colloidal carriers were invented as an alternative to conventional carrier systems such as liposomes, polymeric nanoparticles, and emulsions (Nair et al., 2011). SLNs are a good candidate for drug delivery systems, due to their low cost and scalability. Moreover, there is no specific solvent required during synthesis, they are also stable in the long term and are much easier to manufacture than biopolymer nanoparticles. It has also been found that the toxicity of SLNs to human granulocytes is extremely low (Ekambaram et al., 2018). In terms of their composition, SLNs consist of solid lipids, a surface-active agent (also known as emulsifiers or surfactant), and an aqueous solution (Silva et al., 2015; Kotmakci et al., 2017). The lipid materials used for the SLNs have biocompatibility, biodegradable features, and a high melting point and include fatty acids, triglycerides, monoglycerides, diglycerides, steroids, and waxes (Battaglia et al., 2014; Ekambaram et al., 2018). These physiological properties of the selected lipids are important for the safe delivery of the drug at the required site of action and to minimize the toxicity of the drug. For the emulsification and stabilisation of lipid dispersions, various types of emulsifiers such as soybean lecithin and polysorbates, for instance, had been used by several researchers (Kulkarni et al., 2011; Geszke-Moritz et al., 2016; Umerska et al., 2016; Khatak & Dureja, 2018). Co-surfactant, which is optional along with preservatives, cryoprotectant, and

charge modifiers are also added for the synthesis of SLNs (Mishra et al., 2018). An overview of ingredients commonly used for the preparation of SLNs is provided in Table 2.3.

Table 2.3: Ingredients used in solid lipid nanoparticles based formulations

Ingredients	Examples
Lipid component	beeswax, stearic acid, cholesterol, triglyceride (tricaprin, trilaurin, trimyristin tripalmitin, tristearin, hydrogenated coco-glyceride), monoglycerides, diglyceride, fatty acids (stearic acid palmitic acid, decanoic acid behenic acid)
Surfactant/Emulsifiers	soybean lecithin, egg lecithin, phosphatidylcholine, poloxamer, poloxamine, polysorbate 80
Co-surfactant	sodium dodecyl sulfate, tyloxopol, sodium oleate, taurocholate sodium salt, sodium glycocholate, butanol, taurocholic acid sodium salt, butyric acid, dioctyl sodium sulfosuccinate, mono-octyl phosphoric acid sodium
Preservative	Thiomersa
Cryoprotectant	gelatin, glucose, mannose, maltose, lactose, sorbitol, mannitol, glycine, polyvinyl alcohol, polyvinyl pyrrolidone
Charge modifiers	dipalmitoylphosphatidylcholine, stearyl amine, dicetylphosphate, dimyristoyl, phosphatidylglycerol

Adapted from (Mishra et al., 2018)

Qushawi et al. (2016) formulated and evaluated the antibacterial activity of SLNs loaded with an antibiotic (tilmicosin). They found that the formulation was effective against *Escherichia coli* and *Staphylococcus aureus* at a concentration of 8 µg/mL. Dinarvand et al. (2012) found that the efficiency of the formulated SLNs is achieved when there is better penetration of the nanoparticles into bacterial cells and better delivery of the drug to its site of action. Shazly (2017), in his study, found that antibiotic-loaded SLNs exhibited superior antibacterial activity against *Pseudomonas aeruginosa and Staphylococcus aureus* than the free antibiotic. A similar result was observed by other researchers like Severino et al. (2017); and Ghaderkhani et al. (2019). Din et al. (2017) showed that antibiotics can be incorporated into SLNs in three ways, as shown in Figure 2.9. It can be dispersed homogeneously in the lipid matrix (a), it can be incorporated into the shell surrounding said matrix (b), or it can be distributed in the outer shell

(c). It must be noted that the authors used the lipids only as nanocarriers for Drug Delivery and did not check the antimicrobial effect of the lipid itself.
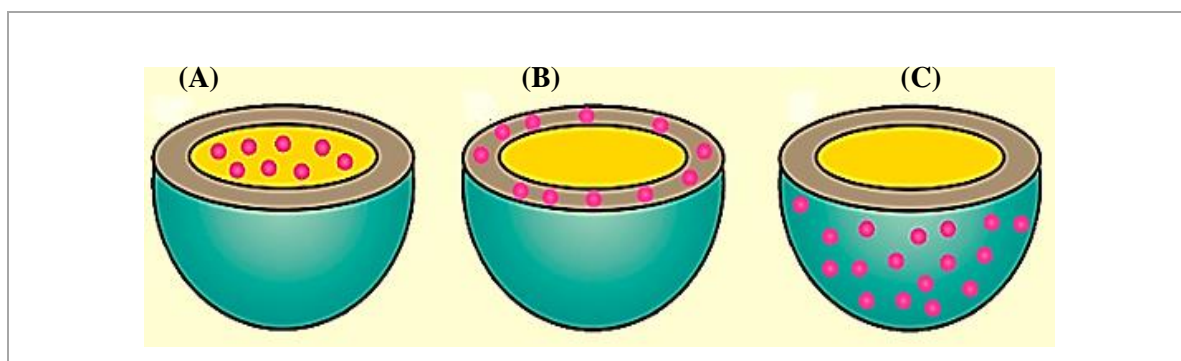
Figure 2.9: Possible methods of incorporating a drug (pink) in solid lipid nanoparticles (Din et al., 2017)

A few years back, instead of loading the SLNs with an antibiotic, Taylor et al. (2014) in their study loaded the SLNs with fatty acids (lauric acid and oleic acid) to eradicate *Pseudomonas aeruginosa*. They were also able to successfully enhance the antimicrobial activity of SLNs formulated with lauric acid by adding oleic acid into the formulation. Research has been done on solid lipid nanoparticles (SLNs) for drug application and has continued to be studied until today. Ozturk et al. (2019) point out that studies focusing on the effects of the type of lipids used in the formulation of the SLNs are lacking. This motivated the author in elucidating the influence of three types of lipids namely glyceryl behenate (lipid used in the cosmetic industry as an emulsifying agent), tripalmitin, and stearic acid on the properties (particle size, polydispersity index, and drug content) of the formulated SLNs. The outcomes of their study showed that the chain length of the lipids influenced particle size. It must be noted that particle size is important criteria of SLNs which affects drug release rate, bio distribution, etc. Higher particle sizes were obtained in SLN formulations prepared with tripalmitin while lower particle sizes were obtained with stearic acid. This resulted in the highest drug content in the formulation prepared with tripalmitin and therefore a better antimicrobial activity against *Staphylococcus aureus* (Ozturk et al., 2019).

A new strategy for manipulating SLNs formulations has been reported by various researchers. A combination consisting of polysaccharide polymers (chitosan, fucoidan, pectin, and

methylcellulose) and lipids to produce solid lipid-polymer hybrid nanoparticles have gained interest in the pharmaceutical field (Hadinoto et al., 2013; Wang & Luo, 2018; Khan et al., 2019; Mukherjee et al., 2019). Chitosan, a cationic polymer derived from chitin is often selected in the SLNs formulations because it forms stable lipid nanoparticles (Shin & Kim, 2018). Moreover, it is biodegradable and non-toxic and has been generally recognised as a safe material (Shin & Kim, 2018). The combination of chitosan with SLN has been proven effective as a strong antimicrobial agent as it combines the advantages of SLNs with the biological properties of chitosan (Friedman et al., 2013). SLN are very complex systems having more advantageous properties compared to other colloidal carriers. According to Ekambaram et al. (2018), further work needs to be done to understand their structure and dynamics on the molecular level in vitro and in vivo studies. The next section highlights the different methods used by various researchers to produce SLNs.

2.9 Production of solid lipid nanoparticles

Solid lipid nanoparticles (SLN) as mentioned previously are made up of solid lipid, emulsifier, and water. The selection of the different methods to synthesize SLNs depends on the nature of the product to be incorporated, the type of lipid and emulsifier as well as the route of administration. The widely reported preparation techniques for the production of SLNs are high-pressure homogenization, ultrasonication/high-speed homogenization, a solvent evaporation method, solvent emulsification–diffusion method, supercritical fluid method, microemulsion based method, spray drying method, or double emulsion method (Ganesan & Narayanasamy, 2017; Duan et al., 2020; Shanaghi et al., 2020). All these methods have their advantages and disadvantages. Table 2.4 highlights the advantages and disadvantages of each method.

Table 2.4: Advantages and disadvantages of wide methods of preparation of solid lipid nanoparticles.

Method	Advantages	Disadvantages
High-pressure homogenization (Hot and Cold)	High encapsulation efficiency. High reproducibility. Organic solvent-free method	Energy-intensive process. High-temperature process. Possible product degradation
Ultrasonication method	Low operational cost. Process intensification. Smaller particle size	Physical instability upon storage. Difficulty in scale-up. Broad particle size distribution
Microemulsion based method	Organic solvent-free method. Not an energy-consuming process. Easy to scale up	Extremely sensitive to change. Labour intensive formulation work. Low nanoparticle concentrations.
Spray drying method	Simple and single-step process. Cost-effective. No need for particle separation. Can be scaled up	Low yield. High maintenance. Not suitable for heat-sensitive materials. High moisture content in the product. High energy and pressure requirement
Double emulsion method	It provides an advantage of encapsulation of both hydrophilic and hydrophobic actives	Large and non-uniform particles. Two-step process. Difficult to scale up
Single emulsion method	Provides high entrapment of lipophilic actives.	The entrapment of hydrophilic drugs is poor. It is difficult to scale up.
Emulsion diffusion method	It allows the incorporation of thermosensitive drugs. Reduces mean particle size and narrow size distribution. Use of nontoxic solvents.	Possible organic solvent residues in the final formulation. Poor encapsulation of hydrophilic drugs. A longer time of emulsion agitation is required.

Adapted from (Iqbal et al., 2015; Shrimal et al., 2020)

2.9.1 Electrospraying: A novel technique for the synthesis of nanoparticles

Electrospraying is an electrohydrodynamic process in which a matrix solution is sprayed through the application of a high potential electric field to obtain particles at a micro or nano scale (Bhushani, 2014). In review, Tapia-Hernández et al. (2015) pointed out that electrospraying is regarded as one of the best methods for developing nanoparticles compared to other techniques such as nanoprecipitation, emulsion-broadcasting, and dual emulsification. According to Trotta et al. (2010), few studies have reported the use of electrospraying to produce lipid-based nanoparticles. This is because the technique was mostly known for the preparation of polymers, and to date over 200 polymers have been electrospun successfully (Bhardwaj & Kundu, 2010). A critical analysis of this method, based on its functionality gives a clear pointer that it could be the appropriate method for the production of nanoparticles in this study. The typical setup for electrospraying shown in Figure 2.10 consists of four main components: a high voltage source (up to 30 kV), stainless steel needle, a syringe pump, and a collector (aluminium foil) (Bhushani & Anandharamakrishnan, 2014).
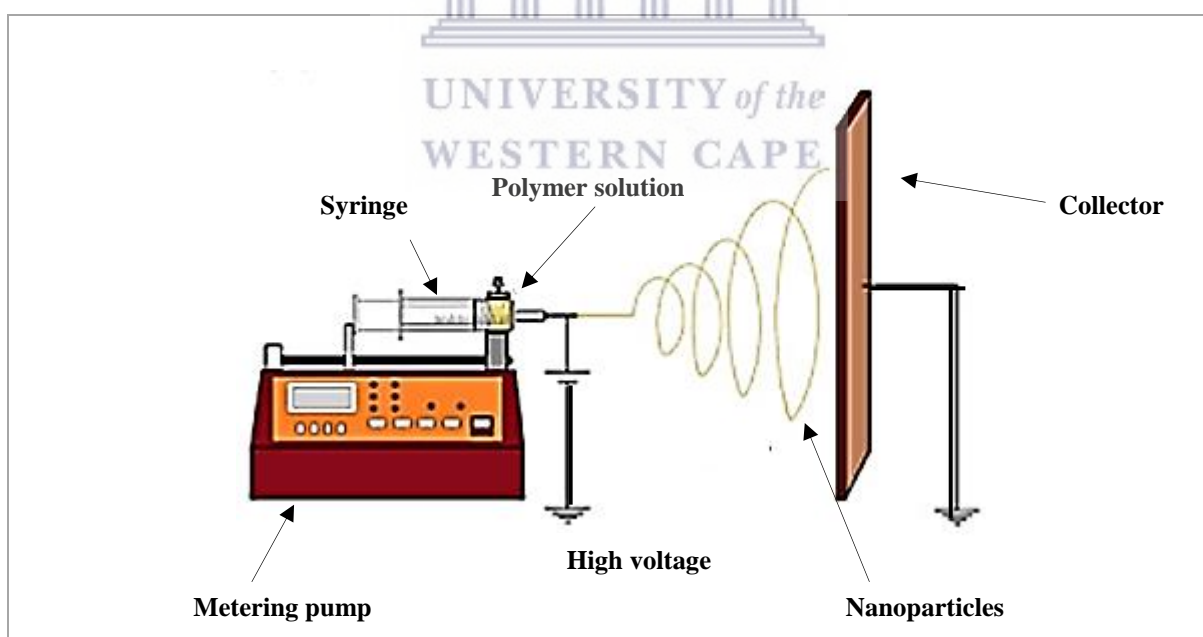
Figure 2.10: Schematic diagram of set up of electrospraying apparatus (Islam et al., 2019)

In this study, the electrospraying method was deemed the best route for the synthesis of the lipid nanoparticle over other methods because it is a single-step process, which does not use

potentially risky organic substances. Moreover, the technique is simple and low cost. It does not use surfactants and can be used to produce a wide range of micro and nanoscale materials (Miranda et al., 2006; Bhushani & Anandharamakrishnan, 2014).

2.10 Chapter Summary

This review revealed that black soldier fly (BSF) larvae could convert organic wastes into valuable biomass rich in protein and lipid. The lipid and protein extracted from the biomass could be applied as a substitute for fish meal and animal fed. Furthermore, the remaining solid waste of the BSF larvae after lipid extraction could be used for agricultural purposes. This is due to their high content of minerals useful to plants and animals. However, the use of BSF for the benefit mentioned above have not been fully or widely adopted. The same trend can be observed in medicine. For instance, in developing countries, approximately 80% of the population still depends on bioactive substances derived from plants, microorganisms, and marine species. These have long been recognised as important sources of bioactive substances which have led to the development of a large variety of drugs to treat human diseases. However, due to the increase in demand for these products and limited available land to cultivate a large quantity of these plants, high competition exists relating to land use. Hence, scientists need to direct their search to a feasible non-food feedstock as a source of bioactive substances. The separate studies done by Gołebiowski et al. (2014), Zdybicka-Barabas et al. (2017), and Prather & Laws (2018), showed that one of the proven ways is through the cultivation of insects. Among the family of insects, BSF larvae have been explored in the search of new active substances. BSF larvae were found to be a source of bioactive chemicals with therapeutic potential (Chu et al., 2014; Müller et al., 2017b). These bioactive compounds enabled the insects to survive in very harsh environments, such as manures and compost, inhabited by a variety of harmful microorganisms including bacteria, viruses, and protozoa. A few examples of those bioactive compounds include antimicrobial peptides, lipid, and chitosan/chitin. This study explored the bioactive compounds present in the BSF larvae with lipid being the main compound of interest. Lipid is a complex set of substances, containing saturated and unsaturated fatty acids as well as glyceride compounds. Lauric acid was found to be the major constituent of the fatty acid. The glyceride compounds present in lipid are monoglycerides, diglycerides, and triglycerides. These bioactive compounds could be a candidate for new drugs that will contribute to solving the challenges associated with multidrug-resistant bacteria. The antimicrobial properties of fatty acids and glyceride compounds have been reviewed. The

review showed that fatty acids and monoglycerides have a strong antimicrobial property that is useful to the health and well-being of humans. Antimicrobial lipids exhibit several promising properties such as low cost, and a broad spectrum of activity that makes them appealing options for antibacterial applications. Giacometti et al. (2002), Bui et al. (2016), and Danish & Nizami (2019) reported on the fractionation of lipid from different sources. To date, there are limited or no studies available that have reported on the effective method(s) of fractionation and isolation of those bioactive compounds from the BSF larvae. Several researchers studied the extraction of lipid from different sources. Rodríguez-Miranda et al. (2014), Ali et al. (2015), Efthymiopoulos et al. (2018), Ali et al. (2015) , and Tesfaye & Tefera. (2017), used the Soxhlet method on seed lipid, but none of them did a study to compare the yields of the extraction methods under the same condition. The studies by these researchers serve as a foundation for this present study.

Although the reviewed literature demonstrated the effectiveness of antimicrobial lipid and that their nanoparticle form could enhance their efficiency, none reported on the BSF larvae antimicrobial efficacy either in their normal state or nanoparticle form. The nanoparticles are intended to ensure biocompatibility, storage stability, and to prevent the degradation of incorporated drugs (Iqbal et al., 2015; Severino et al., 2017; Wang & Luo, 2018). Solid lipid nanoparticles were one of the nanoparticle formulations found in the literature reviewed. During the synthesis of the solid lipid nanoparticles, these authors only focused on lipid nanoparticles as a protective substance for drug encapsulation. None of them studied the antimicrobial properties of lipid itself. This study focused solely on the antimicrobial properties of BSF larvae lipids, with no drugs included.

This review has also highlighted the various methods (high-pressure homogenization, ultrasonication/high-speed homogenization, solvent evaporation, solvent emulsification–diffusion, supercritical fluid, microemulsion, spray drying, or double emulsion) used for the synthesising of solid lipid nanoparticles. These techniques depend on the type of lipid and drug to be used. Some of these methods (microemulsion, double emulsion) have limitations such as intensive labour, the use of risky chemical substances, time-consuming, and requiring high maintenance. The electrospraying method seems the best route for the synthesis of the lipid nanoparticle over other methods. To the best of our knowledge, no previous studies have reported on the formulation of lipid nanoparticles from BSF larvae using the electrospraying technique. This was addressed in this study to determine whether lipids isolated from BSF larvae lipid could form nanoparticles using the electrospraying technique.

CHAPTER 3: RESEARCH CONCEPTS AND PROCEDURES

3.1 Introduction

This chapter explains the experimental approaches used to achieve the study's aims and goals. It contains a list of the chemicals and materials used in this research. The various methods for preparing samples are described. It describes the extraction of black soldier fly (BSF) larvae lipids using three methods (conventional Soxhlet, maceration, and ultrasonic-assisted). It explains the process of fractionating and isolating lipids into various lipid groups. It also explains the electrospray technique used to make nanoparticles from the BSF larvae lipids. The various characterisation approaches and analytical techniques used are also described in this chapter. Gas chromatography flame ionisation detection (GC-FID), Fourier-transform infrared spectroscopy (FTIR), scanning electron microscopy (SEM), and nuclear magnetic resonance (NMR) are among the methods used for characterisation of the BSF larvae lipids. Finally, this research looked into the antimicrobial function of lipids isolated from BSF larvae and their nanoparticle formulations. All of the experimental processes used in this study were summarised in Figure 1.1, which is defined in Chapter 1.

3.2 Materials and chemicals

Agriprotein, a company based in Cape Town, South Africa, provided the black soldier fly (BSF) larvae used in this research. Analytical grade reagents were purchased from Sigma-Aldrich and Kimix Chemicals (South Africa). Those chemicals were crucial for the extraction of the lipid from BSF larvae as well as the synthesis of the lipid nanoparticles. The following section provides a list of chemicals and equipment.

3.2.1 List of chemicals

The list of chemicals, their sources, and percentage purity used in this study are presented in Table 3.1.

Table 3.1: List of chemicals

Reagents	Source	Specification/ /purity (%)
Petroleum ether	Sigma Aldrich	99.9
Dichloromethane	Sigma Aldrich	99.9
Hexane	Sigma Aldrich	99.9
Methanol	Sigma Aldrich	99.9
Acetone	Sigma Aldrich	99.9
Pyridine	Sigma Aldrich	99.9
Acetic acid	Kimix Chemicals	99.9
Ethanol	Sigma Aldrich	99.9
Diethyl ether	Sigma Aldrich	99.9
Agar	Sigma-Aldrich	-
Yeast Extract	Sigma-Aldrich	-
Tryptone	Sigma-Aldrich	-
Vanillin	Kimix Chemicals	99
Silica gel 60	Sigma-Aldrich	-
Standard glycerides	Sigma Aldrich	-
Antibiotic: ampicillin	Sigma Aldrich	-
Bacterial strains :	Sigma Aldrich	-
Pseudomonas aeruginosa		
Micrococcus luteus		
Commercial chitosan	Sigma Aldrich	50 – 190 KDa and 75 – 85% degree of deacetylation
Standards:	Sigma Aldrich	
Lauric acid, palmitic acid, oleic acid,		
caprylic acid, capric acid, arachidic acid,		
myristic acid, palmitoleic acid, stearic		
acid, linolenic acid, linoleic acid,		
trilaurin, tristearin, tripalmitin		
triolein, trilinolenin, trilinolein,		
dipalmitin, 1,3 distearin, dilaurin,		
monolaurin, monopalmitin,		
monomyristin		

3.2.2 List of equipment

The equipment used in this report, as well as their different applications, are summarised in Table 3.2.

Table 3.2: List of equipment and its applications

Equipment	Applications
Bacterial inoculating loops	To pick up bacterial samples from colonies growing on media plates or from liquid media.
Micropipette	To transfer a small amount of sample on the antibiotic disc.
Antibiotic discs	For antimicrobial test. Antibiotic discs were impregnated with antibiotics and the sample.
Petri dish	To culture microorganisms.
Bunsen burner	To sterilise equipment for the antimicrobial test and to create an updraft that pushes airborne pollutants away from the workplace.
UV-visible spectrometer ((JENWAY 6305)	To measure the concentration of the bacteria culture.
Column chromatography	To fractionate the BSF larvae lipids into lipid classes.
Soxhlet extraction apparatus	To extract lipids from the BSF larvae.
Ultrasonic-assisted extraction	To extract lipids from the BSF larvae.
Buchi rotavapor (RE 111)	For gentle removal of solvents from samples by evaporation.
Fourier transform infrared spectroscopy (Thermo Scientific, Nicolet iS10)	To determine the functional groups of the lipid isolated from the BSF larvae class and the formulated lipids nanoparticles.
Gas chromatography- FID (Agilent technologie 7820A and 7890 B	To determine the lipids and fatty acids composition of the BSF larvae lipids.
Nuclear magnetic resonance (Bruker Avance III HD 400 MHz)	To characterise the lipid fractions isolate from BSF larvae.
Telstar laboratory freeze dryer (Telstar LyoQuest-55)	To dry the BSF larvae sample.
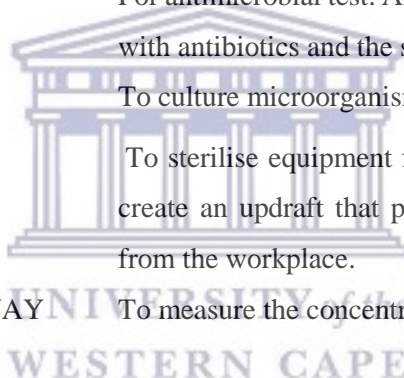
Waring laboratory blender (Thomas Scientific)	To grind the sample into a powder form.
High voltage direct current potential	To supply high voltage during the electrospraying process.
TLC plate	To monitor the efficacy of separation of the lipid fraction.

3.3   Experimental methods of the study

The experimental method for this analysis includes four major procedures: sample preparation, BSF larvae lipids extraction methods, fractionation of the BSF larvae lipid into lipid groups, synthesis of lipid nanoparticles using an electrospraying technique, and finally antimicrobial activity of the lipid classes and nanoparticle formulations.

3.3.1   Black soldier fly larvae sample preparation

Approximately 5 kg of the black soldier fly (BSF) larvae supplied by Agriprotein (South Africa) were divided into portions of 500 g then washed with distilled water. Each portion was transferred to plastic bags and frozen at -20 °C for 6 h. Then the BSF larvae sample was dried using Telstar laboratory freeze dryer (Telstar LyoQuest-55) at 25 °C and 0.20 bar for 5 days. Freeze-dried samples shown in Figure 3.1a were pulverised into powder to a size of 1 mm (Figure 3.1b) using a waring laboratory blender (Thomas Scientific) and stored at -20 °C until analysis.

(a)   (b)

Figure 3.1: Freeze-dried black soldier fly larvae (a), Ground black soldier fly larvae (b)

3.3.2 Extraction of lipids from black soldier fly larvae

Black soldier fly (BSF) larvae lipid has great potential that can be exploited in various industries due to its high lipid content and fatty acid profile. Therefore the extraction of its lipid requires finding cost effective, and high recovery extraction techniques. In this study, three extraction methods such as Soxhlet extraction (SE), ultrasonic-assisted extraction (UAE), and maceration extraction (ME), and their effects on the lipid yield and fatty acid composition of the BSF larvae lipid have been investigated. The procedure involved in the lipid extraction using these methods are presented in the follow up sections

3.3.2.1 Extraction of lipids from black soldier fly larvae using Soxhlet extraction

This method employs the solvent reflux and siphon principles to constantly extract the wanted constituents from a sample mixture. The BSF larvae sample was put in a filter paper then placed in the extraction chamber. When the solvent is heated to boiling temperature, the vapour rises through the air tube and condenses into a liquid that falls into the extractor. When the solvent level surpasses the siphon's highest point, the solution is returned to the flask. This allows a portion of the compound to dissolve in the solvent. Soxhlet extraction set up shown in Figure 3.2 consists of a heating mantle, boiling flask, extraction solvent, thimble, extraction chamber, and a condenser.
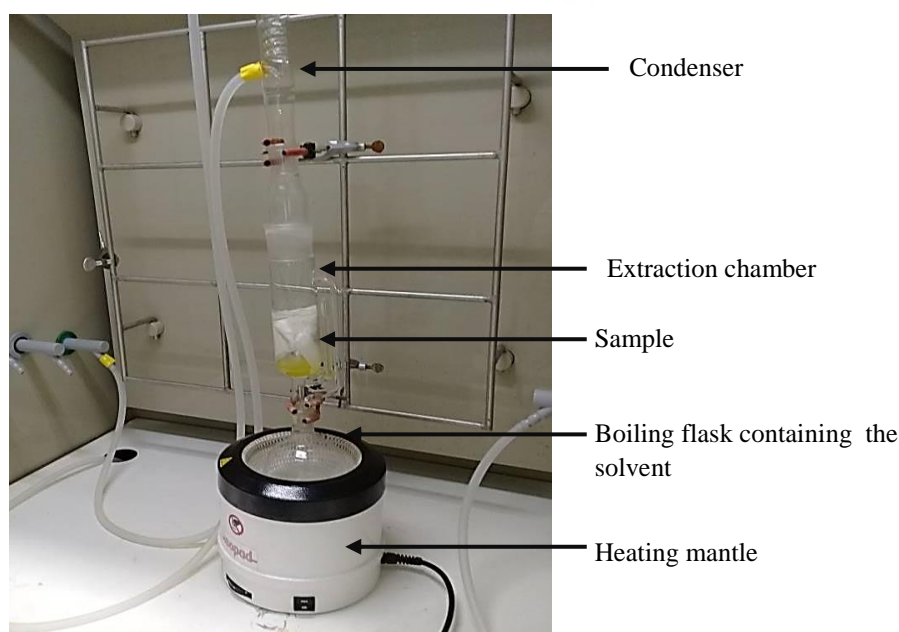
Figure 3.2: Soxhlet extraction apparatus set up

On the extraction of BSF larvae lipids, three important operating parameters (time, the ratio of the sample to solvent, and the solvent used) were considered and their effects on the extraction yield were studied using Soxhlet extraction. The investigation process is detailed in the sections below.

3.3.2.1.1 Effect of extraction time

The effect of the extraction time using Soxhlet extraction was investigated. The study involved three extraction times: 2, 4, and 6 h. The fixed parameters were the mass of the sample (8 g), the volume of the solvent (300 mL), and the temperature for (70 °C). The operating conditions are summarised in Table 3.3.

Table 3.3: Effect of extraction time on the lipids yield using Soxhlet extraction

Varied	Fixed		
Extraction time (h)	Mass of sample (g)	Volume of solvent (mL)	Temperature (°C)
2	8	300	70
4	8	300	70
6	8	300	70

3.3.2.1.2 The effect of the ratio of sample to solvent

The effect of the ratio of sample to solvent on the lipid yield using Soxhlet extraction was carried out at three extraction weights: 5, 8, and 11 g with 300 mL of solvent to give a solid to solvent-ratios of 0.02 0.03 and 0.04 g/mL. The fixed parameters were the extraction time (4 h), the volume of the solvent (300 mL), and the temperature (70°C). The operating conditions are presented in Table 3.4.

Table 3.4: Effect of solid to solvent ratio on the lipid yield using Soxhlet extraction

Varied	Fixed		
Solid to solvent ratio (g/mL)	Extraction time (h)	Volume of solvent (mL)	Temperature (°C)
0.02	4	300	70
0.03	4	300	70
0.04	4	300	70

3.3.2.1.3 The effect of different solvents polarity

The effect of different solvents' polarity on the lipid yield and fatty acid composition using Soxhlet extraction was investigated. The different solvents used were non-polar solvents such as hexane (Hex), petroleum ether (PE) dichloromethane (DCM), and polar solvents such as methanol (Met), and) and ethyl acetate (EA). The fixed parameters were: The mass of the sample (8 g), the volume of the solvent (300 ml), the extraction time (4 h), and the temperature (70 °C). The operating conditions are shown in Table 3.5

Table 3.5: Effect of solvent polarity on the lipid yield using Soxhlet extraction

Varied	Fixed			
Solvent type	Extraction time (h)	Volume of solvent (mL)	Temperature (°C)	Mass of the sample (g)
EA	4	300	70	8
Hex	4	300	70	8
Met	4	300	70	8
PE	4	300	70	8
DCM	4	300	70	8

The physical and chemical properties of the different solvents are presented in Table 3.6. Solvents with dielectric constants greater than about 5 are considered polar while those with dielectric constants less than 5 are considered non-polar (Monder et al., 2020).

Table 3.6: Extraction solvents characteristics

Parameters	EA	Hex	Met	PE	DCM
Refractive Index at 25 °C	1.3720	1.3750	1.3314	1.370	1.4240
Boiling point	77.1	68.7	64.7	60-90	39.8
Density (g/mL) at 25 °C	0.90	0.659	0.8	0.77	1.326
Dielectric constant	6.08	1.88	32.6	1.9	8.93
Polarity	polar	non polar	polar	non polar	polar

(https://www.shodexhplc.com/applications/physical-chemistry-properties-of-solvents/)

3.3.2.1.4 Solvent evaporation

At the end of the extraction, the compound of interest is mixed with the solvent. Hence the solvent needs to be removed to leave behind the compound (BSF larvae lipids). In this experiment, the solvent was removed using a Buchi Rotavapor (RE 111) under reduced pressure at 350 mbar in a water bath at 40 ^{0}C for about 10 min. The main components of the rotary evaporator are: The condenser, receiving flask, water bath, evaporating flask, and temperature control panel. The percentage of the lipid obtained after evaporation of the solvent was calculated as shown in (Equation 3.1).

$$\% \text{ Lipid} = \frac{\text{Lipid}}{\text{Sample}} \times 100 \qquad \textbf{Equation 3.1}$$

The extractions were carried out in triplicate and the percentage lipid yield was calculated gravimetrically according to the Equation 3.1. BSF larvae lipid was kept at -20 °C and in the dark until analysis. Figure 3.3 shows the evaporation process.

| Lipids+ solvent | Evaporation | Final product (lipid extract) |
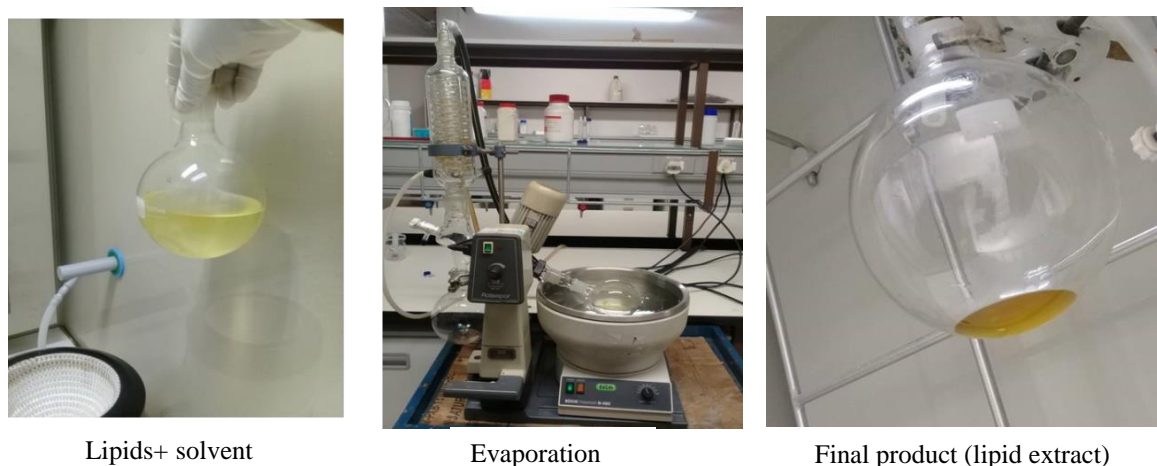
Figure 3.3: Solvent evaporation by rotary evaporator

3.3.2.2   Maceration extraction

Maceration extraction was performed by putting 8 g of the dry powdered BSF larvae sample into a filter bag which was soaked in 300 mL petroleum ether at room temperature for 48 h (Figure 3.4). The lipid extract was then obtained by evaporating petroleum ether with a rotary evaporator at 40 ^{0}C for 10 min until no solvent remained. The extractions were carried out in triplicate and the percentage yield was calculated gravimetrically.

24 h   48 h

Figure 3.4: Maceration method at 24 h and 48 h

3.3.2.3   Ultrasonic-assisted extraction (UAE)

Ultrasonic-assisted extraction (UAE) shown in Figure 3.5 was carried out by placing 8 g BSF larvae powder in a 500 mL glass beaker and mixed with 300 mL petroleum ether. The ultrasound probe was lowered into the mixture about 2/3 depth below the mixture surface for

ultrasound pre-treatment. At the end of the extraction, the extract was pumped out and filtered using filter paper (Whatman no. 1). The fixed parameters for that experiment were: A frequency at 40 kHz and an extraction time of 60 min. The organic solvent was removed at 40 ^{0}C under reduced pressure for about 10 min using a rotary evaporator at 350 mbar until no solvent remained. The lipid yield percentage was calculated.
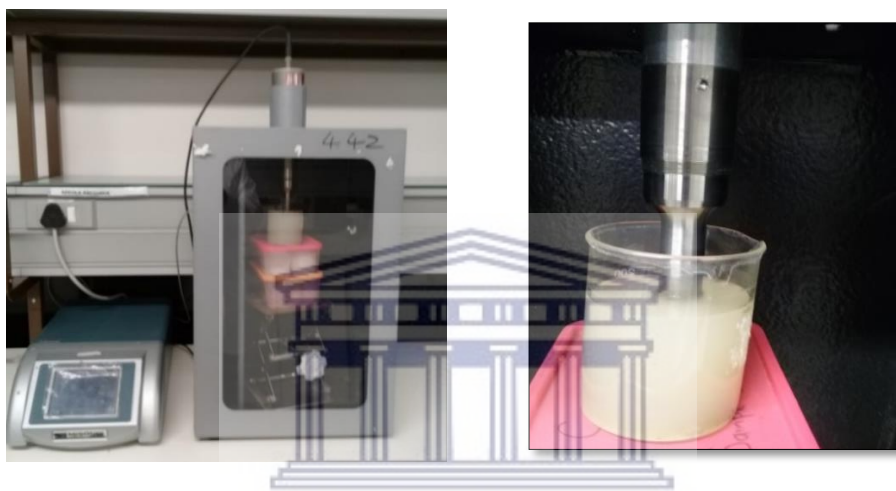
Figure 3.5: Ultrasonic-assisted extraction method

3.3.3 Fractionation of lipid classes with glass column chromatography and thin-layer chromatography (TLC)

BSF larvae lipid was fractionated into lipid classes using glass column chromatography. TLC was carried out to determine the number of components present in the BSF larvae lipid sample. This was done to monitor the efficacy of the separation of the lipid fractions.

3.3.3.1 Column chromatography set up

The chromatography column (6 cm i.d. x 70 cm length), fitted with a stopcock on one side was prepared using a dry packing method. The column was packed by adding a small amount of cotton wool at the bottom of the cylindrical glass column to prevent the loss of the stationary phase. The column was then filled with silica gel 60 (activated overnight at 110 °C for 12 h) to give a column height of 40 cm, before adding the dried lipid sample (50 g) obtained by mixing the lipid with silica gel which was then dried at room temperature for 24 h. The column

containing the silica gel was conditioned by flowing through a mobile phase which flows through the column. The sample (lipid + silica) was added to the column, followed by another 10 g of silica gel. After the sample has been loaded, the column is eluted with a series of solvent mixtures of increasing polarity. The eluted fractions are collected in a 25 mL conical flask. The column chromatography setup is shown in Figure 3.6.
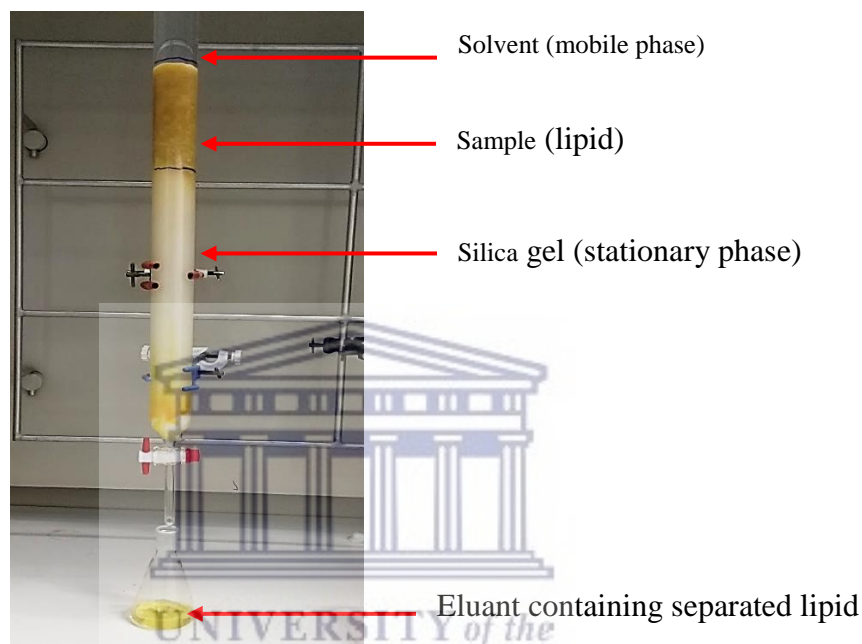
Figure 3.6: Column chromatography set up

The BSF larvae lipid contains a mixture of compound classes which are: cholesterol esters, triglycerides fatty acids, cholesterols, diglycerides, and monoglycerides (Ushakova et al., 2016). The fractionation of the lipid classes was achieved by serial elution with 250 mL of 100 % hexane, 400 mL of 5% diethyl ether in hexane, 400 mL of 15% diethyl ether in hexane, 350 mL of 25% diethyl ether in hexane, 400 mL of 50% diethyl ether in hexane, and 300 mL of 2% methanol in diethyl. An equal volume (15 mL) of the eluates was collected sequentially into a 25 mL conical flask and carefully labelled for TLC analysis. Diethy eher is miscible with hexane in all proportion because it has a low dielectric constant and a dipolar moment of 1.3 therefore considered as non-polar solvent. The elution scheme for the fractionation of the lipid into the lipid classes is shown in Table 3.7.

Table 3.7: Elution scheme for the fractionation of the lipid

Eluting solvent	Volume (mL)	Lipids Eluted
100% Hexane	250	Cholesterol esters
5% diethyl ether in hexane	400	Triglycerides
15% diethyl ether in hexane	400	Fatty acids
25% diethyl ether in hexane	350	Cholesterols
50% diethyl ether in hexane	400	Diglycerides
2% methanol in diethyl ether	300	Monoglycerides

After fractionation, the solvent was removed using a Buchi Rotavapor (RE 111) under reduced pressure at 350 mbar in a water bath at 40 ^{0}C for about 10 min. The mass percentage of the lipid fractions obtained after evaporation of the solvent was calculated as shown in (Equation 3.2).

$$\text{mass percent} = \frac{\text{mass lipid fraction (g)}}{\text{mass of the lipid (g)}} \times 100 \,\% \qquad \textbf{Equation 3.2}$$

3.3.3.2   Thin-layer chromatography (TLC)

The purity of the fractions was checked by TLC in a single dimension with pre-coated silica gel 60 F254 plates with a 0.2 mm layer thickness as adsorbent. The TLC plate was pre-developed with chloroform/methanol 1:1 (v/v) in a clean tank and air-dried in a fume hood to remove impurities from the TLC. The lipid was first dissolved in hexane. Then the diluted sample was separated by TLC in a single dimension. The TLC plate was developed in a developing chamber (Figure 3.7) containing a solvent system of hexane, diethyl ether, and acetic acid in the ratio 85:25:2 (v/v/v).
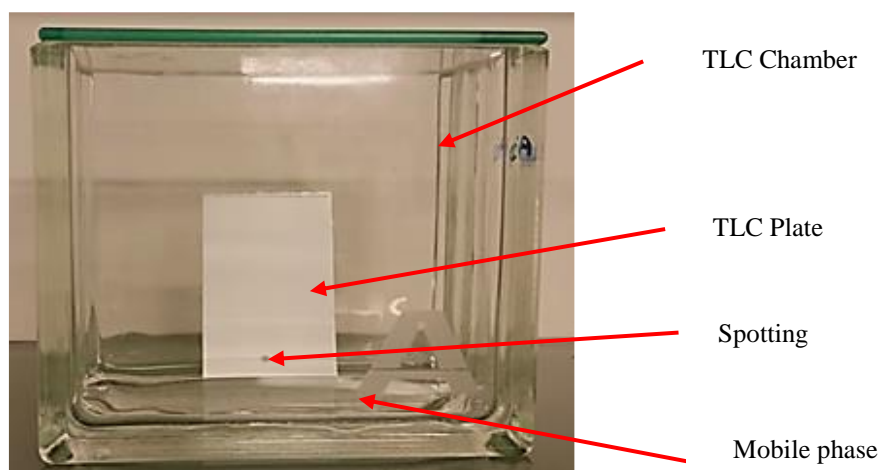
Figure 3.7: Thin layer chromatography

Visualisation of the TLC spots was carried out under UV light at 254 nm and/or 366 nm, and further detection of compounds was achieved by spraying with vanillin spray reagent (prepared by dissolving 15 g of vanillin in 250 mL ethanol followed by the addition of 2.5 mL concentrated sulphuric acid). After spraying, the TLC plates were heated on a hot plate until spots became visible. The purity was assured by comparing the isolated fraction with standard materials. The next section describes the preparation of nanoparticles from the fractionated lipids.

3.3.4 Experimental electrospray set-up

This experiment investigates the feasibility of producing lipid nanoparticles in powder form using the electrospray technique. The electrospray setup involves the use of high voltage which is applied between needles and the collector plate. The two steel needles (0.8 mm inner diameter) were fitted to two 10 mL syringes. The syringes were filled with the sample solution (see section 3.3.4.1) and connected to an infusion pump (Harvard Apparatus 33 Twin Syringe Pump). The sample solution was pumped through a syringe at a constant rate forming a droplet at the end of the needle. The jet formed was ejected toward a collector (aluminium foil). The experimental electrospray set up is shown in Figure 3.8.

High voltage (power supply)　　Syringe pump　　Syringe (containing the sample)　　Electrode　　Collector
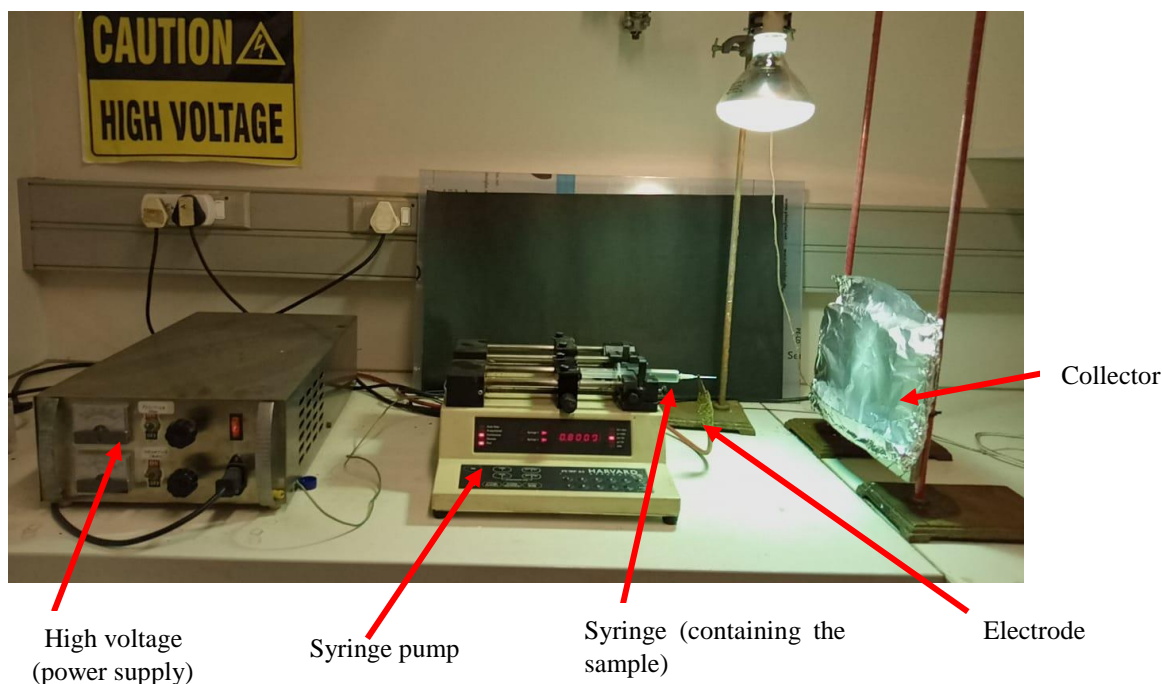
Figure 3.8: Electrospraying setup

Due to the oily nature of the lipids, it was impossible to obtain the lipid nanoparticle powder form, hence the lipids were mixed with chitosan. Chitosan was chosen over other biopolymers because it could form thermally stable nanoparticles that enhance the new product's properties. Chitosan combined with lipids to create the new hybrid (chitosan-lipid nanoparticle) is expected to surpass the effectiveness of the lipids or chitosan alone. The preparation of the sample solutions for the electrospray is described in section 3.3.4.1. The sample solutions comprised of chitosan solution as well as chitosan mixed with lipid.

3.3.4.1　Preparation of the chitosan solution for electrospray

The effect of the concentration of the commercial chitosan solution without lipid-containing and the stirring time was investigated in this study. The electrospray instrument's settings such as the applied voltage, flow rate, and tip-to-collector distance were maintained constant throughout the experiment. The next section details the optimisation of chitosan concentration.

3.3.4.2　Effect of chitosan concentration on the formation of nanoparticle

This experiment was performed to investigate the effect of the chitosan concentration on the electrospraying process to form solid nanoparticles. The concentration of the commercial chitosan was varied while all other parameters such as flow rate (0.5 mL/h), applied voltage

(25 kV), and tip to collector distance (10 cm) were fixed. The optimisation conditions are shown in Table 3.8.

Table 3.8: Electrospraying conditions at different chitosan solution concentrations

Sample code	Fixed			Varied	
	Collector distance (cm)	Voltage (KV)	Flow rate (mL/h)	Concentration of chitosan (wt %)	Weight of the chitosan (g)
CH 1-C	10	25	0.5	0.5	0.05
CH 2-C	10	25	0.5	1	0.11
CH 3-C	10	25	0.5	2	0.22
CH 4-C	10	25	0.5	3	0.32
CH 5-C	10	25	0.5	4	0.43

Commercial chitosan was prepared at different weight percentages of 0.5, 1, 2, 3 and 4 wt % by dissolving approximatively 0.05, 0.11, 0.22, 0.32 and 0.43 g of the chitosan in 10 mL of 90 % acetic acid, respectively. The chitosan solutions were stirred at room temperature for 24 h at a constant speed of 700 rpm with a magnetic stirrer until the chitosan powder was completely dissolved. The chitosan solution was loaded into a 10 mL plastic syringe, fitted with a 21-gauge BD conventional needle. The syringe was inserted on the programmable syringe pump and the electrospraying was carried out at room temperature at a flow rate (0.5 mL/h), applied voltage (25 KV), and tip to collector distance (10 cm). The deposited chitosan nanoparticles were air dried for 24 h to remove any trace of acetic acid and water possibly remaining after the electrospraying. The chitosan nanoparticles were characterised with scanning electron microscope (SEM).

3.3.4.3 Stirring time effects on the formation of the chitosan nanoparticles

This experiment was performed to study the effect of stirring time on the formation of chitosan nanoparticles. The stirring time was varied while all other parameters such as the voltage (25 KV), the flow rate (0.5 mL/h), tip to collector distance (10 cm) were fixed. The optimised

concentration of the chitosan solution was described in section 3.3.3.4.1. The experimental parameters used in this experiment are listed in Table 3.9.

Table 3.9: Electrospraying conditions for the chitosan solution prepared at different stirring times

| Sample code | Fixed | | | | | Varied |
| | Voltage | Collector distance | Concentration of chitosan (wt %) | Weight of the chitosan | Flow rate | Stirring time |
	(kV)	(cm)		(g)	(mL/h)	(h)
CH 1-T	25	10	1	0.1	0.5	12
CH 2-T	25	10	1	0.1	0.5	24
CH 3-T	25	10	1	0.1	0.5	48

Three samples composed of 1 wt % of the chitosan solution were prepared by dissolving 0.1 g of the commercial chitosan in 10 mL of 90 % acetic acid. The samples were stirred independently at a constant stirring speed of 700 rpm for 12, 24, and 48 h, respectively at room temperature. The chitosan solution was loaded into a 10 mL plastic syringe and the electrospraying was carried out at room temperature at a flow rate (0.5 mL/h), applied voltage (25 kV), and tip to collector distance (10 cm) conditions. After electrospraying, the deposited chitosan nanoparticles were air dried for 24 h to remove any traces of acetic acid and water. A scanning electron microscope (SEM) was used to examine the chitosan nanoparticles.

3.3.4.4 Preparation of chitosan-lipid hybrid nanoparticles

This experiment was performed to investigate the effect of chitosan-lipid concentration to obtain the best formulation of the chitosan-lipid hybrid nanoparticles. The concentration of the chitosan-lipid was varied (0.02-0.04 g/mL) while all other parameters such as concentration of the chitosan solution (1wt %), flow rate (0.5 mL/h), applied voltage (25 KV), and tip to collector distance (10 cm) were fixed. The concentration of the chitosan solution (1wt %) and

stirring time (48 h) were previously optimised in sections 3.3.3.4.1 and 3.3.3.4.2. The operating electrospraying conditions are summarised in Table 3.10.

Table 3.10: Electrospraying conditions at different chitosan- lipid concentrations

Sample code	Fixed				Varied
	Collector distance (cm)	Voltage (KV)	Flow rate (mL/h)	Concentration of chitosan (wt %)	Chitosan–lipid concentrations (g/mL)
CH-LIP 1	10	25	0.5	1	0.02
CH-LIP 2	10	25	0.5	1	0.03
CH-LIP 3	10	25	0.5	1	0.04

The chitosan-lipid solutions were prepared at three different concentrations of 0.02, 0.03, and 0.04 g/mL by dissolving 0.2, 0.3, and 0.4 g of the lipid fractions (Triglycerides, diglycerides, monoglycerides, and fatty acids) in liquid form in 1 wt % of the chitosan solution prepared by dissolving 0.1 g of the commercial chitosan in 10 mL of 90 % acetic acid. The lipid was added into 10 mL chitosan solution previously stirred for 48 h at a constant stirring speed of 700 rpm. The chitosan-lipid mixture was then stirred for 24 h using a magnetic stirrer at 500 rpm to form a homogeneous solution. The viscous solution was loaded into a 10 mL plastic syringe and then electrosprayed at room temperature at a flow rate (0.5 mL/h), applied voltage (25 KV), and tip to collector distance (10 cm) conditions. The deposited chitosan- lipid nanoparticles were air dried for 24 h to remove any trace of acetic acid and water possibly remaining after the electrospraying. The nanoparticles were characterised with scanning electron microscope (SEM) and Fourier transform infrared spectroscopy (FTIR). The next section presents the different characterisation methods used in this study.

3.3.5 Characterisation techniques

This section discusses the characterisation techniques used in this study. The analysis of the samples was achieved using four different instruments. Gas chromatography was used to determine the glyceride and fatty acid profile of the BSF larvae lipid. Fourier transform infrared spectroscopy (FTIR) and nuclear magnetic resonance (NMR) were used to identify the

functional group of the lipid classes by recording the type of vibrations produced by their chemical bonds. Scanning electron microscopy (SEM) was used to determine the morphology of the nanoparticle formulated.

3.3.5.1   Chromatographic methods

In this study gas chromatograph Agilent technology 7820 A and Agilent 7890 B were used for the characterisation of the BSF larvae lipid. Agilent 7820 A was specifically used for triglyceride, diglyceride, and monoglyceride composition, while the gas chromatography Agilent 7890 B was used for fatty acids composition. The type of column used in each type of gas chromatography is the key difference between the two. The Agilent 7820 A uses a cyanopropyl-phenyl chemically bonded polyethylene glycol (CP – TAP CB) column that is suitable for high-temperature applications (up to 380 °C), while the Agilent 7890 B uses a high polarity column that contains 88 % Cyanopropy-aryl-polysiloxane (CP-Sil 88) phase and has a temperature limit of 250/260 °C. The next section details the method used for the fatty acid profile of the BSF larvae lipid using gas chromatograph Agilent 7890 B.

3.3.5.1.1   Gas chromatography for fatty acids

- **Sample preparation of the fatty acids**

The fatty acid composition of the black soldier fly larvae lipid extract and lipid fractions (Triglycerides, diglycerides, monoglycerides) were analysed using gas chromatography after derivatization to fatty acid methyl esters with a methanolic solution of sodium hydroxide according to (Cullere et al. (2018) with slight modification. Briefly, a 100 mg BSF larvae lipid was weighed into a 10 mL micro reaction vessel containing a magnetic stirrer. Then 1 mL of hexane and 2 mL of 4 M methanolic potassium hydroxide were added. The mixture was placed on a water bath then heated for 15 min at 50 °C with constant stirring. After that, the mixture was cooled to room temperature for 10 min. The mixture was transferred into a 20 mL centrifuged tube and centrifuge for about 2 min. After phase separation, 1 mL of the organic layer containing the fatty acid methyl esters was transferred into the 1.5 mL GC vial for gas chromatography analysis.

- **Instrument set up**

The determination of the fatty acids composition was performed on an Agilent 7890 B. Gas Chromatograph which was equipped with a flame ionization detector (FID) and the capillary

column was an HP-88 (60 m X 250 µm i.d. X 0.2 µm). The injector and detector temperatures were maintained at 250 and 280 °C respectively. The oven was programmed for 1 min at 120 °C to 175 °C at 6 °C/min, maintained for 2 min at 220 °C, increased further to 230 °C at 5 °C/min and finally maintained for 5 min at 230 °C. The carrier gas, helium was used at a flow rate of 1.8 mL/min. The injection volume was 1 µL, with a split ratio of 1:50. The experimental conditions are summarised in Table 3.11.

Table 3.11: GC operating configuration for fatty acids

Chromatographic system	
GC system	Agilent 7890 B
Inlet	Split/Splitless
Detector	FID
Column	CP-Sil 88 for FAME/HP-88 (60 m X 250 µm ID, 0.2 µm)
Phase	CP-Sil 88 for FAME/HP-88
Experimental Conditions	
Inlet temperature	250 °C
Injection	1µl of 0.05 % lipid in hexane
Split ratio	1/50
Carrier gas	Helium
Head pressure	1.8 mL/min constant flow
Oven temperature	120 °C, 1min, 6 °C/min to 175 °C, 10min, 3 °C/min to 220 °C, 5min; Post-run 230 °C, 1min.
Detector temperature	280 °C
Detector gases	Air: 400 mL/min
	Hydrogen: 30 mL/min
	Makeup gas (N_2): 25 mL/min

- **Quantitative analysis of the Fatty acids**

The percentages of the fatty acids were calculated using the following steps:

Step 1: Calculation of the response factor (RF) of the fatty acid standards $$RF\ (std) = \frac{Peak\ area(std)}{Concentration\ (std)}$$	**Equation 3.3**
Step 2: Calculation of the unknown concentration (C1 unk) of the fatty acids $$C1\ unk = \frac{Peak\ area(unk)}{Response\ factor\ (std)}$$	**Equation 3.4**
Step 3: Conversion of the percent concentration to mg/mL $$(C2\ unk = C1x\ X\ 10)$$	**Equation 3.5**
Step 4: Concentration in mg/10 mL $$(C3\ unk = C2\ unk\ X\ 10)$$	**Equation 3.6**
Step 5: Calculation of the mass (mg) of the fatty acids in 10 mL $$Mass\ (FA) = \frac{Molar\ mass\ of\ the\ acid\ X\ C3\ unk}{Molar\ mass\ of\ the\ ester}$$	**Equation 3.7**
Step 6: Calculation of the mass percent of fatty acids (% mass FA) $$\%\ FA\ (m/m) = \frac{Mass\ of\ FA\ in\ 10\ mL}{Mass\ of\ the\ sample}$$	**Equation 3.8**
Step 7: Calculation of the percentage of the fatty acid (% FA) $$\%\ FA = \frac{Mass\ percent\ FA\ X\ 100}{Total\ mass\ percent\ FA}$$	**Equation 3.9**

3.3.5.1.2 Gas chromatography for glycerides

- **Sample preparation**

This experiment was performed to investigate the glyceride content of the BSF larvae lipid. This was performed on an Agilent 7820A equipped with an FID. Approximately 1 mg of the

various lipid fractions (tri, di, and monoglycerides) was dissolved in 2 mL of hexane, and 1 mL of this mixture was transferred into the GC vial.

- **Instrument set up**

The triglycerides, diglycerides, and monoglycerides were separated on a medium-polarity open-tubular (WCOT) fused silica capillary column (25 m × 0.25 mm i.d.) coated with a 0.1 µm layer of methyl-65 % phenyl-silicone TG CB-type phase (TAP). The carrier gas was helium set at 4 mL/min and the injector and detector temperatures were set at 250 °C and 380 °C, respectively. The oven temperature was programmed from 70 °C to 280 °C at 40 °C/min, raised to 280 °C at 10 °C/min, and then programmed at 30 °C/min up to 380 °C. The final temperature was held for 4.67 min. The instrumental and experimental conditions are summarised in Table 3.12.

Table 3.12: GC operating configuration for glycerides

Chromatographic systems	
Gas chromatography	Agilent 7820A
Technique	GC-capillary
Detector	FID
Column	Agilent CP-TAP CB, 0.25 mm x 25 m WCOT fused silica coated with TAP (0.10 μm)
Injector	Cool-on-column inlet with electronic pneumatics control (EPC); oven track
Experimental conditions	
Carrier gas	Helium; 4mL/min (constant flow)
Flow mode	Constant flow
Detector temperature	380 °C
Injection	0.5 μL of 0.05 % lipid in hexane
Oven program	Initial temperature 70 °C, programmed at 40 °C/min up to 280 °C, programmed at 30 °C/min up to 380 °C, final temperature hold for 4.67 min.
Total run time	16 min.
Auxiliary gas	Hydrogen flow: 30.0 mL/min Air flow: 400.0 mL/min

Makeup flow: 5 mL/min (Nitrogen)

- **Quantification of triglycerides, diglycerides, and monoglycerides sub compounds**

The mass percentage (%) of triglycerides (TGA), diglycerides (DG), and monoglycerides (MG) sub-components were calculated using Equation 3.10, 3.11, and 3.12, respectively, whereby PA TGA, PA DG, and PA MG refers to the peak area of the TGA, DG, and MG, respectively, PA std1, PA std2, and PA std3 refer to the peak area of the internal standard for the TGA, DG, and MG, respectively. M std1, M std2, and M std3 refer to the mass of the internal standard in mg, m refers to the mass in mg of the sample inserted.

Mass percent (%) of triglyceride (TGA) sub components $$\% \text{ TGA (m/m)} = \frac{PA\ TGA}{PA\ std1} \text{ X } \frac{M\ std\ 1}{m}$$	**Equation 3.10**
Mass percent (%) of diglycerides (DG) sub components $$\% \text{ DG (m/m)} = \frac{PA\ DG}{PA\ std\ 2} \text{ X } \frac{M\ std\ 2}{m}$$	**Equation 3.11**
Mass percent (%) of monoglycerides (MG) sub components $$\% \text{ MG (m/m)} = \frac{PA\ MG}{PA\ std\ 3} \text{ X } \frac{100}{m}$$	**Equation 3.12**

3.3.5.2   Fourier transform infrared spectroscopy (FTIR)

Fourier transform infrared spectroscopy is a technique that produces an infrared absorption spectrum to identify chemical bonds in a molecule. In this study, FTIR was used to identify the functional groups of the lipid fraction obtained in section 3.3.3.1 and the chitosan-lipid nanoparticles synthesised in section 3.3.3.5. Approximately 10 mg of the lipid and nanoparticles sample in solid form was carefully placed on the diamond ATR crystal. Then ATR anvil holder was pressed down to ensure full contact of the solid sample with the crystal. The FTIR was programmed to scan 64 times at a resolution of 2.0 cm^{-1} around the wavelength

range of 4000 cm^{-1} to 500 cm^{-1} against the transmittance. Following each scan, the baseline was corrected using the background spectrum obtained from the blank scan.

3.3.5.3 Nuclear magnetic resonance (NMR)

The structures of the lipid fractions were determined using nuclear magnetic resonance (NMR). For the NMR analysis, only lipid fractions (Triglycerides, diglycerides, monoglycerides, and fatty acids) obtained in section 3.3.3.1 were used. Approximately 50 mg of the various lipids in solid form were transferred into the test tube for proton NMR and carbon NMR analysis. Then, 0.8 mL of deuterated chloroform (CDCl$_3$) was pipetted into the test tube. The mixture was vigorously shaken until the lipid sample was completely dissolved. The sample mixture was then filtered with a short pipette in which a small quantity of cotton wool was inserted, then transferred into a 5 mm NMR glass tube for the analysis. NMR spectra were registered on a Bruker -400 MHz NMR. The chemical shifts are expressed in ppm. The experimental condition are summarised in Table 3.13

Table 3.13: Some important operating parameters for 1H NMR and 13C NMR experiment

The experimental parameters	^{1}H NMR	^{13}C NMR
Pre-scan delay	10.38 usec	6.50 usec
Dwell time	62.400 usec	20.80 usec
FID resolution	0.244532 Hz	0.73 Hz
Temperature	297.2 K	297.2 K
Pulse delay	1 s	1s
Number of scans	16	1024
Number of dummy scans	2	4
Time domain	4.0894465 sec	1.3631488 sec
Spectral width	8012.820 Hz	24038.46 Hz
Solvent	CDCl3	CDCl3
Size of the real spectrum (SI)	65536	32768
Line broadening	0.30 Hz	1 Hz

3.3.5.4 Scanning electron microscope (SEM)

The morphology of the chitosan nanoparticles after electrospraying made according to section 3.3.3.4 and the chitosan-lipid nanoparticle made according to section 3.3.3.5 was examined using a scanning electron microscope (FEI, Quanta Feg 250, USA). To prepare the samples, first, adhesive conductive carbon discs (carbon tabs) were placed on an aluminium SEM pin stub. Then a small amount of the nanoparticles sample in powder form was placed on the carbon adhesive disc. The samples were then placed in the analyser, where scanning electron micrographs of each sample were taken. The samples were analysed under a low vacuum with a distance of 19.11 mm and at an acceleration voltage of 5 kV.

3.3.6 Antimicrobial activity

In this work, the antimicrobial effects of lipid fractions and chitosan-lipid nanoparticles obtained in sections 3.3.3.1 and 3.3.3.5 respectively were investigated. The samples were tested against gram-positive bacteria (*Micrococcus luteus*) and gram-negative bacteria (*Pseudomonas aeruginosa*). These two bacteria were selected for this study because they presented multiple antibiotic resistances. The positive control was ampicillin for both bacteria and the antimicrobial test was performed using the disc diffusion method.

3.3.6.1 Preparation of agar medium and solution

LB agar was prepared by mixing 5 g of tryptone, 2.5 g of yeast, 5 g of NaCl, and 7.5 g of agar in 500 mL distilled water while NB agar was prepared by mixing 15 g of agar with 16 g of nutrient broth and 1 L of distilled water. The LB/NB solution was without the agar. The two solutions were then sterilized by autoclaving at 121 °C for 15 min at 15 psi. The LB and NB agar medium were cooled to about 60 °C then poured into sterile plastic petri dishes to a uniform depth of 4 mm. The plates were allowed to solidify and stored at 2-8°C in sealed containers to avoid loss of moisture until further analysis.

3.3.6.2 Preparation of lipid fraction for antimicrobial test

0.4 mg of the individual lipid fractions in solid form (Triglycerides, diglycerides, monoglycerides, and fatty acids) were dissolved in 1 mL of hexane. The mixture was shaken until the lipid was completely dissolved.

3.3.6.3 Preparation of chitosan-lipid nanoparticle for antimicrobial test

0.004 mg of the individual chitosan-lipid nanoparticles in powder form: chitosan-triglycerides (CH-TGA), chitosan-diglycerides (CH-DG), chitosan-monoglycerides (CH-MG), and chitosan- fatty acids (CH-FA) nanoparticles was dissolved in 10 mL of 90 % acetic acid. The mixtures were stirred at room temperature for 24 h at a constant speed of 700 rpm with a magnetic stirrer until the chitosan- lipid nanoparticles powder was completely dispersed.

3.3.6.4 Antimicrobial test

The antimicrobial activity of the samples was determined by the disc diffusion method. A single colony of the different bacteria was collected with a loop then transferred into 10 mL LB and NB solution. Then incubated for 24 h at 30 and 37 °C for *Micrococcus luteus* and *Pseudomonas aeruginosa*, respectively. After the incubation period, the concentration of the bacteria which indicates the growth stage of the cultured cell population was determined using UV-Visible Spectrometer (JENWAY 6305). The absorption analysis was carried out from 360 nm to 460 nm and distilled water was used as a reference blank. The concentration of the bacteria was diluted to an optical density at 600 nm (OD$_{600nm}$) of 0.2 before plating out. The OD$_{600nm}$ value indicates the percentage of light that passes through a sample. When using UV spectroscopy to measure microbial growth, OD$_{600nm}$ is preferred because the cells are not killed as they would be under higher UV light. A sterile pipet tip was used to transfer 120 µL suspension of an OD600$_{nm}$ of 0.2 of the bacteria on the surface agar layer of the Petri dish. The bacteria were spread across the entire plate with a sterile bead.

For the antimicrobial test of the lipid fractions and the chitosan-lipid fractions, 120 µL *Micrococcus luteus* and *Pseudomonas aeruginosa* were spread across the surface agar layer of the plate separately. The antibiotic discs were impregnated with 20 µL of 0.4 mg/mL of each lipid fraction prepared in section 3.3.6.2 and 0.0004 mg/mL of each chitosan-lipid nanoparticles prepared in section 3.3.6.3 the different antibiotic discs impregnated with the sample (lipid fraction / chitosan-lipid nanoparticles) were placed in each quadrant of the plate as shown in Figure 3.9. The control experiment was carried out by impregnating 1 antibiotic disc with 20 µL of the pure solvent which served as a negative control. Hexane and acetic acid were used as a negative control to check the effect of the solvent used for the lipids and nanoparticles, respectively. For the positive control, 20 µL of the antibiotic (ampicillin) was placed on a separate agar plate.

The plates were put into the incubator for 24 h at 30 and 37 °C for *Micrococcus luteus* and *Pseudomonas aeruginosa*, respectively. The experiments were carried out in triplicate. After 24 hours, the plates were viewed. If the bacteria are susceptible to the lipid fraction of the nanoparticles, an area of cleaning will surround the disc where the bacteria are not capable of growing (Figure 3.9). The clean zone is referred to as the zone of inhibition. The zone of inhibition is measured in millimetres, including the diameter of the antibiotic disc
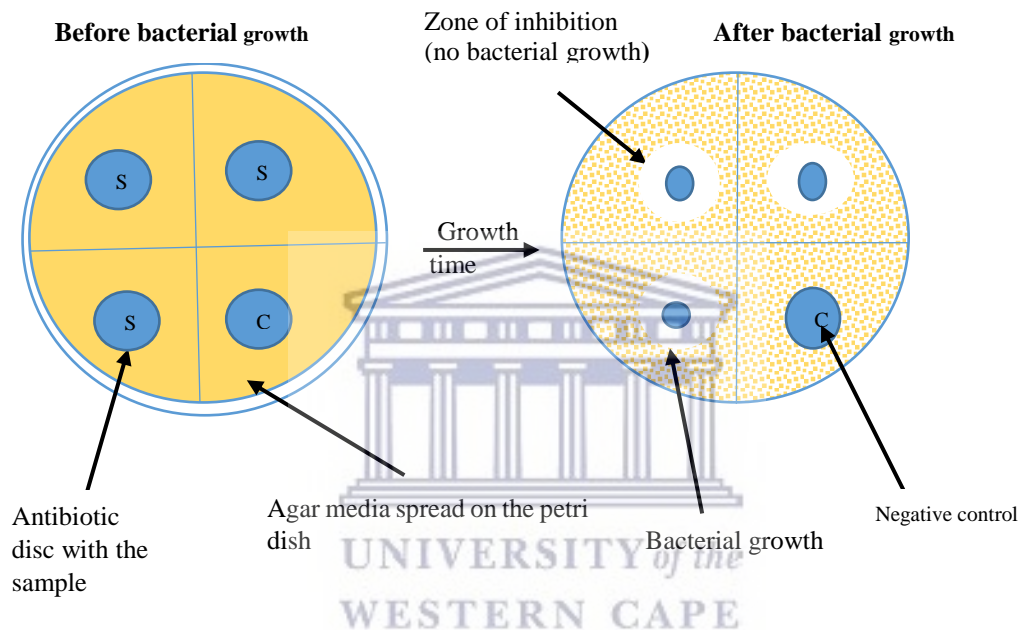
Figure 3.9: Antimicrobial test before and after bacterial growth

CHAPTER 4: A COMPARATIVE ANALYSIS OF DIFFERENT METHODS TO EXTRACT LIPID FROM BLACK SOLDIER FLY LARVAE

Abstract

Various extraction methods have been used to extract lipid from different sources. However, the effective extraction of lipid depends on the extraction method employed and the source of the lipid. Efforts have also been put in towards the extraction conditions (solvent type, temperature, time) surrounding the extraction processes. But few reports show the extraction from black soldier fly (BSF) larvae or the conditions of extraction for better yield. The work presented in this chapter aimed at extracting lipid from BSF larvae and to compare different extraction methods used under the same conditions to determine a suitable method for the extraction of lipid from BSF larvae for maximum yield. Three extraction methods (Soxhlet extraction, ultrasonic-assisted extraction, and maceration extraction) were investigated for their lipid yield and fatty acid composition. Soxhlet extraction proved to be the appropriate method for BSF larvae lipid extraction due to its high lipid yield (40.68 %). Gas chromatography flame ionisation detection (GC-FID) revealed that the lipid extracted from the BSF larvae was found to be a rich source of saturated fatty acids with lauric acid being the most abundant fatty acid. The extraction conditions influencing the BSF larvae lipid yield and fatty acid composition were discussed and the results obtained showed that a high yield of the BSF larvae lipid and fatty acids composition was achieved using petroleum ether at 70°C, a solvent to solid ratio of 0.03 g/mL and an extraction time of 4 h using Soxhlet extraction

Graphical abstract
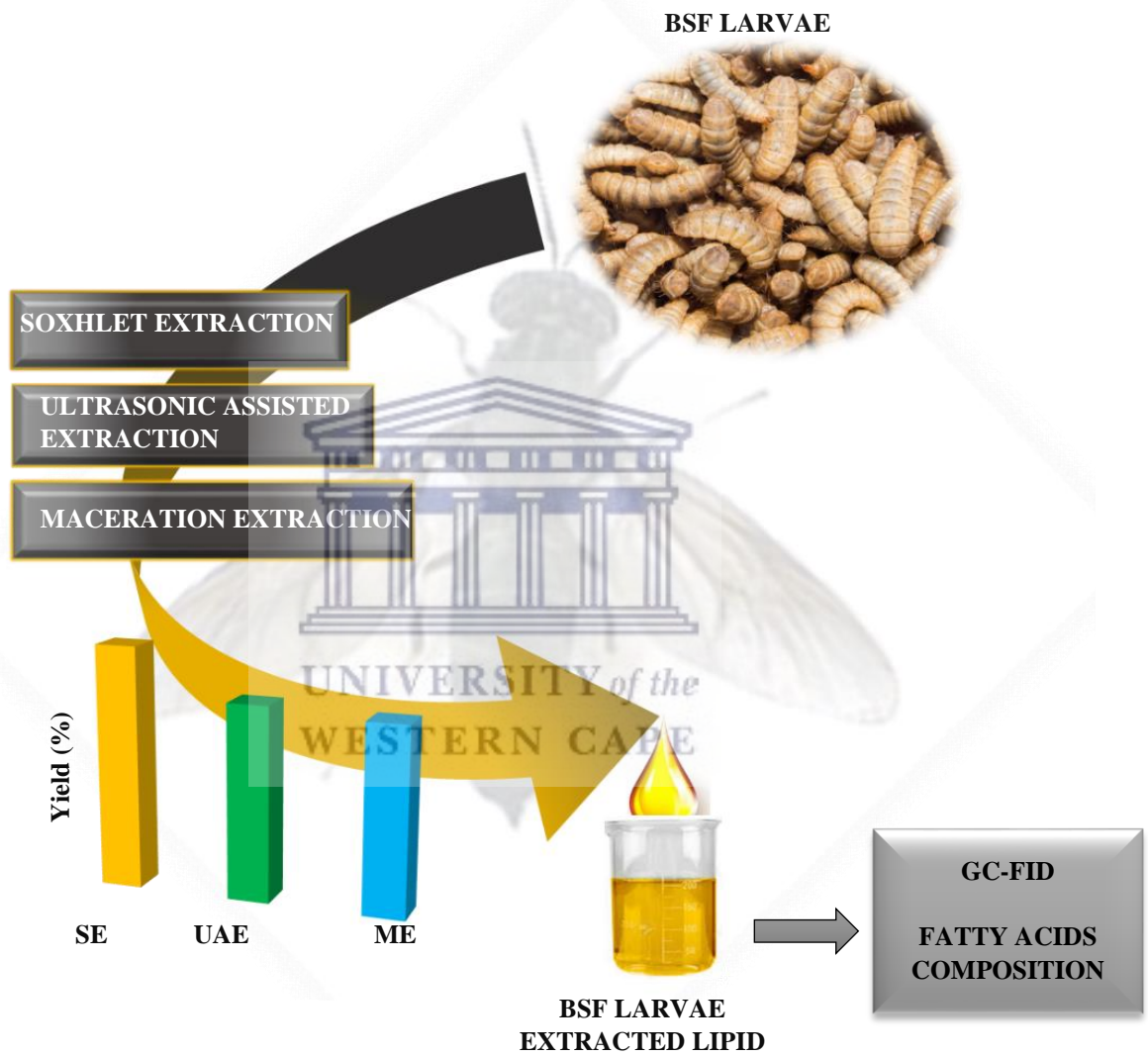
4.1 Introduction

The increased demand for lipids in the food and pharmaceutical industries has highlighted the need for a suitable, selective, cost-effective, and environmentally friendly lipid extraction method capable of producing a high yield. According to research, the most commonly used extraction methods for this purpose are conventional Soxhlet extraction, microwave-assisted extraction, maceration, and ultrasonic-assisted extraction methods. (Pichai & Krit, 2015; Kanadea & Bhatkhandeb, 2016; Smets, Verbinnen, et al., 2020). To achieve the desired result, these extraction methods must be used in conjunction with other extraction parameters such as solute to solvent ratio, time, and solvent polarity, all of which promote efficiency and higher yield recovery. Those extraction parameters are well documented in the literature to improve the efficacy of the lipid yield, and thus optimal extraction parameters are the key success factor for a high recovery (Elboughdiri, 2018; Jisieike & Betiku, 2020). Furthermore, there are numerous solvents available for lipid extraction namely, methanol, ethyl acetate, dichloromethane, hexane, and petroleum ether (Nezhdbahadori et al., 2018), but it is necessary to investigate which of them will provide the desired lipid yield and fatty acid composition.

4.2 Effect of extraction methods on the black soldier fly larvae lipid yield

This section presents and compares the results of the effect of Soxhlet extraction (SE), ultrasonic-assisted extraction (UAE), and maceration extraction (ME) on black soldier fly (BSF) larvae lipid yield. The experiments were carried out to compare the effectiveness of the three extraction methods in terms of their ability to produce high lipid yield. The SE procedure detailed in section 3.3.2.1 was performed for 4 h at 70 °C in which 8 g freeze-dried BSF larvae powder, was packed in a thimble made from filter paper then placed in a Soxhlet extractor with 300 mL of the petroleum ether. The maceration extraction procedure, detailed in section 3.3.2.2 was carried out at room temperature (25 °C) for 48 h in which 8 g freeze-dried BSF larvae powder was placed into a filter bag then immersed in 300 mL petroleum ether. The ultrasonic-assisted extraction procedure described in section 3.3.2.3 used 8 g of freeze-dried BSF larvae powder mixed with 300 mL of petroleum ether, which was then sonicated for 30 minutes at room temperature (25 °C) at a frequency of 40 kHz and extraction power of 200 W. Each extraction method was repeated five times, and the percent lipid yield was calculated using equation 3.1 in section 3.3.2 based on sample weight loss. Table 4.1 summarises the various

parameters used in each extraction procedure. All of the parameters were fixed and chosen based on the best condition obtained during the preliminary work.

Table 4.1:Extraction condition parameters of SE, UAE, and ME techniques

Extraction Methods	Time (min, h)	Temperature (°C)	Extraction Power (W)	Volume of the solvent (mL)	weight of the sample (g)	Frequency (kHz)
SE	4 h	70	/	300	8	/
UAE	30 min	25	200	300	8	20
ME	48 h	25	/	300	8	/

Table 4.2 shows the results of lipid extraction from BSF larvae using the SE, UAE, and ME procedures.

Table 4.2: BSF larvae lipid yield using SE, UAE, and ME method (n = 5, experimental conditions: Volume of petroleum ether = 300 mL, weight of sample = 8 g)

Replication	Extraction yield (%)		
	SE	UAE	ME
1	40.66	30.40	31.72
2	40.65	37.35	31.58
3	41.47	31.30	32.75
4	41.00	32.66	30.83
5	39.60	31.50	30.26
Mean ± SD	40.68 ± 0.69	32.64 ± 2.75	31.42 ± 0.94

The results shown in Table 4.2, revealed that the extraction methods significantly affected the lipid yield ($P < 0.05$). SE achieved the highest lipid yield (40.68 %), followed by the UAE (32.64 %), and the ME (31.42 %). Figure 4.1 depicts a graph comparing the three extraction methods.
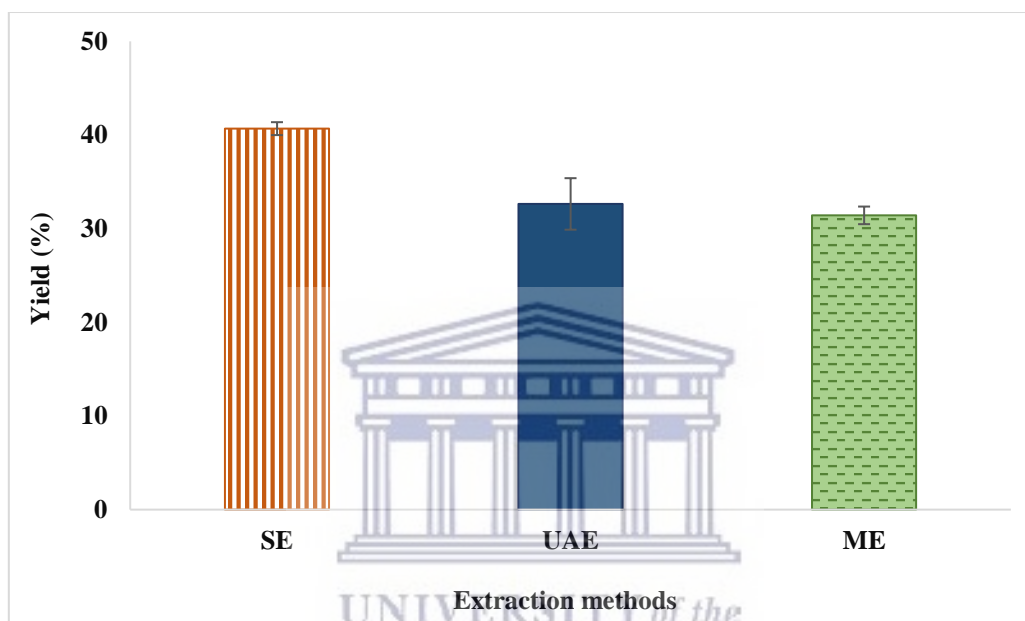
Figure 4.1: Comparison of different lipid extraction methods (Experimental conditions: Volume of petroleum ether = 300 mL, weight of sample = 8 g)

The high lipid yield obtained from the SE could be attributed to the temperature (70 °C) involved in Soxhlet extraction. According to Spigno et al. (2007), heat promotes extraction by increasing diffusion and solubility. When heat is applied during extraction, the physical properties of the solvent, such as density will decrease, thus increasing the rate of diffusion and facilitating the solvent's movement across the sample's adipose tissue. Lower temperatures on the other hand reduce the energy of the molecules, resulting in a slower rate of diffusion. However, high temperature cannot benefit thermolabile (heat sensitive) compounds during extraction because it can cause their degradation or lead solvents to evaporate, resulting in extracts containing undesirable impurities (Zhang et al., 2018).

Another explanation could be that the sample is repeatedly brought into contact with a fresh solvent during SE, ensuring that the lipid from the sample is completely extracted (Luque de Castro & Priego-Capote, 2010). A lower yield observed with ME and UAE compared to SE could also be due to the fact that the UAE used in this study required filtration after extraction, which could have resulted in lipid loss during filtration. ME had the lowest yield of all the methods used in this study, which could be due to an incomplete lipid extraction from the sample.

Several researchers have used various methods to extract lipid from the larvae of the black soldier fly. For example, Li et al. (2011) and Wong et al. (2019) used maceration extraction to extract lipid from black soldier fly larvae using petroleum ether as the extraction solvent, with lipid yields of 30.01 % and 34.23 % obtained, respectively. The lipid yield obtained by Li et al. (2011) was close to the one reported in this study (31.42 %), whereas the lipid yield obtained by Wong et al. (2019) was slightly higher. Other researchers, including Wang et al. (2017) and Hao et al. (2021), used microwave-assisted extraction and petroleum ether as the extraction solvent, with lipid yields of 30.53 % and 37.73 %, respectively. To the best of our knowledge, very few studies on the lipid yield of BSF larvae using Soxhlet extractions have been published. Among them, Smets et al. (2020) reported a lipid yield of 35.67 % when using petroleum ether and a lipid yield of 40.34% when using hexane as the extracting solvent. Their yields were lower than the ones reported in this study (40.68 %).

The extraction parameters used by the aforementioned authors differ in terms of sample preparation, extraction conditions (solvent type and solid to solvent ratio), the type of substrates the larvae were fed on, and the developmental stage of the larvae, all of which can affect the lipid yield and composition of the BSF fly (Karthikeyan et al., 2020). Due to the aforementioned factors, it was difficult to ascertain which method was capable of producing a high lipid yield. As a result, it was critical to conduct a comparative study between extraction methods in this study. One important aspect of this study was that all parameters such as extraction conditions (type and volume of solvent, mass of sample), sample preparation, and larval developmental stage were kept constant for the SE, UAE, and ME methods. This comparative study was done to find a simple, reliable method that will give high lipid yield.

According to the findings of the comparative study, SE was found to be a suitable method for extracting lipid from BSF larvae due to its simplicity, low cost, and high oil recovery when

compared to ME and UAE. Even though Soxhlet extraction is a traditional method of extraction, this study demonstrated that it is a suitable method that can be used on an industrial scale for the extraction of lipid from BSF larvae. However, more comparative extraction methods need to be investigated to broaden the selection of extraction methods. The following section investigates the effect of extraction methods (SE, UAE, and ME) on the fatty acids composition of BSF larvae lipids.

4.3   Effect of the extraction methods on the fatty acids composition

The fatty acids composition of lipid extracted from BSF larvae using Soxhlet extraction (SE), ultrasonic-assisted extraction (UAE), and maceration extraction (ME) are presented in this section. As described in section 3.3.5.1.1, fatty acids were determined using gas chromatography coupled with an FID detection (GC-FID). Each experiment was repeated three times, and the final value was the average of all three. Table 4.3 shows the fatty acid composition of the lipid extracted from BSF larvae using SE, UAE, and ME.

Table 4.3: Fatty acids composition of BSF larvae lipid obtained by SE, UAE, and ME techniques (n = 3, GC condition: CP-Sil 88 for FAME/HP-88 column (60 m X 250 µm ID, 0.2 µm), oven programming from 120 to 230 °C. run time (16 min), FID 280 °C, Injection volume (0.5 µL of 0.05 % lipid in hexane. Carrier gas (Helium; 4 mL/min)

Fatty acids	Fatty acids composition (%)		
	SE	UAE	ME
Lauric acid (C12:0)	31.99 ± 0.03	30.45 ± 0.01	19.71 ± 0.01
Palmitic acid (C16:0)	19.36 ± 0.02	16.30 ± 0.82	14.50 ± 0.04
Oleic acid (C18:1)	0.60 ± 0.02	0.42 ± 0.01	0.32 ± 0.04
Caprylic acid (C8:0)	2.13 ± 0.01	2.55 ± 0.01	2.64 ± 0.02

Capric acid (C10:0)	7.68 ± 1.04	8.13 ± 0.02	8.37 ± 0.02
Arachidic acid (C20:0)	0.18 ± 0.02	0.18 ± 0.01	0.21 ± 0.03
Myristic acid (C14:0)	6.94 ± 0.96	4.98 ± 0.01	2.20 ± 0.03
Palmitoleic acid (C16:1)	1.52 ± 0.01	1.67 ± 0.01	2.43 ± 0.02
Stearic acid (C18:0)	0.38 ± 0.01	0.07 ± 0.01	0.07 ± 0.02
Linolenic acid (C18:3)	0.17 ± 0.02	0.08 ± 0.05	0.19 ± 0.03
Linoleic acid (C18:2)	3.39 ± 0.01	2.88 ± 0.05	3.39 ± 0.02
∑ SFAs	68.64 ± 0.18	62.65 ± 0.88	47.70 ± 2.06
∑ MUFAs	2.12 ± 0.06	2.08 ± 0.02	2.75 ± 0.03
∑ PUFAs	3.56 ± 0.39	2.96 ± 0.21	3.58 ± 0.03

∑ SFA= sum all saturated fatty acids (lauric acid+ palmitic acid + caprylic acid + capric acid + arachidic acid + myristic acid); ∑ MUFA = sum of all monounsaturated fatty acids (oleic acid+ palmitoleic acid); ∑ PUFA = sum of all polyunsaturated fatty acids (linolenic acid+ linoleic acid)

The saturated fatty acids (SFA), monounsaturated fatty acids (MUFA), and polyunsaturated fatty acids (PUFA) determined using Gas chromatography- flame ionisation detection (GC-FID were all detected in the three extraction methods from the BSF larvae, but with different percentage yields (Figure 4.2).
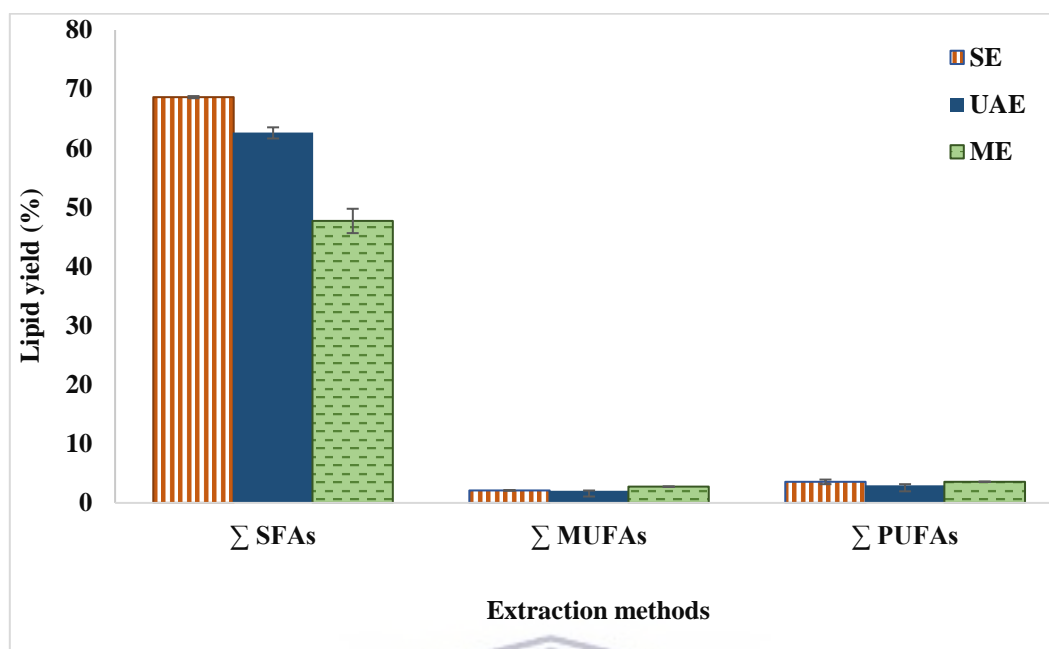
Figure 4.2: Effect of the extraction methods on the saturated, monosaturated, and polyunsaturated fatty acids

Between the three extraction methods, the percentage of total saturated fatty acids ($\sum$ SFA) was significantly different (P < 0.05). The $\sum$ SFAs were 68.64% obtained from the SE method, 62.65% resulted from the UAE method and 47.70 % from the ME method. However, there was no significant difference in the percentage of total monounsaturated fatty acids ($\sum$ MUFA) and polyunsaturated fatty acids ($\sum$ PUFA) between the three methods (P>0.05) The $\sum$ PUFA were 3.56, 2.96, and 3.58 % for SE, UAE, and ME methods, respectively while the $\sum$ MUFA were 2.12, 2.08 and 2.75 % for SE, UAE and ME methods, respectively.

Seven type of saturated fatty acids were detected in the BSF larvae lipid, including lauric acid, palmitic acid, caprylic acid, capric acid , arachidic acid, myristic acid and stearic acid which presented by 31.99 %, 19.36 %, 2.13 %, 0.18 %, 6.94 % and 0.38 respectively, in SE method and 30.45 %, 16.30 %, 2.55 %, 8.13 %, 0.18 %, 4.98 % and 0.07%, respectively in UAE method and 19.71 %, 14.50 %, 2.64 %, 8.37 %, 0.21 %, 2.20 % and 0.07 %, an ME method, respectively. Among the saturated fatty acids, stearic acid was detected in very low percentage in ME and UAE methods (0.07%) (Figure 4.3)
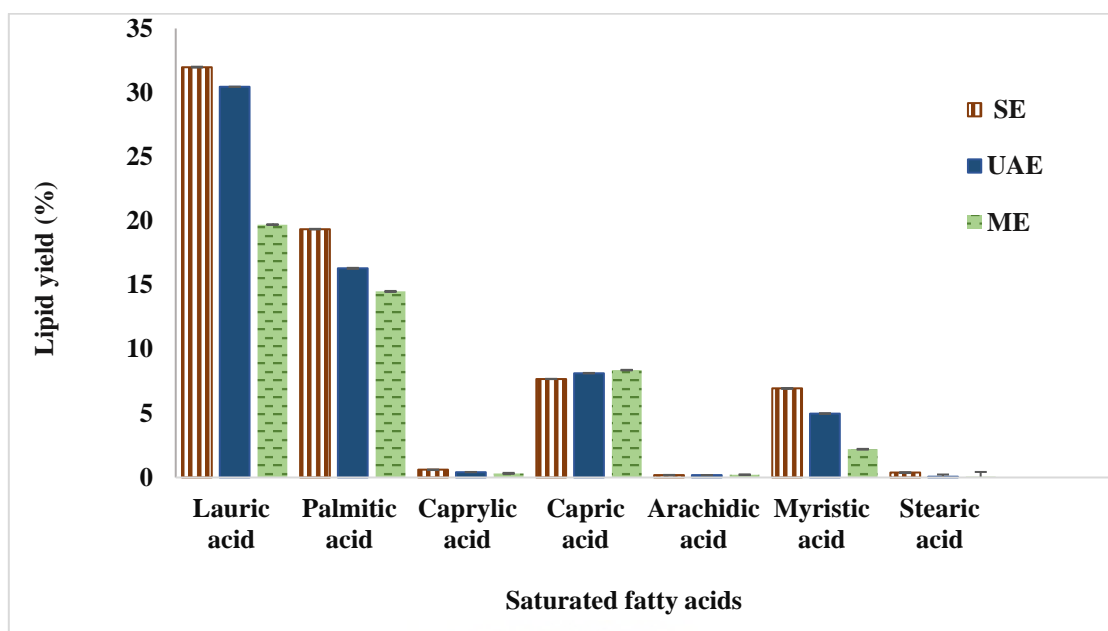
Figure 4.3: Percentage yield of saturated fatty acids using SE, UAE, and ME methods

Only two types of polyunsaturated fatty acids (linolenic acid and linoleic acid) were detected in BSF larvae lipid and were 0.17 %, 0.08 %, and 0.19 % in SE, UAE, and ME methods, respectively for linolenic acid and 3.39, 2.88, and 3.39 % in SE, UAE and ME methods, respectively for linoleic acid. Two monounsaturated fatty acids (oleic acid and palmitoleic acid) were detected in the three extraction methods which were 0.60, 0.42, and 0.32 % for oleic acid and 1.52, 1.67, and 2.43 % for palmitoleic acid in SE, UAE, and ME methods, respectively. The percentage yield of unsaturated fatty acids (mono and polyunsaturated fatty acids) using the SE, UAE, and ME methods is shown in Figure 4.4.

http://etd.uwc.ac.za/
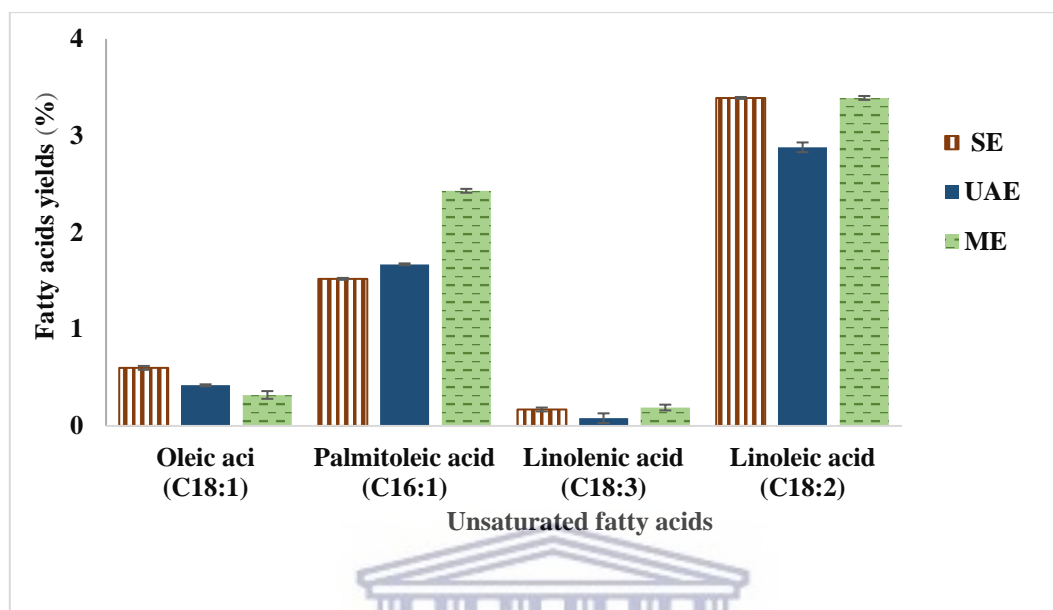
Figure 4.4: The percentage yield of unsaturated fatty acids using SE, UAE, and ME methods.

This study's findings were consistent with previously published works (Liland et al., 2017; Ravi et al., 2019), which revealed a similar fatty acid trend. In all previous research that investigated the fatty acid profile of BSF larvae, lauric acid was found to be the most abundant fatty acid (Zheng et al., 2012; Wang et al., 2017; Ravi et al., 2019; Ewald et al., 2020). The high amount of lauric acid found in BSF larvae could be attributed to the fact that lauric acid is naturally produced by black soldier fly larvae and is more polar than other fatty acids, making it less dependent on chylomicron and lipoproteins for transport. This leads to increased absorption of enterocytes compared to other fatty acids leading to its high content in the lipids of the black soldier fly larvae (Belghit et al., 2019). As mentioned in Chapter 2 (section 2.5.2.1), lauric acid has numerous health benefits. It has been shown to increase high-density lipoprotein (HDL) cholesterol, also known as good cholesterol (Feinman, 2010; Masson et al., 2015), and it has high potency in fighting cancer cells and preventing their growth. Lauric acid has also been shown to lower blood pressure and heart rate, as well as fight various pathogens, as reported by Thormar et al, (2013). It is interesting to note that the fatty acid composition of BSF larvae differs from other insect species, which are dominated by monosaturated and polyunsaturated fatty acids, whereas the largest lipid fraction of BSF larvae is dominated by

saturated fatty acid (Belghit et al., 2019), making the BSF larvae lipid attractive for biodiesel production (Li et al., 2011). Furthermore, Soleimanifar et al. (2019) found that saturated fatty acids are more resistant to oxidation than unsaturated and polyunsaturated fatty acids. The fact that BSF larvae are a good source of saturated fatty acids makes them a viable and long-term animal feed (Belghit et al., 2019). In this study, it was found that the larvae of the BSF contained predominantly SFA, which is due to the fact that SFA is naturally produced by the larvae, as opposed to PUFA, which is primarily derived from their diet (Ewald et al., 2020). Based on this, research should look into the incorporation of omega-3 fatty acids (alpha-linolenic acid, eicosapentaenoic acid, and docosahexaenoic acid) from the diet into the larval lipid of the BSF. When compared to this study, Ewald et al. (2020) reported significantly higher percentages of SFA (up to 76%), MUFA (up to 32%), and PUFA (up to 32%). This could be due to a variety of factors such as larval weight, diet, and extraction method, all of which could influence the fatty acids composition (Dabbou et al., 2021).

The findings of this study revealed that the fatty acids composition of the BSF larvae is affected by the lipid extraction method used. As a result, it was critical not to focus solely on the lipid yield obtained from SE, UAE, and ME, but also to ensure the quality of the fatty acid extracted during the extraction process. The following section examined how critical SE parameters can be improved since the method showed a better acid profile and lipid yield than ME and UAE procedures.

4.4 Optimizations of the extraction conditions using Soxhlet extraction

This experiment was intended to investigate the effect of important parameters during Soxhlet extraction (SE). Those parameters are solvent polarity, extraction time, and solute-solvent ratio. The change of these operating conditions is one of the most important factors influencing the quality and the yield of lipid produced.

4.4.1 Solvent performance on the lipid yield and fatty acid profile

This experiment investigated the effect of solvent polarity on the lipid yield and fatty acid composition of the BSF larvae. It was important to investigate the extraction capacity of solvents on BSF larvae lipid based on polarity since this has been shown to affect the lipid yield and fatty acid composition (Tir et al., 2012; Jisieike & Betiku, 2020).

4.4.1.1 Effect of the solvent types on the black soldier larvae lipid yield

The effect of the different solvent polarities of ethyl acetate (EA), hexane (Hex), methanol (Met), petroleum ether (PE), and dichloromethane (DCM) was tested for their efficiency to extract BSF larvae lipid using Soxhlet extraction. The parameters kept constant during the Soxhlet extraction was the volume of the solvent (300 mL), the weight of the sample (8 g), the temperature (70 ^{0}C), and the extraction time (4 h). The amount of lipid was calculated as % of the total lipid present in the BSF larvae. Each experiment was performed 5 times. Table 4.4 shows   the yields of BSF larvae lipid using various extraction solvents (EA, Hex, Met, PE, and DCM)

Table 4.4: Effect of the solvent polarity on the BSF larvae lipid yield using Soxhlet extraction method (n = 5, Reaction condition: Temperature = 70 ^{0}C, Volume of solvent = 300 mL , weight of the sample = 8 g, Extraction time = 4 h)

	Extraction lipid yield (%)				
Replicate	**EA**	**Hex**	**Met**	**PE**	**DCM**
1	32.96	36.77	26.12	40.33	36.15
2	32.78	36.69	26.41	40.96	36.12
3	32.23	36.78	26.62	40.42	36.28
4	31.11	37.03	26.47	40.16	36.32
5	32.09	36.84	25.92	40.19	36.21
Mean ± SD	32.27 ± 0.83	36.82 ± 0.15	26.41 ± 0.21	40.47 ± 0.35	36.22 ± 0.10

The BSF larvae lipid yields obtained from the different solvents were 32.27, 36.82, 26.41, 40.47, and 36.22 % for EA, Hex, Met, PE, and DCM, respectively. The lipid yields obtained differed significantly ($P < 0.05$) depending on the extraction solvent except for Hex (36.82 %) and DCM (36.22 %) where no significant difference was observed ($P > 0.05$). Figure 4.5 shows the variation of the lipid yields when different extraction solvents are used.
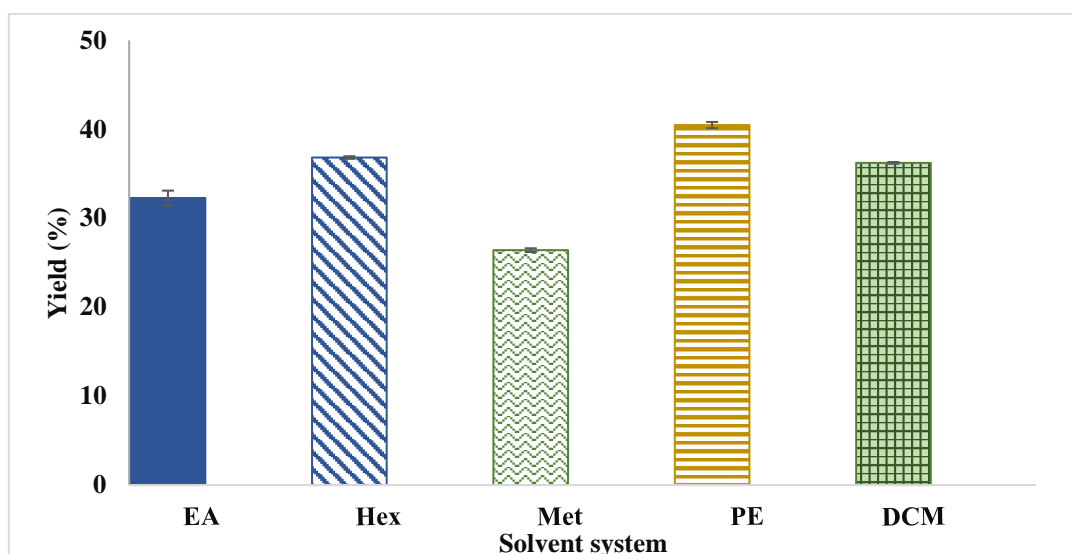
Figure 4.5: Effect of solvent type on the total amount of lipids extracted from BSF larvae using Soxhlet extraction (Reaction condition: Temperature = 70 °C, volume of petroleum ether = 300 mL, weight of sample = 8 g, extraction time = 4 h)

The results showed that BSF larvae lipid yield is better with non-polar solvents (PE and Hex) compared to the yield obtained with polar solvents (Met, DCM, and EA). The dielectric constants of the different solvents which are a measure of their polarity are tabulated in section 3.3.2.1.3. The fact that BSF larvae lipid was effectively extracted with non-polar solvents could be attributed to the fact that BSF larvae lipid contains a higher percentage of non-polar lipids than polar lipids. Non-polar solvents have a higher affinity for non-polar lipids while polar solvents will have an affinity towards polar compounds which are not predominant in BSF larvae lipids. Figure 4.6 depicts the physical appearance of the lipid extracted from BSF larvae (a) using various solvents and their thin layer chromatography separation (b).

(a)   (b)
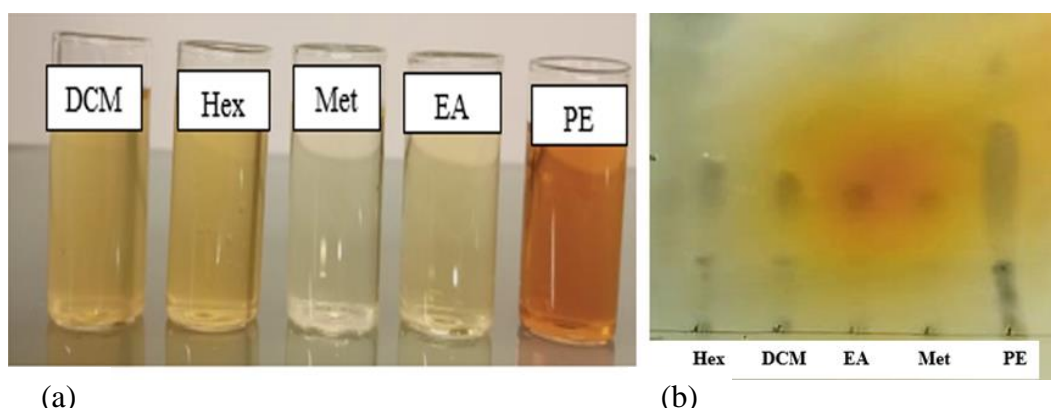
Figure 4.6: The physical appearance of the extract (a) and TLC (b)

Based on the physical appearance of the extracts, the colour ranged from light yellow to deep yellow. The observation on the thin layer chromatography (TLC) plate shows the extraction of the non-polar lipids increased as the polarity of the solvent decreased. The polar lipid compounds were not well extracted when using a polar solvent (Met) while non-polar compounds were mostly extracted when using non-polar solvents such as PE. From that observation, it is clear that solvent polarity significantly ($P < 0.05$) affected the lipid yield from the BSF larvae.

Several researchers studied the ability of various solvents to extract lipids and discovered that the lipid extraction process is strongly related to the physicochemical properties of the extraction solvent, such as polarity and dielectric constant (Wang et al., 2017; Juhaimi, et al., 2019a; Feng et al., 2020). Wang et al. (2017) extracted lipid from BSF larvae using a variety of solvents (hexane, petroleum ether, chloroform, acetone, and methanol) and their mixtures. The authors reported that methanol resulted in a higher lipid yield (43.26 %) when compared to the other solvents, which was significantly higher than the yield (26.41 %) obtained in this study when methanol was used. The high lipid yield reported by Wang et al. (2017) was due to the fact that the methanol extract contained solid impurities that were not present in other solvent extracts, hence influencing the yield of lipids during the extraction process. Similar phenomena was observed by Hidalgo et al. (2015) in which the methanol extract after the extraction process had solid impurities.

In this study petroleum ether (40.47 %) gave yield higher than solvent mixture (chloroform-methanol; 34.06 % or hexane-methanol; 32.51 % mixture) used by Wang et al. (2017) and the

yield was lower than the solvent mixture (hexane-ethanol; 65.79 or petroleum ether-ethanol; 67.57) used by Feng et al. (2020) for the lipid extraction of BSF larvae. According to Feng et al. (2020), the mixture of polar and non-polar solvents showed better performance than polar or non-polar solvents alone on the lipid extraction efficiency. The reason for this is that nonpolar solvents can only extract neutral lipids, causing polar lipids to be lost in the process. However, some organic solvents, such as chloroform and hexane, are expensive and toxic. As a result of its low toxicity, petroleum ether was found to be a suitable solvent for extracting lipid from BSF larvae in this study, and the yield obtained was comparable to that obtained by other researchers. The effect of solvent polarity on the fatty acid composition of the BSF larvae lipid was investigated in the following section.

4.4.1.2 Effect of the solvent type on the fatty acid profile of black soldier larvae lipid

This section investigates the effect of solvent polarity on the fatty acid composition of each solvent extract discussed in section 4.3.3.1. For that purpose, the fatty acid was determined by GC-FID according to the analytical procedure discussed in chapter 3 (section 3.4.1.1). Each analysis was performed in triplicate. The experiment conditions used for the GC-FID are given in section 3.4.1.1. The concentration of individual fatty acids was calculated using the response factor according to equation 2 (section 3.4.1.1). Table 4.5 shows the fatty acids composition of BSF larvae lipid obtained by Soxhlet extraction using petroleum ether (PE), hexane (Hex), dichloromethane (DCM) ethyl acetate (EA), and methanol (Met).

Table 4.5: Fatty acid composition of BSF larvae lipid obtained by Soxhlet extraction using different solvents. Values are represented as mean ± SD of three independent measurements n=3)

Fatty acids	Fatty acid composition (%)

	PE	Hex	DCM	EA	MET
Lauric acid (C12:0)	32.10 ± 0.04	30.50 ± 0.03	29.31 ± 0.16	24.84 ± 0.02	21.69 ± 0.01
Palmitic acid (C16:0)	18.79 ± 0.02	15.70 ± 0.01	15.23 ± 0.03	15.71 ± 0.02	17.53 ± 0.03
Oleic acid (C18:1)	0.63 ± 0.03	0.69 ± 0.01	0.68± 0.02	0.12± 0.04	0.09 ± 0.01
Caprylic acid (C8:0)	2.12 ± 0.01	2.29 ± 0.02	1.77± 0.01	0.92± 0.02	0.40 ± 0.03
Capric acid (C10:0)	7.55 ± 0.03	6.04 ± 0.01	6.25± 0.01	9.01 ± 0.04	3.89 ± 0.01
Arachidic acid (C20:0)	0.17 ± 0.09	0.20 ± 0.01	0.10± 0.01	0.03 ± 0.03	0.03 ± 0.02
Myristic acid (C14:0)	6.50 ± 0.04	6.74 ± 0.01	6.88± 0.01	0.67 ± 0.01	0.09 ± 0.01
Palmitoleic acid (C16:1)	1.40 ± 0.02	0.07 ± 0.01	0.20± 0.04	0.57 ± 0.06	0.87 ± 0.02
Stearic acid (C18:0)	0.40 ± 0.08	0.36 ± 0.01	0.20± 0.01	0.07 ± 0.02	0.52 ± 0.10
Linolenic acid (C18:3)	0.20 ± 0.01	0.14 ± 0.01	0.10± 0.02	0.09 ± 0.01	0.06 ± 0.01
Linoleic acid (C18:2)	3.50 ± 0.31	0.08 ± 0.45	0.07± 0.01	0.11 ± 0.03	0.01 ± 0.01
∑SFAs	67.46 ± 0.05	61.83 ± 0.10	59.74 ± 0.24	51.25 ± 0.15	44.15 ± 0.18
∑MUFAs	2.03 ± 0.05	0.76 ± 0.02	0.88 ± 0.07	0.69 ± 0.10	0.95 ± 0.11
∑PUFAs	3.07 ± 0.02	0.22 ± 0.46	0.17 ± 0.02	0.20 ± 0.04	0.07 ± 0.02

∑ SFA= sum all saturated fatty acids (lauric acid+ palmitic acid + caprylic acid + capric acid + arachidic acid +
myristic acid); ∑ MUFA = sum of all monounsaturated fatty acids (oleic acid+ palmitoleic acid); ∑ PUFA = sum
of all polyunsaturated fatty acids (linolenic acid+ linoleic acid)

The total saturated fatty acids (∑ SFA), monounsaturated fatty acids (∑ MUFA), and
polyunsaturated fatty acids (∑ PUFA) were significantly different ($P < 0.05$) depending on the
solvent type. The ∑ SFAs were 67.46, 61.83, 59.74, 51.25, 44.15 % for PE, Hex, DCM, EA,
and MET, respectively. The ∑ MUFA were 2.03, 0.76, 0.88, 0.69 and 0.95 % while the ∑ PUFA
were 3.07, 0.22, 0.17, 0.20 and 0.07 % for PE, Hex, DCM, EA and MET, respectively. Petroleum
ether gave the highest percentage of the ∑ SFAs (67.46 %), ∑ MUFA (2.03 %), and ∑ PUFA
(3.07 %) followed by Hex, DCM, EA, and ME. MUFA and PUFA were almost undetectable
in Hex, DCM, EA, and MET extracts with a percentage yield < 1% (Figure 4.7)
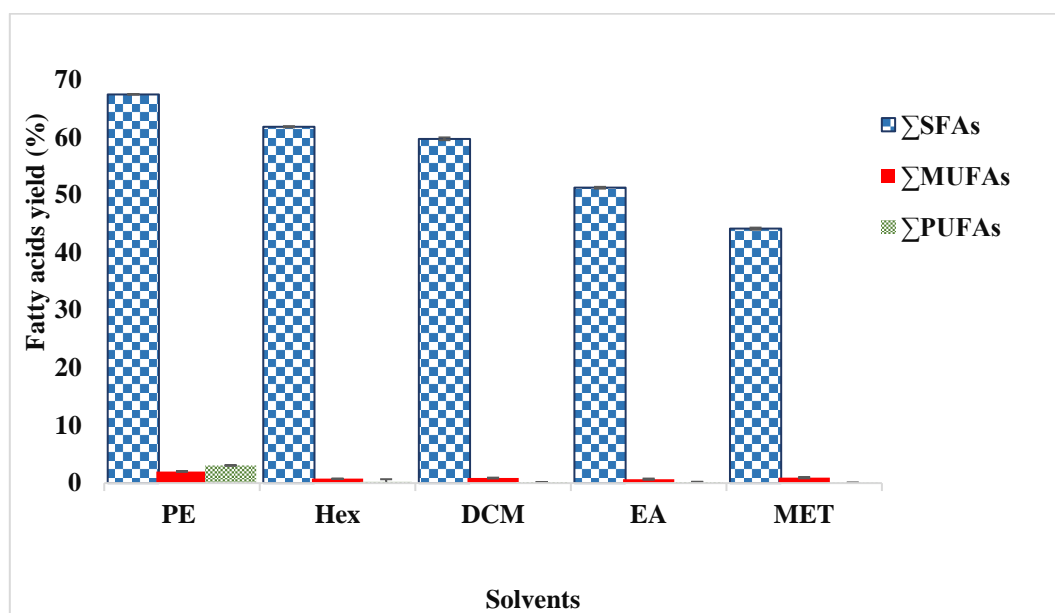
Figure 4.7: Effect of solvent polarity on the yield of saturated fatty acids ($\sum$ SFA), monounsaturated fatty acids ($\sum$ MUFA), and polyunsaturated fatty acids ($\sum$ PUFA) from BSF larvae lipid

Lauric acid was the dominant fatty acid among the saturated fatty acids, ranging from 21.69 % (MET) to 32.10 % (PE), followed by palmitic acid, which ranged from 15.23 % (DCM) to 18.79 % (PE). Among the saturated fatty acids, stearic acid (EA; 0.07 to PE; 0.40 %) and caprylic acid (MET; 3.89 to PE; 2.12 %) were found in lower percentages. The percentage yields of linoleic acid produced by Hex (0.08 %) and DCM (0.07 %) were not significant (p >0.05). This study's findings were consistent with previous research, which revealed a similar trend in fatty acids and suggested that solvent polarity influenced the fatty acid composition of BSF larvae lipids (Nezhdbahadori et al., 2018; Juhaimi, et al., 2019; Ravi et al., 2019). The next section discusses the principal component of statistical analysis

4.4.1.3 Principal component analysis (PCA)

The principal component (PCA) is a statistical method used to reduce a large set of variables into a new set of variables known as principal components. PCA was used in this study to visualise the position of the variables in two-dimensional space and to explain the effect of solvent type (DCM, EA, MET, Hex, and PE) on BSF larvae lipid yield and fatty acid composition. PCA was also used to demonstrate the relationships between individual fatty

acids. The projection of the PCA biplots on the plane which is formed by the first principal component (PC 1) and the second principal component (PC 2) is illustrated in Figure 4.8.
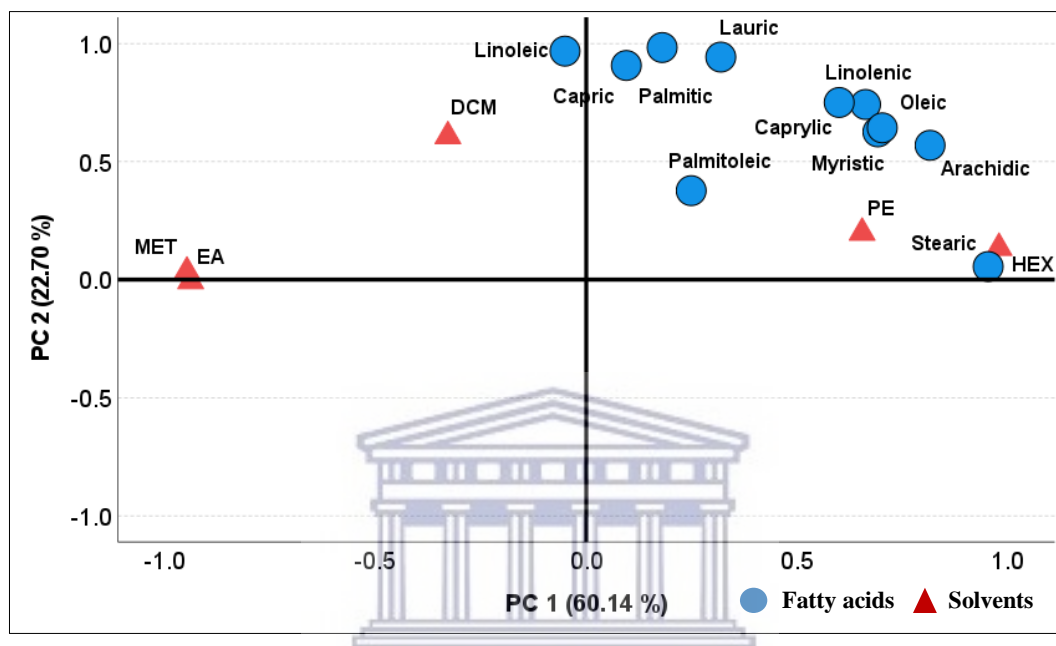
Figure 4.8: Component analysis （PCA） showing the effects of solvent types lipid yield and fatty acid composition of BSF larvae lipid

PC 1 and PC 2 account for 82.84 % of the data variance. The first principal component (PC 1) explained 60.14 % of the variability in the data set, while the second (PC 2) explained 22.70 %. According to the Kaiser rule, principal components with eigenvalues greater than one are retained. Eigenvalues are the coefficients of loadings that explain whether the PCA describes all variables in the data. The biplot in Figure 4.8 clearly showed that the solvents were grouped based on their polarity. Non-polar solvents (PE and Hex) are clustered together, resulting in higher lipid yield and fatty acids: Lauric acid, palmitic acid, oleic acid, caprylic acid, capric acid, arachidic acid, myristic acid, palmitoleic acid, stearic acid, linolenic acid, and linoleic acid. Whereas Met and EA, which are polar solvents, were observed to have the lowest lipid and fatty acid contents. DCM was found to have higher lipid and fatty content than Met and EA. These findings demonstrated that solvent polarity has a significant impact on the BSF larvae's lipid yield and fatty acid composition. Similarly, studies indicated that solvent polarity

influenced the lipid yield and fatty acid profile of BSF larvae lipids (Juhaimi, Uslu, Elfadıl E Babiker, et al., 2019; Jisieike & Betiku, 2020). The relationships between the different fatty acids were evaluated from PCA loading plots shown in Figure 4.9.
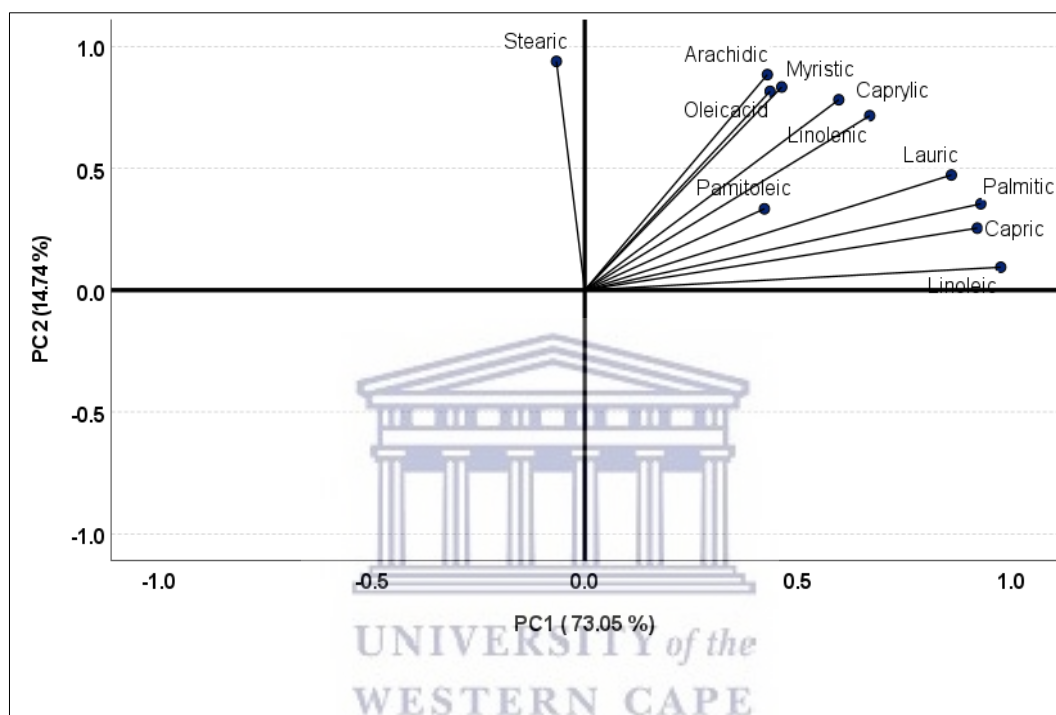
Figure 4.9: Component analysis（PCA）showing the correlation between fatty acids of the BSF larvae lipid

 PC 1 and PC 2 the Biplot (Figure 4.9) described 87.79 % of the total variation of the fatty acid extracted. PC 1 and PC 2 described 73.05 and 14.74 % of the total variance, respectively. To interpret how variables correlate with one another on the loading plots, a small angle between variables and the closeness between them implies a positive correlation between them, while variables opposite one another or forming an angle of about 180 ° suggests a negative correlation. There is no correlation between two variables when an angle of about 90 ° is formed between two variables. From the biplot, the two vectors formed by linoleic acid and stearic acid form an angle of approximatively 90 ° suggesting that there is no correlation between the two fatty acids. Lauric acid on the other hand was close to most of the fatty acids.

For instance, it has a strong positive correlation with palmitic acid, caprylic acid, and linoleic acid and a positive correlation with the other fatty acids except for palmitoleic acid and stearic acid where there was a very weak correlation. Palmitic acid has a strong positive correlation with capric acid and linoleic acid. Oleic acid has a strong positive correlation with caprylic acid, arachidic acid, and myristic acid. Caprylic acid and arachidic acid were both strongly positively correlated with linolenic acid. In this study, no negative correlation was found among the individual fatty acids in the BSF larvae.

4.4.2   Effect of extraction time on black soldier fly larvae lipid yield

This section presents the effect of extraction time on the BSF larvae lipid yield. Extraction time was taken into consideration because appropriate timing allows maximum interaction between the solvent and the lipid molecules to achieve the maximum lipid yield. The experiment was conducted in a Soxhlet apparatus using 8 g freeze-dried BSF larvae powder and 300 mL petroleum ether at 70 ^{0}C according to the analytical procedure detail in section 3.3.2.1.1. Three different extraction times (which were 2, 4, and 6 h) were investigated to ascertain the optimum extraction time. Each experiment was conducted 5 times and the final value was the average of all. Table 4.6 showed the amount of lipid extracted from the BSF larvae at different extraction times.

Table 4.6: Variation of BSF larvae lipid yield according to the extraction time using Soxhlet extraction technique (n = 5 Reaction condition: Temperature = 70 ^{0}C, Volume petroleum ether = 300 mL , weight of the sample = 8 g)

	Lipid yield (%)		
Replication	2 h	4 h	6 h
1	31.41	43.03	33.25
2	31.11	37.00	34.68
3	34.87	45.10	34.42
4	31.50	43.60	34.50
5	31.20	43.95	34.75
Mean ± SD	32.02 ± 1.60	42.54 ± 3.19	34.32 ± 0.61

From the obtained results, it was observed that the extraction time significantly ($P < 0.05$) influenced the BSF larvae lipid yield (32.02, 42.54, and 34.32 % for 2, 4, and 6 h of extraction, respectively). The BSF larvae lipid yield increased significantly from 2 h (32.02 %) to 4 h (42.54 %) then decreased to 34.32 % at 6 h of extraction time (Figure 4.10). As a result, 4 h was chosen as the optimal time for the extraction of BSF larvae lipid
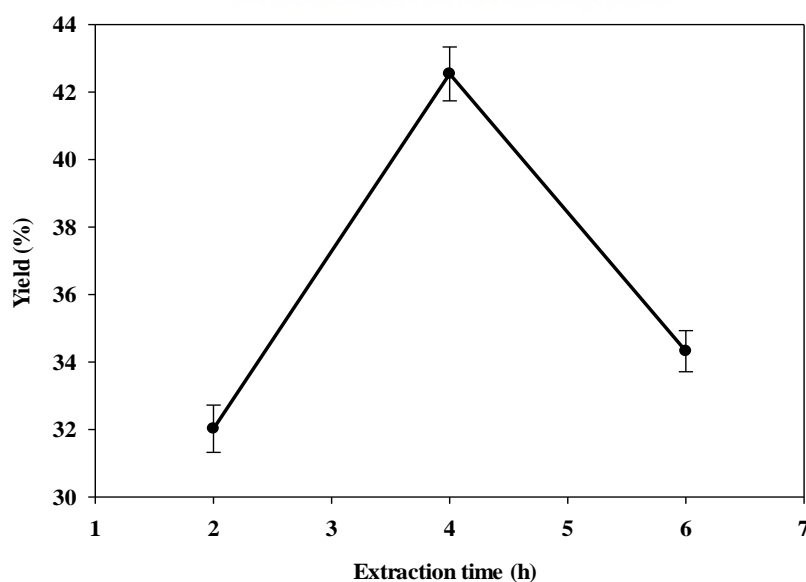
Figure 4.10: Effect of extraction time on the BSF larvae lipid yield using Soxhlet extraction (Reaction condition: Temperature = 70 °C, Volume of petroleum ether = 300 mL, weight of sample = 8 g)

The fact that the amount of lipid extracted increased from 2 h (32.02 %) to 4 h (42.54 %) could indicate that there was enough time to ensure that all of the lipids were extracted at that point. However, after 4 h of extraction, there was no further increase and the lipid yield decreased to 34.32 %, most likely due to bioactive substance losses during the longer heating time of the Soxhlet extraction process. The findings of this study agree with those of several other researchers (Al-sumri et al., 2016; Niawanti et al., 2019). The effect of extraction time on BSF larvae lipid yield has been investigated in a few studies. Ishak et al. (2018) reported a BSF larvae lipid yield of 56 % using 30 g of dried BS larvae, petroleum ether as a solvent, and a 6 h extraction time. On the other hand, Ravi et al. (2019) reported a lipid yield of 36.41 % when using 25 g dried BSF larvae, 6 h extraction time with hexane. Their yields were lower than the one reported in this study since 8 g of BSF larvae yielded a lipid of 42.54 % after 4 h of extraction time, as opposed to the larger quantity of BSF larvae sample and longer extraction time used by Ishak et al. (2018) and Ravi et al. (2019). It is believed that they may have achieved a higher yield by increasing the volume of the solvent used, as theirs was only about 250 mL, which may not have been enough to dissolve all of the lipids from the BSF larvae sample or by increasing their extraction time.

The current study found that extracting 8 g of BSF larvae lipid for 4 h was sufficient to dissolve the optimum amount of lipid in the extraction solvent (300 mL petroleum ether) at a temperature of 70 °C. Based on the findings of this study, researchers should select an extraction time that allows the solvent to dissolve all of the lipids in the sample while also preventing the degradation of the sample lipid's constituents. The effect of the extraction time on the fatty acids composition of the BSF larvae, which can be further explored, was not investigated in this study. The following section investigated the effect of the solid to solvent ratio on lipid yield.

4.4.3 Effect of the solid to solvent ratio on the yield of extracted lipid

The results of the effect of the solid to solvent ratio on lipid yield are presented in this sub-section. The solid to solvent ratio is expressed as the ratio of the weight of the extraction sample (g) to the volume of solvent (mL) (Elboughdiri, 2018). This is an important parameter that must be studied to reduce the costs and the quantity of the solvent to be used. Soxhlet extraction (SE) was carried out on three extraction weights, 5, 8, or 11 g, with 300 mL of petroleum ether to give a solid to solvent-ratios of 0.02 0.03 or 0.04 g/mL respectively. The fixed parameters were the extraction time (4 h) and the temperature (70 ºC). Table 4.7shows the effect of the solid to solvent ratio on the yield of extracted lipid.

Table 4.7: Effect of solid to solvent ratio on the BSF larvae lipid yield using Soxhlet extraction method (n = 5, Reaction condition: Temperature = 70 ^{0}C, Volume petroleum ether = 300 mL).

Replicate	Lipid yield (%)		
	0.02 g/mL	**0.03 g/mL**	**0.04 g/mL**
1	37.55	43.03	38.26
2	34.00	37.00	35.00
3	29.71	45.10	35.00
4	34.60	45.20	35.10
5	34.12	43.42	35.24
Mean ± SD	33.75 ± 3.93	41.71 ± 4.21	36.09 ± 1.88

The results in Table 4.7 indicate that the lipid yield was significantly affected by the solid to solvent ratio ($P < 0.05$). The optimum lipid yield was obtained with a solute-solvent ratio of 0.03 g/mL (41.71 %) followed by 0.04 g/mL (36.09 %) and 0.02 g/mL (33.75 %) (Figure 4.11)
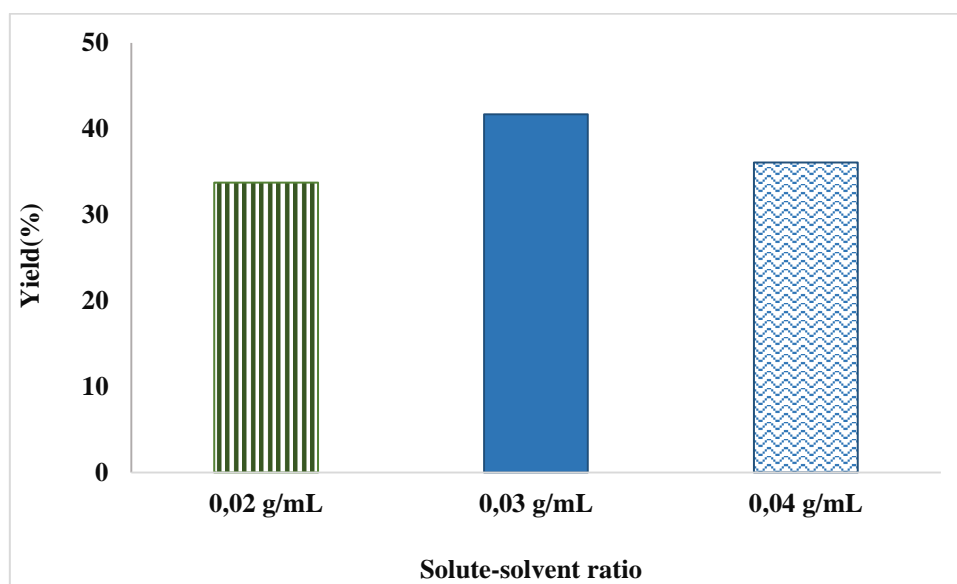
Figure 4.11: Effect of solid to solvent ratio on the BSF larvae lipid yield using Soxhlet extraction (Reaction conditions: Temperature = 70 °C, Volume of petroleum ether = 300 mL, Extraction time = 4 h)

The solute-solvent ratio of 0.02 g/mL gave the lowest lipid yield (33.75 %). This was probably because the solution might reach a saturated state in which some of the lipids in the sample remained unextracted. Therefore, an excess amount of sample might require more solvent volume and extraction time to achieve the optimum yield of extracted lipids. The result in this study agrees with Norshazila et al. (2017) in which the amount of carotenoids extracted from pumpkin increased as the solid to solvent ratio increased until the equilibrium was reached. Elboughdiri (2018) also discovered a similar result after extracting phenolic compounds from olive leaves. However, in this present study further increase of the solid to solvent ratio thus did not increase the lipid yield. This was attributed to the fact that 300 mL of solvent was not able to extract all the lipid from the sample (11 g). Hence, sufficient solvent is needed to reach the equilibrium between solid and solvent. Therefore in this study, the optimum conditions; 0.03 g/mL (solid to solvent ratio) and extraction time 4 h at 70 °C gave the best lipid yield.

The solid to solvent ratio has a high impact on lipid yield; however, researchers have yet to investigate the variation of this parameter in BSF larvae lipid using Soxhlet extraction. For example, Smets et al. (2020) investigated lipid extraction from BSFL larvae, using 5 g dried BSF larvae and 120 mL solvent (or a solid to solvent ratio of 1:24 g/mL), while other

parameters such as solvent polarity were varied. Ravi et al. (2019) used Soxhlet extraction with 25 g of BSF larvae and 250 mL to study the effect of different solvents on BSF larvae to identify an optimal green solvent from a wide array of solvents. As a result, the current study was critical to propose an optimal solid to solvent ratio to reduce extraction costs (solid to solvent ratio, and extraction time). In this study, a solid-to-solvent ratio of 0.03 g/mL was found to be the optimal ratio for achieving a high yield of the BSF lipid.

4.5   Chapter summary

This chapter explained the effects of experimental parameters which needed to be optimized for optimal lipid extraction from BSF larvae and investigated the extraction conditions influencing the extraction yield. BSF larvae lipid was extracted using three extraction methods such as maceration (ME), Soxhlet (SE), and ultrasonic-assisted extraction (UAE)). The type of extraction method was found to affect significantly ($P < 0.05$) both the lipid yield and the fatty acids composition. Among the extraction methods investigated in this study, SE was found to be a more suitable method due to its high lipid yield and good fatty acid composition while the maceration extraction method gave the lowest lipid yield and fatty acid composition. Although Soxhlet extraction is a traditional method of extraction, this current study has shown that it is an appropriate method for extracting lipid from BSF larvae, which can be carried out at an industrial level.

The findings from this study confirm that methods used for the extraction affect the fatty acids composition of the BSF larvae. As a result, it was critical to pay attention not only to the lipid yield obtained from SE, UAE, and ME but also to the components of the fatty acid recovered during the extraction process. It was found that BSF larvae lipid contained mainly saturated fatty acids (SFAs) with lauric acid as the dominant SFA in all the methods of extraction used. This was explained by the fact that SFAs are naturally produced by larvae (Spranghers et al., 2017). Also, BSF larvae store SFA as their source of energy at the adult stage since they are less prone to oxidation (Ewald et al., 2020). On the other hand, polyunsaturated fatty acids (PUFAs) such as linoleic acid (0.08-0.19%) and linolenic (2.88-3.39 %) were found at a low percentage in the BSF larvae lipid. This suggests that the BSF larvae are not able to synthesise them and originated from their feed. In terms of lipid and fatty acid content, BSF larvae are a promising source for exploitation and studies should be conducted to investigate the incorporation of omega-3 fatty acids (linolenic acid, eicosapentaenoic acid, and

docosahexaenoic acid) from the diet into the larval lipid of the BSF, as they have been shown to have medical applications.

Because SE produced a better fatty acid profile and lipid yield than the ME and UAE method, extraction parameters such as time, solvent to solid ratio, and solvent polarity were investigated to determine the optimum extraction conditions of the Soxhlet extraction method. The results show that a good recovery of the BSF larvae lipid and fatty acids composition was achieved using petroleum ether (PE) at 70°C, a solvent to solid ratio of 0.03 g/mL, and an extraction time of 4 h. BSF larvae lipid was better extracted with non-polar solvents such as PE and Hex as they resulted in a higher yield compared to the other solvents. A polar solvent such as methanol gave the lowest lipid recovery which might be attributed to poor solubility of the non-polar lipids in the most polar solvent. The findings of this study prove that there is an alternative more environmentally friendly solvent (petroleum ether) that could replace the often used solvent (chloroform) which is known for its toxicity. The application of PE in this study could be the first step toward implementing the process on a large scale, as well as a good starting point for further research into continuous process optimisation, which is of great industrial interest
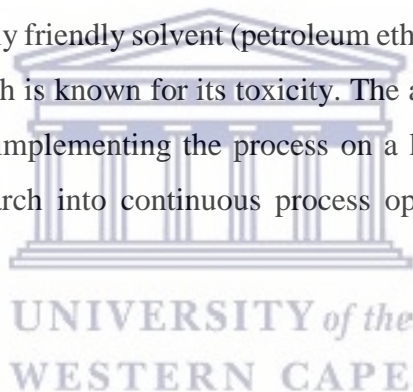
CHAPTER 5: BLACK SOLDIER FLY LARVAE LIPID FRACTIONATION AND CHARACTERISATION

Abstract

Lipids are made up of a diverse group of compounds that must be separated into individual lipid fractions for various applications. This chapter aimed at fractionating the lipid extracted from black soldier fly (BSF) larvae into separated constituents and further characterise each lipid fraction. Thin layer chromatography (TLC) and a silica gel column chromatographic procedure were used to fractionate the lipid while gas chromatography flame ionisation (GC-FID), Fourier-transform infrared spectroscopy (FTIR), and nuclear magnetic resonance (NMR) spectroscopy were used to characterise the lipid fractions. The chromatography on a single silica column with solvent mixtures of increasing polarity resulted in the complete separation of cholesterol esters, triglycerides, cholesterol, fatty acids, diglycerides, and monoglycerides. Triglyceride was the main component of BSF larvae lipid while cholesterol esters and cholesterol were the least abundant lipid fractions. The composition of the triglycerides, diglycerides, monoglycerides, and fatty acids subcomponents were further determined using gas chromatography flame ionisation detection (GC-FID) and the results showed that lauric acid, trilaurin, dilaurin, and monolaurin were the main subcomponent of the fatty acids, triglycerides, diglycerides, and monoglycerides fractions. The fractionation methods were effective for separating the lipid classes from BSF larvae lipid

Graphical abstract

Black soldier fly larvae lipid

Fractionation

Lipid fractions

CE   TGA   FA   C   DG   MG

CHARACTERISATION

GC-FID FTIR, NMR
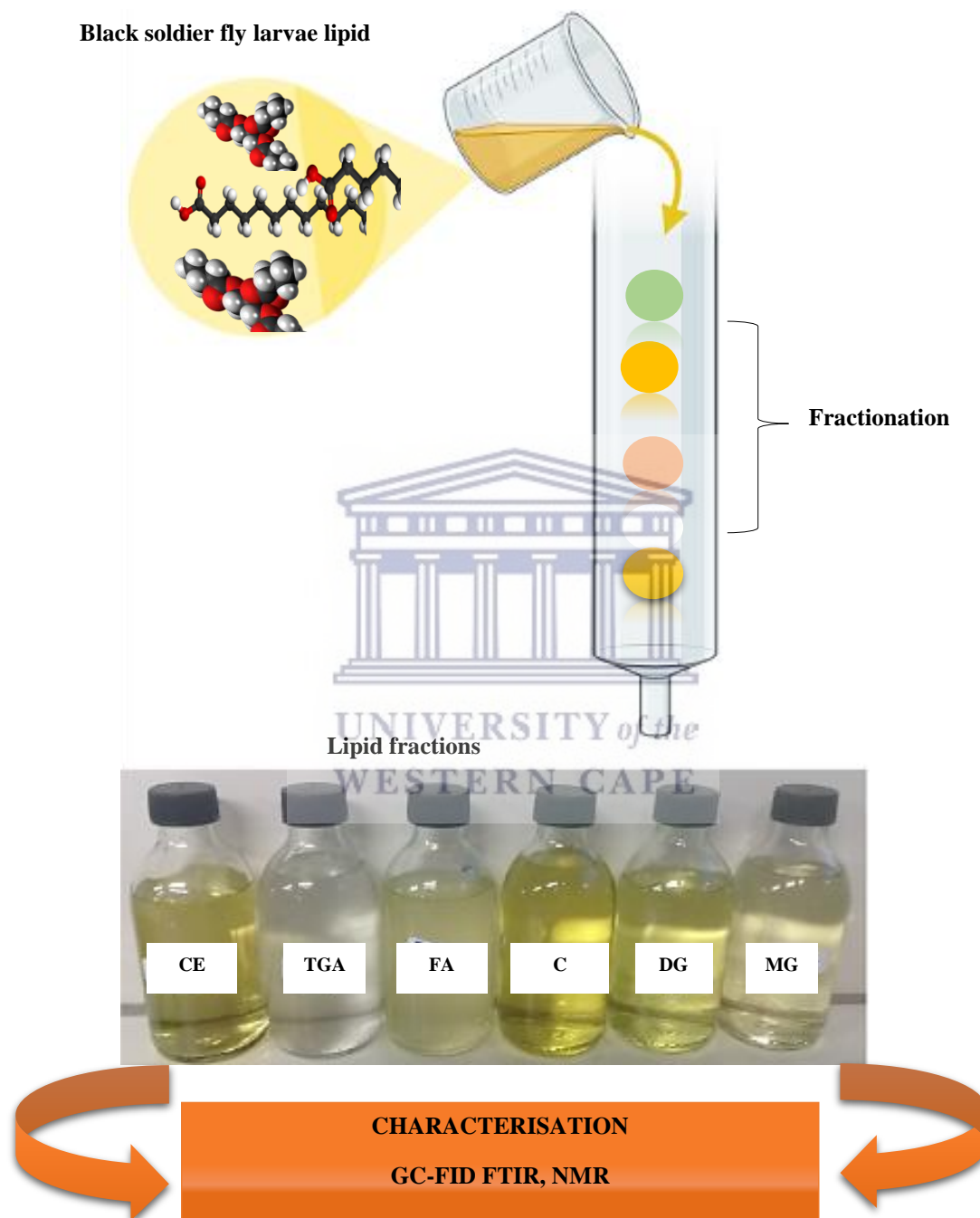
5.1   Introduction

Column chromatography was found to be a useful procedure for the fractionation of lipid from various samples (Yang et al., 2017; Hudiyanti et al., 2018; Soetjipto et al., 2019). Among the type of column chromatography (adsorption chromatography, ion-exchange chromatography, and partition chromatography) adsorption chromatography is based on the distribution of the sample between the stationary (silica) and the mobile (solvents) phases. This technique is considered the most used method for separating lipid components. After the sample has eluted from the column, the purity is checked using thin layer chromatography (TLC). Several characterisation methods have proven to be useful and effective for the quantification and qualification of the lipids and the method to employ depends on the compounds present and of interest. Gas chromatography flame ionisation in this study (GC-FID-7820 A and GC-FID-7890 B) among all techniques proved to be the most effective method in the characterisation of the lipid into groups and further characterisation of each group into sub-groups, giving their percentage compositions. The gas chromatography used in this study (Agilent 7820 A) was applied specifically to determine the subcomponents of the triglycerides, diglycerides, and monoglycerides, while the gas chromatography (Agilent 7890 B) was used for fatty acids analysis. The type of column used in each type of gas chromatography is the key difference between the two. The Agilent 7820 A column is suitable for high-temperature applications (up to 380 °C), while the Agilent 7890 B column has a temperature limit of 250/260 °C. Spectroscopy methods such as Fourier-transform infrared spectroscopy (FTIR) and nuclear magnetic resonance (NMR) spectroscopy are also other possible characterisation methods that can give good results useful for validating the results of the gas chromatography.

5.2   Fractionation of lipids from the black soldier fly larvae

This section investigated the fractionation of the lipid extracted from the black soldier fly (BSF) larvae using silica gel column chromatography and thin-layer chromatography (TLC). The fractionation of lipid from the BSF larvae into lipid groups using silica gel column chromatography is detailed in section 3.3.3.1. Briefly, BSF larvae lipid was fractionated by loading 50 g of lipid into a glass chromatographic column (6 cm i.d. x 70 cm L) packed with approximately 40 g of silica gel. The different lipid fractions, which include cholesterol esters (CE), triglycerides (TGA), fatty acids (FA), cholesterols (C), diglycerides (DG), and monoglycerides (MG), were eluted sequentially with 100 % of hexane, a mixture of 5 % diethyl

100

ether in hexane, 15 % diethyl ether in hexane, 25 % diethyl ether in hexane, 50 % diethyl ether in hexane and 2 % methanol in diethyl ether respectively. Elution carried out at room temperature was collected in 10 mL fractions. A 25 µL aliquot of each fraction eluted from the column was analysed using thin-layer chromatography (TLC) to identify the lipid class present and evaluate the completeness of separation. The TLC procedure as detailed in section 3.3.3.2 and involves two phases: A stationary phase which consisted of a plate made of a plastic sheet coated with silica and a mobile phase which consisted of a solvent system composed of hexane, diethyl ether, and acetic acid in the ratio 85:25:2 (v/v/v). Subsequently, the TLC plate was then inserted into the developing chamber containing the mobile phase. The developing chamber was sealed to prevent evaporation of the solvent. After the TLC plate's development, spots representing the different lipid fractions on the TLC plates were visualised by spraying the plate with vanillin. Thereafter, it was heated up on a hot plate to char the organic material, allowing the spots to be visible. Eluate fractions containing the same lipid class were combined, and the solvents were evaporated using a rotary evaporator as described in section 3.3.2.1.4. The mass percentage was calculated using Equation 3.2 (section 3.3.3.1)

$$mass\ percent = \frac{mass\ lipid\ fraction\ (g)}{mass\ of\ the\ lipid\ (g)} x 100\ \% \quad \text{Equation 3.2}$$

Table 5.1 shows the mass (g) and mass percent (%) obtained from the different lipid fractions as well as their physical characteristics

Table 5.1: Mass, mass percent, and physical appearance of the lipid fractions isolated from column chromatography (Elution condition: Mass of the lipid= 50 g, elution time = 6 h, elution solvent= 100 % of hexane, 5 % diethyl ether in hexane, 15 % diethyl ether in hexane, 25 % diethyl ether in hexane, 50 % diethyl ether in hexane, 2 % methanol in diethyl ether to elute CE, TGA, FA, C, DG, and MG, respectively)

Lipid fractions	Mass (g)	Mass (%)	Physical Appearance
CE	0.8	1.6	yellow
TGA	15	30	milky white

FA	8	16	light orange
C	0.3	0.6	yellow
DG	10	20	green
MG	5	10	brown

CE=Cholesterol esters, TGA= Triglycerides, FA= Fatty acids, C=Cholesterol, DG= Diglycerides, MG= Monoglycerides

The mass of the lipid fractions CE, TGA, FA, C, DG, and MG were 0.8, 15, 8, 0.3, 10, and 5 g for and their mass percentage was 1.6, 30, 16, 0.6, 20, and 10 %, respectively. The most abundant lipid group was the TGA (30%), followed by the DG (20 %) and the FA (16 %). CE (1.6 %) and C (0.6 %) were the least abundant lipid fractions (Figure 5.1).
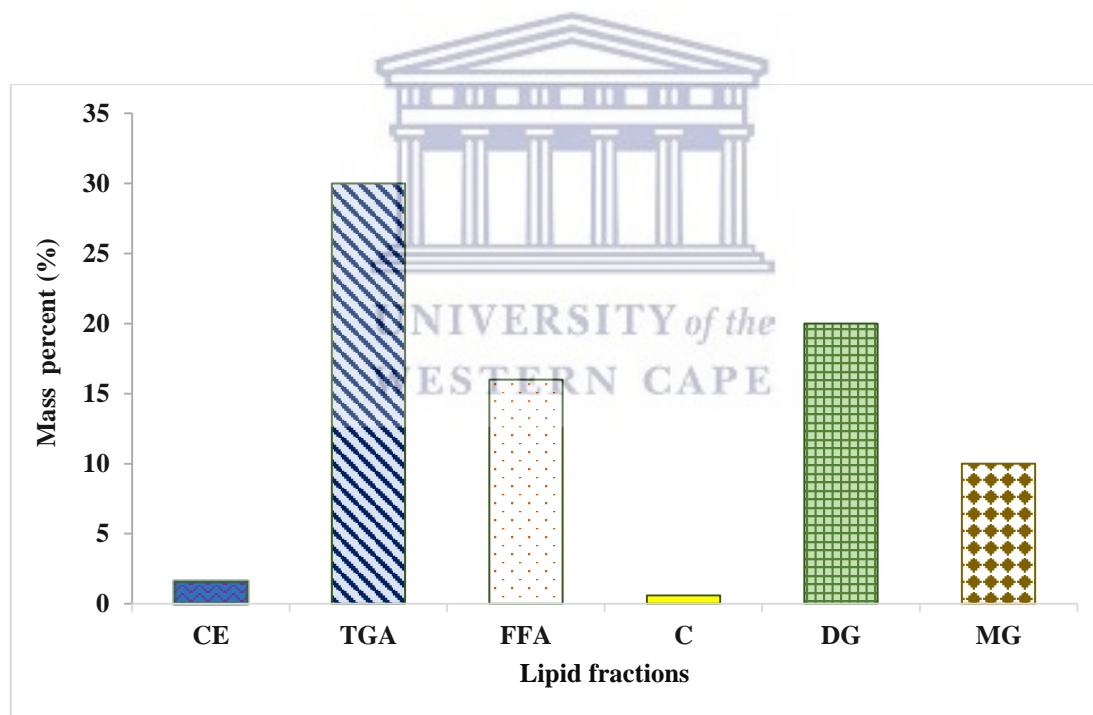
Figure 5.1: Mass percent of different lipid fractions (Elution condition: elution time = 6 h, elution volume = 100 % of hexane, 5 % diethyl ether in hexane, 15 % diethyl ether in hexane, 25 % diethyl ether in hexane, 50 % diethyl ether in hexane, 2% methanol in diethyl ether to elute CE, TGA, FA, C, DG, and MG, respectively)

The different fractions are solid at room temperature with a distinguishable colour as shown in Figure 5.2. They appear as yellowish for (C and CE), milky white (TGA), orange (FA), green (DG), and brown (MG).
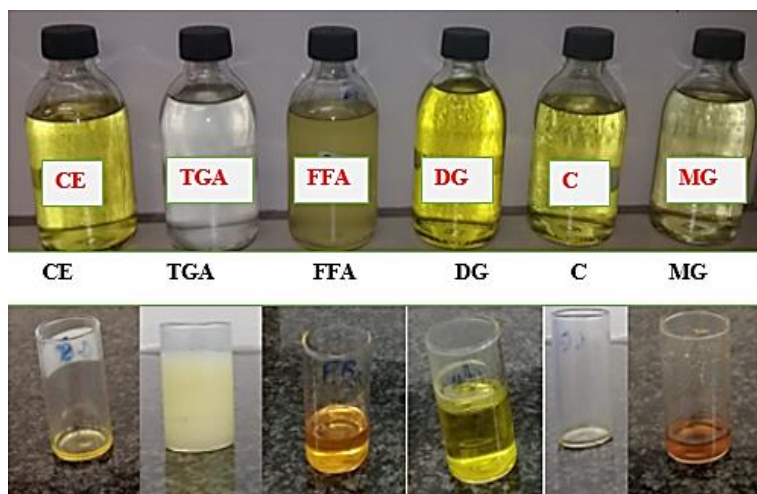
Figure 5.2: Lipid fractions eluted from column chromatography (Elution condition: elution time = 6 h, elution volume = 100 % of hexane, 5 % diethyl ether in hexane, 15 % diethyl ether in hexane, 25 % diethyl ether in hexane, 50 % diethyl ether in hexane, 2 % methanol in diethyl ether to elute CE, TGA, FA, C, DG, and MG, respectively)

Figure 5.3 shows the TLC chromatographic plate of the lipid fractions (a) and the lipid extracted (b) from the BSF larvae. The TLC chromatographic plate was developed in a solvent mixture of hexane, diethyl ether, and acetic acid in the ratio 85:25:2 (v/v/v).
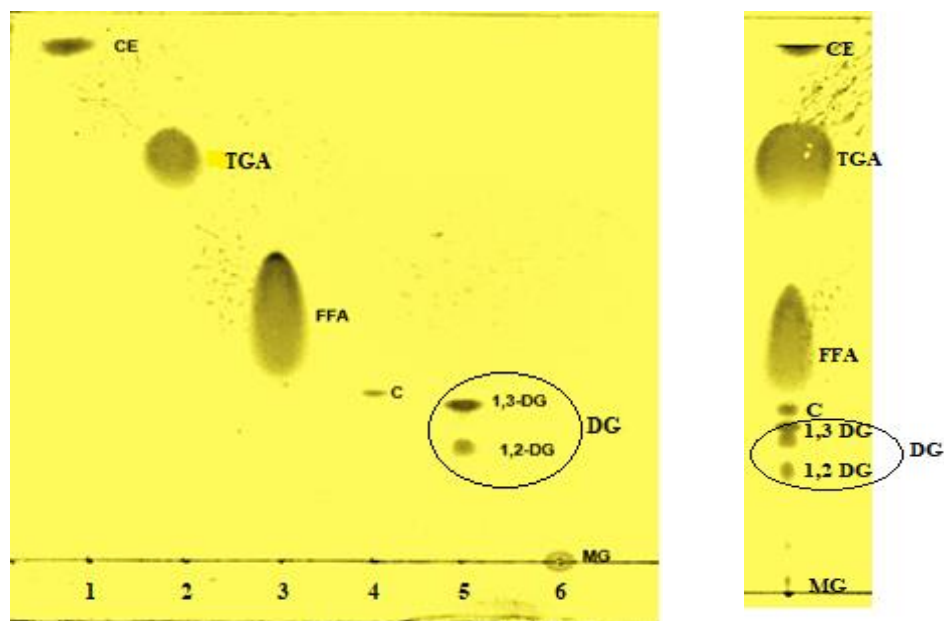
lipid fractions (a)   BSF larvae lipid
                                                       extract (b)

Figure 5.3: TLC chromatographic plate of lipid fractions obtained by column chromatography and the lipid extract (b) (TLC Solvent system: hexane, diethyl ether, and acetic acid in the ratio 85:25:2 (v/v/v)

Each spot (1 to 6) on the TLC chromatographic plate (Figure 5.3a) represents a combination of eluted fractions containing the same lipid class. Before the fractionation of the BSF larvae lipid using silica gel glass chromatography, TLC analysis of the BSF larvae lipid (b) was performed to ascertain how many classes of components are present in the BSF larvae lipid. The TLC chromatographic plate revealed six spots separated from the BSF larvae lipid indicating that there are six compounds present in the BSF larvae lipid. Those compounds were identified as cholesterol esters (CE), triglycerides (TGA), fatty acid (FA), cholesterol (C) diglycerides (DG), and monoglycerides (MG) by comparing them to the literature (Pengon et al., 2012; Nasopoulou et al., 2013; Oellig et al., 2018). As can be seen in Figure 5.3b, DG has two structural isomers (1, 2-DG and 1, 3-DG) indicated in the two circled spots. The retention factor (Rf) values of the lipid fractions were summarised in Table 5.2.

Table 5.2: Retention factor (Rf) values of the lipid groups in a solvent system of hexane, diethyl ether, and acetic acid in the ratio 85:25:2 (v/v/v)

Lipids	Rf value	Polarity
CE	0.94	Non-polar
TGA	0.75	Non- polar
FA	0.44	polar
C	0.30	polar
1,3-DG	0.25	polar
1,2-DG	0.22	polar
MG	0	polar

The retention factor (Rf) which is a unitless number is calculated as the ratio of the distance travelled by the compound to the distance travelled by the mobile phase (solvent). The Rf values for the different lipid fractions were 0.94, 0.75, 0.44, 0.3, 0.25, 0.22 and 0 for CE, TGA, FA, C, DG (1, 3-DG and 1, 2-DG) and MG fractions, respectively. This is characterised by the polarity of the compound, indicated by the number of hydrocarbon chain(s) and the presence or absence of hydroxyl group. The Rf values as seen from the table decreases in this order: MG < DG < C < FA < TGA < CE. The difference in the Rf values of the lipid fractions was due to their different interaction with the polar adsorbent silanol group (Si–O–H) of the silica gel coated on the TLC plate. The higher polar compound interacts strongly with the silanol group on silica gel when compared to the less polar compounds.

The highest Rf values were obtained by CE (0.94) and TGA (0.77), indicating that they were the least polar compounds hence have less interaction with the polar adsorbent on the TLC plate. The MG fraction, on the other hand, did not deviate from the baseline due to its high affinity for the polar adsorbent. However, it must be noted that the inability of the MG to deviate was based on the effect of the solvent system (hexane: diethyl ether: acetic acid 85:25:2 v/v/v) used as the mobile. This means that the solvent system was not polar enough to remove the polar compound (MG) off the extremely polar silica gel.

MG has two free hydroxyl groups (OH) and one hydrocarbon chain, making it a more polar compound than DG with one free OH and two hydrocarbon chains, and TGA, with three

hydrocarbon chains and no free OH, is the least polar compound among the three. The lipid fractions' Rf values were in good agreement with their polarity as well as similar results reported by (Pengon et al., 2012; Sonam et al., 2017; Oellig et al., 2018).

The study revealed that the lipid of the BSF larvae is made of complex mixtures of TGA, DG, MG, FA, and other minor components such as cholesterol and cholesterol esters which were present in small amounts. The TGA fraction had a greater mass percentage (30 %) than the other lipid fractions because BSF stores primarily TGA during the larval stage to aid their survival at the adult stage, where they do not feed (Bertinetti et al., 2019; Tomberlin & van Huis, 2020). The BSF survives in the adult stage without food by recycling the TGA stored in the larval stage. TGA is broken down into MG and DG during digestion with the help of enzymes and then converted back to TGA once in the bloodstream (Alves-Bezerra & Cohen, 2018). Because DG, MG, and FA have numerous applications in the food industry, maximizing their yield can be very beneficial. This can be accomplished through the transesterification reaction, which is a chemical conversion process that uses a conventional catalyst (e.g., NaOH and KOH) to break down TGA into either MG, DG, or FA. To demonstrate this, an experiment was carried out in this study to synthesize FA from the TGA of BSF larvae. The result was a white solid made of FA (Appendix 1). Other researchers such as Ezigbo & Emmanuella, (2016), have done a similar experiment with coconut lipid rich in TGA. They identified the end product as lauric acid which is a saturated fatty acid.

Analytical procedures for the separation of lipid from various sources have become increasingly complex in recent years, and as a result, they have become more expensive. However, even with a relatively simple analytical procedure, good results can be obtained. This was demonstrated in this study by the optimisation of solvent mixtures to separate the different lipid classes using thin-layer chromatography (TLC) and silica gel column chromatography techniques. TLC and column chromatography procedures developed in this study proved to be effective in separating lipid from BSF larvae into lipid groups. Several researchers have developed various solvent mixture schemes to fractionate lipids from various sources into lipid classes using TLC and column chromatography (De Clercq et al., 2008; Nasopoulou et al., 2013) The aforementioned researchers used a solvent mixture of chloroform, acetone-methanol, and acetic acid in different ratio as a mobile phase for the TLC separation. However, in this study, highly toxic chloroform and acetone were replaced with less toxic hexane and diethyl ether.

Solid-phase extraction (SPE) was used by several researchers (Anna et al., 2017; Traversier et al., 2018; Wolfshorndl et al., 2019; Alves et al., 2020) to separate lipids into lipid classes. This method applies the same chromatographic principles as column chromatography but is only effective for the separation of lipid into lipid classes in very small quantities (as per mg) also, some researchers used high-performance liquid chromatography (HPLC) for the separation of lipid since it offers the possibility of collecting fractions for further analysis. However, the use of the SPE and HPLC were not suitable for this current study because a large amount (as measured in grams) of lipid classes was needed for further analysis. The next section discusses the different characterisation methods for the lipid fractions.

5.3   Characterisation methods

In the section, the purity and quantification of the isolated compounds were further validated using three characterisation techniques: Gas chromatography (GC-FID), Fourier-transform infrared spectroscopy (FTIR), and nuclear magnetic resonance (NMR) spectroscopy. The following subsection discussed the separation and identification of the different lipid fraction sub-components using gas chromatography flame ionisation (GC-FID).

5.3.1   Gas chromatography (GC-FID)

Gas chromatography analysis was carried out in triplicate to determine the composition of the triglycerides (TGA), diglycerides (DG), monoglycerides (MG), and fatty acids (FA) subcomponents. Gas chromatography was performed according to the analytical methods discussed in section 3.3.5.1.2. Each compound was identified by comparing its retention time to the retention time of a known standard listed in section 3.2.1. The mass percent of the TGA, DG and MG subcomponents were calculated according to Equations 3.7, 3.8, and 3.9 in section 3.3.5.1.2 respectively. Tables 5.3 and 5.4 summarises the composition of the lipid subcomponents in each class and the fatty acids composition in TGA, DG, and MG fractions, respectively.

Table 5.3: BSF larvae lipid subcomponents in each class using GC-FID. Values are represented as mean ± SE of three independent measurements n = 3. GC condition: CP-TAP-CB capillary column (25 m x 0.25 mm, 0.10 µm), oven programming from 70 to 380 °C. run time (16 min), FID 380 °C, Injection volume (0.5 µL of 0.05 % lipid in hexane) Carrier gas (Helium; 4 mL/min)

Lipid subcomponents	% composition of the lipid subcomponents
Triglyceride subcomponents	
Trilaurin	27.32 ± 0.03
Tristearin	12.40 ± 0.15
Tripalmitin	13.10 ± 0.06
Triolein	11.27 ± 0.06
Trilinolenin	17.17 ± 0.01
Trilinolein	16.21 ± 0.01
Diglyceride subcomponents	
Dipalmitin	25.10 ± 0.01
1,3 Distearin	18.12 ± 0.01
Dilaurin	29.26 ± 0.06
Monoglyceride subcomponents	
Monolaurin	14.50 ± 0.06
Monopalmitin	13.58 ± 0.01
Monomyristin	10.77 ± 0.04
Fatty acids subcomponents	
Lauric acid (C12:0)	27.65 ± 0.02
Myrisitc acid (C14:0)	4.85 ± 0.01
Palmitic acid (C16:0)	11.33 ± 0.03
Stearic acid (C18:0)	1.45 ± 0.09
Arachidic acid (C20:0)	2.52 ± 0.10
Palmitoleic (C16:1)	1.45 ± 0.01
Oleic acid (C18:1)	5.93 ± 0.02
Linoleic acid (C18:2)	13.07 ± 0.02
Capric acid (C10:0)	14.93 ± 0.02

Table 5.4: Fatty acids present in TGA, DG, and MG fractions. Values are represented as mean ± SE of three independent measurements n = 3. GC condition: CP-Sil 88 for FAME/HP-88 column (60 m X 250 µm ID, 0.2 µm), oven programming from 120 to 230 °C, run time (16 min), FID 280 °C, Injection volume (0.5 µL of 0.05 % lipid in hexane) Carrier gas (Helium; 4 mL/min)

(%) Fatty acid compositions in each lipid fractions		
Lipid fractions		
Fatty acids	**Triglycerides**	**Diglycerides**	**Monoglycerides**
Lauric acid	16.64 ± 0.03	19.10 ± 0.02	22.70 ± 0.01
Myristic acid	4.90 ± 0.01	3.24 ± 0.13	0.95 ± 0.02
Palmitic acid	15.95 ± 0.10	5.62 ± 0.05	5.06 ± 0.01
Stearic acid	2.44 ± 0.04	0.65 ± 0.03	0.68 ± 0.10
Arachidic acid	1.89 ± 0.11	1.55 ± 0.02	0.68 ± 0.02
Palmitoleic Acid	1.56 ± 0.02	0.77 ± 0.01	0.04 ± 0.12
Oleic acid	7.98 ± 0.01	3.22 ± 0.10	0.44 ± 0.02
Linoleic acid	13.8 ± 0.01	7.68 ± 0.02	0.26 ± 0.13

In Table 5.3, the triglycerides (TGA) fraction was found to contain 7 types of subcomponents which are trilaurin, tristearin, tripalmitin, triolein, trilinolenin, and trilinolein with a percentage of 27.32, 12.40, 13.10, 11.27, 17.17, and 16.21 %, respectively. The TGA fraction was dominated by trilaurin (27.32 %). Triolein was found to have the lowest concentration (11, 27 %). The DG fraction was composed of dipalmitin (25.10 %), 1, 3 distearin, (18.12 %), and dilaurin (29.26 %) having the highest concentration. The MG fraction comprises of monolaurin (14, 50 %), monopalmitin (13, 58 %), and monomyristin (10, 77 %). The FA fraction consists of lauric acid (27.65 %), myristic acid (4.85 %) palmitic acid (11.33 %), stearic acid (1.45 %), arachidic acid (2.52 %), palmitoleic acid (1.45 %), oleic acid (5.93 %), and linoleic acid (13.07 %) and capric acid (14.93 %). Both stearic and palmitoleic acid were found at a low concentration of 1.45 %. The results of the analysis show that lauric acid was the major fatty acid (27.75 %) followed by palmitic acid (11, 33 %). Lauric acid and its esters (trilaurin, dilaurin, and monolaurin) represented were the main subcomponents of each lipid fraction.

In tern of their fatty acids composition, the TGA, DG, and MG fractions were composed lauric acid, myristic acid, palmitic acid, stearic acid, arachidic acid, palmitoleic acid, oleic acid, and linoleic acid at different percentages as seen in Table 5.4. The percentage of lauric acid in TGA, DG, and MG were 16.64, 19.10, and 22.70 %, respectively. Myristic acid was 4.90, 3.24, and

0.95 % in TGA, DG, and MG, respectively. Palmitic acid was 15.95, 5.62, and 5.06 % in TGA, DG, and MG, respectively. Stearic acid was 2.44, 0.65, and 0.68 % in TGA, DG, and MG, respectively. Arachidic acid 1.89, 1.55, and 0.68 % in TGA, DG, and MG, respectively. Palmitoleic Acid was 1.56, 0.77 and 0.04% in TGA, DG and MG, respectively. Oleic acid was 7.98, 3.22, and 0.44% in TGA, DG, and MG, respectively. Linoleic acid 13.8, 7.68, and 0.15 % TGA, DG, and MG, respectively.

Several researchers had investigated the mono, di, and triglycerides composition using gas chromatography flame ionisation detection (GC-FID). However, the fundamental limitation of GC-FID lies in its inability to analyse directly less volatile substances. The substances must be volatile so that a finite fraction of them is distributed in the gaseous phase. Because of the low volatility of the lipid compounds, they cannot be analysed directly by the GC-FID. To make it possible, a derivatisation step, which is a process of converting a compound into a product with a similar chemical structure known as a derivative, is required. In recent years, many derivatisation techniques to increase the volatility of lipid compounds in various samples have been reported (Ponphaiboon et al., 2014; Zhang et al., 2015; Alleman et al., 2019). In the analysis of mono, di, and trilaurin from coconut oil, Ponphaiboon et al. (2014), described a derivatisation technique using silytation reaction by reacting the lipid samples with an excess amount of N,O-bis (trimethylsilyl) trifluoroacetamide (BSTFA). Alleman et al. (2019), presented the derivatisation method for monoglycerides in biodiesel samples using N-methyl n-trimethylsilyltrifluoracetamide (MSTFA). However, the derivatisation process is not a preferred option due to several issues, including a longer analysis time, high cost and instability of certain derivatisation reagents, and the chance of the formation of side products due to an incomplete or unstable reaction with the derivatisation compounds (Makahleh et al., 2010).

To overcome the shortcomings of the derivatisation step, GC-FID equipped with a medium polarity capillary column (25 m x 0.25 mm x 0.1 μm) coated with a cyanopropyl-phenyl chemically bonded polyethylene glycol (CP-TAP-CB) was employed for direct analysis of mono, di and triglyceride compounds. The capillary column type was suitable for high boiling points compounds facilitating their evaporation and detection. To the best of the author's knowledge, no study has reported on the analysis of underivatised mono, di, and triglyceride from the BSF larvae using GC-FID equipped with a medium polarity capillary column CP-TAP-CB.

5.3.2 Spectroscopy analysis

Fourier-transformed infrared spectroscopy, ^{1}H nuclear magnetic resonance spectroscopy, and ^{13}C nuclear magnetic resonance spectroscopy were used to characterise the lipid fraction. Spectroscopic analysis was carried out to confirm the identity of the lipid classes isolated from BSF larvae by assessing their functional groups.

5.3.2.1 Fourier-transformed infrared spectroscopy (FTIR)

Fourier-transformed infrared spectroscopy (FTIR) examines the functional groups of the molecules by recording the type of vibrations (stretching and bending) produced by their chemical bonds. This method was used to determine the structural features of the triglycerides (TGA), diglycerides (DG), monoglycerides (MG) and the fatty acids (FA) classes since every lipid class has unique infrared spectra. The FTIR analysis of the TGA, DG, MG and FA fractions was done as described in section 3.3.5.2 over the wavelength range of 500 to 4000 cm.[-1] Table 5.5 summarises the identification and assignment of each lipid fraction based on their FTIR absorption bands.
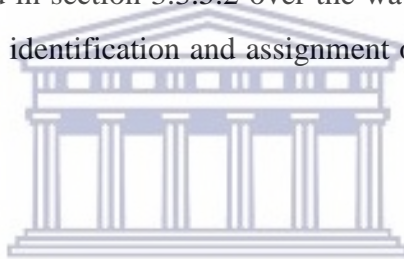
Table 5.5: Assignments of the FTIR absorption bands of the lipid fractions

Functional group	C = O	C - C - O	O – C - C	O - H	CH$_3$	CH$_2$
Vibration Intensity	Stretching medium sharp	Stretching strong broad	stretching medium	stretching strong broad	stretching Strong, sharp	stretching Strong sharp
Wavenumbers * (cm^{-1})	1760 - 1690	1210 - 1160	1100 - 1030	3300 - 2500	2950 - 2872	2920 - 2830
TGA	1753	1171	1108	none	2947	2863
DG	1747	1181	1065	3429	2932	2857
MG	1661	1117	1060	3302	2911	2958
FA	1721	1304	none	2963	2915	2866

*(Kiefer et al., 2010; Goeel, 2018; Mohammadi et al., 2020)

Assignments of the FTIR absorption bands of the lipid fractions showed that FA belongs to the carboxylic group while TGA, DG, and MG belong to the ester group. The infrared spectra of the TGA, DG, MG and FA are shown in Figures 5.4, 5.5, 5.6, and 5.7, respectively.
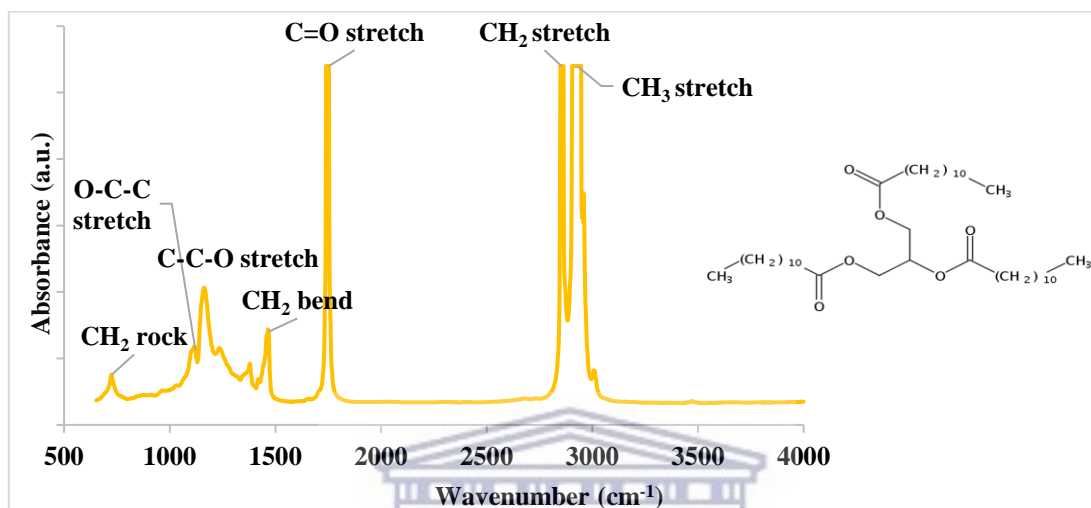
Figure 5.4: FTIR TGA fraction
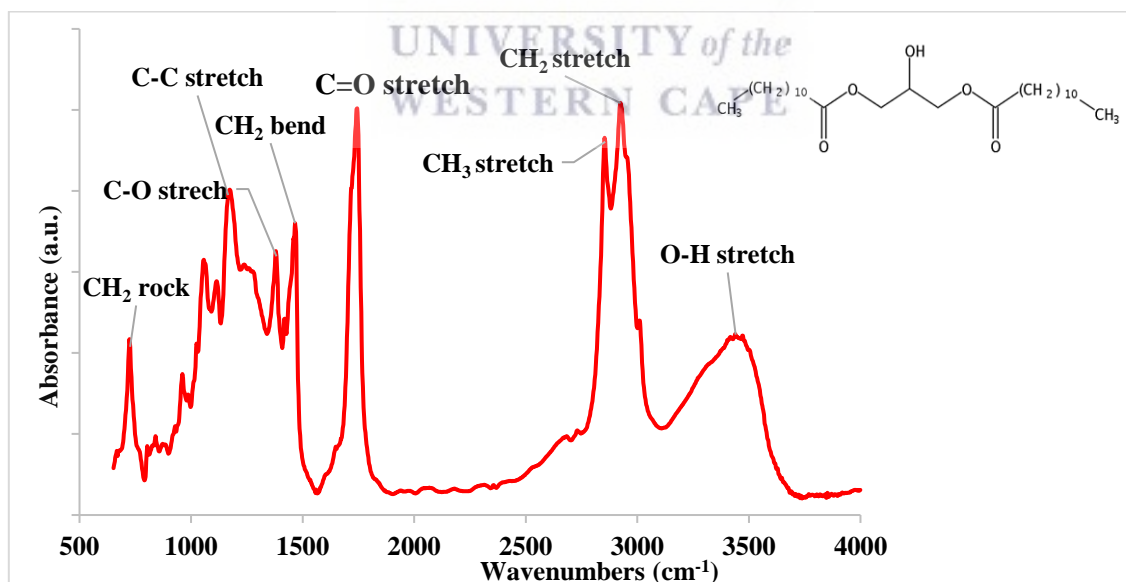
Figure 5.5: FTIR of DG fraction
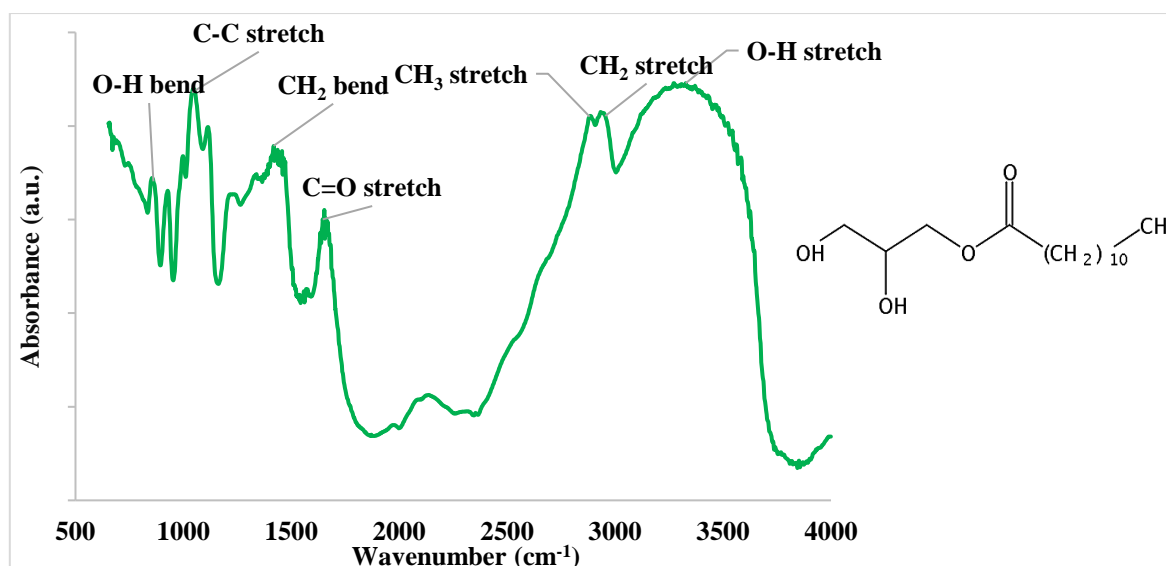
Figure 5.6: FTIR of MG fraction
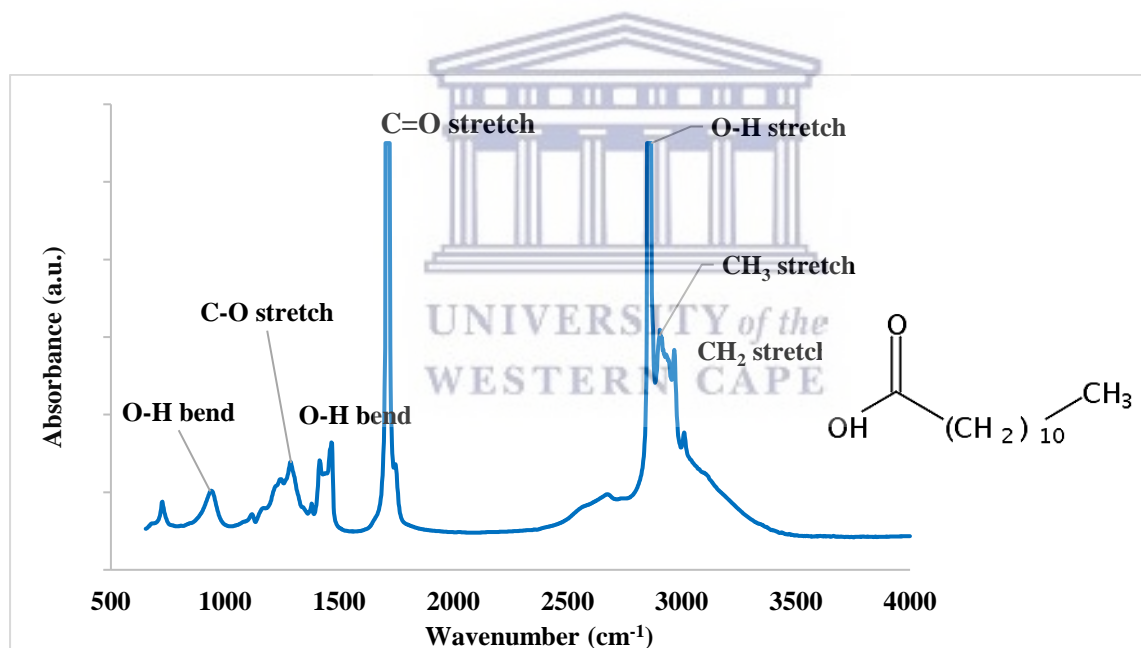
Figure 5.7: FTIR of FA fraction

These infrared spectra reveal several prominent absorption bands that are specific to each lipid class. In the spectra of the triglyceride (Figure 5.4) it can be deduced that the hydroxyl group is absent (O-H) while it was present in the spectra of DG (Figure 5.5), MG (Figure 5.6), and FA (Figure 5.7). The O-H stretching vibration of the carboxylic acid and ester usually appears as a strong and broad signal in the region of 3200 to 3500 cm^{-1} of the spectra (Lucarini et al., 2018). O-H stretching was more prominent in the MG than in DG. This might indicate the

113

presence of the primary and secondary O-H groups of the MG as opposed to one O-H of a DG. These findings are in line with the work done by Aly et al. (2020). The O-H stretching in the spectra of the FA was not found in the region of 3200 to 3500 but at about 2963 cm^{-1} region which is unique to all fatty acids compounds. A broad peak due to the O-H stretch of the fatty acid superimposed on the sharp C-H stretching bands which are in the same region was also reported by Lucarini et al. (2018).

The spectra of the TGA showed two strong and sharp peaks in the region 2950 - 2872 cm^{-1} and 2920 - 2830 cm^{-1} which conforms with the work of Oleszko et al. (2017). Those peaks are due to aliphatic CH_2 and CH_3 symmetric and asymmetric stretching, respectively, conforming with the research of other scholars like Mohammadi et al. (2020). The CH_2 and CH_3 stretching which appears less sharp due to the presence of O-H were also present in the DG and MG spectra. Based on the above observations, it can be confirmed that the TGA did not contain a trace of DG, MG, or FA impurity during column chromatography separation as shown also by the TLC presented in section 5.2.

In the fingerprint region, below 2000 cm^{-1} almost every organic compound produces a unique pattern. TGA, DG, MG, and FA produced different patterns but shared some similarities in their functional groups such as the carbonyl group (C=O). The carbonyl stretch C=O of a carboxylic acid (FA) and the ester (TGA, DG, and MG) all appear as an intense peak in the region 1760 - 1690 cm^{-1} also found by Gaweł et al. (2014) and Gocen et al. (2018). For instance, TGA, DG, MG, and FA peaks occur at 1753, 1747, 1661, and 1721 cm^{-1} respectively. Oleszko et al. (2017) and Kudo & Nakashima (2020), in their separate research also reported a similar trend. In line with the findings of Goeel (2018), the stretching vibrations of the C-O bond of the FA appeared in the region 1320 - 1210 cm^{-1} as expected. In this study, it occurs at about 1304 cm^{-1}. On the other hand, stretching vibrations of the C-O bond of esters are composed of two coupled asymmetric vibrations C-C-O (1210 - 1160 cm^{-1}) and O-C-C (1100 - 1030 cm^{-1}). The peaks that originated from C-C-O occurred at 1171, 1181, and 1117 for TGA, DG, and MG, respectively while the O-C-C stretch occurred at 1108, 1065, and 1060 cm^{-1} for TGA, DG, and MG, respectively. CH_2 bending present at about 1377 cm^{-1} could be attributed to the glycerol group of the TGA, DG, and MG. The region of the appearance of the C-C-O, O-C-C, and CH_2 bending was supported by the work of Lazzari et al. (2018) and Uncu et al. (2019) respectively.

5.3.2.2 ^{1}H nuclear magnetic resonance spectroscopy

^{1}H nuclear magnetic resonance spectroscopy (^{1}H NMR) was applied to investigate the functional groups of the different lipid fractions. This was done to confirm the structure of the TGA, DG, MG, and FA. The characterisation of the lipids fractions was performed as described in section 3.3.5.3. The ^{1}H NMR signals of the TGA, DG, MG and FA fractions are assigned to different types of protons and are presented in Table 5.6.

Table 5.6: ^{1}H NMR signals of TGA, DG, MG, and FA isolated from BSF larvae

Chemical shift (ppm)	Functional group	Type of proton	Attribution
0.8	acyl group	$-CH_3-$	FA, TGA, DG, MG
1.2	acyl group	$-(CH2)n-$	TGA
1.3	acyl group	$-(CH2)n-$	FA, DG
1.4	acyl group	$-(CH_2)n-$	FA
1.5	acyl group	$-(CH_2)n-$	MG, TGA
1.6	acyl group	$-OCO-CH_2-CH_2-$	DG, FA
1.8	acyl group	$-OCO-CH_2-CH_2-$	DG
2	acyl group	$-OCO-CH_2-CH_2-$	TGA, FA
2.7	acyl group	$-OCO-CH_2-CH_2-$	TGA
2.8	acyl group	$-OCO-CH_2-CH_2-$	DG, FA
3.5	glyceryl group	$ROCH_2-CH(OR)-CH_2OR$	DG, MG
3.7	glyceryl group	$ROCH_2-CH(OR)-CH_2OR$	DG-MG
4	glyceryl group	$ROCH_2-CH(OR)-CH_2OR$	TGA, MG
4.1	glyceryl group	$ROCH_2-CH(OR)-CH_2OR$	MG
4.2	glyceryl group	$ROCH_2-CH(OR)-CH_2OR$	TGA
4.3	glyceryl group	$ROCH_2-CH(OR)-CH_2OR$	DG
5	glyceryl group	$ROCH_2-CH(OR)-CH_2OR$	MG
5.3	glyceryl group	$ROCH_2-CH(OR)-CH_2OR$	TGA
5.4	acyl group	$-OCO-CH_2-CH_2-$	FA (unsaturated fatty acids)

The different lipid classes display signals coming from the protons on the acyl and glyceryl group carbon. For the TGA (Figure 5.8) the protons on the acyl groups resonate at about six (6) signals (0.8, 1.2, 1.5, 2, 2.3, and 2.7 ppm) while the protons attached to the glycerol group give rise to 3 peaks appearing at a downfield of 4.0, 4.2 and 5.3 ppm.
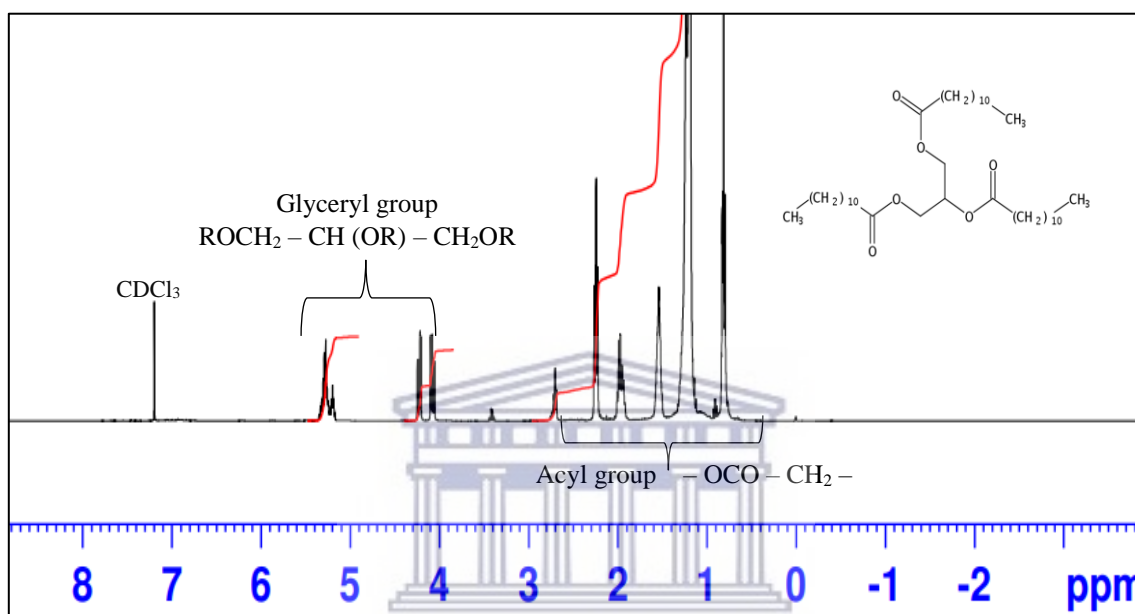
Figure 5.8: ^{1}HNMR of TGA fraction in deuterated chloroform (CDCl₃)

In DG, five up-field acyl group signals were observed at 0.7, 0.8, 1, 1.3, 1.6 1.8, 2.0, 2.3, and 2.8 ppm while six downfield glycerol groups were observed at 3.5, 3.7, 4.1, 4.3, 5.1 and 5.4 ppm (Figure 5.10)
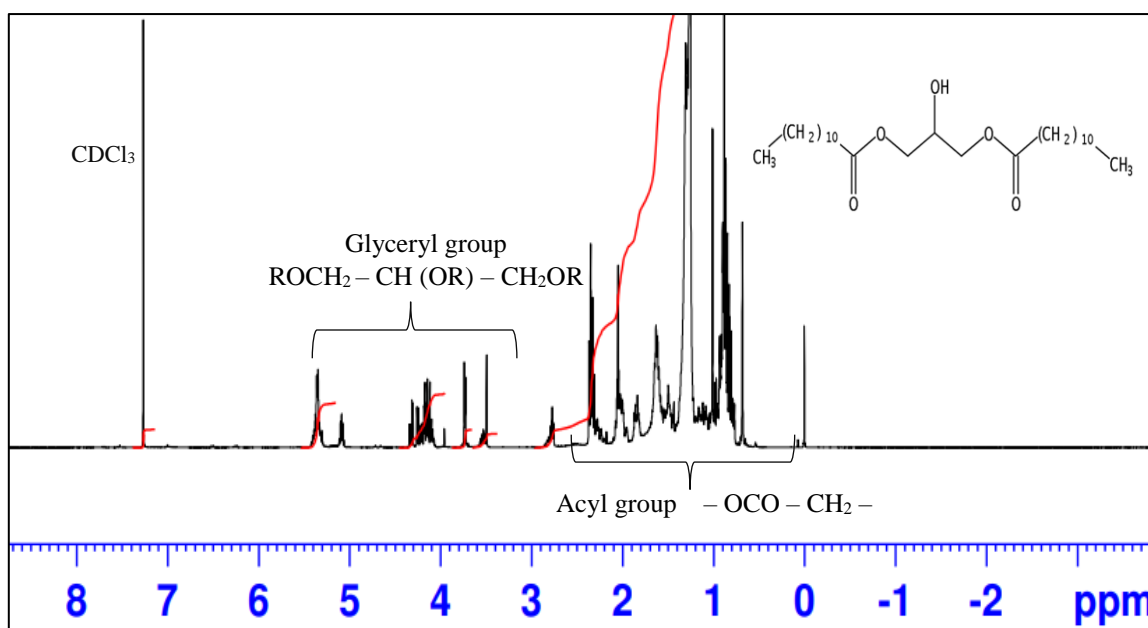
Figure 5.9: ¹HNMR of DG in deuterated chloroform (CDCl₃)

The ^{1}H NMR spectrum of the MG (Figure 5.10) showed resonances at 5.0, 4.1, and 3.7, 3.5 ppm which indicated the presence of the glycerol group. Consequently, the acyl group showed a signal at 2.3, 2.1, 2, 1.5, 1.3, and 0.8 ppm. In the MG protons from the glycerol groups clustered mostly toward the downfield of the spectrum. The behaviour is probably due to the loss of the high electron density of the acyl group. Jin et al. (2007) found the same behaviour in the vegetable lipid lipids

117
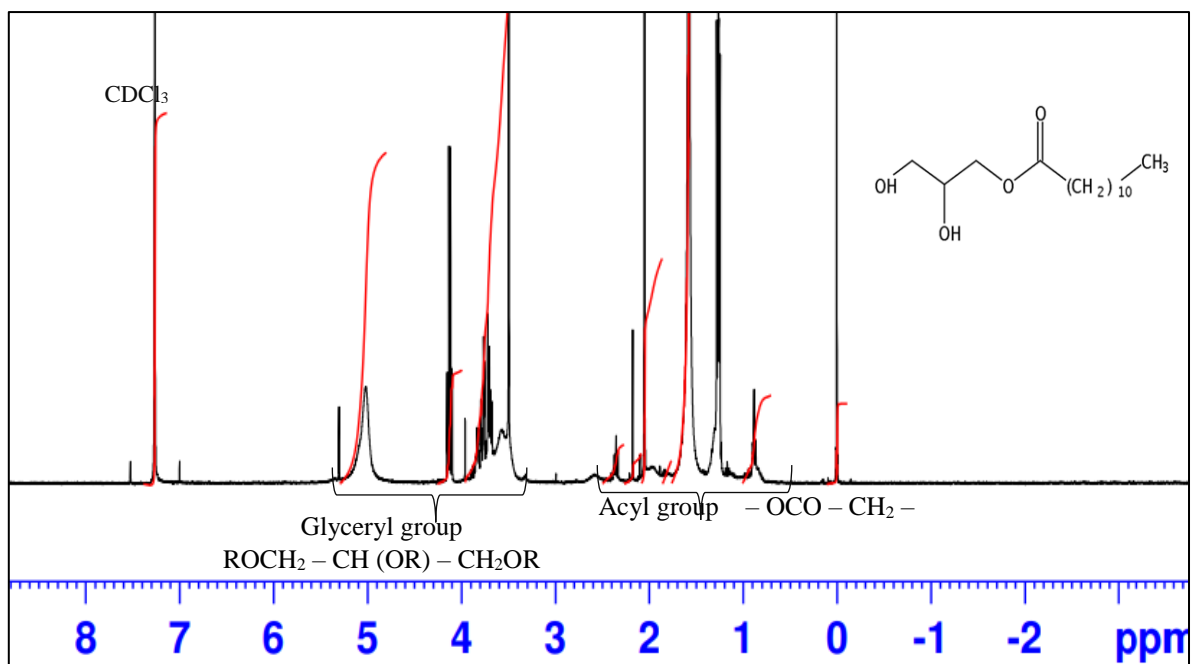
Figure 5.10: ^{1}HNMR of MG in deuterated chloroform (CDCl$_3$)

The ^{1}H NMR spectrum of the FA (Figure 5.11) shows an acyl group to the higher frequency of the spectrum (5.4 ppm) which probably indicated the presence of unsaturated fatty acids. The other acyl groups were observed at 2.8, 2.3, 2, 1.6, 1.4, and 0.8 ppm at the lower frequency of the spectrum.
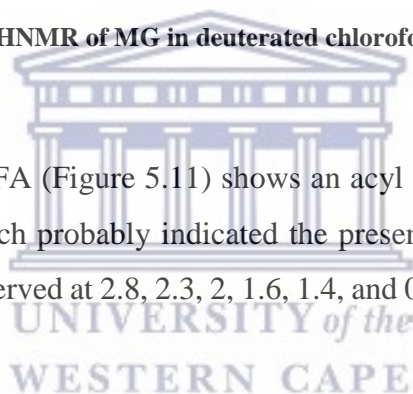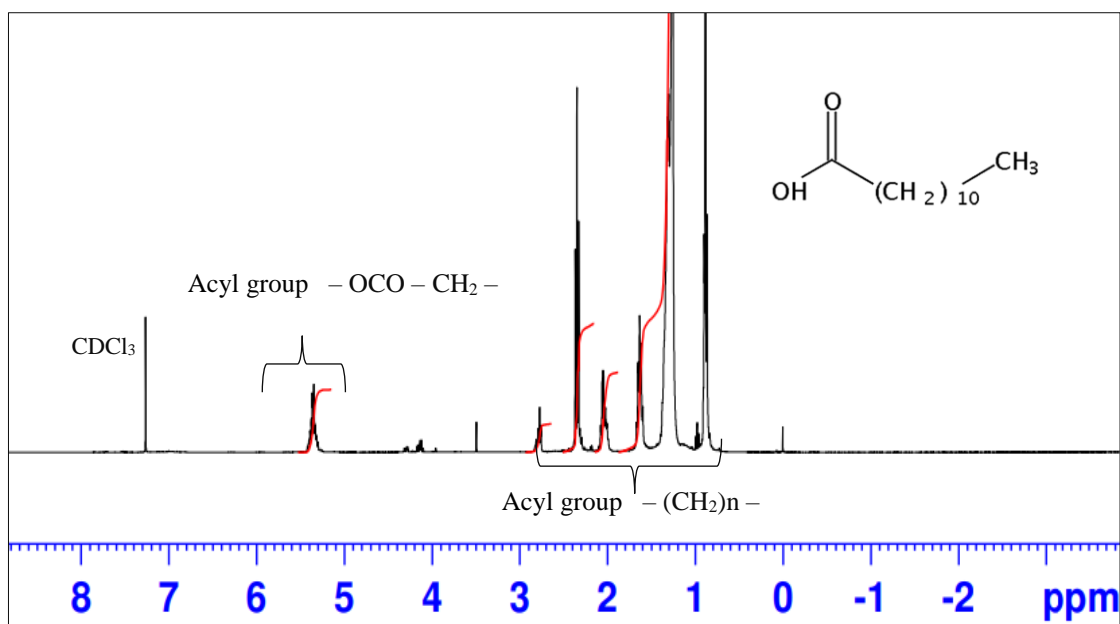
Figure 5.11: ¹HNMR of FA in deuterated chloroform (CDCl₃)

5.3.2.3   ¹³C nuclear magnetic resonance spectroscopy

For further confirmation of the results obtained by ¹H NMR analysis, ¹³C NMR identification
was also carried out as described in section 3.4.6. ¹³C NMR provides a large number of signals
covering a wide range of chemical shifts (Di Pietro et al., 2020). The carbon spectra of the
triglyceride (TGA), diglycerides (DG), and monoglycerides (MG) were visible with a
distinctive peak except for the carbon spectra of MG which appears messy hence does not
permit the identification of the peaks. Based on this, only the spectrums of TGA, DG, and FA
were considered. Table 5.7 shows the chemical shift and assignment of the TGA, DG, and FA
for 13^C NMR.

Table 5.7: Chemical shift and assignment of TGA, DG, and FA FOR 13^C NMR

Functional group	Methylenic region	Glycerol region	Olefinic region	Carbonyl region
Chemical shift [**]	10 to 35	60 to 72	124 to 134	172 to 174
TCA	22 - 34	62 - 77	127 - 130	172 - 173
DG	22 - 39	61 - 77	121 - 140	173
FA	14 - 34	none	127 - 130	180

(**) Burri et al., 2016

119

In the attempt to identify the constituent carbon atoms from the lipid fractions, attention was paid specifically to four major sets of signals from ^{13}C resonances which are: methylene, glycerol, olefin (alkene), and carbonyl carbons. The carbon spectra of the TGA, DG and FA are shown in Figure 5:12, Figure 5:13, Figure 5:14, respectively.
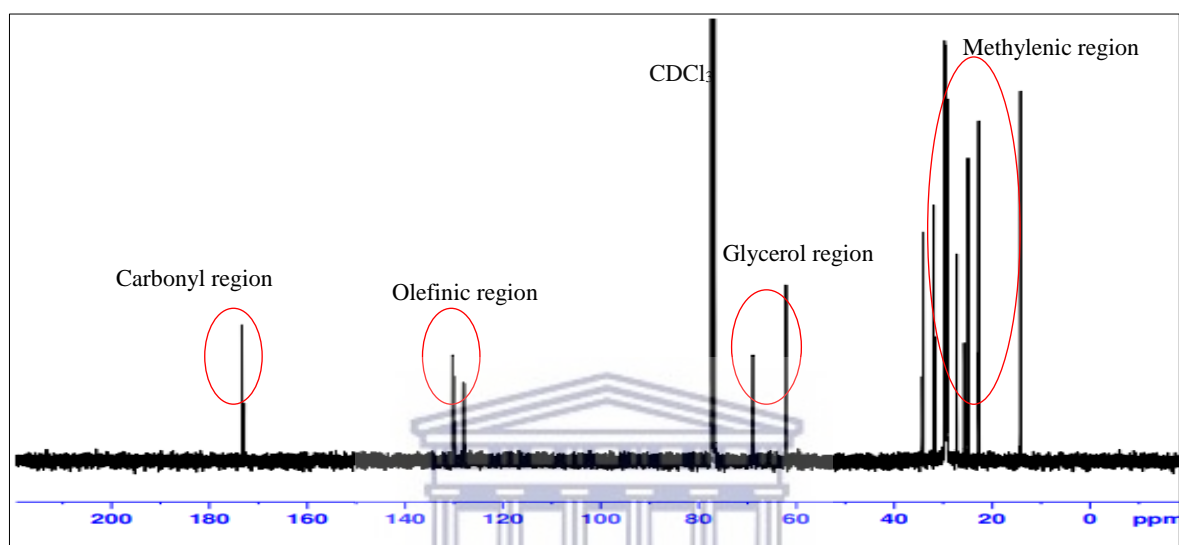
Figure 5.12: ^{13}C NMR spectrum of TGA in deuterated chloroform (CDCl$_3$)
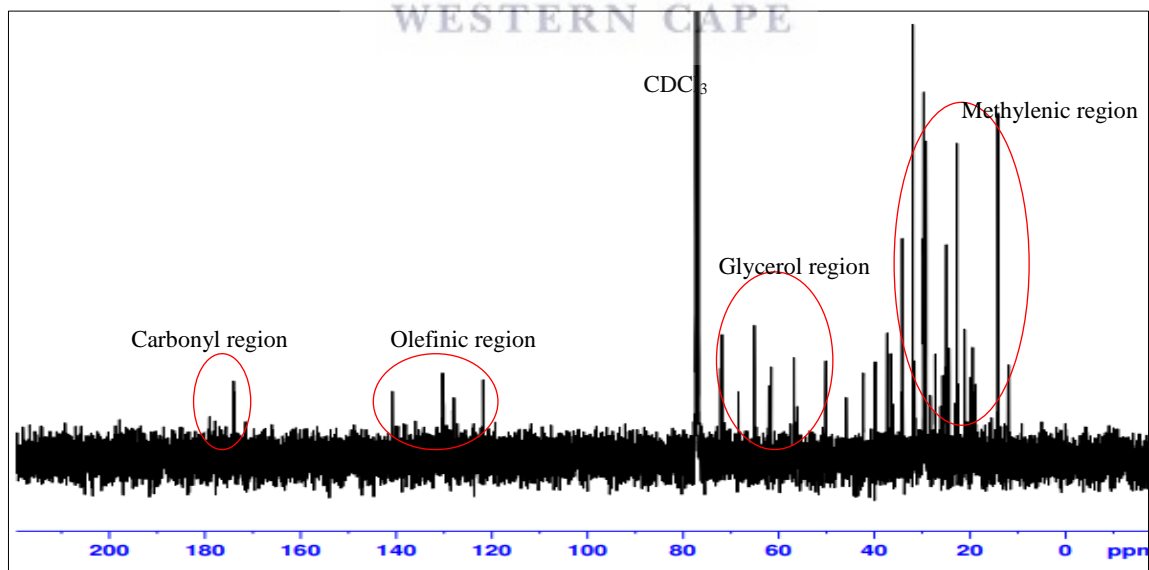
Figure 5.13: ^{13}C NMR spectrum of DG in deuterated chloroform (CDCl$_3$)
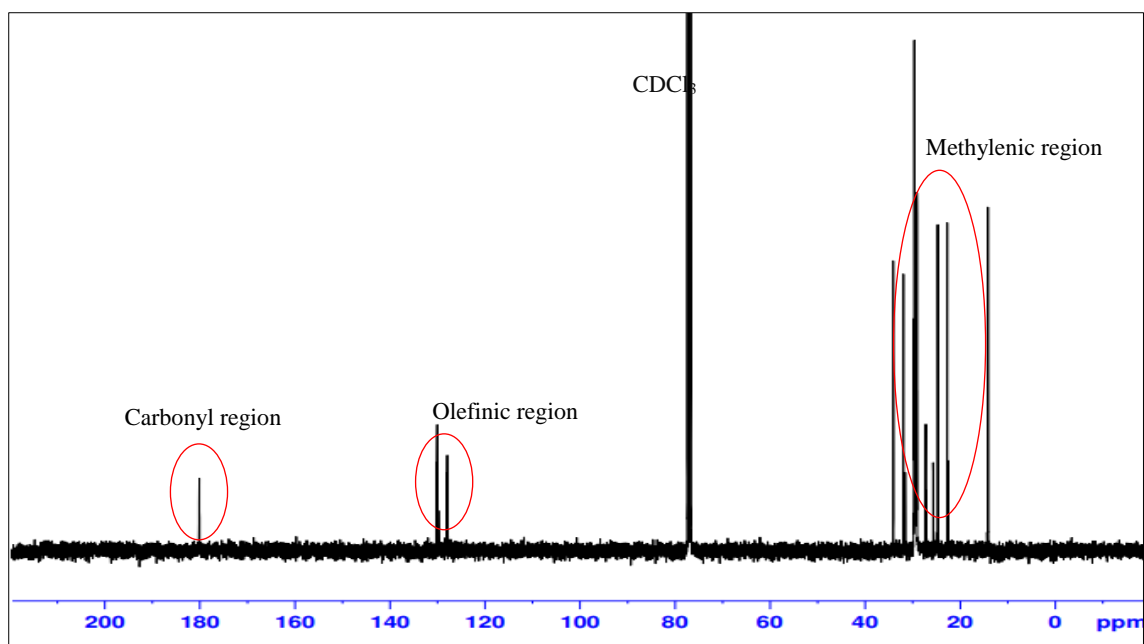
Figure 5.14: ^{13}C NMR spectrum of FA in deuterated chloroform (CDCl$_3$)

The methylenic carbon of the TGA, DG and FA resonated from 22 - 31, 22 - 39, and 14 - 34 ppm respectively. Glycerol region corresponding to the resonances from the glycerol backbone carbons resonated from 62 - 77 and 61 - 77 ppm for the TGA, and DG. FA does not contain the glycerol backbone since they are carboxylic acid with an aliphatic chain. The olefinic carbon of the TGA resonated from 127 to 130 ppm, DG from 121 to 140 ppm, and FA from 127 to 130 ppm. The carbonyl carbons from the fatty acyl chains appeared from 172 to 173 ppm for the TGA, 173 ppm for DG, and 180 ppm for the FA

According to the literature, methylenic carbon for the lipids resonates from 10 to 35 ppm (Burri et al., 2016; Truzzi et al., 2021). Researchers have found that this probably corresponds to the resonances of methyl (- CH$_3$) and methylene (- CH$_2$) carbons from the saturated and unsaturated fatty acyl chains. Truzzi et al. (2021) reported that the olefinic region is found from 124 to 134 ppm, which corresponds to the unsaturated carbon resonances. In this study, similar ranges were found. From the ^{13}C NMR results, a high level of conformity with the result found by ^{1}H NMR was noted.

5.4   Chapter summary

This chapter aimed to fractionate the lipid of the black soldier fly (BSF) larvae into lipid classes using column chromatography and thin-layer chromatography (TLC) and to characterise them

121

using gas chromatography (GC-FID), Fourier-transform infrared spectroscopy (FTIR), and nuclear magnetic resonance (NMR) spectroscopy. The column chromatography and TLC procedure developed in this study proved to be effective in separating lipid from BSF larvae into lipid classes. The results showed that the lipid of the BSF larvae is made of complex mixtures of triglycerides (TGA), diglycerides (DG), monoglycerides (MG), fatty acids (FA), and other minor components such as cholesterols (C) and cholesterol esters (CE) which were present in small amounts. The TGA fraction had a greater mass percentage (30 %) compared to the other lipid fractions, followed by DG and FA. To the best of our knowledge, the fractionation of the lipid extracted from the BSF larvae has not been published before. Non-polar solvent (100 % hexane) was used to isolate a non-polar lipid (CE) from BSF larvae. The other non-polar lipid classes were isolated with a solvent combination of increasing polarity of 5 % diethyl ether in hexane, 15 % diethyl ether in hexane, 25 % diethyl ether in hexane for TGA, FA, and C, respectively. The polar lipid classes on the other hand can be separated with 50 % diethyl ether in hexane and 2 % methanol in diethyl ether for the DG and MG respectively.

GC-FID was noted to be used by several researchers for sole analysis of volatile samples or samples that can be made volatile through derivatisation. The side product formation of substances during derivatisation made it not an appreciable method for the substances (mono, di, and triglycerides) under investigation. To overcome this challenge, GC-FID equipped with a medium polarity capillary column CP-TAP-CB was employed. This improved GC-FID with the advantage of directly analysing non-volatile substances with high boiling points, such as mono, di, and triglycerides, without the need for derivatisation. The results of Fourier-transform infrared spectroscopy (FTIR) and nuclear magnetic resonance (NMR) spectroscopy were consistent with the column chromatography results.

CHAPTER 6: SYNTHESIS OF CHITOSAN-LIPID HYBRID NANOPARTICLES

Abstract

Lipid-polymer nanoparticles are nanomaterials made up of a polymer and lipid which exhibit complementary characteristics of both polymer and lipid. They are of interest as antimicrobial agents due to their unique physical and chemical properties. Fabrication of lipid-polymer nanoparticles using electrohydrodynamic atomization (electrospraying) appears to be a novel strategy to produce nanoparticles. This chapter informs about manufacturing chitosan-lipid hybrid nanoparticles with the electrospraying technique. For this purpose, the lipid fractions (triglycerides, diglycerides monoglycerides, and fatty acids) isolated from BSF larvae were individually mixed with commercial chitosan. The effects of the chitosan concentration and stirring time on the formation of the nanoparticles were investigated to bring chitosan to the state possible for it to form an effective hybrid with the lipids. The effect of chitosan-lipid concentrations 0.02, 0.03, and 0.04 g/mL was investigated to obtain the best formulation of the chitosan-lipid hybrid nanoparticles. Chitosan- lipid nanoparticles in powder form were obtained when 1 wt % of chitosan solution in 90 % acetic acid was stirred for a long period of 48 h. The chitosan-lipid nanoparticles were characterised in terms of their molecular structure using Fourier transform infrared spectroscopy and their morphology using scanning electron microscopy. The results from this study showed that chitosan-lipid hybrid nanoparticles were successfully prepared using the electrospray method.

Graphical abstract
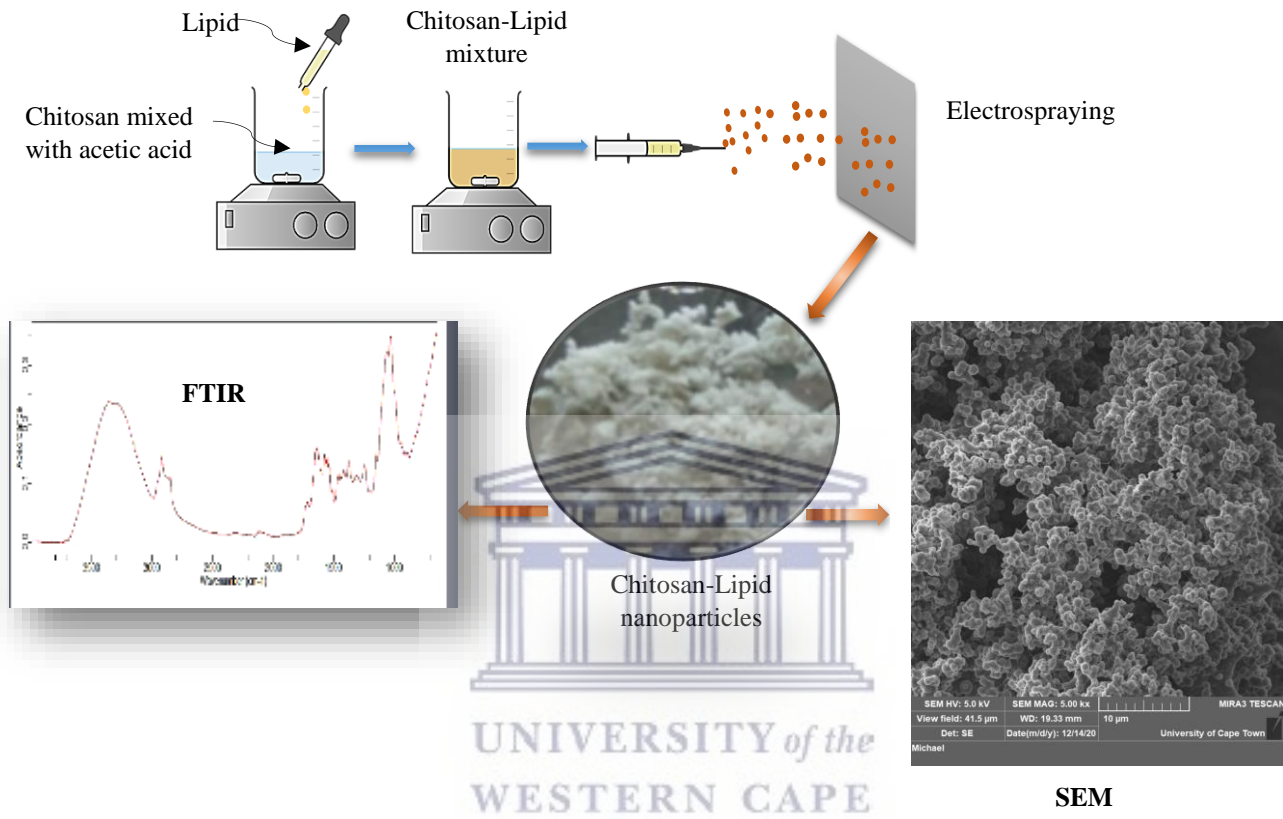
6.1 Introduction

Nanoparticle synthesis has evolved in recent years. In different fields, depending on the end product and its application, nanoparticles have been synthesised using diverse materials. Its application is extensive in cosmetic, catalysis, environmental remediation, medical and pharmaceutical fields (Mishra et al., 2018). The properties of nanoparticles in particular their size (1-100 nm) offer substantial advantages over their large-scale structures. Also, the flexibility in adapting them to unique requirements emphasizes its effectiveness. Besides, nanoparticles are more effective, reactive, easy to manipulate, and have high long-term stability (Wang et al., 2018; Bayón-Cordero et al., 2019; Dave et al., 2019). These properties further increase their request for use in various industries.

Lipids, being the subject of this research with their antimicrobial effectiveness, were synthesised into solid nanoparticles. Lipids are not typically easy to synthesize into powder form due to their oily nature. Hence, they need to be transformed into hybrid substances for structural and mechanical purposes. The lipids in hybrid form enhance and maximize their effectiveness (Scopel et al., 2020). Several substances can effectively form a hybrid with lipids but some will not offer any additional benefit to the substance order than structural and mechanical re-enforcement (Dave et al., 2019). Due to the purpose of this study, which is to test the antimicrobial efficacy of the lipids, chitosan was chosen by the author for the advantage of its antimicrobial properties, its non-toxicity, and biocompatibility, mechanical and thermal stability (Ardila et al., 2018). Based on the above-mentioned properties of chitosan, it is expected that the efficacy of the hybrid compound will surpass that of lipids or chitosan alone.

In synthesizing nanoparticles, depending on the application and the final product, several methods are employed (Ganesan & Narayanasamy, 2017; Duan et al., 2020; Shanaghi et al., 2020). Among the methods (high-pressure homogenization, ultrasonication, supercritical fluid, microemulsion, spray drying, reverse micellar method, etc.) as described in section 2.9.1, the electrospraying method has been widely used due to its low cost, its simplicity, and the fact that it does not require the use of harmful organic substances (surfactants) (Ardila et al., 2018). This work involves the mixture of chitosan with four different lipid classes (triglycerides, fatty acid, diglyceride, monoglyceride) isolated from the BSF Larvae presented in Chapter five. The mixture of the lipids and chitosan was synthesised to form chitosan-lipid-hybrid nanoparticles using the electrospray method. To form an effective hybrid of chitosan and lipids, several considerations such as the concentration of the chitosan solution is optimised to bring chitosan

to the state possible for it to form a hybrid with the lipids. Also the effect of stirring time on the formation of the chitosan-lipids nanoparticles were optimised. This must be done when trying to synthesise nanoparticles involving chitosan and lipids to produce a high-quality product.

6.2 Synthesis of chitosan-lipids hybrid nanoparticles

Before mixing the chitosan with lipids to form the chitosan - lipids hybrid nanoparticles, it was important to first investigate the appropriate solution parameters of the chitosan. According to Ardila et al. (2018), the most critical solution parameters of interest for this production are concentration (viscosity) and stirring time for the dissolution to achieve the desired end product (chitosan nanoparticle). The electrospray instrument parameters such as flow rate (0.5 mL/h), applied voltage (25 kV), and tip to collector distance (10 cm) were kept constant. The following sub-section discusses the effect of chitosan concentration on nanoparticle formation.

6.2.1 Nanoparticles formation dependency on chitosan concentration

This section presents the results of the effect of the chitosan concentration on the formation of the chitosan nanoparticles. The concentration of the chitosan is an important factor of interest when synthesising nanoparticles using electrospraying as it determines the nature of the product formed (nanofibre, nanofilm, and nanoparticle) (Zhang & Kawakami, 2010; Islam et al., 2019). Not upon just the nature of the end product formed, but also upon the formation of a solution, the viscosity of the solvent needs to be suitable for passing into the needle of the syringe the source material solution for electrospraying treatment. The preparation of the different chitosan concentrations is detailed in section 3.3.4.2. Briefly, commercial chitosan was prepared at different weight percentages of 0.5, 1, 2, 3 and 4 wt % by dissolving approximatively 0.05, 0.11, 0.22, 0.32 and 0.43 g of the chitosan in 10 mL of 90 % acetic acid. The electrospraying parameter was fixed: flow rate (0.5 mL/h), applied voltage (25 kV), and tip to collector distance (10 cm). The electrospraying conditions for the formation of chitosan nanoparticles are summarised in Table 6.1.

Table 6.1: Electrospraying conditions at different chitosan solution concentrations

	Fixed			Varied	
Sample code	Collector distance (cm)	Voltage (kV)	Flow rate (mL/h)	Concentration of chitosan (wt %)	Weight of the chitosan (g)
CH 1-C	10	25	0.5	0.5	0.05
CH 2-C	10	25	0.5	1	0.11
CH 3-C	10	25	0.5	2	0.22
CH 4-C	10	25	0.5	3	0.32
CH 5-C	10	25	0.5	4	0.43

This range of concentrations produced a range of viscosities. Some chitosan solutions were either too viscous (high viscosity) to spray through the syringe or had too low viscosity causing it to drop and did not give the desired result (powder particles). Chitosan concentration of less than 1wt % produced a viscosity considered too low. This can be explained by the fact that the evaporation of the solvent (90 % acetic acid) may not be rapid enough to form solid nanoparticles with a solution with a low concentration (Park et al., 2007). In contrast, the chitosan solutions with a concentration of 3 and 4 wt % were too viscous to electrospray. This is due to the high viscosity of the chitosan solution which impedes the continuous flow through the needle. Consequently, only solutions between 1 and 2 wt % of chitosan in 90 % acetic acid were within the viscosities which were spinnable hence were electrosprayed and tested for the quality desired. However, at a concentration of 2 wt %, the electric field could deform the polymer but was unable to completely break the droplet at the needle tip. The deformation resulted in low particles per collector surface unit area. Due to this, only 1 wt % chitosan solution concentration was considered and used for the rest of the synthesis. The chitosan solution of 1 wt % was spinnable, however, it did not result in the formation of a solid nanoparticle. It instead resulted in the formation of a chitosan film. Zhong et al.(2019) reported that a chitosan film is usually formed when the surface tension of the solution is high. Therefore

it was necessary to investigate ways to lower surface tension to reduce the chances of producing undesired chitosan film. Therefore the following section investigated the effect of the stirring on the formation of nanoparticles.

6.2.2 Stirring time effects on the formation of the chitosan nanoparticles

This section presents the result of the effect of stirring time on the formation of the chitosan-lipids nanoparticles. As detailed in section 3.3.4.2.2, 1 wt % of the chitosan solution was stirred three different times: 12, 24, and 48 h at 700 rmp. The electrospray parameters such as the flow rate (0.5 mL/h), applied voltage (25 kV), and tip to collector distance (10 cm) were maintained constant throughout the experiment. The electrospraying conditions are shown in Table 6.2.

Table 6.2: Electrospraying conditions for the chitosan solution prepared at different stirring times

	Fixed					Varied
Sample code	Voltage	Collector distance	Concentration of chitosan	Weight of the chitosan	Flow rate	Stirring time
	(kV)	(cm)	(wt %)	(g)	(mL/h)	(h)
CH 1-T	25	10	1	0.1	0.5	12
CH 2-T	25	10	1	0.1	0.5	24
CH 3-T	25	10	1	0.1	0.5	48

Figures 6.1, 6.2, and 6.3 show the morphology of the nanoparticles of 1 wt % chitosan solution stirred at 700 rmp for 12, 24, and 48 h, respectively at optimised electrospraying conditions (a voltage of 25 kV, a flow rate of 0.5 mL/h, and 10 cm tip to collector distance). The chitosan nanoparticles were visualised using a scanning electron microscope (FEI, Quanta Feg 250, USA) at 5 kx: right and 20 kx: left.

| High magnification | Low magnification |
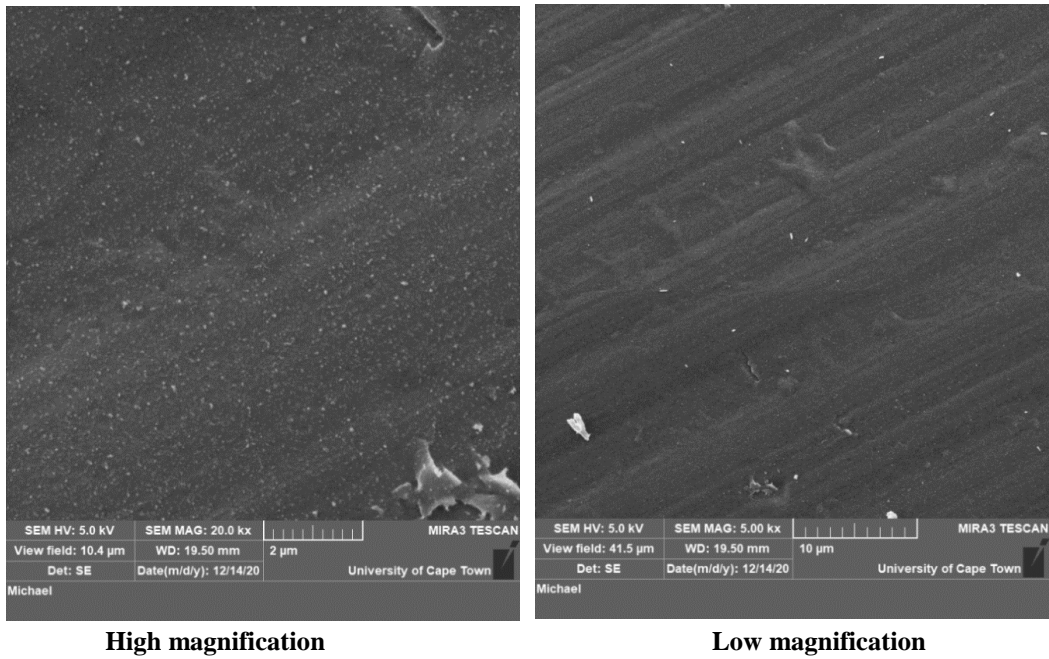
Figure 6.1: SEM micrographs of 1 wt % chitosan solution stirred for 12 h at 700 rmp at optimised electrospraying conditions (a voltage of 25 kV, a flow rate of 0.5 mL/h, and 10 cm tip to collector distance).

| High magnification | Low magnification |
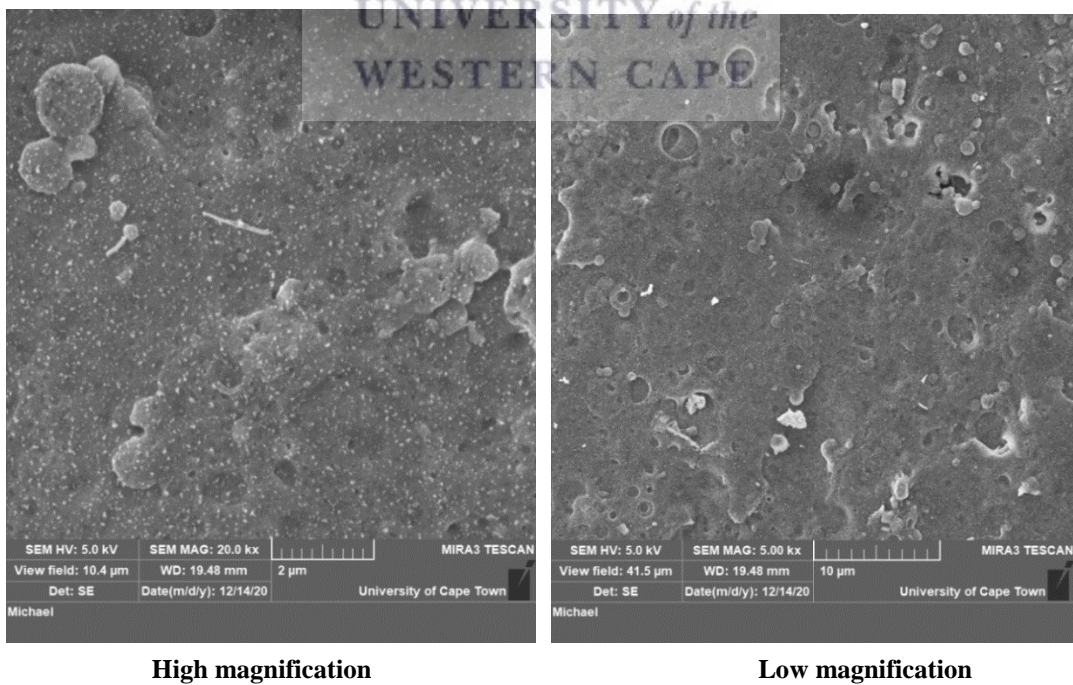
Figure 6.2: SEM micrographs of 1 wt % chitosan solution stirred for 24 h at 700 rmp at optimised electrospraying conditions (a voltage of 25 kV, a flow rate of 0.5 mL/h, and 10 cm tip to collector distance).

http://etd.uwc.ac.za/

129
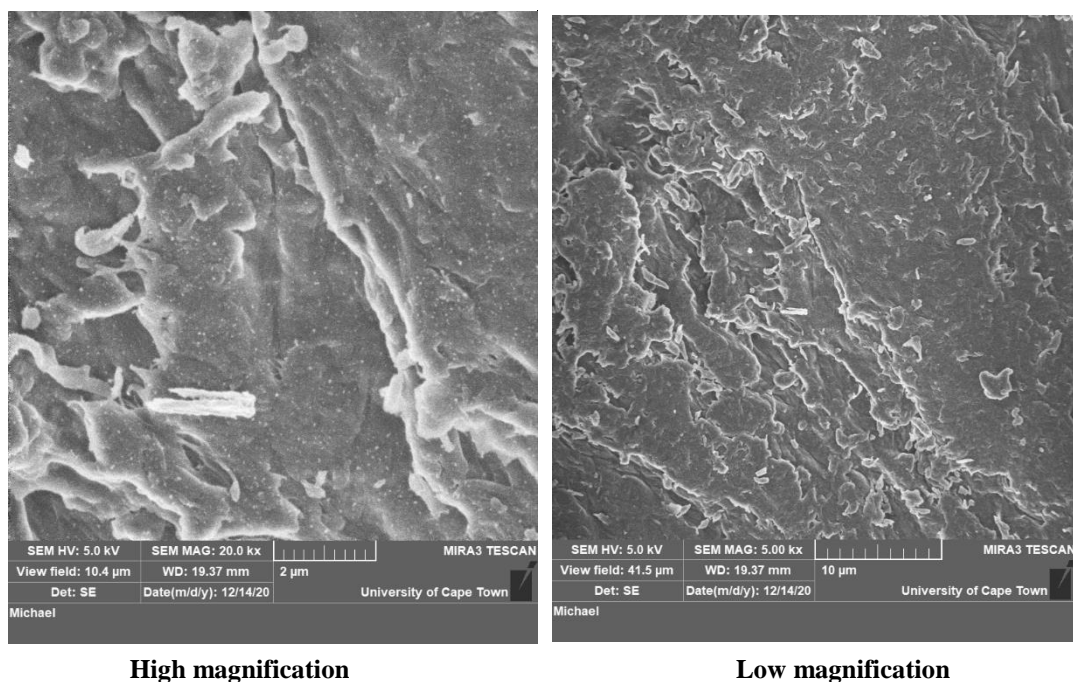
| High magnification | Low magnification |

Figure 6.3: SEM micrographs of 1 wt % chitosan solution stirred for 48 h at 700 rmp at optimised electrospraying conditions (a voltage of 25 kV, a flow rate of 0.5 mL/h, and 10 cm tip to collector distance).

The electrospray of 1 wt % chitosan solution stirred for 12 h (Figure 6.1) lead to the formation of a strong chitosan film which appears smooth and non-porous surface. At 24 h stirring the solution also lead to the formation of a chitosan film which was more fragile compared to the one produced when stirred for 12 h. Also, the film has a rough surface area with a porous internal structure and irregular pores (Figure 6.2). After 48 h stirring the chitosan solution lead to a drastic reduction of a film with a rough surface area and lead to the formation of large and small particles, as shown in Figure 6.3. The transition in the morphology from chitosan films into chitosan nanoparticles from 12h to 48 stirring times might result from the low surface tension of the chitosan solution induced when the chitosan solution was stirred for a long period. As the chitosan solution was stirred for a longer duration (48 h), the intermolecular forces of the chitosan bonds might have decreased due to the breakdown of molecular chains.

The findings of this study agreed with those of other studies (Hussain & Sahudin, 2016; Thandapani et al., 2017; Debnath et al., 2018), which indicated a significant impact of stirring time and stirring speed on the formation of chitosan nanoparticles. Several researchers have demonstrated a relationship between the result of chitosan (nanoparticle, fiber, or film) and the

stirring speed and time (Wang & Jing, 2016; Thandapani et al., 2017). In the study conducted by Wang & Jing. (2016), the stirring speed was varied while the stirring time was constant, however in this study, stirring speed was kept constant while the stirring time was varied.

Thandapani et al. (2017) investigated the effects of stirring time on the formation of chitosan nanoparticles. The chitosan nanoparticles were prepared at different stirring times while keeping the stirring speed constant. Their stirring time (30, 60, and 120 min) were shorter than the stirring time used in this study. However, Marinho et al. (2018) reported that longer stirring time favour the breakdown of the largest particles and increase the number of particles compared to shorter stirring time. Although not further investigated in this study, chitosan films are of interest due to their oxygen and carbon dioxide barrier properties (Bhuvaneshwari et al., 2011) which are important in food packaging since they extend food shelf life (Wang & Jing, 2016). The next section discusses the preparation of chitosan -lipid nanoparticles.

6.3   Preparation of chitosan lipid nanoparticles

This section presents the results of the effect of chitosan-lipids concentrations: chitosan-triglycerides (CH-TGA), chitosan-diglycerides (CH-DG), chitosan-monoglycerides (CH-MG), and chitosan-fatty acids (CH-FA). The chitosan-lipid concentrations were investigated to obtain the best formulation of the lipid-chitosan nanoparticles, detailed in section 3.3.4.4. The chitosan-lipid solutions were prepared at three different concentrations of 0.02, 0.03, and 0.04 g/mL by dissolving 0.2, 0.3, and 0.4 g of each lipid fraction (triglycerides, diglycerides, monoglycerides, and fatty acids) in liquid form in 1 wt % of the chitosan solution prepared by dissolving 0.1 g of the commercial chitosan in 10 mL of 90 % acetic acid. The applied conditions shown in Table 6.3 were a voltage of 25 kV, a flow rate of 0.5 mL/h, and a 10 cm tip to collector distance.

Table 6.3: Electrospraying conditions at different chitosan- lipid concentrations

Sample code	Fixed				Varied
	Collector distance (cm)	Voltage (kV)	Flow rate (mL/h)	Concentration of chitosan (wt %)	Chitosan–lipid concentrations (g/mL)
CH-LIP C	10	25	0.5	1	0.02
CH-LIP C	10	25	0.5	1	0.03
CH-LIP C	10	25	0.5	1	0.04

Figure 6.4 showed the chitosan-lipid deposition on the aluminium foil at a chitosan-lipid concentrations of 0.02 g/mL (a), 0.03 g/mL (b) and 0.04 g/mL (c) using the electrospray method.
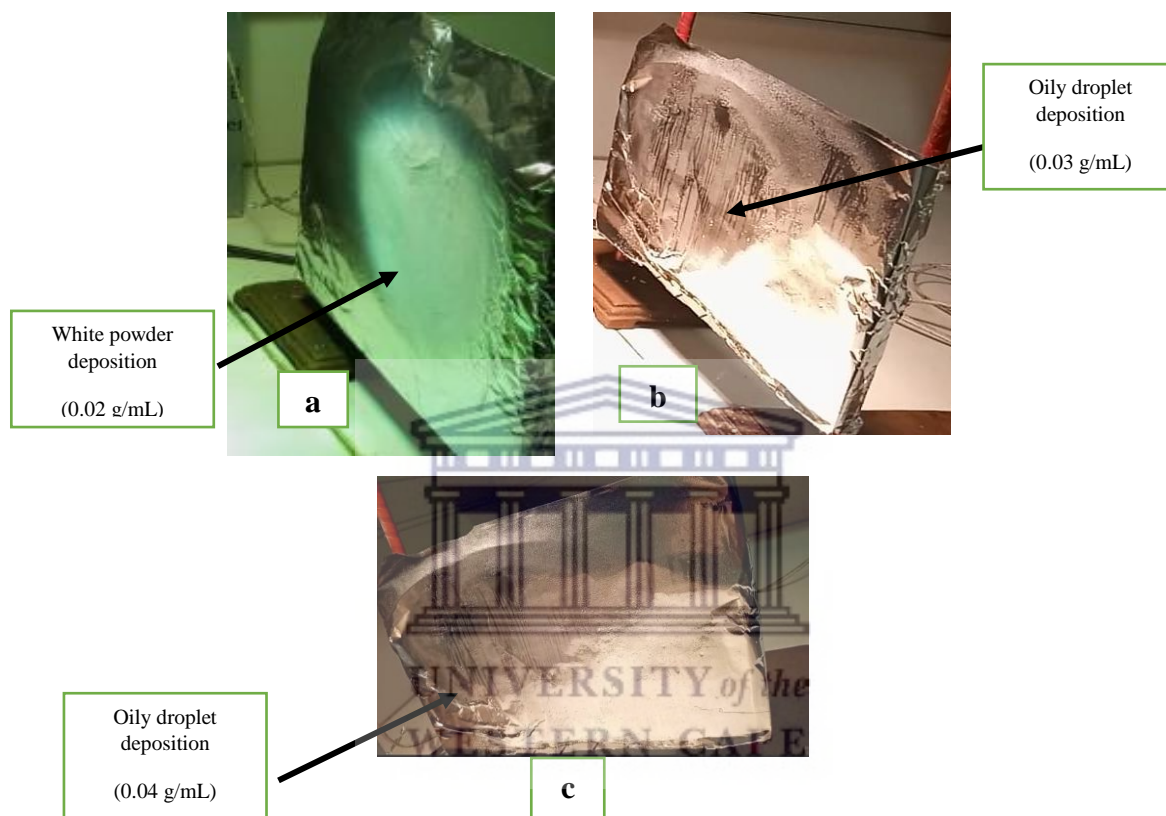
Figure 6.4: Preparation of the chitosan-lipid concentrations of 0.02 g/mL (a), 0.03 g/mL (b) and 0.04 g/mL (c) using the electrospray method. Electrospraying conditions (a voltage of 25 kV, a flow rate of 0.5 mL/h, and 10 cm tip to collector distance).

Lipid-chitosan hybrid nanoparticles were synthesised at various doses to achieve the best formulation. The chitosan-lipid concentrations of 0.03 and 0.04 g/mL resulted in an oily droplet being deposited on the collector during electrospraying, whereas the chitosan-lipid concentration of 0.02 g/mL resulted in a white solid powder being deposited on the collector. The desirable white solid product was the lipid-chitosan hybrid nanoparticles therefore the chitosan-lipids concentration of 0.02 g/mL was the optimum concentration for the formulation

of the nanoparticles. It must be noted that each lipid fraction (triglycerides, diglycerides, monoglycerides, and fatty acids) mixed with the chitosan were all able to form solid powder nanoparticles at a concentration of 0.02 g/mL.

Lipid-polymer hybrid nanoparticles have been formulated by several researchers as a delivery system (Singh & Dutta, 2016; Dave et al., 2019; Khan et al., 2019). The common aspect in their studies was the fact that they used both commercial lipids and polymers for the formulation of the lipid-polymer hybrid nanoparticles. Singh & Dutta (2016) used commercial chitosan and lauric acid for the formulation of chitosan-lauric acid hybrid nanoparticles. This current study, on the other hand, demonstrated that lipid fractions from the black soldier fly (BSF) larvae could also form hybrid nanoparticles. As previously said, lipid-polymer hybrid nanoparticles are mostly used for drug delivery by various researchers. However, no study has been conducted to explore the potential of lipid-chitosan hybrid nanoparticles as an antibacterial agent in the absence of drug incorporation, which was further discussed in the following chapter.

6.4 Characterisation of chitosan lipid hybrid nanoparticles

The section compiles the investigations done about the characterization of chitosan-lipid hybrid nanoparticles. Fourier transform infrared spectroscopy (FTIR) and Scanning electron microscopy (SEM) was used to study the structural components of the particles in solvents.

6.4.1 Fourier transform infrared spectroscopy (FTIR)

Fourier transform infrared spectroscopy (FTIR) analysis was performed to investigate the functional groups of the chitosan lipid nanoparticles. The analysis was also done to compare the spectra of the different chitosan- lipid nanoparticle formulations: chitosan-triglycerides (CH-TGA)Np, chitosan-diglycerides (CH-DG)Np, chitosan-monoglycerides (CH-MG)Np, and chitosan-fatty acids (CH-FA)Np with the chitosan (CH) as well as the lipid fractions in the free form triglycerides (TGA), diglycerides (DG), monoglycerides (MG), and fatty acids (FA). The FTIR data of the different nanoparticle formulations are recorded in Table 6.4.

Table 6.4: Wavenumber and absorbance bands from FTIR spectra of chitosan and chitosan - lipid nanoparticles

Wavenumber (cm^{-1})	Vibration modes or possible assignment
842 - 864	N - H bending of chitosan
1080 - 1132	C - N Stretching in amine group of chitosan
1150 - 1040	C – O - C in the glycosidic bond
	O - C - C stretching of TGA, DG, MG,
1253 - 1294	CH$_3$ in an amine group
	C - C - O stretching of TGA, DG, MG,
1563 - 1578	N - H bending in an amine group
1650 - 1671	C = O stretching vibration in the amide group
1743 - 1758	C = O stretching vibration in the TGA, DG, MG, and FA
2870 - 2893	CH$_3$ stretching of TGA, DG, MG, FA, and chitosan
2926 - 2971	CH$_2$ stretching of TGA, DG, MG, FA, and chitosan
3036 - 3392	N- H Stretching in amine group and OH stretching of chitosan
	O - H stretching in FA, DG, MG

The spectra of the commercial chitosan nanoparticle shown in Figure 6.5 was obtained from 1% chitosan in 90 % acetic acid and was electrosprayed at optimised conditions (a voltage of 25 kV, a flow rate of 0.5 mL/h, and 10 cm tip to collector distance) as described in section 3.3.4.1.
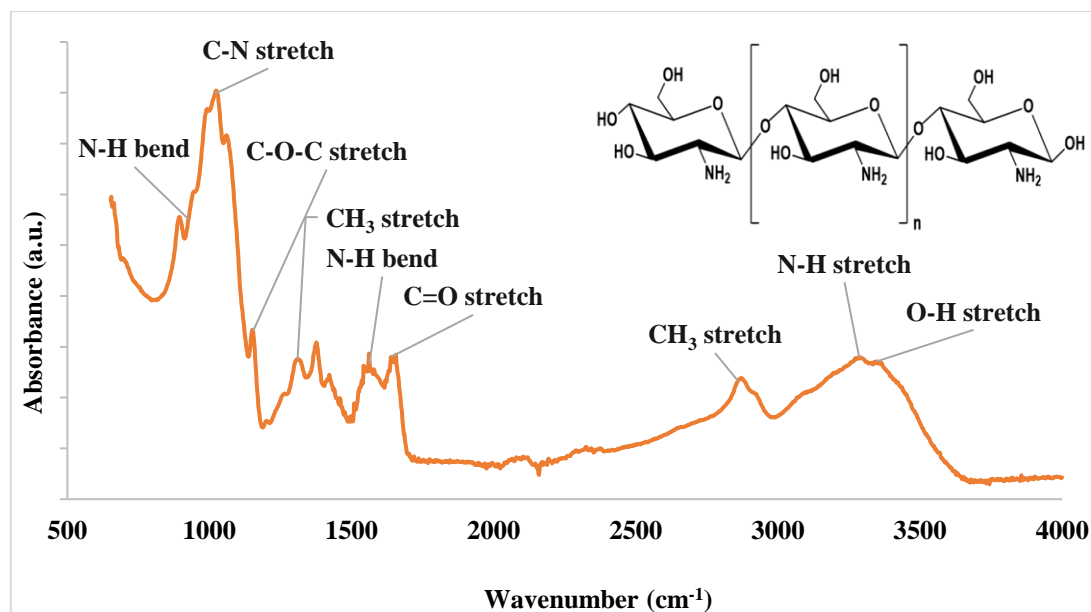
Figure 6.5: FTIR spectrum of chitosan nanoparticles. Electrospraying conditions (a voltage of 25 kV, a flow rate of 0.5 mL/h, and 10 cm tip to collector distance).

The spectrum of the commercial chitosan nanoparticles had a major characteristic band dominated by the amine (I and II), amide, and hydroxyl, groups. The absorption associated with the amide (I) was observed at 1650 - 1671 cm^{-1} and was assigned to C = O stretching vibrations. The peak in the region of 1040 - 1150 cm^{-1} was attributed to the C-O stretching vibration found in the glycosidic linkage of the chitosan which conforms to the observation of Sudatta et al. (2020), in their study. The N-H stretching of the amide (II) group was found in the region of 3036 - 3392 cm^{-1} and the N-H bend of the amine (I) was observed around 1563 - 1578 cm^{-1}. A strong absorption band due to O-H stretching was found at 3036 - 3396 cm^{-1}. That band overlapped with the N-H stretch of the amide (II) which is in close confirmation with the result reported by Kazemi et al. (2019). A weak band of the aliphatic amines was observed in the region 1080-1132 cm^{-1} which is assigned to C-N stretching. CH$_2$ stretch in chitosan is observed at 2870 - 2893 cm^{-1} and it is attributed to a pyranose ring comprising of five carbon atoms and one oxygen, a typical characteristic for saccharide compounds (Zawadzki & Kaczmarek, 2010; Sudatta et al., 2020).

A comparison of the different chitosan- lipid formulations: (CH-TGA)Np, (CH-DG)Np, (CH-MG)Np, and (CH-FA)Np are shown in Figure 6.6, 6.7, 6.8, and 6.9, respectively.
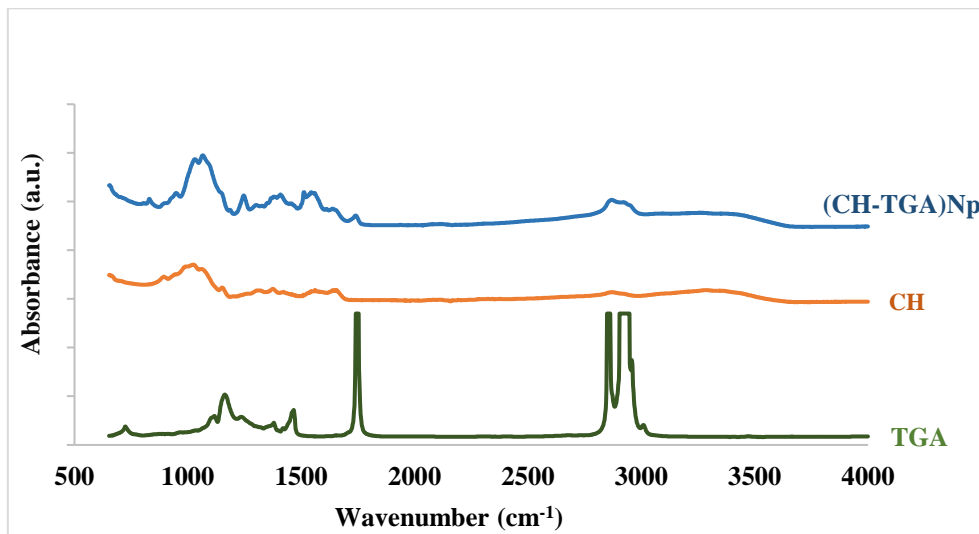
Figure 6.6: FTIR spectra of (CH - TGA) Np, CH, and TGA
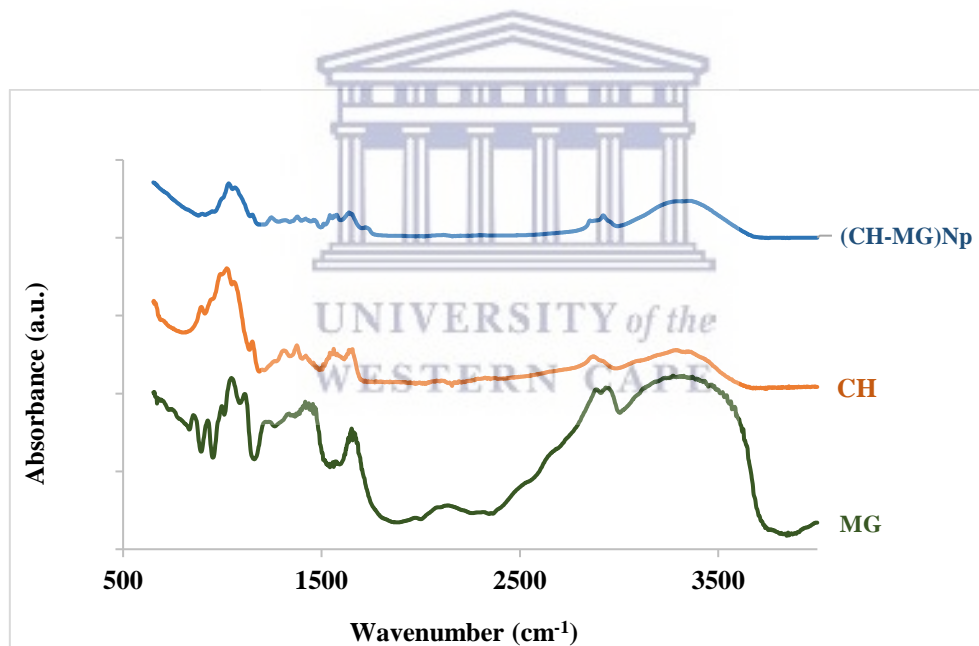
Figure 6.7: FTIR spectra (CH - MG) Np, CH, and MG

136
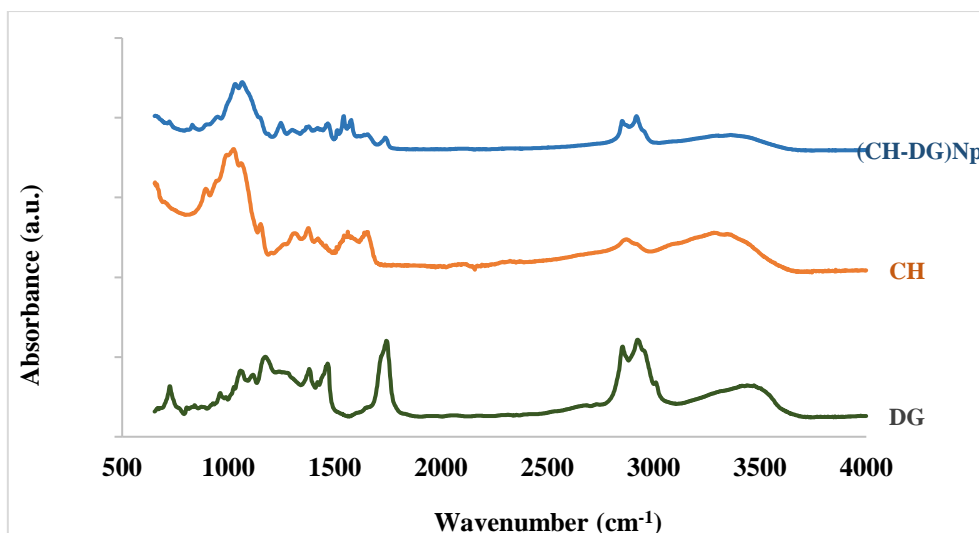
Figure 6.8: FTIR spectra of (CH - DG) Np, CH, and DG
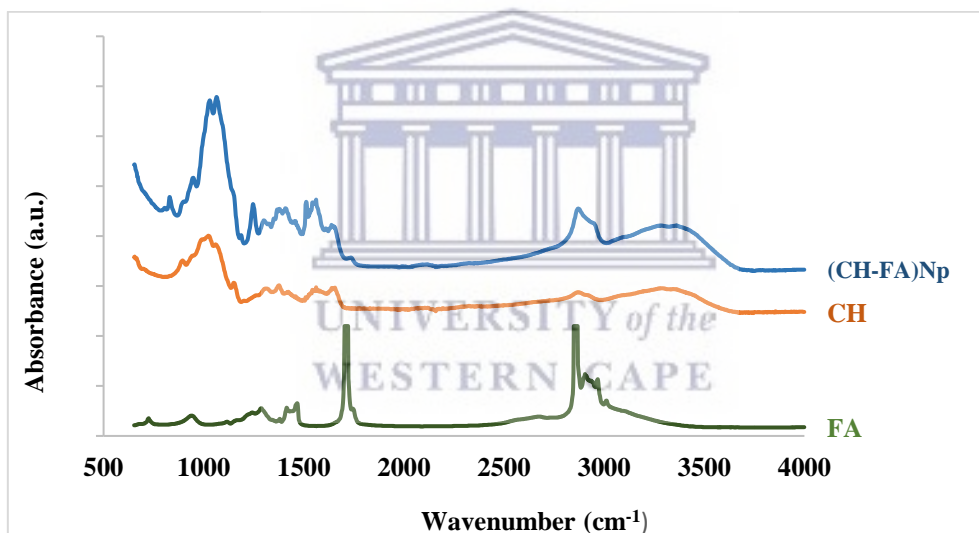
Figure 6.9: FTIR spectra of (CH - FA), CH, and FA

Chitosan in the different formulations was identified by the increase in N-H bending in the region 842 - 864 cm^{-1}, C-N stretching in the region 1080 - 132 cm^{-1}, N-H bending in the region 1563 - 1578 cm^{-1}, C = O stretching in the region 1650 - 1671 cm^{-1} and absorption band assigned to O-H stretching at about 3396 cm^{-1}. The presence of the lipids in the formulation was identified by the existence of a major band in the region 1743 - 1758 cm^{-1} assigned to C=O stretching vibration. Other major brands of the different lipids overlapped with those from the chitosan since they appear around the same region. The overlapping bands included CH_3 stretching, CH_2 stretching, O-H stretching, O-C-C stretching, and C-C-O stretching. The above

observation of a proper co-existence of chitosan and lipids to form a hybrid compound, without any chemical reactions leading to the loss of chemical properties of the individual substance serves as a strong motivation for the use of chitosan to provide structural and mechanical strengthening to the lipids.

In this study, there was no substantial shift in the pattern of peaks of the chitosan and lipid fractions in the FTIR spectra of chitosan-lipid hybrid nanoparticles; all of the major bands of the chitosan and lipid were still present in the nanoparticle formulations. This indicates that the chemical bonds of the compounds did not degrade during the electrospraying process. Similar results were reported by other researchers (Dave et al., 2017; Tahir et al., 2019). They found that the FTIR peaks of lipid-polymer hybrid nanoparticles did not change much, indicating that there was no interaction between the lipid and polymer.

6.4.2   Scanning electron microscopy (SEM)

Scanning electron microscopy (SEM) at two magnifications (5 kx: right and 20 kx: left) of the different formulation: Chitosan-triglycerides (CH-TGA)Np, chitosan-diglycerides (CH-DG)Np, chitosan-monoglycerides (CH-MG)Np, and chitosan-fatty acids (CH-FA)Np presented in Figures 6.10, 6.11, 6.12 and 6.13, respectively.
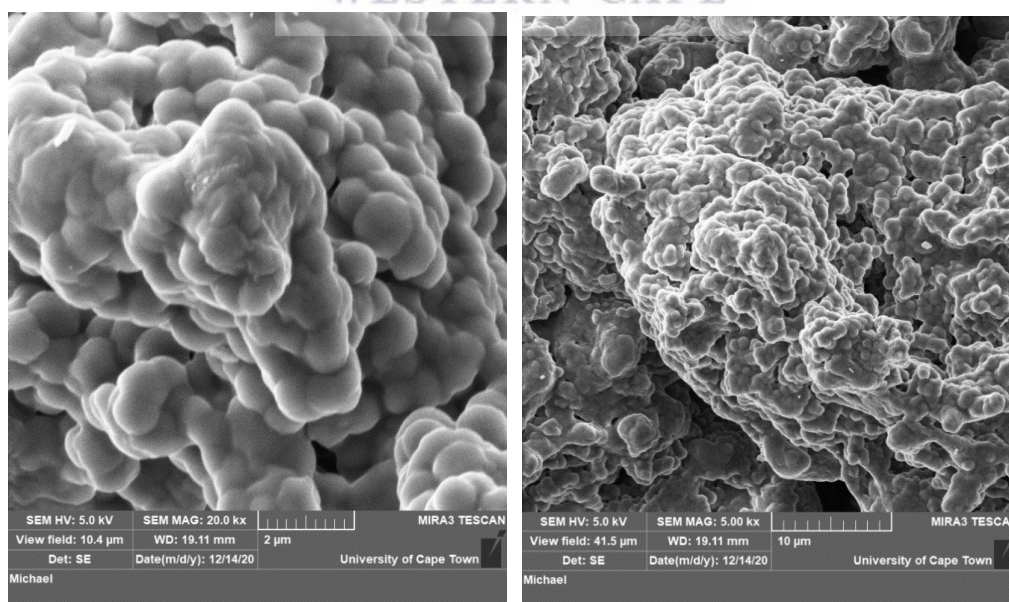
| High magnification | Low magnification |

Figure 6.10: SEM micrographs of (CH-TGA)Np at optimised electrospraying conditions (a voltage of 25 kV, a flow rate of 0.5 mL/h, and 10 cm tip to collector distance).
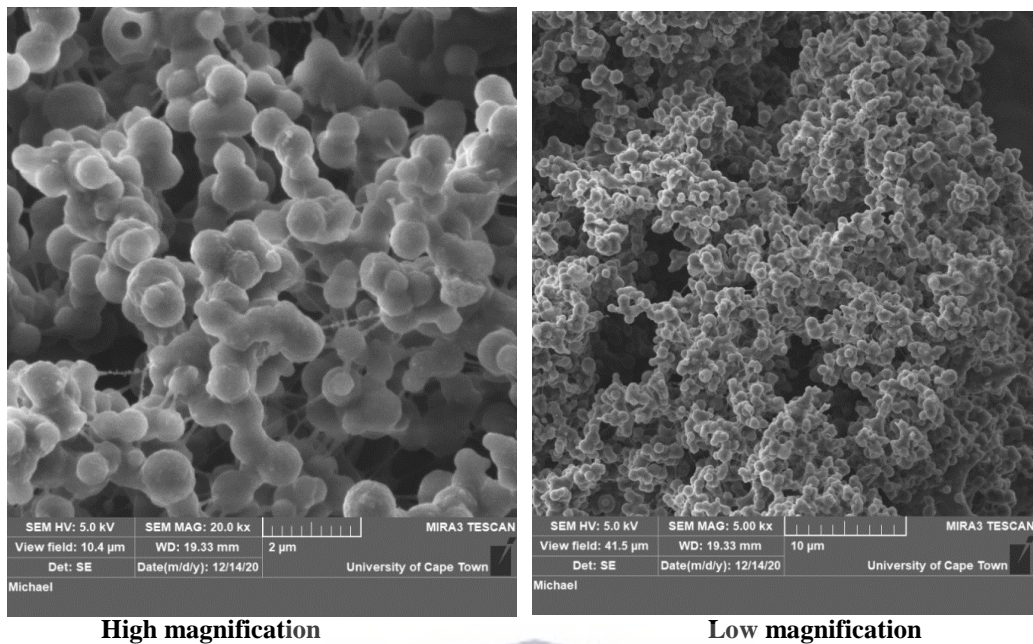
High magnification   Low magnification

Figure 6.11: SEM micrographs of (CH – DG)Np at optimised electrospraying conditions (a voltage of 25 kV, a flow rate of 0.5 mL/h, and 10 cm tip to collector distance).
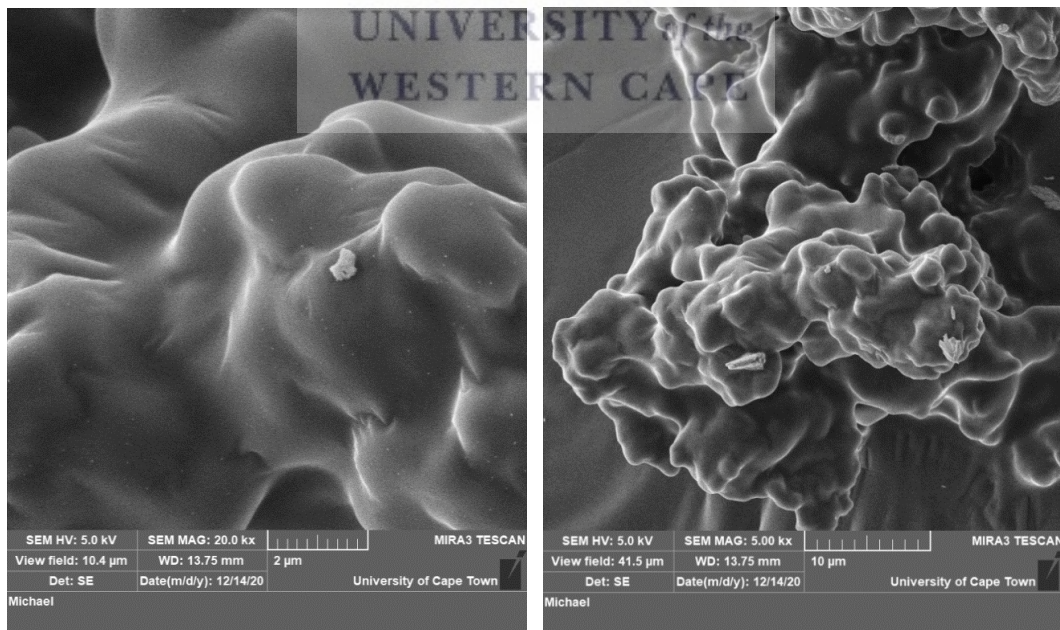
High magnification   Low magnification

Figure 6.12: SEM micrographs of (CH- MG)Np at optimised electrospraying conditions (a voltage of 25 kV, a flow rate of 0.5 mL/h, and 10 cm tip to collector distance).

| High magnification | Low magnification |
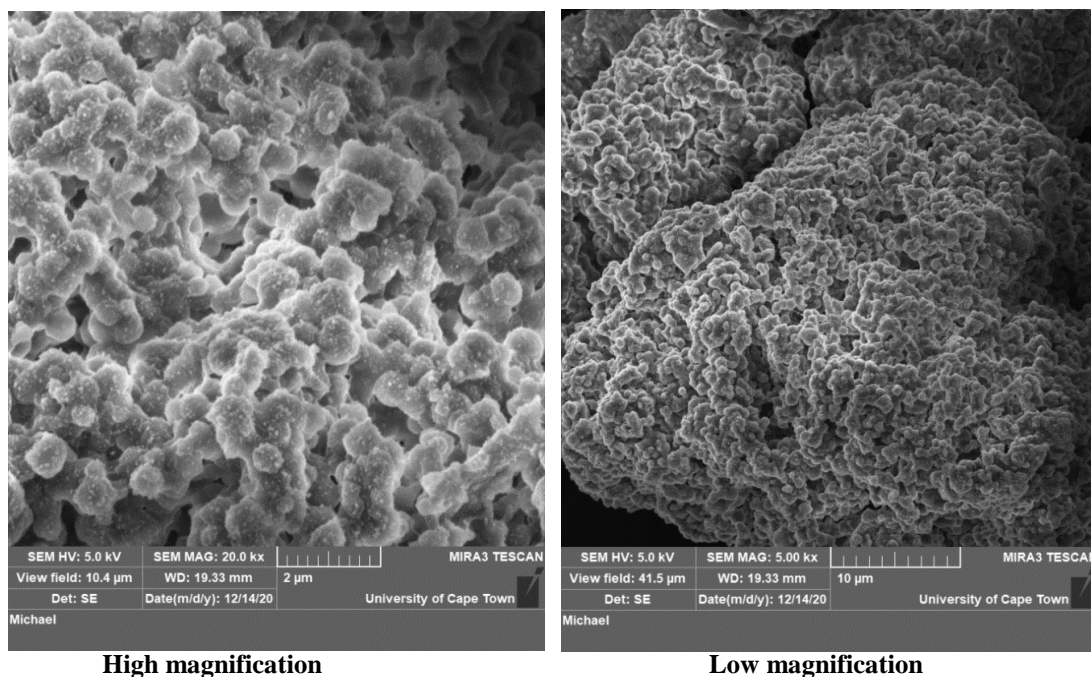
Figure 6.13: SEM micrographs of (CH – FA)Np at optimised electrospraying conditions (a voltage of 25 kV, a flow rate of 0.5 mL/h, and 10 cm tip to collector distance).

The SEM micrographs of (CH-TGA)Np, (CH-DG)Np, (CH-MG)Np, and (CH-FA)Np in Figures 6.10, 6.11, 6.12, and 6.13, respectively, demonstrated that all three chitosan-lipid hybrid nanoparticle formulations had spherical particles and were forming clumps. (CH-DG)Np and (CH-FA)Np contain spherical particles as well as very fine fibers, indicating the presence of the chitosan. On SEM micrographs of (CH-TGA)Np and (CH-MG)Np, those fine fibers were not visible.

The findings of this investigation were consistent with those of several other studies, which indicated that the SEM micrograph of lipid-polymer hybrid nanoparticles has a spherical shape with the presence of small polymer fibers (Dave et al., 2017; Q. Wang et al., 2017; Khan et al., 2019). Dave et al. (2017) produced lipid-polymer hybrid nanoparticles using soya lecithin (lipid) and poly lactic acid (polymer), which had a spherical form and a roughed surface. Khan et al. (2019) synthesised lipid-polymer hybrid nanoparticles produced from soybean phospholipids (lipid) and chitosan (polymer), which also displayed spherical nanoparticles. Their studies were different from this present study in terms of the type of lipid and polymer used.

6.5   Chapter summary

Several methods have been employed for the production of lipid-polymer hybrid nanoparticles however, in this study, the electrospraying technique was used for the production the chitosan-lipid hybrid nanoparticles (chitosan-triglycerides, chitosan-diglycerides, chitosan-monoglycerides, and chitosan-fatty acids nanoparticles). The chitosan-lipid mixture was produced because it was difficult to electrospray lipid on its own without oil droplets deposited on the collector during electrospraying. Chitosan was chosen over other polymers because of its antimicrobial properties, biocompatibility, mechanical and thermal stability. For chitosan to form an effective hybrid with the lipid fractions from the black soldier fly larvae, different concentrations of chitosan (0.5, 1, 2, 3, and 4 wt %) and stirring times (12, 24, and 48 h) were investigated. The findings revealed that those two parameters were crucial for the formation of the desired product and the optimum parameter were stirring time of 48 h and a chitosan concentration of 1 wt %). The effect of chitosan-lipid concentration was investigated at three different concentrations of 0.02, 0.03, and 0.04 g/mL to find the best formulation of the chitosan-lipid hybrid nanoparticle. The best result was achieved with 0.02 g/mL chitosan-lipid concentration.

The chitosan-lipid nanoparticles were characterised in terms of their molecular structures using Fourier transform infrared spectroscopy (FTIR) and morphological using scanning electron microscopy (SEM). The SEM micrograph of the chitosan-lipid hybrid nanoparticles showed that the various particles were slightly spherical and formed small aggregates. The presence of the chitosan in the formulations was shown by the presence of fine fibers on the chitosan-diglyceride and chitosan fatty acid nanoparticles but was not visible in the chitosan-triglyceride and chitosan-monoglyceride nanoparticles. The presence of the lipid fractions and chitosan in the formulation was identified by the existence of major bands of each molecule shown in the different FTIR spectra.

The study is paving a way to produce chitosan-lipid hybrid nanoparticles via electrospray technique using the lipid fractions from the BSF larvae. The antimicrobial effect of each chitosan-lipid hybrid nanoparticles were tested against *Micrococcus luteus* and *Pseudomonas aeruginosa* in the following chapter

CHAPTER 7: ANTIBACTERIAL ACTIVITY OF THE LIPIDS AND CHITOSAN-LIPID HYBRID NANOPARTICLES FROM BLACK SOLDIER FLY LARVAE AGAINST *MICROCOCCUS LUTEUS* AND *PSEUDOMONAS AERUGINOSA*.

Abstract

The emergence of antibiotic-resistant strains of *Micrococcus luteus* and *Pseudomonas aeruginosa* is a major public health concern worldwide. This calls for the development of new antimicrobial agents to combat the ineffectiveness of current clinical treatment. Lipids have been shown to have antimicrobial activity against a variety of pathogens in this regard. In nanoparticle form, they may be more effective and a candidate for fighting multidrug-resistant bacteria. Therefore this chapter aimed to examine the antibacterial activities of the isolated lipids fractions (triglycerides, fatty acids, diglycerides, and monoglycerides) from the BSF larvae and their nanoparticles against *Micrococcus luteus* and *Pseudomonas aeruginosa*. The antimicrobial activity of the lipid fraction and lipid-chitosan nanoparticles were determined by the agar disc diffusion method. Commercial chitosan was combined with each lipid class in the nanoparticle fabrication process to enhance the lipid's antibacterial activity against bacteria. The result of the study showed that lipid fractions were effective in inhibiting *Micrococcus luteus* growth with the fatty acid exhibiting the largest zone of inhibition on the other hand the lipid fractions did not have antibacterial activity against *Pseudomonas aeruginosa*. However, the individual chitosan-lipid nanoparticles (chitosan-triglyceride, chitosan-diglyceride, chitosan-monoglyceride, and chitosan-fatty acids nanoparticles) were strongly active against *Micrococcus luteus* and *Pseudomonas aeruginosa* with the chitosan-fatty acid nanoparticle having the largest zone of inhibition against the two bacteria.

Graphical abstract
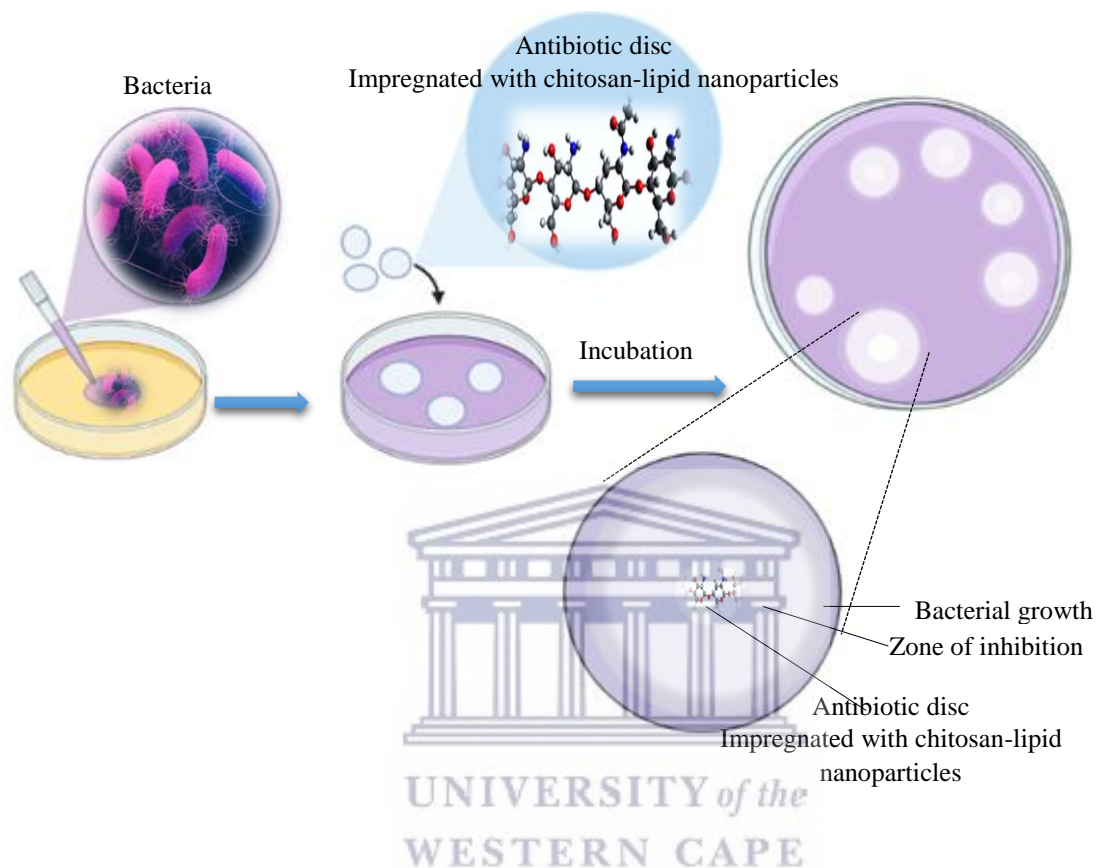
7.1   Introduction

The challenges of drug-resistant bacteria have increased over time, researchers are constantly trying to develop new groups of antibiotics from different sources. The antibacterial properties of lipids have been explored in numerous reports (Nguyen et al., 2017; Anacarso et al., 2018; Yoon et al., 2018). A certain class of lipids such as monoglycerides and fatty acids for instance has attracted researchers' attention as antibacterial agents due to their broad spectrum of activity. To date, the antibacterial properties of the lipids from the black soldier fly larvae have not been explored against *Pseudomonas aeruginosa* (Gram-negative bacteria) and *Micrococcus luteus* (gram-positive bacteria). *Pseudomonas aeruginosa* and *Micrococcus luteus* were selected because they are multidrug-resistant bacteria. They are commonly found in the environment and wildlife, including humans where they can cause life-threatening acute and chronic infections (Alam et al., 2019). Several studies have reported that lipid groups can be used in combined therapy with existing antibiotics to improve their effectiveness (Churchward et al., 2018). Hence the antibacterial activity of the individual lipid fractions combined with commercial chitosan was tested against *Micrococcus luteus* and *Pseudomonas aeruginosa.*

7.2   Antimicrobial activity of the lipid fractions isolated from black soldier fly larvae

This section presents the antimicrobial activity of triglycerides (TGA), diglycerides (DG), monoglycerides (MG), and fatty acids (FA) isolated from the BSF larvae against *Micrococcus luteus* and *Pseudomonas aeruginosa*. The different lipid fractions were obtained by fractionating 50 g of the oil extracted from the BSF larvae using a glass column packed with silica in fractioning the lipids with chromatography. Solvents with different polarities were added into the column sequentially to separate the different lipids into lipid groups as described in section 3.3.3.1. The antimicrobial test was performed using the disc diffusion method as described in section 3.3.6.2. Briefly, 120 µL *Micrococcus luteus* and *Pseudomonas aeruginosa* were spread across the surface agar layer of the plate separately. Several antibiotic discs were impregnated with 20 µL of 0.4 mg/mL each lipid fraction. The different discs were placed on the plate that contained the bacteria. The plates were incubated for 24 h at 30 °C and 37 °C for *Micrococcus luteus* and *Pseudomonas aeruginosa*, respectively. Each experiment was carried out in triplicate. After incubation, the zone of inhibitions appearing on the antibiotic disc was measured. 20 µL of the commercial antibiotic (ampicillin) was used as the positive control while 20 µL hexane was used as the negative control since it was used to dissolve the lipid

fractions. The negative control was necessary to ensure that any zone of inhibition appearing on the disc comes from the product only. The mean of three measurements of inhibition zone diameter of the TGA, DG, FA, MG, and BSF larvae lipid is summarised in Table 7.1.

Table 7.1: Antibacterial activity of the lipid fractions using disc diffusion method (Incubation: Time = 24 h, temperature = 30°C and 37 °C for *Micrococcus luteus* and *Pseudomonas aeruginosa*, respectively)

Lipid fractions	Inhibition zones (mm)	
	Gram-positive bacteria *Micrococcus luteus*	Gram negative bacteria *Pseudomonas aeruginosa*
TGA	$6.56 \pm 0{,}46$	none
FA	8.75 ± 0.36	none
DG	7.77 ± 0.48	none
MG	8.59 ± 0.30	none
BSF larvae extract	7.64 ± 0.33	none
Negative control (hexane)	none	none
Positive control (ampicillin)	11.28	11.12

In Figure 7.1, TGA, DG, FA, and MG show antimicrobial activity against *Micrococcus luteus* and no inhibitory zones for *Pseudomonas aeruginosa.*
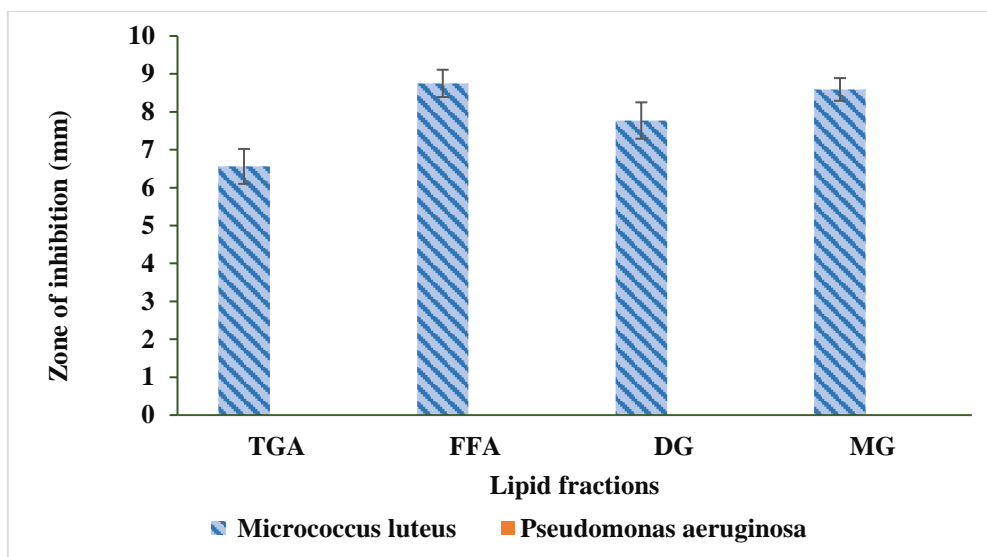
Figure 7.1: Antibacterial activity test of chitosan-lipid nanoparticle against *Pseudomonas aeruginosa* and *Micrococcus luteus*.

Figures 7.2 and 7.3 showed the agar plates with *Pseudomonas aeruginosa* and *Micrococcus luteus*, respectively.
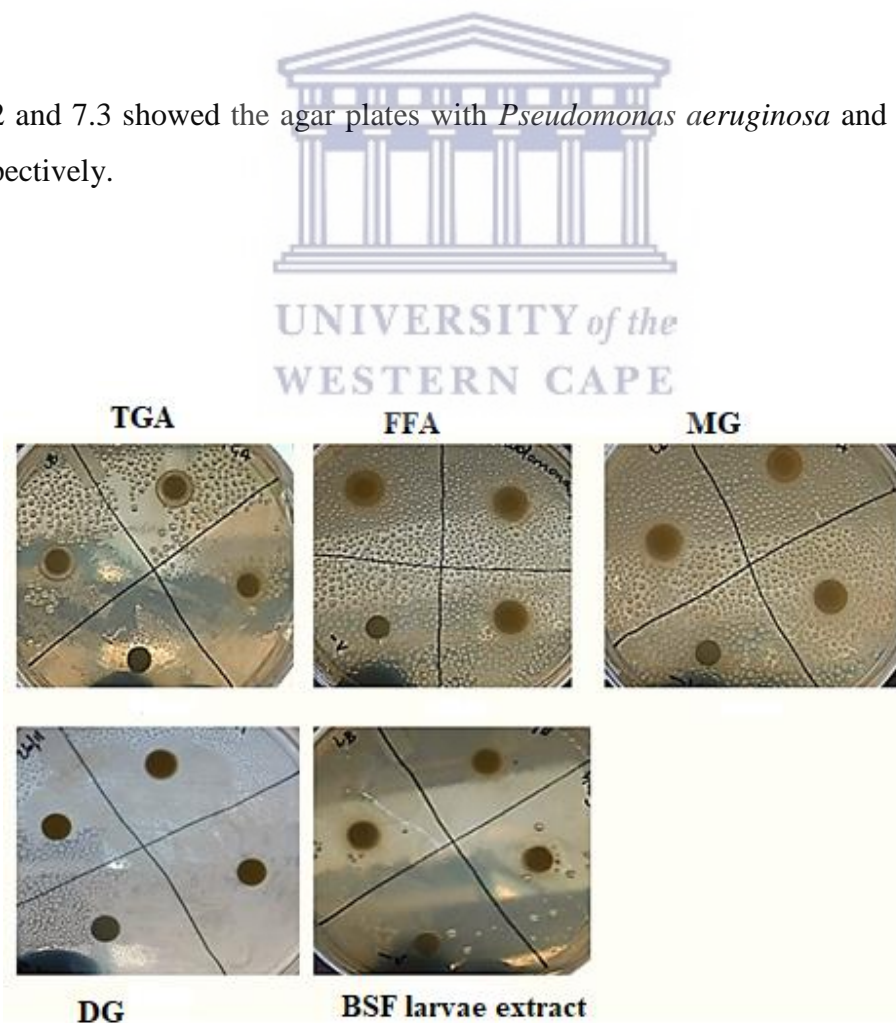
Figure 7.2: Antibacterial activity of the lipid fractions against *Pseudomonas aeruginosa*
(Incubation: Time = 24 h, temperature = 37°C)
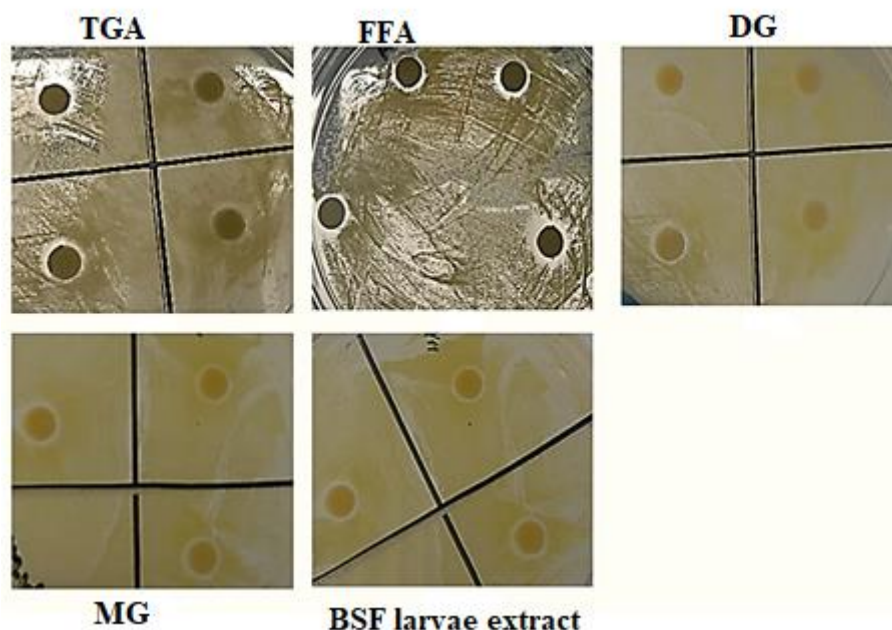
Figure 7.3: Antibacterial activity of the lipid fractions against *Micrococcus luteus* (Incubation: Time = 24 h, temperature = 30°C)

The result of the antimicrobial test indicated that *Pseudomonas aeruginosa* was resistant to TGA, DG, FA, MG lipid fractions, and the BSF larvae extract, and no inhibitory zones were observed (Figures 7.2). On the other hand, TGA, DG, FA, MG, and the BSF larvae extract showed antimicrobial activity against *Micrococcus luteus* and the zone of inhibitions were 6.56, 8.75, 7.77, 8.59, and 7.64 mm for TGA, FA, DG, MG, and BSF larvae extract, respectively (Figure 7.3). FA gave the highest zone of inhibition (8.75 mm) among the lipid fractions, followed by MG (8.59 mm). The lowest antibacterial activity was shown by the TGA fraction (6.56 mm). Commercial antibiotics ampicillin gave a zone of inhibition of 11.28 and 11.12 mm for *Micrococcus luteus* and *Pseudomonas aeruginosa,* respectively. The negative control (hexane) did not show a zone of inhibition for *Micrococcus luteus* and *Pseudomonas aeruginosa* which has confirmed that any zone of inhibition appearing on the disc comes from the lipid fractions only. Based on the diameter of zones of inhibition, the evaluation of inhibition can be classified into three categories which are very active (above 11 mm), medium activity or active (between 6-11 mm), and non-active (< 6 mm). Due to that classification, it can be concluded that the lipid fractions isolated from the BSF larvae were active as antimicrobial compounds against *Micrococcus luteus* since the zones of inhibition reported in this study were between 6.56 and 8.75mm. The higher percentage of lauric acid present in the

FA fraction reported in chapter 5 section 3.3.1 could explain its largest zone of inhibition when compared to TGA and DG and MG fractions. The percentages of lauric acid were 27.65, 22.70, 19.10, and 16.64 % for FA, MG, DG, and TGA, respectively (section 3.3.1).

Similar results were reported by Silalahi, (2019). From their study, they found that the difference in fatty acid composition of the vegetal oils (virgin coconut oil, soybean oil, and palm oil) affected their antibacterial activity. In their study, the virgin coconut oil showing the highest antibacterial activity against *Salmonella typhi* was dominated by lauric acid (48%).

In this present study gram-negative bacteria (*Pseudomonas aeruginosa)* were resistant to the antibacterial action of the different lipid fractions (TGA, DG, MG, and FA) as opposed to the gram-positive bacteria (*Micrococcus luteus).* The reason for that may be due to the cell structure differences of the two bacteria. *Pseudomonas aeruginosa* and *Micrococcus luteus* both possess a cell wall composed of peptidoglycan, in addition to that, *Pseudomonas aeruginosa* has an extra outer membrane composed of lipopolysaccharide which provides an effective barrier against antimicrobial compounds (Alam et al., 2019; Pang et al., 2019). A similar result was reported in other studies (Pang et al., 2019). However, the study conducted by Urbanek et al. (2012) has reported contradicting results in which fatty acids extracted from the larvae of *Forcipomyia nigra* exhibited low antimicrobial activity against *Pseudomonas aeruginosa.* A possible reason for the observed results may be due to the presence of O-antigen or O-polysaccharide attached to the lipopolysaccharide membrane of *Pseudomonas aeruginosa.* The presence or absence of O-antigen can determine how easily antimicrobial lipid compounds can penetrate the lipopolysaccharide of the bacteria (Churchward et al., 2018). The absence or a few O-antigen can make the lipopolysaccharide of the bacteria more hydrophobic while the presence of many O-antigen would make the lipopolysaccharide of the bacteria less hydrophobic (Churchward et al., 2018). This could explain why the different lipids with hydrophobic carbon chains, were unable to penetrate a less hydrophobic lipopolysaccharide membrane of the *Pseudomonas aeruginosa* if it is assumed that o- antigen was present in the lipopolysaccharide membrane. Further study can be conducted by exploring the interaction between the lipid fractions to identify synergistic combinations to improve their antimicrobial activity. For instance, the most active lipid fraction which was the fatty acid can be combined with other lipids showing good antibacterial activity.

The next section discusses the antimicrobial activity of the aforementioned mentioned lipid fractions mixed with commercial chitosan.

7.3 Antimicrobial testing of chitosan-lipid nanoparticles against *Micrococcus luteus* and *Pseudomonas aeruginosa*.

This section presents the antimicrobial activity of chitosan-lipid nanoparticles against *Micrococcus luteus* and *Pseudomonas aeruginosa*. The chitosan-lipid nanoparticles were prepared by dissolving 0.2 g of each of the lipid fractions in 1 wt % of the chitosan solution prepared The chitosan-lipid mixtures were stirred for 24 h using a magnetic stirrer at 500 rpm to form a homogeneous solution. The mixture was loaded into a 10 mL plastic syringe and then electrosprayed room temperature at a flow rate (0.5 mL/h), applied voltage (25 kV), and tip to collector distance (10 cm) conditions as detailed in section 3.3.4.4. The antimicrobial testing of the chitosan-lipid nanoparticles was performed to see the antimicrobial effect of adding commercial chitosan to the lipid fractions extracted from the black soldier fly larvae. The antimicrobial test was performed using the disc diffusion method as described in section 3.3.6.2. Briefly, 120 µL *Micrococcus luteus* and *Pseudomonas aeruginosa* were spread across the surface agar layer of the plate separately. The antibiotic discs were impregnated with 20 µL of 0.0004 mg/mL the chitosan-lipid nanoparticles. The different antibiotic discs were placed on the plate that contained the bacteria. The plates were incubated for 24 h at 30°C and 37 °C for *Micrococcus luteus* and *Pseudomonas aeruginosa*, respectively. Each experiment was carried out in triplicate. After incubation, the zone of inhibitions appearing on the antibiotic disc was measured. The antimicrobial activity of the chitosan-lipid nanoparticles tested against *Micrococcus luteus* and *Pseudomonas aeruginosa* are presented in Table7.2.

Table 7.2: Antibacterial activity of chitosan - lipids nanoparticles using disc method. (Incubation: Time = 24 h, temperature = 30°C and 37 °C for *Micrococcus luteus* and *Pseudomonas aeruginosa*, respectively)

Chitosan-lipid nanoparticles	Inhibition zones (mm)	
	Gram-positive bacteria Micrococcus luteus	Gram-negative bacteria *Pseudomonas aeruginosa*
(CH-TGA)Np	14.37 ± 0.32	9.75 ± 0.97
(CH-FA)Np	21.90 ± 0.13	12.10 ± 0.05
(CH-DG)Np	18.29 ± 1.52	10.70 ± 0.61
(CH-MG)Np	15.12 ± 1.08	10.13 ± 0.63

(CH)Np	11.41 ± 1.81	9.40 ± 0.72
CH	11.09 ± 1.31	9.13 ± 0.36
Positive control (ampicillin)	11.26 ± 0.20	11.24 ± 0.21
Negative control (Acetic acid)	none	none

All the chitosan- lipid nanoparticles were more effective against *Micrococcus luteus* giving a larger zone of inhibition compared to *Pseudomonas aeruginosa* (Figure 7.4).
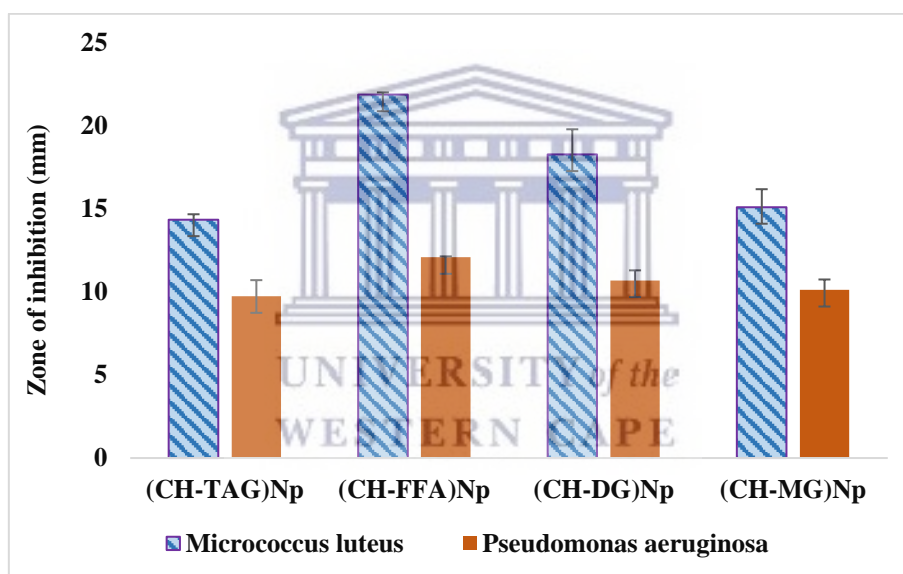
Figure 7.4: Antibacterial activity test of chitosan-lipid nanoparticle against *Pseudomonas aeruginosa* and *Micrococcus luteus*

Figures 7.5 and 7.6 show the zone of inhibitions on agar plates streaked with *Micrococcus luteus* and *Pseudomonas aeruginosa,* respectively.
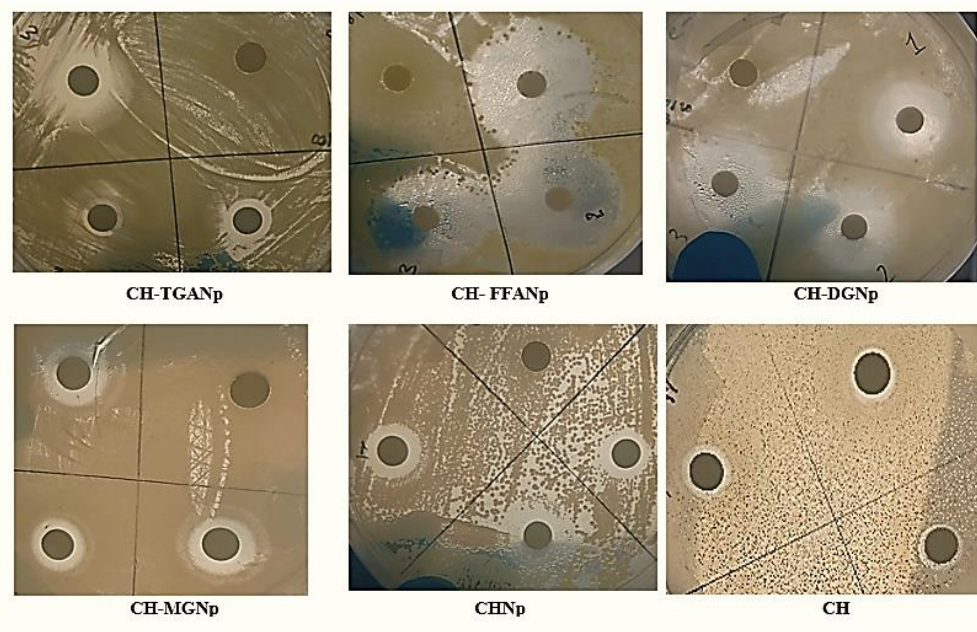
Figure 7.5: Antibacterial activity of the chitosan-lipid nanoparticles against *Micrococcus luteus* (Incubation: Time = 24 h, temperature = 30°C)
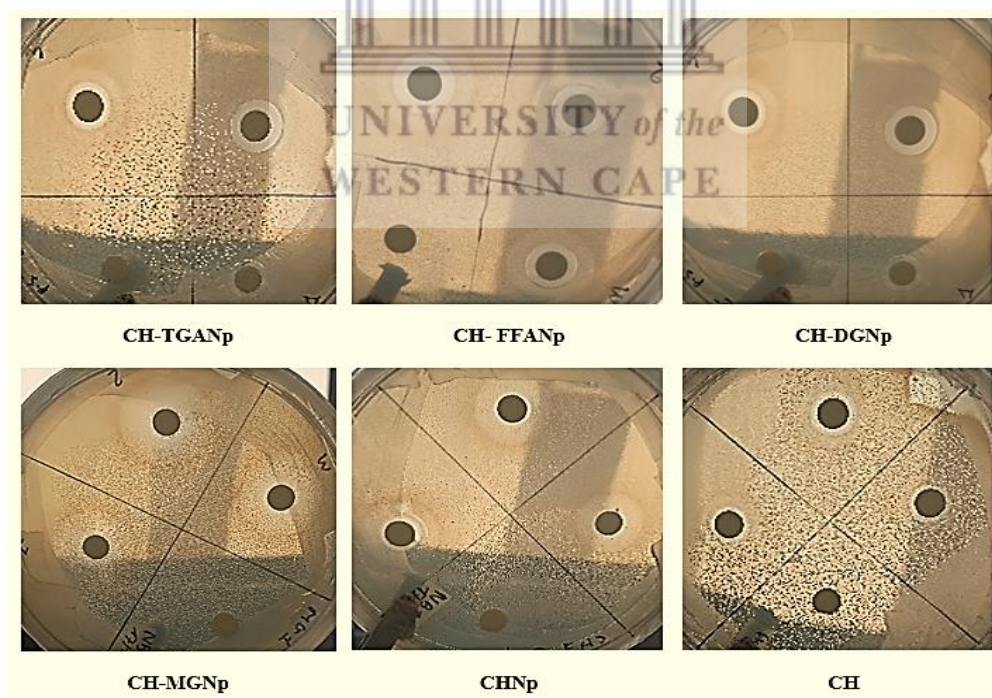
Figure 7.6: Antibacterial activity of the chitosan-lipid nanoparticles against *Pseudomonas aeruginosa* (Incubation: Time = 24 h, temperature = 37 °C)

The inhibition zone of chitosan-lipid nanoparticles for *Micrococcus luteus* were 14.37, 21.90, 18.29, 15.12, 11.41, 11.41 and 11.09 mm, for (CH -TGA)Np, (CH – FA)Np, (CH – DG)Np, (CH –MG)Np, CHNp and CH, respectively. For *Pseudomonas aeruginosa,* the inhibition zone were 9.75, 12.10, 10.70, 10.13, 9.40, and 9.13 mm for (CH-TGA)Np, (CH- FA)Np, (CH-DG)Np, (CH-MG)Np, CHNp, and CH, respectively. It was also interesting to find out that the nanoparticles exhibited a higher inhibition zone when compared to a positive control (ampicillin). Ampicillin gave a zone of inhibition of 11.26 and 11.24 mm for *Micrococcus luteus* and *Pseudomonas aeruginosa* respectively. No zone of inhibition was observed in the two bacteria cultures when using the negative control (acetic acid). Chitosan-lipid nanoparticles formulated in this study were very active as an antimicrobial against *Micrococcus luteus* zones of inhibition were above 11 mm. Only (CH-FA)Np was very active against *Pseudomonas aeruginosa* sinc*e* its zone of inhibition was 12.10 mm while (CH-TAG)Np, (CH-DG)Np, (CH-MG)Np were moderately active against *Pseudomonas aeruginosa*.

The fact that the chitosan-lipid nanoparticles were very active against *Micrococcus luteus* compared to *Pseudomonas aeruginosa* can be explained by the fact that gram-positive bacteria have cell walls composed of teichoic acid which is the major component of the gram-positive cell wall which is made of an anionic phosphate group (PO_4^{3-}) (Arifin et al., 2016). When the anionic phosphate groups react with the cationic amine groups (NH_3^+) of the chitosan, an electrostatic interaction is generated between the two groups (Arifin et al., 2016). This electrostatic interaction will cause the effect of the antimicrobial activity of the gram-positive bacteria to be higher. The strength of the electrostatic interactions depends on the number of the anionic phosphate group to the cationic amine group. However, as opposed to the gram-positive bacteria, gram-negative bacteria have a fewer anionic phosphate group leading to a weak electrostatic interaction, hence a smaller zone of inhibition.

In this study, it was also observed that the different chitosan- lipid nanoparticle formulated exhibited higher antimicrobial activity when they were in combined form compared to the lipid on its own. One of the reasons might be because at the nanoscale, the chitosan-lipid nanoparticles will have a larger surface area, and thus it might easily penetrate the bacterial cell walls as compared to their uncombined form. Another reason for that is when chitosan is mixed with lipid fractions, the functional group of the lipids (COOH) reacts with the amine group (NH_2) of the chitosan. The amine group becomes protonated to form a cationic amine group (NH_3^+). The cationic amine group interacts with the cell membrane of the bacteria having a negative charge which triggers bacterial cell lysis.

Several old and new studies have investigated the combination of two antibiotics to increase their effectiveness against bacteria, some other studies have incorporated antibiotics in lipid as a drug delivery system. The challenge of the bacteria to develop resistance against antibiotics remain unsolved. This current study did not use a combination of antibiotics with the lipid fraction instead the lipid class was mixed with commercial chitosan which is a biopolymer. Their combined effect on the bacteria was found more effective than their effect when acting individually against the bacteria. Most importantly, Anacarso et al. (2018) have reported bacteria do not develop resistance to lipid compounds such as fatty acids and monoglycerides.

In this generation of antibiotic resistance, *Pseudomonas aeurogenosa* and *Micrococcus luteus*, are one of the most significant antibiotic resistant pathogens. This study has demonstrated the therapeutic potential of the CH - TGA, CH - FA, CH - DG, and CH - MG nanoparticles as an antimicrobial against *Pseudomonas aeruginosa* and *Micrococcus luteus*. Further investigation can be conducted on other antibiotic-resistant ESKAPE (*Enterococcus faecium, Staphylococcus aureus, Klebsiella pneumoniae, Acinetobacter baumannii, Pseudomonas aeruginosa, and Enterobacter* species) pathogens which pose a threat to human health.

7.4 Chapter summary

In this study, the antimicrobial properties of lipid classes (triglycerides, diglycerides, monoglycerides, and fatty acids) isolated from black soldier fly larvae lipid were investigated as well as their nanoparticle formulations. *Micrococcus luteus* and *Pseudomonas aeruginosa* were tested against triglycerides (TGA), diglycerides (DG), monoglycerides (MG), and fatty acids (FA). Those lipids classes on their own were found to have potent antibacterial properties against *Micrococcus luteus* but not for *Pseudomonas aeruginosa* probably due to the outer membrane of *Pseudomonas aeruginosa* which is composed of lipopolysaccharide and which provides an effective barrier against the lipid fraction. However, in this study, the nanoparticle formulation of the isolated lipid fractions mixed with commercial chitosan to form chitosan-lipid hybrid nanoparticles was more efficient against the two bacteria when compared to their component materials on their own.

After a thorough review of the literature, the author could not find any previous study that has investigated the antimicrobial efficacy of the lipid classes (triglycerides, diglycerides, monoglycerides, and fatty acids) combined with commercial chitosan in nanoparticle formulation against *Micrococcus luteus* and *Pseudomonas aeruginosa*. This study demonstrated the possibility of using the antimicrobial lipid fractions and the chitosan-lipid

nanoparticles against *Micrococcus luteus* and *Pseudomonas aeruginosa*. The obtained data highlighted the potential of using various lipid fractions from the black soldier fly larvae as alternative treatment options to the antibiotic therapy of *Micrococcus luteus* and *Pseudomonas aeruginosa* as well as other antibiotic resistant ESKAPE pathogens which pose a threat to human health.

CHAPTER 8: CONCLUSIONS, NOVELTY, AND RECOMMENDATIONS

8.1 Conclusion

Finding an alternative and low-cost source of bioactive compounds has been a quest for researchers in recent times. This study revealed that the lipid of BSF larvae contains important compounds for the food, pharmaceutical, and cosmetics industries. Several objectives were outlined to accomplish the aims of this study, and they were as follows: (i) to compare extraction methods of the lipid from BSF larvae, (ii) to fractionate the extracted lipids into individual lipid classes using column chromatography and thin-layer chromatography, (iii) to characterise the lipid fractions from the BSF larvae lipid using FTIR and NMR, (iv) to synthesise lipid nanoparticle using the electrospraying technique and to characterise the nanoparticle formulated, (v) to test antibacterial activities of the lipid fractions and their nanoparticle formulations on *Micrococcus luteus* and *Pseudomonas aeruginosa* using disc diffusion method. The results from this study indicate that the aforementioned objectives have been achieved and below are the answers to the research questions of this study:

- **What is the percentage recovery of lipid extracted from black soldier fly larvae using different extraction methods?**

The important factor usually considered when dealing with the extraction of any substance is the percentage yield which influenced the researcher's choice of extraction method. Lipid from BSF larvae was extracted using Soxhlet extraction, ultrasonic-assisted extraction, and maceration extraction with 8 g freeze-dried BSF larvae powder and 300 mL of petroleum ether as the extraction solvent. The results showed that the extraction methods had a significant effect on the lipid yield ($P < 0.05$). Soxhlet extraction produced the highest lipid yield (40.68 %), followed by ultrasonic-assisted (32.64 %) and maceration extractions (31.42 %).

- **What is the influence of the extraction methods on the fatty acids composition of the black soldier fly larvae lipid**

Different extraction methods have been used to extract lipids, and they have demonstrated an influence on the fatty acids composition of the lipid. The findings, particularly for BSFL lipid, were consistent with previous studies, showing that the percentage of saturated fatty acids (SFAs) varied significantly ($P < 0.05$), depending on the extraction methods. The Soxhlet extraction method yielded 68.64 % of the SFAs, ultrasonic-assisted extraction yielded 62.65 %, and maceration extraction yielded 47.70 %. The percentage of total monounsaturated fatty acids (MUFA) and polyunsaturated fatty acids (PUFA) did not differ significantly ($P > 0.05$) between the three methods. The ∑ PUFA and ∑ MUFA ranged from 2.96 to 3.58 % and from 2.08 to 2.75 %, respectively.

- **What are the optimal extraction conditions of the lipid from black soldier fly larvae using Soxhlet extraction?**

Extensive research revealed that extraction conditions must be examined to determine the optimal extraction parameters that will give the best yield. The solvent types, time, and solid to solvent ratio were all investigated to determine the best Soxhlet extraction conditions. The extraction yield was strongly influenced by the solvent type due to their different polarities as well as the polarity of the compounds extracted. Organic solvents of higher polarity such as methanol, ethyl acetate, and dichloromethane were not as effective compared to non-polar solvents (petroleum ether and hexane) for high lipid recovery from the BSF larvae. The effects of these different solvents on lipid recovery agree with the fact that the lipid of the BSF larvae is mainly composed of non-polar compounds that dissolved more easily in non-polar solvents. Among the non-polar solvents investigated, petroleum ether (lowest toxicity), gave the highest lipid yield. Among the polar solvents methanol which is the most polar solvent resulted in the lowest lipid yield.

The extraction time affects the solubility and stability of the lipid compounds. The diffusion rate increases significantly as the extraction time increases. However, there is a maximum extraction time that should not be exceeded, else, there could be a resultant degradation of the lipid compounds. On 2, 4, and 6 h extraction time investigated, 4 h gave the highest yield.

The solid to solvent ratio, expressed as the weight of the extraction sample (g) divided by the volume of solvent (mL), was an important factor in the extraction of lipid from BSF larvae. The solvent to solid ratios investigated was (0.02, 0.03, or 0.04 g/mL), with 0.03 g/mL giving the best yield.

- **Can column chromatography be suitable for the fractionation of the lipid from black soldier fly larvae?**

The steps for determining the effectiveness of column chromatography for fractionating lipid from BSL larvae were presented in Section 5.1. The lipid extracts from BSF larva were loaded onto a column containing silica gel and were separated into six fractions with the order of elution from the column being cholesterol esters, triglycerides, fatty acids, cholesterol, diglycerides, and monoglycerides. The lipid classes fractionated revealed that triglycerides were the most abundant lipid class and accounted for 30 % of the total lipid mixture. Triglycerides are stored in large quantities in the larva because they will be used as food in the adult stage. The small amount of cholesterols (0.3 %) and cholesterol esters (1.6 %) found in this study was consistent with previous research, suggesting that those two compounds are not stored in larvae. In addition to the aforementioned lipid class, diglycerides (20 %), fatty acids (16 %) were also found in a large percentage compared to monoglycerides with a percentage of 10 %.

- **Can the lipids be formulated as nanoparticles?**

Electrospraying is a proven technique for the production of nanoparticles for different sources. However, due to the inability to spray the lipid compound effectively without oily droplets deposition, electrospraying was not a favourable technique for the production of lipid nanoparticles. To use electrospraying for the production of lipid nanoparticles, the lipid was mixed with commercial chitosan. The purpose was to increase the mechanical and structural properties of the lipid and additionally, enhance its antimicrobial property. Electrospray solution parameters (concentration, stirring time, and chitosan-lipid ratio) were investigated, chitosan concentrations of 0.5, 2, 3, and 4 wt % were not suitable for electrospraying. Only 1 wt % chitosan solution stirred for a period of 48 h gave the optimum electrospray condition hence, this was used for the synthesis of chitosan-lipid nanoparticles. The chitosan-lipid solutions were thereafter prepared at three different concentrations of 0.02, 0.03, and 0.04 g/mL. The concentration of 0.02 g/mL obtained by dissolving 0.2 g of the liquid lipid in 10 mL 1 wt % of the chitosan resulted in the formation of chitosan-lipid hybrid nanoparticles as a white solid powder deposit on the collector. The optimum electrospraying conditions were: Flow rate (0.5 mL/h), applied voltage (25 kV), and tip to collector distance (10 cm). The chitosan-lipid hybrid nanoparticles were characterised using Fourier transform infrared spectroscopy (FTIR) and Scanning electron microscopy (SEM). The FTIR spectra of chitosan-

lipid hybrid nanoparticles showed no significant changes in the pattern of peaks of the chitosan and the lipid fractions; all of the major bands from the chitosan and the lipid fractions bands were still present in the FTIR of the nanoparticle formulations. The images from SEM revealed that the chitosan-lipid hybrid nanoparticles were slightly spherical and were forming aggregates composed of smaller particles.

- **Are lipid fractions able to inhibit the growth of *Micrococcus luteus* and *Pseudomonas aeruginosa*?**

In this era of antibiotic resistance, *Micrococcus luteus* and *Pseudomonas aeruginosa* represent one of the most alarming pathogens involved in antibiotic resistance. When tested against the different lipid fractions (triglycerides, diglycerides, monoglycerides, and fatty acids) *Pseudomonas aeruginosa* which is categorised as a gram-negative bacteria remained resistant, no zone of inhibition was observed. On the other hand, each lipid fraction successfully inhibited the growth of the gram-positive *Micrococcus luteus*, with fatty acid exhibiting the largest zone of inhibition compared to the other lipid fractions. The lipid fractions were active as antimicrobial compounds against *Micrococcus luteus* since the zones of inhibition were greater than 6 mm. Also, the higher percentage of lauric acid (27.65 %) present in the FA fraction reported in section 3.3.1 could explain its largest zone of inhibition when compared to TGA and DG, and MG fractions.

- **Are nanoparticles formulated with chitosan more effective in inhibiting the growth of *Micrococcus luteus* and *Pseudomonas aeruginosa* compared to their free lipid form?**

Nanoparticle-based materials are increasingly being exploited as a new line of defense against multidrug resistance (MDR) and microbial resistance. In this study, chitosan-lipid nanoparticles (chitosan-triglyceride, chitosan-diglyceride, chitosan-monoglyceride, and chitosan-fatty acid nanoparticles) were found to be highly effective against *Micrococcus luteus* and *Pseudomonas aeruginosa*, with the chitosan-fatty acid nanoparticle having the largest zone of inhibition. The antibacterial activity of chitosan-lipid nanoparticles against *Micrococcus luteus* was quite high, with inhibition zones exceeding 11 mm. For *Pseudomonas aeruginosa*, only (CH-FA)Np was very active against with a zone of inhibition of 12.10 mm, while (CH-TAG)Np, (CH-DG)Np, and (CH-MG)Np were only moderately effective with a zone of inhibition between 9.75-11.24 mm.

8.2   Novelty

➢   This study proposed new extraction conditions that can effectively and efficiently extract lipid from the black soldier fly (BSF). The results show that Soxhlet extraction with 300 mL of petroleum ether at 70 °C, a solid to solvent ratio of 0.03 g/mL, and an extraction time of 4 h resulted in good recovery of the BSF larvae lipid and saturated fatty acids such as lauric acid and Palmitic acid. The extraction conditions could be the first step toward implementing the process on a large scale, as well as a good starting point for future research into continuous process optimization.

➢   A new preparation scheme was proposed to fractionate non-polar lipids and polar lipids from the black soldier fly (BSF) larvae lipid using silica gel column chromatography. The optimised extraction scheme consisted of 250 mL of 100 % hexane, 400 mL of 5 % diethyl ether in hexane, 400 mL of 15 % diethyl ether in hexane, 350 mL of 25 % diethyl ether in hexane to obtain non-polar lipid cholesterol, triglycerides, fatty acids, and cholesterol esters, respectively followed by 400 mL of 50 % diethyl ether in hexane and 300 mL of 2 % methanol in diethyl ether to obtain polar lipid diglycerides and monoglycerides, respectively.

➢   A new polymer-lipid hybrid nanoparticles was proposed to enhance the antimicrobial activity of the aforementioned lipid classes (triglyceride, diglyceride, monoglyceride, and fatty acid) extracted from the BSF larvae lipids. The new polymer-lipid hybrid nanoparticles were composed of chitosan as the polymer and the lipids were triglycerides, diglycerides, monoglycerides, and fatty acids. The chitosan-lipid hybrid nanoparticles were more effective compared to lipid fractions and chitosan on their own. The chitosan-lipid hybrid nanoparticles worked best due to the combined antimicrobial properties of the chitosan and the lipids.

8.3   Recommendations

The aim and research questions of this study were completely addressed giving rise to new propositions of knowledge. However, some challenges were encountered as well as certain observations were made through the process of conducting this study. Based on these challenges and observations, some recommendations are made for future research in this area.

➢   When compared to ME and UAE, the comparative study found SE to be a suitable method for extracting lipid from BSF larvae due to its simplicity, low cost, and high oil

recovery. Even though Soxhlet extraction is a traditional method of extraction, this study demonstrated that it is a suitable method for extracting lipid from BSF larvae on an industrial scale. However, more comparative extraction methods need to be investigated to broaden the extraction method selection spectrum.

➢ Further study can be conducted by exploring the interaction between the lipid fractions to identify synergistic combinations to improve their antimicrobial activity. For instance, the most active lipid fraction, the fatty acid may in the future be combined with other lipids that have good antibacterial activity.

➢ This study only tested the antimicrobial activity of lipid fractions against *Pseudomonas aeurogenosa* and *Micrococcus luteus*. Further investigation should be conducted on other antibiotic-resistant ESKAPE (*Enterococcus faecium, Staphylococcus aureus, Klebsiella pneumoniae, Acinetobacter baumannii, Pseudomonas aeruginosa, and Enterobacter* species) pathogens that pose a threat to human health.

➢ This study only focuses on the fractionation of the black soldier fly (BSF) larvae lipid into lipid classes using column chromatography. It will be interesting to further fractionate each lipid class into its lipid subcomponents. This will provide a better understanding of the subcomponents that contribute or do not contribute to the antimicrobial property of the lipid class.

➢ BSF larvae could be a new source of lauric acid, a saturated fatty acid found in a variety of plant and animal fats that has several applications. As a result, researchers can investigate further to establish an effective strategy for isolating lauric acid from BSF larvae lipids.

➢ Chitosan was used to provide mechanical and structural stability to lipid making electrospraying possible. Further investigations are envisaged to bring lipid to the state that can be sprayed on an electrospraying machine to form solid nanoparticles without oily droplets.

APPENDIX

Appendix 1: Transesterification reaction of triglycerides into lauric acid.

REFERENCES

Abdolshahi, A., Abdolshahi, A. & Shaebani, A.A. 2011. The Effect of solvent extraction techniques on fatty acid composition of pistachio oil.

Adhikari, B.K., Barrington, S. & Martinez, J. 2006. Predicted growth of world urban food waste and methane production. *Waste Management & Research*, 24(5): 421–433. http://journals.sagepub.com/doi/10.1177/0734242X06067767 4 May 2020.

Agren, J.J., Julkunen, A. & Penttila, and I. 1992. Rapid separation of serum lipids for fatty acid analysis by a single aminopropyl column. *Journal of Lipid Research*, 33: 1871–1876.

Ahmad, A.L., Yasin, N.H.M., Derek, C.J.C. & Lim, J.K. 2011. Microalgae as a sustainable energy source for biodiesel production: A review. *Renewable and Sustainable Energy Reviews*, 15(1): 584–593. https://linkinghub.elsevier.com/retrieve/pii/S1364032110003059 4 May 2020.

Al-bukhaiti, W.Q., Noman, A., Qasim, A.S. & Al-farga, A. 2017. Gas Chromatography : Principles , Advantages and Applications in Food Analysis. , 6(1).

Al-sumri, A., Al-siyabi, N., Al-saadi, R., Al-rasbi, S. & Al-dallal, A. 2017. Study on the Extraction of Date Palm Seed Oil using Soxhlet Apparatus. , (January): 3–8.

Al-sumri, A., Al-siyabi, N., Al-saadi, R., Al-rasbi, S. & Al-dallal, A. 2016. Study on the Extraction of Date Palm Seed Oil using Soxhlet Apparatus. , 7(12): 1266–1270.

Alam, S.T., Le, T.A.N., Park, J.S., Kwon, H.C. & Kang, K. 2019. Antimicrobial biophotonic treatment of ampicillin-resistant Pseudomonas aeruginosa with hypericin and ampicillin cotreatment followed by orange light. *Pharmaceutics*, 11(12).

Aldridge, M. 2020. Review of the antiviral activity and pharmacology of monoglycerides and implications for treatment of COVID-19. : 1–10.

Ali, M.A., Al-hattab, T.A. & Al-hydary, I.A. 2015. E XTRACTION O F D ATE P ALM S EED O IL (P HOENIX D ACTYLIFERA) B Y S OXHLET A PPARATUS. , 8(3): 261–271.

Alleman, T.L., Christensen, E.D. & Moser, B.R. 2019. Improving biodiesel monoglyceride determination by ASTM method D6584-17. *Fuel*, 241(December 2018): 65–70. https://doi.org/10.1016/j.fuel.2018.12.019.

Alves-Bezerra, M. & Cohen, D.E. 2018. Triglyceride metabolism in the liver. *Comprehensive Physiology*, 8(1): 1–22.

Alves, E., Simoes, A. & Domingues, M.R. 2020. Fruit seeds and their oils as promising sources

of value-added lipids from agro-industrial byproducts: oil content, lipid composition, lipid analysis, biological activity and potential biotechnological applications. *Critical Reviews in Food Science and Nutrition*, 0(0): 1–35. https://doi.org/10.1080/10408398.2020.1757617.

Aly, K.I., Sun, J., Kuckling, D. & Younis, O. 2020. Polyester resins based on soybean oil: synthesis and characterization. *Journal of Polymer Research*, 27(9).

Anacarso, I., Quartieri, A., De Leo, R. & Pulvirenti, A. 2018. Evaluation of the antimicrobial activity of a blend of monoglycerides against Escherichia coli and Enterococci with multiple drug resistance. *Archives of Microbiology*, 200(1): 85–89.

Anna, SobaNska, J.P. & BrzeziNska, E. 2017. SPE / TLC / Densitometric Quantification of Selected Synthetic Food Dyes in Liquid Foodstuffs and Pharmaceutical Preparations. *Journal of Analytical Methods in Chemistry*, 2017.

Anu Bhushani, J. & Anandharamakrishnan, C. 2014. Electrospinning and electrospraying techniques: Potential food based applications. *Trends in Food Science and Technology*, 38(1): 21–33. http://dx.doi.org/10.1016/j.tifs.2014.03.004.

Anzaku, A.A. 2017. Antimicrobial Activity of Coconut Oil and its Derivative (Lauric Acid) on Some Selected Clinical Isolates. *International Journal of Medical Science and Clinical Inventions*, 4(8).

Anzaku, A.A., Akyala, J.I., Juliet, A. & Obianuju, E.C. 2017a. Antibacterial Activity of Lauric Acid on Some Selected Clinical Isolates iMedPub Journals Antibacterial Activity of Lauric Acid on Some Selected Clinical Isolates Lauric acid or systematically dodecanoic acid is saturated. , (January).

Anzaku, A.A., Akyala, J.I., Juliet, A. & Obianuju, E.C. 2017b. iMedPub Journals Antibacterial Activity of Lauric Acid on Some Selected Clinical Isolates. : 1–5.

Ardila, N., Ajji, Z., Heuzey, M.C. & Ajji, A. 2018. Chitosan electrospraying: Mapping of process stability and micro and nanoparticle formation. *Journal of Aerosol Science*, 126(June): 85–98. https://doi.org/10.1016/j.jaerosci.2018.08.010.

Arifin, B., Sugita, P. & Masyudi, D.E. 2016. Chitosan and lauric acid addition to corn starch-film based effect: Physical properties and antimicrobial activity study. *International Journal of Chemical Sciences*, 14(2): 529–544.

Arsenault, A.B., Gunsalus, K.T.W., Laforce-Nesbitt, S.S., Przystac, L., Deangelis, E.J., Hurley, M.E., Vorel, E.S., Tucker, R., Matthan, N.R., Lichtenstein, A.H., Kumamoto, C.A. & Bliss, J.M. 2019. Dietary supplementation with medium-chain triglycerides reduces candida gastrointestinal colonization in preterm infants. *Pediatric Infectious*

Disease Journal, 38(2): 164–168.

Arutyunov, V.S. & Lisichkin, G. V. 2017. Energy resources of the 21st century: problems and forecasts. Can renewable energy sources replace fossil fuels? *Russian Chemical Reviews*, 86(8): 777–804.

Banks, I.J. 2014. To assess the impact of black soldier fly (*Hermetia illucens*) larvae on faecal reduction in pit latrines. *Dissertations and Theses*, (2014): 1–231.

Barragan-Fonseca, K.B., Gort, G., Dicke, M. & van Loon, J.J.A. 2019. Effects of dietary protein and carbohydrate on life-history traits and body protein and fat contents of the black soldier fly Hermetia illucens. *Physiological Entomology*, 44(2): 148–159.

Batovska, D.I., Todorova, I.T., Tsvetkova, I. V. & Najdenski, H.M. 2009. Antibacterial study of the medium chain fatty acids and their 1-monoglycerides: Individual effects and synergistic relationships. *Polish Journal of Microbiology*, 58(1): 43–47.

Battaglia, L., Gallarate, M., Panciani, P.P., Ugazio, E., Sapino, S., Peira, E. & Chirio, D. 2014. Techniques for the Preparation of Solid Lipid Nano and Microparticles. *Application of Nanotechnology in Drug Delivery*, (August).

Bayón-Cordero, L., Alkorta, I. & Arana, L. 2019. Application of solid lipid nanoparticles to improve the efficiency of anticancer drugs. *Nanomaterials*, 9(3).

Belattmania, Z., Engelen, A.H., Pereira, H., Serrão, E.A., Barakate, M., Elatouani, S., Zrid, R., Bentiss, F., Chahboun, N., Reani, A. & Sabour, B. 2016. Potential uses of the brown seaweed Cystoseira humilis biomass: 2- Fatty acid composition, antioxidant and antibacterial activities. *Journal of Materials and Environmental Science*, 7(6): 2074–2081.

Belghit, I., Liland, N.S., Gjesdal, P., Biancarosa, I., Menchetti, E., Li, Y., Waagbø, R., Krogdahl, Å. & Lock, E.J. 2019. Black soldier fly larvae meal can replace fish meal in diets of sea-water phase Atlantic salmon (Salmo salar). *Aquaculture*, 503(October 2018): 609–619. https://doi.org/10.1016/j.aquaculture.2018.12.032.

Belghit, I., Waagbø, R., Lock, E.J. & Liland, N.S. 2019. Insect-based diets high in lauric acid reduce liver lipids in freshwater Atlantic salmon. *Aquaculture Nutrition*, 25(2): 343–357.

Belyagoubi, L., Belyagoubi-Benhammou, N., Jurado, V., Dupont, J., Lacoste, S., Djebbah, F., Ounadjela, F.Z., Benaissa, S., Habi, S., Abdelouahid, D.E. & Saiz-Jimenez, C. 2018. Antimicrobial activities of culturable microorganisms (Actinomycetes and fungi) isolated from Chaabe Cave, Algeria. *International Journal of Speleology*, 47(2): 189–199.

Bendif, H., Adouni, K., Miara, M.D., Baranauskienė, R., Kraujalis, P., Venskutonis, P.R., Nabavi, S.M. & Maggi, F. 2018. Essential oils (EOs), pressurized liquid extracts (PLE)

and carbon dioxide supercritical fluid extracts (SFE-CO2) from Algerian Thymus munbyanus as valuable sources of antioxidants to be used on an industrial level. *Food Chemistry*, 260: 289–298. https://doi.org/10.1016/j.foodchem.2018.03.108.

Bertinetti, C., Samayoa, A.C. & Hwang, S.Y. 2019. Effects of feeding adults of hermetia illucens (Diptera: Stratiomyidae) on longevity, oviposition, and egg hatchability: Insights into optimizing egg production. *Journal of Insect Science*, 19(1): 1–7.

Beskin, K. V., Holcomb, C.D., Cammack, J.A., Crippen, T.L., Knap, A.H., Sweet, S.T. & Tomberlin, J.K. 2018. Larval digestion of different manure types by the black soldier fly (Diptera: Stratiomyidae) impacts associated volatile emissions. *Waste Management*, 74: 213–220. https://doi.org/10.1016/j.wasman.2018.01.019.

Bhushani, J.A. 2014. Electrospinning and electrospraying techniques : Potential food based applications. *Trends in Food Science & Technology*, 38(1): 21–33. http://dx.doi.org/10.1016/j.tifs.2014.03.004.

Bligh, E.G. and Dyer, W.J. 1959. Canadian Journal of Biochemistry and Physiology. *Canadian Journal of Biochemistry and Physiology*, 37(8).

Bojor, O.I. 2008. Evaluation of an alternative organic waste disposal system in Chevron-Escravos : A case study. , (November).

Branen, J.K. & Davidson, P.M. 2004. Enhancement of nisin, lysozyme, and monolaurin antimicrobial activities by ethylenediaminetetraacetic acid and lactoferrin. *International Journal of Food Microbiology*, 90(1): 63–74.

Browne, A.J., Kashef Hamadani, B.H., Kumaran, E.A.P., Rao, P., Longbottom, J., Harriss, E., Moore, C.E., Dunachie, S., Basnyat, B., Baker, S., Lopez, A.D., Day, N.P.J., Hay, S.I. & Dolecek, C. 2020. Drug-resistant enteric fever worldwide, 1990 to 2018: A systematic review and meta-analysis. *BMC Medicine*, 18(1): 1–22.

Bui, Q.H.D., Fried, B. & Sherma, J. 2016. Thin-Layer Chromatographic Analysis of Lipids and Lipophilic Pigments in Snails. , 28(2015): 99–107.

Bundhoo, Z.M.A. 2018. Solid waste management in least developed countries: current status and challenges faced. *Journal of Material Cycles and Waste Management*, 20(3): 1867–1877. http://dx.doi.org/10.1007/s10163-018-0728-3.

Byeon, S.K., Lee, J.Y. & Moon, M.H. 2012. Optimized extraction of phospholipids and lysophospholipids for nanoflow liquid chromatography-electrospray ionization-tandem mass spectrometry. *Analyst*, 137(2): 451–458.

Caligiani, A., Marseglia, A., Leni, G., Baldassarre, S., Maistrello, L., Dossena, A. & Sforza, S. 2018. Composition of black soldier fly prepupae and systematic approaches for extraction

and fractionation of proteins, lipids and chitin. *Food Research International*, 105: 812–820.

Cansizoglu, M.F. & Toprak, E. 2017. Fighting against evolution of antibiotic resistance by utilizing evolvable antimicrobial drugs. *Current Genetics*, 63(6): 973–976.

Chatterjee, P., Fernando, M., Fernando, B., Dias, C.B., Shah, T., Silva, R., Williams, S., Pedrini, S., Hillebrandt, H., Goozee, K., Barin, E., Sohrabi, H.R., Garg, M., Cunnane, S. & Martins, R.N. 2020. Potential of coconut oil and medium chain triglycerides in the prevention and treatment of Alzheimer's disease. *Mechanisms of Ageing and Development*, 186(December 2019): 111209. https://doi.org/10.1016/j.mad.2020.111209.

Chen, S., Hoene, M., Li, J., Li, Y., Zhao, X., Häring, H.U., Schleicher, E.D., Weigert, C., Xu, G. & Lehmann, R. 2013. Simultaneous extraction of metabolome and lipidome with methyl tert-butyl ether from a single small tissue sample for ultra-high performance liquid chromatography/mass spectrometry. *Journal of Chromatography A*, 1298: 9–16. http://dx.doi.org/10.1016/j.chroma.2013.05.019.

Choi, J.S., Park, N.H., Hwang, S.Y., Sohn, J.H., Kwak, I., Cho, K.K. & Choi, I.S. 2013. The antibacterial activity of various saturated and unsaturated fatty acids against several oral pathogens. *Journal of Environmental Biology*, 34(4): 673–676.

Choudhary, V., Choudhary, M., Pandey, S., Chauhan, V.D. & Hasnani, J.J. 2016. Maggot debridement therapy as primary tool to treat chronic wound of animals. *Veterinary World*, 9(4): 403–409.

Chu, K.B., Jeon, G.C. & Quan, F.S. 2014. Hexanedioic acid from Hermetia illucens larvae (Diptera: Stratiomyidae) protects mice against Klebsiella pneumoniae infection. *Entomological Research*, 44(1): 1–8.

Chudasama, C. & Bhupendra, K. 2018. Nanoantibiotics : strategic assets in the fight against drug-resistant superbugs. *International Journal of Nanomedicine*, 13: 3–6.

Churchward, C.P., Alany, R.G. & Snyder, L.A.S. 2018. Alternative antimicrobials: the properties of fatty acids and monoglycerides. *Critical Reviews in Microbiology*, 44(5): 561–570. https://doi.org/10.1080/1040841X.2018.1467875.

Čičková, H., Newton, G.L., Lacy, R.C. & Kozánek, M. 2015. The use of fly larvae for organic waste treatment. *Waste Management*, 35: 68–80.

Ciura, K., Dziomba, S., Nowakowska, J. & Markuszewski, M.J. 2017. Thin layer chromatography in drug discovery process. *Journal of Chromatography A*, 1520: 9–22. http://dx.doi.org/10.1016/j.chroma.2017.09.015.

De Clercq, N., Foubert, I. & Dewettinck, K. 2008. Separation and analysis of acylglycerols by

chromatographic methods. *Lipid Technology*, 20(10): 232–234.

Cullere, M., Tasoniero, G., Giaccone, V., Acuti, G., Marangon, A. & Dalle Zotte, A. 2018. Black soldier fly as dietary protein source for broiler quails: Meat proximate composition, fatty acid and amino acid profile, oxidative status and sensory traits. *Animal*, 12(3): 640–647.

Cullere, M., Tasoniero, G., Giaccone, V., Miotti-Scapin, R., Claeys, E., De Smet, S. & Dalle Zotte, A. 2016. Black soldier fly as dietary protein source for broiler quails: Apparent digestibility, excreta microbial load, feed choice, performance, carcass and meat traits. *Animal*, 10(12): 1923–1930.

Dabbou, S., Lauwaerts, A., Ferrocino, I., Biasato, I., Sirri, F., Zampiga, M., Bergagna, S., Pagliasso, G., Gariglio, M., Colombino, E., Narro, C.G., Gai, F., Capucchio, M.T., Gasco, L., Cocolin, L. & Schiavone, A. 2021. Modified black soldier fly larva fat in broiler diet: Effects on performance, carcass traits, blood parameters, histomorphological features and gut microbiota. *Animals*, 11(6).

Danish, M. & Nizami, M. 2019. Complete fatty acid analysis data of flaxseed oil using GC-FID method. *Data in Brief*, 23: 103845. https://doi.org/10.1016/j.dib.2019.103845.

Danlami, J.M., Arsad, A., Zaini, M.A.A. & Sulaiman, H. 2014. A comparative study of various oil extraction techniques from plants. *Reviews in Chemical Engineering*, 30(6): 605–626.

Dasari, S.R. & Goud, V. V. 2014. Effect of pre-treatment on solvents extraction and physico-chemical properties of castor seed oil. *Journal of Renewable and Sustainable Energy*, 6(6).

Dave, V., Tak, K., Sohgaura, A., Gupta, A., Sadhu, V. & Reddy, K.R. 2019. Lipid-polymer hybrid nanoparticles: Synthesis strategies and biomedical applications. *Journal of Microbiological Methods*, 160(March): 130–142. https://doi.org/10.1016/j.mimet.2019.03.017.

Dave, V., Yadav, R.B., Kushwaha, K., Yadav, S., Sharma, S. & Agrawal, U. 2017. Lipid-polymer hybrid nanoparticles: Development & statistical optimization of norfloxacin for topical drug delivery system. *Bioactive Materials*, 2(4): 269–280. https://doi.org/10.1016/j.bioactmat.2017.07.002.

Dayrit, F.M. 2014. Lauric acid is a medium-chain fatty acid, coconut oil is a medium-chain triglyceride. *Philippine Journal of Science*, 143(2): 157–166.

Debnath, S.K., Saisivam, S., Debanth, M. & Omri, A. 2018. Development and evaluation of Chitosan nanoparticles based dry powder inhalation formulations of Prothionamide. *PLoS ONE*, 13(1): 1–12.

Department of Environmental Affairs. 2018. South Africa State of Waste Report South Africa First draft report. *Government of South Africa*: 68. http://sawic.environment.gov.za/documents/8635.pdf.

Desbois, A.P. & Lawlor, K.C. 2013. Antibacterial activity of long-chain polyunsaturated fatty acids against Propionibacterium acnes and Staphylococcus aureus. *Marine Drugs*, 11(11): 4544–4557.

Desbois, A.P. & Smith, V.J. 2010. Antibacterial Free Fatty Acids : Activities , Mechanisms of Action and. *Appl. Microbiol. Biotechnol*, 44(1334): 1629–1642.

Dey, M.C., Roy, R.N. & Sinhababu, A. 2017. Fatty Acid Composition and Antibacterial Activity of the Leaf Oil of Kleinhovia hospita Linn . *J. Nat. Prod*, 10(3): [cited 2018 Jan 01];p.1102–1105. http://www.sphinxsai.com/2017/ch_vol10_no3/1/(378-384)V10N3CT.pdf%0Ahttps://www.researchgate.net.

Dhouioui, M., Boulila, A., Jemli, M., Schiets, F., Casabianca, H. & Zina, M.S. 2016. Fatty acids composition and antibacterial activity of Aristolochia longa L. and Bryonia dioïca Jacq. Growing wild in Tunisia. *Journal of Oleo Science*, 65(8): 655–661.

Diener, S.;, Zurbrügg, C.;, Roa Gutiérrez, F.;, ; N.D.H., Morel, A.;, Koottatep, T.; & Tockner, K. 2011. Black soldier fly larvae for organic waste treatment – prospects and constraints. WasteSafe 2011 – 2nd Int. Conf. on Solid Waste Management in the Developing Countries, 13-15 February 2011, Khulna, Bangladesh, 52-59. , 52(February): 978–984.

Din, F.U., Aman, W., Ullah, I., Qureshi, O.S., Mustapha, O., Shafique, S. & Zeb, A. 2017. Effective use of nanocarriers as drug delivery systems for the treatment of selected tumors. *International Journal of Nanomedicine*, 12: 7291–7309.

Dinarvand, R., Jafarzadeh Kashi, T., Eskandarion, Esfandyari-Manesh, Samadi, Atyabi, F. & Eshraghi. 2012. Improved drug loading and antibacterial activity of minocycline-loaded PLGA nanoparticles prepared by solid/oil/water ion pairing method. *International Journal of Nanomedicine*, 7: 221–234.

Dissanayake, A.A., Wagner, C.M. & Nair, M.G. 2016. Chemical characterization of lipophilic constituents in the skin of migratory adult sea lamprey from the Great Lakes Region. *PLoS ONE*, 11(12): 1–17.

Dodds, E.D., McCoy, M.R., Rea, L.D. & Kennish, J.M. 2005. Gas chromatographic quantification of fatty acid methyl esters: Flame ionization detection vs. electron impact mass spectrometry. *Lipids*, 40(4): 419–428.

Duan, Y., Dhar, A., Patel, C., Khimani, M., Neogi, S., Sharma, P., Siva Kumar, N. & Vekariya, R.L. 2020. A brief review on solid lipid nanoparticles: Part and parcel of contemporary

drug delivery systems. *RSC Advances*, 10(45): 26777–26791.

Efthymiopoulos, I., Hellier, P., Ladommatos, N., Russo-Profili, A., Eveleigh, A., Aliev, A., Kay, A. & Mills-Lamptey, B. 2018. Influence of solvent selection and extraction temperature on yield and composition of lipids extracted from spent coffee grounds. *Industrial Crops and Products*, 119(April): 49–56.

Ekambaram, P., Sathali, A.A.H. & Priyanka, K. 2018a. Solid lipid nanoparticles : A review SOLID LIPID NANOPARTICLES : A REVIEW. *Sci. Revs. Chem. Commun.*, 2(November 2011): 80–102.

Ekambaram, P., Sathali, A.A.H. & Priyanka, K. 2018b. Solid lipid nanoparticles : A review SOLID LIPID NANOPARTICLES : A REVIEW. , (November 2011).

Elboughdiri, N. 2018. Effect of Time, Solvent-Solid Ratio, Ethanol Concentration and Temperature on Extraction Yield of Phenolic Compounds From Olive Leaves. *Engineering, Technology & Applied Science Research*, 8(2): 2805–2808.

Elhag, O., Zhou, D., Song, Q., Soomro, A.A., Cai, M., Zheng, L., Yu, Z. & Zhang, J. 2017. Screening, expression, purification and functional characterization of novel antimicrobial peptide genes from hermetia illucens (L.). *PLoS ONE*, 12(1): 1–15.

Ewald, N., Vidakovic, A., Langeland, M., Kiessling, A., Sampels, S. & Lalander, C. 2020a. Fatty acid composition of black soldier fly larvae (Hermetia illucens) – Possibilities and limitations for modification through diet. *Waste Management*, 102: 40–47. https://doi.org/10.1016/j.wasman.2019.10.014.

Ewald, N., Vidakovic, A., Langeland, M., Kiessling, A., Sampels, S. & Lalander, C. 2020b. Fatty acid composition of black soldier fly larvae (Hermetia illucens) – Possibilities and limitations for modification through diet. *Waste Management*, 102: 40–47. http://www.sciencedirect.com/science/article/pii/S0956053X19306440.

Ezigbo, O. & Mbaegbu, A. 2017. African journal of education, science and technology. *African Journal of Education,Science and Technology*, 3(3): 59–62. http://ajest.info/index.php/ajest/article/view/32.

Ezigbo, V.O. & Emmanuella, A. 2016. Extraction of Lauric Acid from Coconut Oil, Its Applications and Health Implications On Some Microorganisms. *African Journal of Education Science and Technology*, 3(2): 144–147. http://www.coou.edu.ng/journals/ajest/vol_3_iss_2/extraction_of_lauric_acis_from_coconut_oil.pdf.

Fan, J.X., Zheng, D.W., Rong, L., Zhu, J.Y., Hong, S., Li, C., Xu, Z.S., Cheng, S.X. & Zhang, X.Z. 2017. Targeting epithelial-mesenchymal transition: Metal organic network nano-

complexes for preventing tumor metastasis. *Biomaterials*, 139: 116–126. http://dx.doi.org/10.1016/j.biomaterials.2017.06.007.

Feinman, R.D. 2010. Saturated fat and health: Recent advances in research. *Lipids*, 45(10): 891–892.

Feldlaufer, M.F., Knox, D.A., Lusby, W.R. & Shimanuki, H. 1993. Antimicrobial activity of fatty acids against Bacillus larvae, the causative agent of American foulbrood disease. *Apidologie*, 24(2): 95–99.

Feng, W., Qian, L., Wang, W., Wang, T., Deng, Z., Yang, F., Xiong, J. & Wang, C. 2018. Exploring the potential of lipids from black soldier fly: New paradigm for biodiesel production (II)—Extraction kinetics and thermodynamic. *Renewable Energy*, 119: 12–18. https://doi.org/10.1016/j.renene.2017.11.076.

Feng, W., Xiong, H., Wang, W., Duan, X., Yang, T., Wu, C., Yang, F., Wang, T. & Wang, C. 2020. A facile and mild one-pot process for direct extraction of lipids from wet energy insects of black soldier fl y larvae. *Renewable Energy*, 147: 584–593. https://doi.org/10.1016/j.renene.2019.08.137.

Fernando, I.P.S., Kim, K.N., Kim, D. & Jeon, Y.J. 2019. Algal polysaccharides: potential bioactive substances for cosmeceutical applications. *Critical Reviews in Biotechnology*, 39(1): 99–113. https://doi.org/10.1080/07388551.2018.1503995.

Fife, B. 2010. Coconut Oil and Medium-Chain Triglycerides. : 1–5.

FOLCH, J., LEES, M. & SLOANE STANLEY, G.H. 1957. A simple method for the isolation and purification of total lipides from animal tissues. *The Journal of biological chemistry*, 226(1): 497–509.

Francescangeli, A., Daniele, V., Di Lorenzo, P.A. & Franco, M. 2020. A Novel GC-FID Analytical Strategy Reveals Adulteration of Fuels by Vegetable Oil. *Journal of AOAC INTERNATIONAL*, 103(2): 449–455.

Friedman, A.J., Phan, J., Schairer, D., Champer, J., Qin, M., Blecher, K., Oren, A., Liu, P., Modlin, R.L. & Kim, J. 2013. Nanoparticles : a targeted therapy for cutaneous pathogens. *Journal of Investigative Dermatology*, 133(5): 1231–1239.

Fuchs, B., Süß, R., Teuber, K., Eibisch, M. & Schiller, J. 2011. Lipid analysis by thin-layer chromatography — A review of the current state. *Journal of Chromatography A*, 1218(19): 2754–2774. http://dx.doi.org/10.1016/j.chroma.2010.11.066.

Gachhi, D.B. & Hungund, B.S. 2018. Two-phase extraction, characterization, and biological evaluation of chitin and chitosan from Rhizopus oryzae. *Journal of Applied Pharmaceutical Science*, 8(11): 116–122.

Ganesan, P. & Narayanasamy, D. 2017. Lipid nanoparticles: Different preparation techniques, characterization, hurdles, and strategies for the production of solid lipid nanoparticles and nanostructured lipid carriers for oral drug delivery. *Sustainable Chemistry and Pharmacy*, 6(May): 37–56. http://dx.doi.org/10.1016/j.scp.2017.07.002.

Gao, J., Jing, Y.J., Wang, M.Z., Shi, L.F. & Liu, S.M. 2016. The effects of the unsaturated degree of long-chain fatty acids on the rumen microbial protein content and the activities of transaminases and dehydrogenase in vitro. *Journal of Integrative Agriculture*, 15(2): 424–431. http://dx.doi.org/10.1016/S2095-3119(15)61081-4.

Gaweł, B., Eftekhardadkhah, M. & Øye, G. 2014. Elemental composition and fourier transform infrared spectroscopy analysis of crude oils and their fractions. *Energy and Fuels*, 28(2): 997–1003.

Geszke-Moritz, Małgorzata, Moritz & Michał. 2016. Solid lipid nanoparticles as attractive drug vehicles: Composition, properties and therapeutic strategies. *Materials Science and Engineering C*, 68: 982–994.

Ghaderkhani, J., Yousefimashouf, R., Arabestani, M., Roshanaei, G., Asl, S.S. & Abbasalipourkabir, R. 2019. Improved antibacterial function of Rifampicin-loaded solid lipid nanoparticles on Brucella abortus. *Artificial Cells, Nanomedicine and Biotechnology*, 47(1): 1181–1193. https://doi.org/10.1080/21691401.2019.1593858.

Ghormade, V., Pathan, E.K. & Deshpande, M. V. 2017. Can fungi compete with marine sources for chitosan production? *International Journal of Biological Macromolecules*, 104: 1415–1421. http://dx.doi.org/10.1016/j.ijbiomac.2017.01.112.

Giacometti, J., Milošević, A. & Milin, Č. 2002. Gas chromatographic determination of fatty acids contained in different lipid classes after their separation by solid-phase extraction. *Journal of Chromatography A*, 976(1–2): 47–54.

Gocen, T., Bayari, S.H. & Guven, M.H. 2018. Conformational and vibrational studies of arachidonic acid, light and temperature effects on ATR-FTIR spectra. *Spectrochimica Acta - Part A: Molecular and Biomolecular Spectroscopy*, 203: 263–272.

Goeel, M. 2018. Fatty acids profile and functional group of mixture of yellow striped scad (Selaroides spp) fish and local catfish (Clarias sp) oils. *Oriental Journal of Chemistry*, 34(3): 1380–1386.

Gołebiowski, M., Urbanek, A., Oleszczak, A., Dawgul, M., Kamysz, W., Boguś, M.I. & Stepnowski, P. 2014. The antifungal activity of fatty acids of all stages of Sarcophaga carnaria L. (Diptera: Sarcophagidae). *Microbiological Research*, 169(4): 279–286.

Goud, V. 2014. Effect of pre-treatment on solvents extraction and physico-chemical properties

of castor seed oil. , (September 2016).

Goy, R.C., De Britto, D. & Assis, O.B.G. 2009. A review of the antimicrobial activity of chitosan. *Polimeros*, 19(3): 241–247.

Guglielmo. 2012. On Prediction of Depreciation Time of Fossil Fuel in Malaysia. *Journal of Mathematics and Statistics*, 8(1): 136–143. http://thescipub.com/abstract/10.3844/jmssp.2012.136.143.

Guilhelmelli, F., Vilela, N., Albuquerque, P., Derengowski, L. da S., Silva-Pereira, I. & Kyaw, C.M. 2013. Antibiotic development challenges: The various mechanisms of action of antimicrobial peptides and of bacterial resistance. *Frontiers in Microbiology*, 4(DEC): 1–12.

Gujarathi Gayatri, R. & Pejaver Madhuri, K. 2013. Occurrence of Black Soldier Fly Hermetia illucens (Diptera : Stratiomyidae) in Biocompost. *Research Journal of Recent Sciences*, 2(4): 65–66.

Gunsalus, K.T.W., Tornberg-Belanger, S.N., Matthan, N.R., Lichtenstein, A.H. & Kumamoto, C.A. 2015. Manipulation of Host Diet To Reduce Gastrointestinal Colonization by the. *mSphere*, 1(1): 1–16.

Zaghloul, H.E. and Ibrahim, H., 2019. Comparative study on antimicrobial activity of commercial and extracted chitin and chitosan from Marsupenaeus japonicus shells. *Egyptian Journal of Aquatic Biology and Fisheries*, 23(2): 291-302.

Hadinoto, K., Sundaresan, A. & Cheow, W.S. 2013. Lipid-polymer hybrid nanoparticles as a new generation therapeutic delivery platform: A review. *European Journal of Pharmaceutics and Biopharmaceutics*, 85(3 PART A): 427–443. http://dx.doi.org/10.1016/j.ejpb.2013.07.002.

Hales, K.E., Parker, D.B. & Cole, N.A. 2012. Potential odorous volatile organic compound emissions from feces and urine from cattle fed corn-based diets with wet distillers grains and solubles. *Atmospheric Environment*, 60: 292–297. http://dx.doi.org/10.1016/j.atmosenv.2012.06.080.

Hernández-Santos, B., Rodríguez-Miranda, J., Herman-Lara, E., Torruco-Uco, J.G., Carmona-García, R., Juárez-Barrientos, J.M., Chávez-Zamudio, R. & Martínez-Sánchez, C.E. 2016. Effect of oil extraction assisted by ultrasound on the physicochemical properties and fatty acid profile of pumpkin seed oil (Cucurbita pepo). *Ultrasonics Sonochemistry*, 31: 429–436.

Heussler, C.D., Walter, A., Oberkofler, H., Insam, H., Arthofer, W., Schlick-Steiner, B.C. & Steiner, F.M. 2019. Correction: Influence of three artificial light sources on oviposition

and half-life of the Black Soldier Fly, Hermetia illucens (Diptera: Stratiomyidae): Improving small-scale indoor rearing (PLoS ONE (2018) 13:5 (e0197896) DOI: 10.1371/journal.pone.0197. *PLoS ONE*, 14(12): 40–45.

Hoc, B., Noël, G., Carpentier, J., Francis, F. & Megido, R.C. 2019. Optimization of black soldier fly (Hermetia illucens) artificial reproduction. *PLoS ONE*, 14(4): 1–13.

Huang, W.C., Tsai, T.H., Chuang, L. Te, Li, Y.Y., Zouboulis, C.C. & Tsai, P.J. 2014. Antibacterial and anti-inflammatory properties of capric acid against Propionibacterium acnes: A comparative study with lauric acid. *Journal of Dermatological Science*, 73(3): 232–240. http://dx.doi.org/10.1016/j.jdermsci.2013.10.010.

Hudiyanti, D., Al Khafiz, M.F. & Anam, K. 2018. Coconut (Cocos nucifera L.) lipids: Extraction and characterization. *Oriental Journal of Chemistry*, 34(2): 1136–1140.

Hussain, Z. & Sahudin, S. 2016. Preparation, characterisation and colloidal stability of chitosan-tripolyphosphate nanoparticles: Optimisation of formulation and process parameters. *International Journal of Pharmacy and Pharmaceutical Sciences*, 8(3): 297–308.

Iqbal, M., Zafar, N., Fessi, H. & Elaissari, A. 2015. Double emulsion solvent evaporation techniques used for drug encapsulation. *International Journal of Pharmaceutics*, 496(2): 173–190.

Ishak, S. & Kamari, A. 2019. Biodiesel from black soldier fly larvae grown on restaurant kitchen waste. *Environmental Chemistry Letters*, 17(2): 1143–1150. https://doi.org/10.1007/s10311-018-00844-y.

Ishak, S., Kamari, A., Yusoff, S.N.M. & Halim, A.L.A. 2018. Optimisation of biodiesel production of Black Soldier Fly larvae rearing on restaurant kitchen waste. *Journal of Physics: Conference Series*, 1097(1): 0–8.

Islam, S., Ang, B.C., Andriyana, A., Amalina, · & Afifi, M. 2019. A review on fabrication of nanofibers via electrospinning and their applications. https://doi.org/10.1007/s42452-019-1288-4 10 May 2021.

Iverson, S.J., Lang, S.L.C. & Cooper, M.H. 2001. Comparison of the bligh and dyer and folch methods for total lipid determination in a broad range of marine tissue. *Lipids*, 36(11): 1283–1287.

Jackman, J.A., Yoon, B.K., Li, D. & Cho, N.J. 2016. Nanotechnology formulations for antibacterial free fatty acids and monoglycerides. *Molecules*, 21(3).

Jahan, A., Ahmad, I.Z., Fatima, N., Ansari, V.A. & Akhtar, J. 2017. Algal bioactive compounds in the cosmeceutical industry: A review. *Phycologia*, 56(4): 410–422.

Jin, F., Kawasaki, K., Kishida, H., Tohji, K., Moriya, T. & Enomoto, H. 2007. NMR spectroscopic study on methanolysis reaction of vegetable oil. *Fuel*, 86(7–8): 1201–1207.

Jisieike, C.F. & Betiku, E. 2020. Rubber seed oil extraction: Effects of solvent polarity, extraction time and solid-solvent ratio on its yield and quality. *Biocatalysis and Agricultural Biotechnology*, 24(February): 101522. https://doi.org/10.1016/j.bcab.2020.101522.

Jucker, C., Lupi, D., Moore, C.D., Leonardi, M.G. & Savoldelli, S. 2020. Nutrient recapture from insect farm waste: Bioconversion with hermetia illucens (L.) (Diptera: Stratiomyidae). *Sustainability (Switzerland)*, 12(1): 1–14.

Juhaimi, F. Al, Uslu, N., Babiker, Elfadıl E, Ghafoor, K., Ahmed, I.A.M. & Özcan, M.M. 2019a. The Effect of Different Solvent Types and Extraction Methods on Oil Yields and Fatty Acid Composition of Safflower Seed. , 2019: 1–6.

Juhaimi, F. Al, Uslu, N., Babiker, Elfadıl E, Ghafoor, K., Ahmed, I.A.M. & Özcan, M.M. 2019b. The Effect of Different Solvent Types and Extraction Methods on Oil Yields and Fatty Acid Composition of Safflower Seed. , 1104(11): 1099–1104.

Juhaimi, F. Al, Uslu, N., Babiker, Elfadıl E., Ghafoor, K., Mohamed Ahmed, I.A. & Özcan, M.M. 2019. The effect of different solvent types and extraction methods on oil yields and fatty acid composition of safflower seed. *Journal of Oleo Science*, 68(11): 1099–1104.

Jumina, J., Mada, U.G. & Siswanta, D. 2018. Synthesis and Antibacterial Activity 1-Monolaurin. , (November).

Jung, S.W. & Lee, S.W. 2016. The antibacterial effect of fatty acids on Helicobacter pylori infection. *Korean Journal of Internal Medicine*, 31(1): 30–35.

Jung, S.W., Thamphiwatana, S., Zhang, L. & Obonyo, M. 2015. Mechanism of antibacterial activity of liposomal linolenic acid against helicobacter pylori. *PLoS ONE*, 10(3): 1–13.

Kabara, J.J., Vrable, R. & Lie Ken Jie, M.S.F. 1977. Antimicrobial lipids: Natural and synthetic fatty acids and monoglycerides. *Lipids*, 12(9): 753–759.

Kahsay, A.G. & Muthupandian, S. 2016. A review on Sero diversity and antimicrobial resistance patterns of Shigella species in Africa, Asia and South America, 2001-2014. *BMC Research Notes*, 9(1): 1–6.

Kalhapure, R.S., Mocktar, C., Sikwal, D.R., Sonawane, S.J., Kathiravan, M.K., Skelton, A. & Govender, T. 2014. Ion pairing with linoleic acid simultaneously enhances encapsulation efficiency and antibacterial activity of vancomycin in solid lipid nanoparticles. *Colloids and Surfaces B: Biointerfaces*, 117: 303–311. http://dx.doi.org/10.1016/j.colsurfb.2014.02.045.

Kalus, K., Opaliński, S., Maurer, D., Rice, S., Koziel, J.A., Korczyński, M., Dobrzański, Z., Kołacz, R. & Gutarowska, B. 2017. Odour reducing microbial-mineral additive for poultry manure treatment. *Frontiers of Environmental Science and Engineering*, 11(3): 1–9.

Kaluzny, M.A., Duncan, L.A. & M. V. Merritt, and D.E.E. 1985. Rapid separation of lipid classes in high yield and purity using bonded phase columns. *Journal of Lipid Research*, 26.

Kamau, E., Mutungi, C., Kinyuru, J., Imathiu, S., Tanga, C., Affognon, H., Ekesi, S., Nakimbugwe, D. & Fiaboe, K.K.M. 2018. Moisture adsorption properties and shelf-life estimation of dried and pulverised edible house cricket Acheta domesticus (L.) and black soldier fly larvae Hermetia illucens (L.). *Food Research International*, 106: 420–427. https://doi.org/10.1016/j.foodres.2018.01.012.

Kanadea, R. & Bhatkhandeb, D.S. 2016. Extraction of Ginger Oil Using Different Methods and Effect of Solvents, Time, Temperature to Maximize Yield. *International Journal of Advances in Science Engineering and Technology*, 4(3): 2321–9009.

Karthikeyan, H., Antoine, R., Jérôme, D., Christophe, C. & Farid, T. 2020. Effect of devitalization techniques on the lipid , protein , antioxidant , and chitin fractions of black soldier fly (Hermetia illucens) larvae. *European Food Research and Technology*, 246(12): 2549–2568. https://doi.org/10.1007/s00217-020-03596-8.

Kasiramar, G. 2019. SIGNIFICANT ROLE OF SOXHLET EXTRACTION PROCESS IN PHYTOCHEMICAL Mintage Journal of Pharmaceutical & Medical Sciences SIGNIFICANT ROLE OF SOXHLET EXTRACTION PROCESS IN PHYTOCHEMICAL. , (April).

Kazemi, M.S., Mohammadi, Z., Amini, M., Yousefi, M., Tarighi, P., Eftekhari, S. & Rafiee Tehrani, M. 2019. Thiolated chitosan-lauric acid as a new chitosan derivative: Synthesis, characterization and cytotoxicity. *International Journal of Biological Macromolecules*, 136: 823–830.

Khalil, M.H., Marcelletti, J.F. & Diego, S. 1999. United States Patent (19). , (19).

Khan, M.M., Madni, A., Torchilin, V., Filipczak, N., Pan, J., Tahir, N. & Shah, H. 2019. Lipid-chitosan hybrid nanoparticles for controlled delivery of cisplatin. *Drug Delivery*, 26(1): 765–772. https://doi.org/10.1080/10717544.2019.1642420.

Khan, S.H. 2018. Recent advances in role of insects as alternative protein source in poultry nutrition. *Journal of Applied Animal Research*, 46(1): 1144–1157.

Khan, S.T., Musarrat, J. & Al-Khedhairy, A.A. 2016. Countering drug resistance, infectious

diseases, and sepsis using metal and metal oxides nanoparticles: Current status. *Colloids and Surfaces B: Biointerfaces*, 146: 70–83. http://dx.doi.org/10.1016/j.colsurfb.2016.05.046.

Khatak, S. & Dureja, H. 2018. Structural Composition of Solid Lipid Nanoparticles for Invasive and Noninvasive Drug Delivery. *Current Nanomaterials*, 2(3): 129–153.

Kidadl. 2021. Black Soldier Fly: 19 Facts You Won't Believe! https://kidadl.com/animal-facts/black-soldier-fly-facts 17 September 2021.

Kiefer, J., Noack, K., Bartelmess, J., Walter, C., Dörnenburg, H. & Leipertz, A. 2010. Vibrational structure of the polyunsaturated fatty acids eicosapentaenoic acid and arachidonic acid studied by infrared spectroscopy. *Journal of Molecular Structure*, 965(1–3): 121–124. http://dx.doi.org/10.1016/j.molstruc.2009.11.052.

Kim, Y.B., Kim, D.-H., Jeong, S., Lee, J.-W., Kim, T., Lee, H.-G. & Lee, K. 2020. Black soldier fly larvae oil as an alternative fat source in broiler nutrition. *Poultry Science*. https://doi.org/10.1016/j.psj.2020.01.018.

Kim, Y.G., Lee, J.H., Raorane, C.J., Oh, S.T., Park, J.G. & Lee, J. 2018. Herring oil and omega fatty acids inhibit Staphylococcus aureus biofilm formation and virulence. *Frontiers in Microbiology*, 9(JUN): 1–10.

Kotmakçı, M., Akbaba, H., Erel, G., Ertan, G. & Kantarcı, G. 2017. Improved Method for Solid Lipid Nanoparticle Preparation Based on Hot Microemulsions: Preparation, Characterization, Cytotoxicity, and Hemocompatibility Evaluation. *AAPS PharmSciTech*, 18(4): 1355–1365.

Kudo, S. & Nakashima, S. 2020. Changes in IR band areas and band shifts during water adsorption to lecithin and ceramide. *Spectrochimica Acta - Part A: Molecular and Biomolecular Spectroscopy*, 228: 117779. https://doi.org/10.1016/j.saa.2019.117779.

Kulkarni, P.R., Yadav, J.D. & Vaidya, K.A. 2011. LIPOSOMES: A NOVEL DRUG DELIVERY SYSTEM Review. *International Journal of Current Pharmaceutical Research*, 3(2).

Lalander, C., Diener, S., Magri, M.E., Zurbrügg, C., Lindström, A. & Vinnerås, B. 2013. Faecal sludge management with the larvae of the black soldier fly (Hermetia illucens) - From a hygiene aspect. *Science of the Total Environment*, 458–460: 312–318. http://dx.doi.org/10.1016/j.scitotenv.2013.04.033.

Lalander, C., Diener, S., Zurbrügg, C. & Vinnerås, B. 2019. Effects of feedstock on larval development and process efficiency in waste treatment with black soldier fly (Hermetia illucens). *Journal of Cleaner Production*, 208: 211–219.

https://doi.org/10.1016/j.jclepro.2018.10.017.

Lauritano, C., Martínez, K.A., Battaglia, P., Granata, A., de la Cruz, M., Cautain, B., Martín, J., Reyes, F., Ianora, A. & Guglielmo, L. 2020. First evidence of anticancer and antimicrobial activity in Mediterranean mesopelagic species. *Scientific Reports*, 10(1): 1–8.

Lazzari, E., Schena, T., Marcelo, M.C.A., Primaz, C.T., Silva, A.N., Ferrão, M.F., Bjerk, T. & Caramão, E.B. 2018. Classification of biomass through their pyrolytic bio-oil composition using FTIR and PCA analysis. *Industrial Crops and Products*, 111(November): 856–864. http://dx.doi.org/10.1016/j.indcrop.2017.11.005.

Lee, A.K., Lewis, D.M. & Ashman, P.J. 2012. Disruption of microalgal cells for the extraction of lipids for biofuels: Processes and specific energy requirements. *Biomass and Bioenergy*, 46: 89–101. http://dx.doi.org/10.1016/j.biombioe.2012.06.034.

Li, Q., Cai, T., Huang, Y., Xia, X., Cole, S.P.C. & Cai, Y. 2017. A review of the structure, preparation, and application of NLCs, PNPs, and PLNs. *Nanomaterials*, 7(6): 1–25.

Li, Q., Zheng, L., Cai, H., Garza, E., Yu, Z. & Zhou, S. 2011. From organic waste to biodiesel : Black soldier fly , Hermetia illucens , makes it feasible. *Fuel*, 90(4): 1545–1548. http://dx.doi.org/10.1016/j.fuel.2010.11.016.

Liland, N.S., Biancarosa, I., Araujo, P., Biemans, D., Bruckner, C.G., Waagbø, R., Torstensen, B.E. & Lock, E.J. 2017. Modulation of nutrient composition of black soldier fly (Hermetia illucens) larvae by feeding seaweed-enriched media. *PLoS ONE*, 12(8).

Liu, Q., Tomberlin, J.K., Brady, J.A., Sanford, M.R. & Yu, Z. 2008. Black Soldier Fly (Diptera: Stratiomyidae) Larvae Reduce <I>Escherichia coli</I> in Dairy Manure. *Environmental Entomology*, 37(6): 1525–1530.

Liu, T., Awasthi, M.K., Chen, H., Duan, Y., Awasthi, S.K. & Zhang, Z. 2019. Performance of black soldier fly larvae (Diptera: Stratiomyidae) for manure composting and production of cleaner compost. *Journal of Environmental Management*, 232: 113294

Longyu Zheng, Q.L. 2011. Insect Fat a Promising Resource for Biodiesel. *Journal of Petroleum & Environmental Biotechnology*, s2(01).

López-Colom, P., Castillejos, L., Rod Ríguez-Sorrento, A., Puyalto, M., Mallo, J.J. & Martín-Orúe, S.M. 2019. Efficacy of medium-chain fatty acid salts distilled from coconut oil against two enteric pathogen challenges in weanling piglets. *Journal of Animal Science and Biotechnology*, 10(1): 1–17.

Lucarini, M., Durazzo, A., Sánchez del Pulgar, J., Gabrielli, P. & Lombardi-Boccia, G. 2018. Determination of fatty acid content in meat and meat products: The FTIR-ATR approach.

Food Chemistry, 267: 223–230. https://doi.org/10.1016/j.foodchem.2017.11.042.

Luque de Castro, M.D. & Priego-Capote, F. 2010. Soxhlet extraction: Past and present panacea. *Journal of Chromatography A*, 1217(16): 2383–2389. http://dx.doi.org/10.1016/j.chroma.2009.11.027.

M J Hao, N.H.E., Aminuddin, M.H. & Zainalabidin, N. 2021. Microwave-assisted extraction of black soldier fly larvae (BSFL) lipid. *Earth and Environmental Science*, 765: 1753–1315.

Makahleh, A., Saad, B., Siang, G.H., Saleh, M.I., Osman, H. & Salleh, B. 2010. Determination of underivatized long chain fatty acids using RP-HPLC with capacitively coupled contactless conductivity detection. *Talanta*, 81(1–2): 20–24. http://dx.doi.org/10.1016/j.talanta.2009.11.030.

Makkar, H.P.S., Tran, G., Heuzé, V. & Ankers, P. 2014a. State-of-the-art on use of insects as animal feed. *Animal Feed Science and Technology*, 197: 1–33.

Makkar, H.P.S., Tran, G., Heuzé, V. & Ankers, P. 2014b. State-of-the-art on use of insects as animal feed. *Animal Feed Science and Technology*, 197: 1–33. http://dx.doi.org/10.1016/j.anifeedsci.2014.07.008.

Marinho, R., Horiuchi, L. & Pires, C.A. 2018. Effect of stirring speed on conversion and time to particle stabilization of poly (vinyl chloride) produced by suspension polymerization process at the beginning of reaction. *Brazilian Journal of Chemical Engineering*, 35(2): 631–639.

Martini, M.C., Zhang, T., Williams, J.T., Abramovitch, R.B., Pamela, J., Shell, S.S., Genetics, M. & Lansing, E. 2020. Artemisia annua and Artemisia afra extracts exhibit strong bactericidal activity against Mycobacterium tuberculosis. : 1–13.

Masson, L., Alfaro, T., Camilo, C., Carvalho, A., Illesca, P., Torres, R., Do Carmo, M.T., Mancini-Filho, J. & Bernal, C. 2015. Fatty acid composition of soybean/sunflower mix oil, fish oil and butterfat applying the AOCS Ce 1j-07 method with a modified temperature program. *Grasas y Aceites*, 66(1): 1–16.

Matuszewska, A., Jaszek, M., Stefaniuk, D., Ciszewski, T. & Matuszewski, Ł. 2018. Anticancer, antioxidant, and antibacterial activities of low molecular weight bioactive subfractions isolated from cultures of wood degrading fungus Cerrena unicolor. *PLoS ONE*, 13(6): 1–14.

McBryde, E.S., Meehan, M.T., Doan, T.N., Ragonnet, R., Marais, B.J., Guernier, V. & Trauer, J.M. 2017. The risk of global epidemic replacement with drug-resistant Mycobacterium tuberculosis strains. *International Journal of Infectious Diseases*, 56: 14–20.

http://dx.doi.org/10.1016/j.ijid.2017.01.031.

McNeish, H. 2018. Rocketing smoking rates across Africa stoke TB and HIV fears. *BMJ*, 361: k1884. http://www.bmj.com/lookup/doi/10.1136/bmj.k1884 4 May 2020.

Meneguz, M., Schiavone, A., Gai, F., Dama, A., Lussiana, C., Renna, M. & Gasco, L. 2018. Effect of rearing substrate on growth performance, waste reduction efficiency and chemical composition of black soldier fly (Hermetia illucens) larvae. *Journal of the Science of Food and Agriculture*, 98(15): 5776–5784.

Meng, Z., Wen, D., Sun, D., Gao, F., Li, W., Liao, Y. & Liu, H. 2007. Rapid determination of C12-C26 non-derivatized fatty acids in human serum by fast gas chromatography. *Journal of Separation Science*, 30(10): 1537–1543.

Meticulous. 2014. Top 10 companies in black soldier fly market. https://meticulousblog.org/top-10-companies-in-black-soldier-fly-market/ 11 March 2022.

Mishra, V., Bansal, K.K., Verma, A., Yadav, N., Thakur, S., Sudhakar, K. & Rosenholm, J.M. 2018. Solid lipid nanoparticles: Emerging colloidal nano drug delivery systems. *Pharmaceutics*, 10(4): 1–21.

Mohammadi, M., Khanmohammadi Khorrami, M., Vatani, A., Ghasemzadeh, H., Vatanparast, H., Bahramian, A. & Fallah, A. 2020. Rapid determination and classification of crude oils by ATR-FTIR spectroscopy and chemometric methods. *Spectrochimica Acta - Part A: Molecular and Biomolecular Spectroscopy*, 232: 118157. https://doi.org/10.1016/j.saa.2020.118157.

Molino, A., Larocca, V., Di Sanzo, G., Martino, M., Casella, P., Marino, T., Karatza, D. & Musmarra, D. 2019. Extraction of bioactive compounds using supercritical carbon dioxide. *Molecules*, 24(4).

Momchilova, S. & Nikolova-, B. 2016. Silver Ion Chromatography of Fatty Acids. : 1–6.

Mubarak, M., Shaija, A. & Suchithra, T. V. 2015. A review on the extraction of lipid from microalgae for biodiesel production. *Algal Research*, 7: 117–123. http://dx.doi.org/10.1016/j.algal.2014.10.008.

Mukherjee, A., Waters, A.K., Kalyan, P., Achrol, A.S., Kesari, S. & Yenugonda, V.M. 2019. Lipid-polymer hybrid nanoparticles as a nextgeneration drug delivery platform: State of the art, emerging technologies, and perspectives. *International Journal of Nanomedicine*, 14: 1937–1952.

Müller, A., Wolf, D. & Gutzeit, H.O. 2017a. The black soldier fly, Hermetia illucens - A promising source for sustainable production of proteins, lipids and bioactive substances.

Zeitschrift fur Naturforschung - Section C Journal of Biosciences, 72(9–10): 351–363.

Müller, A., Wolf, D. & Gutzeit, H.O. 2017b. The black soldier fly, Hermetia illucens - A promising source for sustainable production of proteins, lipids and bioactive substances. *Zeitschrift fur Naturforschung - Section C Journal of Biosciences*, 72(9–10): 351–363.

Muniyan, R. & Jayaraman, G. 2016. Lauric acid and myristic acid from Allium sativum inhibit the growth of Mycobacterium tuberculosis H37Ra: in silico analysis reveals possible binding to protein kinase B. *Pharmaceutical Biology*, 54(12): 2814–2821.

Nagappan, S., Devendran, S., Tsai, P.C., Dahms, H.U. & Ponnusamy, V.K. 2019. Potential of two-stage cultivation in microalgae biofuel production. *Fuel*, 252(100): 339–349. https://doi.org/10.1016/j.fuel.2019.04.138.

Nair, R., Kumar, K.S.A., Priya, K.V. & Sevukarajan, M. 2011. Recent Advances in Solid Lipid Nanoparticle Based Drug Delivery Systems. *J Biomed Sci and Res*, 3(2): 368–384.

Nakamura, S., Ichiki, R.T., Shimoda, M. & Morioka, S. 2016. Small-scale rearing of the black soldier fly, Hermetia illucens (Diptera: Stratiomyidae), in the laboratory: low-cost and year-round rearing. *Applied Entomology and Zoology*, 51(1): 161–166.

Nakatsuji, T. & Gallo, R.L. 2012. Antimicrobial peptides: Old molecules with new ideas. *Journal of Investigative Dermatology*, 132(3 PART 2): 887–895. http://dx.doi.org/10.1038/jid.2011.387.

Nasopoulou, C., Gogaki, V., Panagopoulou, E., Demopoulos, C. & Zabetakis, I. 2013. Hen egg yolk lipid fractions with antiatherogenic properties. *Animal Science Journal*, 84(3): 264–271.

Naß, J. & Efferth, T. 2018. The activity of Artemisia spp. and their constituents against Trypanosomiasis. *Phytomedicine*, 47: 184–191. https://doi.org/10.1016/j.phymed.2018.06.002.

Neff, W.E., Zeitoun, A.M. & Weisleder, D. 1992. Resolution of lipolysis mixtures from soybean oil by a solid-phase extraction procedure. *Journal of Chromtography*, 589: 353–357.

Nezhdbahadori, F., Abdoli, M.A., Baghdadi, M. & Ghazban, F. 2018. A comparative study on the efficiency of polar and non-polar solvents in oil sludge recovery using solvent extraction. *Environmental Monitoring and Assessment*, 190(7).

Nguyen, T.T.X., Tomberlin, J.K. & Vanlaerhoven, S. 2015. Ability of Black Soldier Fly (Diptera: Stratiomyidae) Larvae to Recycle Food Waste. *Environmental Entomology*, 44(2): 406–410.

Nguyen, V.T.A., Le, T.D., Phan, H.N. & Tran, L.B. 2017. Antibacterial Activity of Free Fatty

Acids from Hydrolyzed Virgin Coconut Oil Using Lipase from Candida rugosa . *Journal of Lipids*, 2017(2013): 1–7.

Niawanti, H., Lewar, Y.S. & NN, O. 2019. Effect of Extraction Time on Averrhoa bilimbi Leaf Ethanolic Extracts Using Soxhlet Apparatus. : 0–5.

Niemi, C., Lage, S. & Gentili, F.G. 2019. Comparisons of analysis of fatty acid methyl ester (FAME) of microalgae by chromatographic techniques. *Algal Research*, 39(November 2018): 101449. https://doi.org/10.1016/j.algal.2019.101449.

Nitbani, F.O., Jumina, Siswanta, D., Sholikhah, E.N. & Fitriastuti, D. 2018. Synthesis and antibacterial activity of 1-monolaurin. *Oriental Journal of Chemistry*, 34(2): 863–867.

Nobmann, P., Smith, A., Dunne, J., Henehan, G. & Bourke, P. 2009. The antimicrobial efficacy and structure activity relationship of novel carbohydrate fatty acid derivatives against Listeria spp. and food spoilage microorganisms. *International Journal of Food Microbiology*, 128(3): 440–445. http://dx.doi.org/10.1016/j.ijfoodmicro.2008.10.008.

Norshazila, S., Koy, C.N., Rashidi, O., Ho, L.H., Azrina, I., Nurul Zaizuliana, R.A. & Zarinah, Z. 2017. The effect of time, temperature and solid to solvent ratio on pumpkin carotenoids extracted using food grade solvents. *Sains Malaysiana*, 46(2): 231–237.

Obonyoa, M., Li Zhangb, c, 1 & Soracha Thamphiwatanab, c, 1, Dissaya Pornpattananangkulc, d, Victoria Fub, and L.Z. 2012. Antibacterial Activities of Liposomal Linolenic Acids against Antibiotic-resistant Helicobacter pylori. *Mol Pharm*, 9(9): 2677–2685. https://linkinghub.elsevier.com/retrieve/pii/S0022202X15370834.

Oellig, C., Brändle, K. & Schwack, W. 2018. Characterization of E 471 food emulsifiers by high-performance thin-layer chromatography–fluorescence detection. *Journal of Chromatography A*, 1558: 69–76. https://doi.org/10.1016/j.chroma.2018.05.010.

Oleszko, A., Hartwich, J., Wójtowicz, A., Gąsior-Głogowska, M., Huras, H. & Komorowska, M. 2017. Comparison of FTIR-ATR and Raman spectroscopy in determination of VLDL triglycerides in blood serum with PLS regression. *Spectrochimica Acta - Part A: Molecular and Biomolecular Spectroscopy*, 183: 239–246.

Oliveira, F.R., Doelle, K. & Smith, R.P. 2016. External morphology of Hermetia illucens stratiomyidae: Diptera (L.1758) based on electron microscopy. *Annual Research and Review in Biology*, 9(5): 1–10.

Oonincx, D.G.A.B., Volk, N., Diehl, J.J.E., van Loon, J.J.A. & Belušič, G. 2016. Photoreceptor spectral sensitivity of the compound eyes of black soldier fly (Hermetia illucens) informing the design of LED-based illumination to enhance indoor reproduction. *Journal of Insect Physiology*, 95(August 2018): 133–139.

Osman, Y.A., Gbr, M.M., Abdelrazak, A. & Mowafy, A.M. 2018. Fatty acids and survival of bacteria in Hammam Pharaon springs, Egypt. *Egyptian Journal of Basic and Applied Sciences*, 5(2): 165–170. https://doi.org/10.1016/j.ejbas.2018.04.003.

Ouédraogo, J.C.W., Dicko, C., Kini, F.B., Bonzi-Coulibaly, Y.L. & Dey, E.S. 2018. Enhanced extraction of flavonoids from Odontonema strictum leaves with antioxidant activity using supercritical carbon dioxide fluid combined with ethanol. *Journal of Supercritical Fluids*, 131: 66–71. http://dx.doi.org/10.1016/j.supflu.2017.08.017.

Öztürk, A.A., Aygül, A. & Şenel, B. 2019. Influence of glyceryl behenate, tripalmitin and stearic acid on the properties of clarithromycin incorporated solid lipid nanoparticles (SLNs): Formulation, characterization, antibacterial activity and cytotoxicity. *Journal of Drug Delivery Science and Technology*, 54(August): 101240. https://doi.org/10.1016/j.jddst.2019.101240.

Pang, Z., Raudonis, R., Glick, B.R., Lin, T.J. & Cheng, Z. 2019. Antibiotic resistance in Pseudomonas aeruginosa: mechanisms and alternative therapeutic strategies. *Biotechnology Advances*, 37(1): 177–192. https://doi.org/10.1016/j.biotechadv.2018.11.013.

Park, H.H., 2016. Black soldier fly larvae manual. https://scholarworks.umass.edu/sustainableumass_studentshowcase/14/

Park, K.H., Kwak, K.W., Nam, S.H., Choi, J.Y., Hyun, S., Kim, H.G. & Kim, S.H. 2015. Antibacterial activity of larval extract from the black soldier fly Hermetia illucens (Diptera : Stratiomyidae) against plant pathogens. *Journal of Entomology and Zoology Studies*, 3(5): 176–179.

Park, S.I., Chang, B.S. & Yoe, S.M. 2014. Detection of antimicrobial substances from larvae of the black soldier fly, Hermetia illucens (Diptera: Stratiomyidae). *Entomological Research*, 44(2): 58–64.

Park, S.I. & Yoe, S.M. 2017. A novel cecropin-like peptide from black soldier fly, Hermetia illucens: Isolation, structural and functional characterization. *Entomological Research*, 47(2): 115–124.

Pengon, S., Limmatvapirat, C. & Limmatvapirat, S. 2012. Simplified qualitative analysis of glycerides derived from coconut oil using thin layer chromatography. *Advanced Materials Research*, 506: 182–185.

Penta, S. 2016. Antimicrobial Agents. *Advances in Structure and Activity Relationship of Coumarin Derivatives*, 2(1): 9–45.

Perednia, D.A., Anderson, J. & Rice, A. 2017. A Comparison of the Greenhouse Gas

Production of Black Soldier Fly Larvae versus Aerobic Microbial Decomposition of an ... Feed Material. *Research & Reviews: Journal of Ecology and Environmental Sciences*, 5(3): 10–16. http://www.rroij.com/open-access/a-comparison-of-the-greenhouse-gas-production-of-blacksoldier-fly-larvae-versus-aerobic-microbial-decomposition-of-anorganic-feed-.pdf.

Pichai, E. & Krit, S. 2015. Optimization of solid-to-solvent ratio and time for oil extraction process from spent coffee grounds using response surface methodology. *ARPN Journal of Engineering and Applied Sciences*, 10(16): 7049–7052.

Di Pietro, M.E., Mannu, A. & Mele, A. 2020. NMR determination of free fatty acids in vegetable oils. *Processes*, 8(4).

Pinzi, S., Garcia, I.L., Lopez-Gimenez, F.J., Luque de Castro, M.D., Dorado, G. & Dorado, M.P. 2009. The Ideal Vegetable Oil-based Biodiesel Composition: A Review of Social, Economical and Technical Implications. *Energy & Fuels*, 23(5): 2325–2341. https://pubs.acs.org/doi/10.1021/ef801098a.

Ponphaiboon, J., Pengon, S., Chaidedgumjorn, A., Limmatvapirat, S. & Limmatvapirat, C. 2014. Determination of Monolaurin in Solution Preparations Composed of Modified Coconut Oil Using GC-FID. *Advanced Materials Research*, 1060: 203–206.

Prather, C.M. & Laws, A.N. 2018. Insects as a piece of the puzzle to mitigate global problems: an opportunity for ecologists. *Basic and Applied Ecology*, 26: 71–81. http://dx.doi.org/10.1016/j.baae.2017.09.009.

Prete, P.E. 1997. Growth effects of Phaenicia sericata larval extracts on fibroblasts: Mechanism for wound healing by maggot therapy. *Life Sciences*, 60(8): 505–510.

Qushawi, A. Al, Rassouli, A., Atyabi, F., Peighambari, S.M., Esfandyari-Manesh, M., Shams, G.R. & Yazdani, A. 2016. Preparation and characterization of three tilmicosin-loaded lipid nanoparticles: Physicochemical properties and in-vitro antibacterial activities. *Iranian Journal of Pharmaceutical Research*, 15(4): 663–676.

Rabani, V., Cheatsazan, H. & Davani, S. 2019. Proteomics and lipidomics of black soldier fly (Diptera: Stratiomyidae) and blow fly (Diptera: Calliphoridae) larvae. *Journal of Insect Science*, 19(3).

Rach, O., Hadeen, X. & Sachse, D. 2020. An automated solid phase extraction procedure for lipid biomarker purification and stable isotope analysis. *Organic Geochemistry*, 142: 103995. https://doi.org/10.1016/j.orggeochem.2020.103995.

Ravi, H.K., Vian, M.A., Tao, Y., Degrou, A., Costil, J., Trespeuch, C. & Chemat, F. 2019. Alternative solvents for lipid extraction and their effect on protein quality in black soldier

fly (Hermetia illucens) larvae. *Journal of Cleaner Production*, 238(1069).

Raychowdhury, M.K., Goswami, R. & Chakrabarti, P. 1985. Effect of unsaturated fatty acids in growth inhibition of some penicillin-resistant and sensitive bacteria. *Journal of Applied Bacteriology*, 59(2): 183–188.

Rehman, K. ur, Rehman, A., Cai, M., Zheng, L., Xiao, X., Somroo, A.A., Wang, H., Li, W., Yu, Z. & Zhang, J. 2017. Conversion of mixtures of dairy manure and soybean curd residue by black soldier fly larvae (Hermetia illucens L.). *Journal of Cleaner Production*, 154: 366–373.

Renna, M., Schiavone, A., Gai, F., Dabbou, S., Lussiana, C., Malfatto, V., Prearo, M., Capucchio, M.T., Biasato, I., Biasibetti, E., De Marco, M., Brugiapaglia, A., Zoccarato, I. & Gasco, L. 2017. Evaluation of the suitability of a partially defatted black soldier fly (Hermetia illucens L.) larvae meal as ingredient for rainbow trout (Oncorhynchus mykiss Walbaum) diets. *Journal of Animal Science and Biotechnology*, 8(1): 57. http://jasbsci.biomedcentral.com/articles/10.1186/s40104-017-0191-3.

Rial, S.A., Karelis, A.D., Bergeron, K.F. & Mounier, C. 2016. Gut microbiota and metabolic health: The potential beneficial effects of a medium chain triglyceride diet in obese individuals. *Nutrients*, 8(5): 1–19.

Rodríguez-Miranda, J., Hernández-Santos, B., Herman-Lara, E., Gómez-Aldapa, C.A., Garcia, H.S. & Martínez-Sánchez, C.E. 2014. Effect of some variables on oil extraction yield from Mexican pumpkin seeds. *CYTA - Journal of Food*, 12(1): 9–15. http://dx.doi.org/10.1080/19476337.2013.777123.

Ruddaraju, L.K., Pammi, S.V.N., Guntuku, G. sankar, Padavala, V.S. & Kolapalli, V.R.M. 2020. A review on anti-bacterials to combat resistance: From ancient era of plants and metals to present and future perspectives of green nano technological combinations. *Asian Journal of Pharmaceutical Sciences*, 15(1): 42–59.

Ruiz-Gutiérrez, V. & Pérez-Camino, M.C. 2000. Update on solid-phase extraction for the analysis of lipid classes and related compounds. *Journal of Chromatography A*, 885(1–2): 321–341.

Rydlewski, A.A., Silva, P.D., Manin, L.P., Tavares, C.B.G., Paula, M.G., Figueiredo, I.L., Neia, V.B.M.J.C., Santos, O.O. & Visentainer, J. V. 2019. Lipid profile determination by direct infusion ESI-MS and fatty acid composition by GC-FID in human milk pools by Folch and creamatocrit methods. *Journal of the Brazilian Chemical Society*, 30(5): 1063–1073.

S. Bhuvaneshwari *, D.Sruthi*, V. Sivasubramanian* & Niranjana kalyani** and J. Sugunabai

**. 2011. Development and characterization of chitosan film. *International Journal of Engineering Research and Applications (IJERA)*, 1(2): 292–299. http://www.ijera.com/papers/vol 1 issue 2/012292299AL.pdf.

Sado-Kamdem, S.L., Vannini, L. & Guerzoni, M.E. 2009. Effect of α-linolenic, capric and lauric acid on the fatty acid biosynthesis in Staphylococcus aureus. *International Journal of Food Microbiology*, 129(3): 288–294. http://dx.doi.org/10.1016/j.ijfoodmicro.2008.12.010.

Sajilata, M.G., Singhal, R.S. & Kamat, M.Y. 2008. Fractionation of lipids and purification of γ-linolenic acid (GLA) from Spirulina platensis. *Food Chemistry*, 109(3): 580–586.

Sajjadi, B., Raman, A.A.A. & Arandiyan, H. 2016. A comprehensive review on properties of edible and non-edible vegetable oil-based biodiesel: Composition, specifications and prediction models. *Renewable and Sustainable Energy Reviews*, 63: 62–92.

Salomone, R., Saija, G., Mondello, G., Giannetto, A., Fasulo, S. & Savastano, D. 2017. Environmental impact of food waste bioconversion by insects: Application of Life Cycle Assessment to process using Hermetia illucens. *Journal of Cleaner Production*, 140: 890–905. http://dx.doi.org/10.1016/j.jclepro.2016.06.154.

SantosMiranda, M.E., Marcolla, C., Rodriguez, C.A., Wilhelm, H.M., Sierakowski, M.R., BelleBresolin, T.M. & Alves de Freitas, R. 2006. I . The role of N-carboxymethylation of chitosan in the thermal stability and dynamic. *Polym Int*, 55(April 2007): 961–969.

Schlievert, P.M. & Peterson, M.L. 2012. Glycerol monolaurate antibacterial activity in broth and biofilm cultures. *PLoS ONE*, 7(7).

Scopel, R., Falcão, M.A., Cappellari, A.R., Morrone, F.B., Guterres, S.S., Cassel, E., Kasko, A.M. & Vargas, R.M.F. 2020. Lipid-polymer hybrid nanoparticles as a targeted drug delivery system for melanoma treatment. *International Journal of Polymeric Materials and Polymeric Biomaterials*, 0(0): 1–12. https://doi.org/10.1080/00914037.2020.1809406.

Scortichini, S., Boarelli, M.C., Silvi, S. & Fiorini, D. 2020. Development and validation of a GC-FID method for the analysis of short chain fatty acids in rat and human faeces and in fermentation fluids. *Journal of Chromatography B: Analytical Technologies in the Biomedical and Life Sciences*, 1143(September 2019): 121972. https://doi.org/10.1016/j.jchromb.2020.121972.

Seleem, D., Chen, E., Benso, B., Pardi, V. & Murata, R.M. 2016. In vitro evaluation of antifungal activity of monolaurin against Candida albicans biofilms. *PeerJ*, 2016(6): 1–17.

Seleem, D., Freitas-Blanco, V.S., Noguti, J., Zancope, B.R., Pardi, V. & Murata, R.M. 2018. In vivo antifungal activity of monolaurin against Candida albicans biofilms. *Biological and Pharmaceutical Bulletin*, 41(8): 1299–1302.

Severino, P., Silveira, E.F., Loureiro, K., Chaud, M. V., Antonini, D., Lancellotti, M., Sarmento, V.H., da Silva, C.F., Santana, M.H.A. & Souto, E.B. 2017. Antimicrobial activity of polymyxin-loaded solid lipid nanoparticles (PLX-SLN): Characterization of physicochemical properties and in vitro efficacy. *European Journal of Pharmaceutical Sciences*, 106(March): 177–184. https://doi.org/10.1016/j.ejps.2017.05.063.

Shanaghi, E., Aghajani, M., Esmaeli, F., Faramarzi, M.A., Jahandar, H. & Amani, A. 2020. Application of electrospray in preparing solid lipid nanoparticles and optimization of nanoparticles using artificial neural networks. *Avicenna Journal of Medical Biotechnology*, 12(4): 251–254.

Shazly, G.A. 2017. Corrigendum to 'Ciprofloxacin Controlled-Solid Lipid Nanoparticles: Characterization, In Vitro Release, and Antibacterial Activity Assessment'. *BioMed research international*, 2017: 6761452.

Shin, G.H. & Kim, J.T. 2018. Observation of chitosan coated lipid nanoparticles with different lipid compositions under simulated in vitro digestion system. *Food Hydrocolloids*, 84: 146–153. https://doi.org/10.1016/j.foodhyd.2018.05.052.

Shin, S.Y., Bajpai, V.K., Kim, H.R. & Kang, S.C. 2007. Antibacterial activity of eicosapentaenoic acid (EPA) against foodborne and food spoilage microorganisms. *LWT - Food Science and Technology*, 40(9): 1515–1519.

Shinde, V. & Mahadik, K. 2019. Supercritical fluid extraction: A new technology to herbals. *Int J Herb Med*, (January 2019). https://www.researchgate.net/profile/Vaibhav_Shinde2/publication/343288610_Supercritical_fluid_extraction_A_new_technology_to_herbals/links/5f216ccc299bf134048f8a10/Supercritical-fluid-extraction-A-new-technology-to-herbals.pdf.

Shrimal, P., Jadeja, G. & Patel, S. 2020. A review on novel methodologies for drug nanoparticle preparation: Microfluidic approach. *Chemical Engineering Research and Design*, 153: 728–756. https://doi.org/10.1016/j.cherd.2019.11.031.

Silalahi, J. 2015. Antibacterial Activity of Hydrolyzed Oils of Different Fatty Acid Composition against Salmonella Thypi and Lactobacillus Plantarum. , (February).

Silalahi, J. & Putra, E.D.E.L.U.X. 2018. Antibacterial activity of hydrolyzed virgin coconut oil. , (February).

Silva, E.L., Carneiro, G., De Araújo, L.A., Vaz Trindade, M.D.J., Yoshida, M.I., Oréfice, R.L.,

Farias, L.D.M., De Carvalho, M.A.R., Dos Santos, S.G., Goulart, G.A.C., Alves, R.J. & Ferreira, L.A.M. 2015. Solid lipid nanoparticles loaded with retinoic acid and lauric acid as an alternative for topical treatment of acne vulgaris. *Journal of Nanoscience and Nanotechnology*, 15(1): 792–799.

Silva, G.D.P. & Hesselberg, T. 2020. A Review of the Use of Black Soldier Fly Larvae, Hermetia illucens (Diptera: Stratiomyidae), to Compost Organic Waste in Tropical Regions. *Neotropical Entomology*, 49(2): 151–162.

Singh, B.K. & Dutta, P.K. 2016. Preparation and Characterization of Chitosan-Lauric Acid Derivative : Antibacterial Activity and Drug Delivery Study Preparation and Characterization of Chitosan-Lauric Acid Derivative : Antibacterial Activity and Drug. , (February 2017).

Singh, R.P., Singh, P., Araujo, A.S.F., Hakimi Ibrahim, M. & Sulaiman, O. 2011. Management of urban solid waste: Vermicomposting a sustainable option. *Resources, Conservation and Recycling*, 55(7): 719–729. http://dx.doi.org/10.1016/j.resconrec.2011.02.005.

De Smet, J., Wynants, E., Cos, P. & Van Campenhout, L. 2018. Microbial Community Dynamics during Rearing of Black. *Applied and Environmental Microbiology*, 84(9): 1–17.

Smets, R., Goos, P., Claes, J. & Borght, M. Van Der. 2020. Optimisation of the Lipid Extraction of Fresh Black Soldier Fly Larvae (Hermetia illucens) with 2-Methyltetrahydrofuran by Response Surface Methodology †. *Separation and Purification Technology*: 118040. https://doi.org/10.1016/j.seppur.2020.118040.

Smets, R., Verbinnen, B., Van De Voorde, I., Aerts, G., Claes, J. & Van Der Borght, M. 2020. Sequential Extraction and Characterisation of Lipids, Proteins, and Chitin from Black Soldier Fly (Hermetia illucens) Larvae, Prepupae, and Pupae. *Waste and Biomass Valorization*, 11(12): 6455–6466.

Soetemans, L., Uyttebroek, M. & Bastiaens, L. 2020. Characteristics of chitin extracted from black soldier fly in different life stages. *International Journal of Biological Macromolecules*, 165: 3206–3214. https://doi.org/10.1016/j.ijbiomac.2020.11.041.

Soetjipto, H., Pradana, R.C. & Ign Kristijanto, A. 2019. Fatty acid composition and total lipid content of the seed oil of Leucaena leucocephala (Lam) de Wit. *IOP Conference Series: Materials Science and Engineering*, 509(1).

Soleimanifar, M., Niazmand, R. & Jafari, S.M. 2019. Evaluation of oxidative stability, fatty acid profile, and antioxidant properties of black cumin seed oil and extract. *Journal of Food Measurement and Characterization*, 13(1): 383–389.

187

http://dx.doi.org/10.1007/s11694-018-9953-7.

Sonam, M., Singh, R.P. & Saklani, P. 2017. Phytochemical Screening and TLC Profiling of Various Extracts of Reinwardtia indica. *International Journal of Pharmacognosy and Phytochemical Research*, 9(4).

Song, Z., Li, G., Guan, F. & Liu, W. 2018. Application of chitin/chitosan and their derivatives in the papermaking industry. *Polymers*, 10(4).

Spigno, G., Tramelli, L. & De Faveri, D.M. 2007. Effects of extraction time, temperature and solvent on concentration and antioxidant activity of grape marc phenolics. *Journal of Food Engineering*, 81(1): 200–208.

Spranghers, T., Michiels, J., Vrancx, J., Ovyn, A., Eeckhout, M., De Clercq, P. & De Smet, S. 2018. Gut antimicrobial effects and nutritional value of black soldier fly (Hermetia illucens L.) prepupae for weaned piglets. *Animal Feed Science and Technology*, 235(June 2017): 33–42. https://doi.org/10.1016/j.anifeedsci.2017.08.012.

Spranghers, T., Ottoboni, M., Klootwijk, C., Ovyn, A., Deboosere, S., De Meulenaer, B., Michiels, J., Eeckhout, M., De Clercq, P. & De Smet, S. 2017. Nutritional composition of black soldier fly (Hermetia illucens) prepupae reared on different organic waste substrates. *Journal of the Science of Food and Agriculture*, 97(8): 2594–2600.

St-Hilaire, S., Cranfill, K., McGuire, M.A., Mosley, E.E., Tomberlin, J.K., Newton, L., Sealey, W., Sheppard, C. & Irving, S. 2007. Fish offal recycling by the black soldier fly produces a foodstuff high in omega-3 fatty acids. *Journal of the World Aquaculture Society*, 38(2): 309–313.

Ståhls, G., Meier, R., Hauser, M. & Richards, C. 2020. The puzzling mitochondrial phylogeography of the black soldier fly (Hermetia illucens), the commercially most important insect protein species. *Preprint*: 1–25.

Subramani, R., Narayanasamy, M. & Feussner, K.D. 2017. Plant-derived antimicrobials to fight against multi-drug-resistant human pathogens. *3 Biotech*, 7(3): 1–15.

Subroto, E. & Indiarto, R. 2020. Bioactive monolaurin as an antimicrobial and its potential to improve the immune system and against covid-19: A review. *Food Research*, 4(6): 2355–2365.

Sudatta, B.P., Sugumar, V., Varma, R. & Nigariga, P. 2020. International Journal of Biological Macromolecules Extraction , characterization and antimicrobial activity of chitosan from pen shell , Pinna bicolor. *International Journal of Biological Macromolecules*, 163: 423–430. https://doi.org/10.1016/j.ijbiomac.2020.06.291.

Sun, M., Dong, J., Xia, Y. & Shu, R. 2017. Antibacterial activities of docosahexaenoic acid

(DHA) and eicosapentaenoic acid (EPA) against planktonic and biofilm growing Streptococcus mutans. *Microbial Pathogenesis*, 107: 212–218. http://dx.doi.org/10.1016/j.micpath.2017.03.040.

Surendra, K.C., Olivier, R., Tomberlin, J.K., Jha, R. & Khanal, S.K. 2016. Bioconversion of organic wastes into biodiesel and animal feed via insect farming. *Renewable Energy*, 98: 197–202.

Tadesse, B.T., Ashley, E.A., Ongarello, S., Havumaki, J., Wijegoonewardena, M., González, I.J. & Dittrich, S. 2017. Antimicrobial resistance in Africa: A systematic review. *BMC Infectious Diseases*, 17(1): 1–17.

Tadesse, D.A., Zhao, S., Tong, E., Ayers, S., Singh, A., Bartholomew, M.J. & McDermott, P.F. 2012. Antimicrobial drug resistance in Escherichia coli from humans and food animals, United States, 1950-2002. *Emerging Infectious Diseases*, 18(5): 741–749.

Tahir, N., Madni, A., Correia, A., Rehman, M., Balasubramanian, V., Khan, M.M. & Santos, H.A. 2019. Lipid-polymer hybrid nanoparticles for controlled delivery of hydrophilic and lipophilic doxorubicin for breast cancer therapy. *International Journal of Nanomedicine*, 14: 4961–4974.

Tapia-Hernández, J.A., Torres-Chávez, P.I., Ramírez-Wong, B., Rascón-Chu, A., Plascencia-Jatomea, M., Barreras-Urbina, C.G., Rangel-Vázquez, N.A. & Rodríguez-Félix, F. 2015. Micro- and Nanoparticles by Electrospray: Advances and Applications in Foods. *Journal of Agricultural and Food Chemistry*, 63(19): 4699–4707.

Tatsing Foka, F.E., Kumar, A. & Ateba, C.N. 2018. Emergence of vancomycin-resistant enterococci in South Africa: Implications for public health. *South African Journal of Science*, 114(9–10): 1–7.

Taylor, E.N., Kummer, K.M., Dyondi, D., Webster, T.J. & Banerjee, R. 2014. Multi-scale strategy to eradicate Pseudomonas aeruginosa on surfaces using solid lipid nanoparticles loaded with free fatty acids. *Nanoscale*, 6(2): 825–832.

Tesfaye, B. & Tefera, T. 2017. Extraction of Essential Oil from Neem Seed by Using Soxhlet Extraction Methods. , (6): 646–650.

Thamphiwatana, S., Gao, W., Obonyo, M. & Zhang, L. 2014. In vivo treatment of Helicobacter pylori infection with liposomal linolenic acid reduces colonization andameliorates inflammation. *Proceedings of the National Academy of Sciences of the United States of America*, 111(49): 17600–17605.

Thandapani, G., Supriya Prasad, P., Sudha, P.N. & Sukumaran, A. 2017. Size optimization and in vitro biocompatibility studies of chitosan nanoparticles. *International Journal of*

Biological Macromolecules, 104(October): 1794–1806. http://dx.doi.org/10.1016/j.ijbiomac.2017.08.057.

Thormar, H., Hilmarsson, H. & Bergsson, G. 2013. Antimicrobial lipids : Role in innate immunity and potential use in prevention and treatment of infections . *Microbial pathogens and strategies for combating them: science, technology and education*: 1474–1488.

Tir, R., Dutta, P.C. & Badjah-hadj-ahmed, A.Y. 2012. Effect of the extraction solvent polarity on the sesame seeds oil composition. : 1427–1438.

Tomberlin, J.K., Adler, P.H. & Myers, H.M. 2009. Development of the Black Soldier Fly (Diptera: Stratiomyidae) in Relation to Temperature: Table 1. *Environmental Entomology*, 38(3): 930–934.

Tomberlin, J.K. & van Huis, A. 2020. Black soldier fly from pest to 'crown jewel' of the insects as feed industry: An historical perspective. *Journal of Insects as Food and Feed*, 6(1): 1–4.

Tomberlin, J.K. & Sheppard, D.C. 2002. Factors Influencing Mating and Oviposition of Black Soldier Flies (Diptera: Stratiomyidae) in a Colony. *Journal of Entomological Science*, 37(4): 345–352.

Tomberlin, J.K. & Sheppard, D.C. 2001. Lekking Behavior of the Black Soldier Fly (Diptera: Stratiomyidae). *The Florida Entomologist*, 84(4): 729.

Traversier, M., Gaslondes, T., Milesi, S., Michel, S. & Delannay, E. 2018. *Polar lipids in cosmetics: recent trends in extraction, separation, analysis and main applications*.

Trotta, M., Cavalli, R., Trotta, C., Bussano, R. & Costa, L. 2010. Electrospray technique for solid lipid-based particle production. *Drug Development and Industrial Pharmacy*, 36(4): 431–438.

Ulmer, C.Z., Jones, C.M., Yost, R.A., Garrett, T.J. & Bowden, J.A. 2018. Optimization of Folch, Bligh-Dyer, and Matyash sample-to-extraction solvent ratios for human plasma-based lipidomics studies. *Analytica Chimica Acta*, 1037: 351–357. https://doi.org/10.1016/j.aca.2018.08.004.

Umerska, A., Cassisa, V., Matougui, N., Joly-Guillou, M.L., Eveillard, M. & Saulnier, P. 2016. Antibacterial action of lipid nanocapsules containing fatty acids or monoglycerides as co-surfactants. *European Journal of Pharmaceutics and Biopharmaceutics*, 108: 100–110. http://dx.doi.org/10.1016/j.ejpb.2016.09.001.

Uncu, O., Ozen, B. & Tokatli, F. 2019. Use of FTIR and UV–visible spectroscopy in determination of chemical characteristics of olive oils. *Talanta*, 201(February): 65–73.

https://doi.org/10.1016/j.talanta.2019.03.116.

Urbanek, A., Szadziewski, R., Stepnowski, P., Boros-Majewska, J., Gabriel, I., Dawgul, M., Kamysz, W., Sosnowska, D. & Gołeogonekbiowski, M. 2012. Composition and antimicrobial activity of fatty acids detected in the hygroscopic secretion collected from the secretory setae of larvae of the biting midge Forcipomyia nigra (Diptera: Ceratopogonidae). *Journal of Insect Physiology*, 58(9): 1265–1276.

Ushakova, N.A., Brodskii, E.S., Kovalenko, A.A., Bastrakov, A.I., Kozlova, A.A. & Pavlov, D.S. 2016. Characteristics of lipid fractions of larvae of the black soldier fly Hermetia illucens. *Doklady Biochemistry and Biophysics*, 468(1): 209–212.

Wang, C., Qian, L., Wang, W., Wang, T., Deng, Z., Yang, F., Xiong, J. & Feng, W. 2017a. Exploring the potential of lipids from black soldier fl y : New paradigm for biodiesel production (I). *Renewable Energy*, 111: 749–756. http://dx.doi.org/10.1016/j.renene.2017.04.063.

Wang, C., Qian, L., Wang, W., Wang, T., Deng, Z., Yang, F., Xiong, J. & Feng, W. 2017b. Exploring the potential of lipids from black soldier fly: New paradigm for biodiesel production (I). *Renewable Energy*, 111: 749–756. http://dx.doi.org/10.1016/j.renene.2017.04.063.

Wang, C., Qian, L., Wang, W., Wang, T., Deng, Z., Yang, F., Xiong, J. & Feng, W. 2017c. Exploring the potential of lipids from black soldier fly: New paradigm for biodiesel production (I). *Renewable Energy*, 111(I): 749–756.

Wang, Q., Alshaker, H., Böhler, T., Srivats, S., Chao, Y., Cooper, C. & Pchejetski, D. 2017. Core shell lipid-polymer hybrid nanoparticles with combined docetaxel and molecular targeted therapy for the treatment of metastatic prostate cancer. *Scientific Reports*, 7(1): 1–8.

Wang, S. & Jing, Y. 2016. *Effects of a Chitosan Coating Layer on the Surface Properties and Barrier Properties of Kraft Paper*.

Wang, T., Hu, Q., Lee, J.Y. & Luo, Y. 2018. Solid Lipid-Polymer Hybrid Nanoparticles by in Situ Conjugation for Oral Delivery of Astaxanthin. *Journal of Agricultural and Food Chemistry*, 66(36): 9473–9480.

Wang, T. & Luo, Y. 2018. Chitosan hydrogel beads functionalized with thymol-loaded solid lipid–polymer hybrid nanoparticles. *International Journal of Molecular Sciences*, 19(10).

Wardani, G., Mahmiah & Sudjarwo, S.A. 2018. In vitro antibacterial activity of chitosan nanoparticles against mycobacterium tuberculosis. *Pharmacognosy Journal*, 10(1): 162–166.

Warren, C.R. 2019. Does silica solid-phase extraction of soil lipids isolate a pure phospholipid fraction? *Soil Biology and Biochemistry*, 128(October 2018): 175–178. https://doi.org/10.1016/j.soilbio.2018.10.021.

Wei, L., Mu, L., Wang, Y., Bian, H., Li, J., Lu, Y., Han, Y., Liu, T., Lv, J., Feng, C., Wu, J. & Yang, H. 2015. Purification and characterization of a novel defensin from the salivary glands of the black fly, Simulium bannaense. *Parasites and Vectors*, 8(1): 1–11.

Wolfshorndl, M., Danford, R. & Sachs, J.P. 2019. 2H/1H fractionation in microalgal lipids from the North Pacific Ocean: Growth rate and irradiance effects. *Geochimica et Cosmochimica Acta*, 246: 317–338. https://doi.org/10.1016/j.gca.2018.11.027.

Wong, C.Y., Rosli, S.S., Uemura, Y., Ho, Y.C., Leejeerajumnean, A., Kiatkittipong, W., Cheng, C.K., Lam, M.K. & Lim, J.W. 2019. Potential protein and biodiesel sources from black soldier fly larvae: Insights of larval harvesting instar and fermented feeding medium. *Energies*, 12(8).

Yan, L., Chu, J., Li, M., Wang, X., Zong, J., Zhang, X., Song, M. & Wang, S. 2018. Pharmacological Properties of the Medical Maggot: A Novel Therapy Overview. *Evidence-based Complementary and Alternative Medicine*, 2018.

Yang, Y.H., Du, L., Hosokawa, M., Miyashita, K., Kokubun, Y., Arai, H. & Taroda, H. 2017. Fatty acid and lipid class composition of the microalga Phaeodactylum tricornutum. *Journal of Oleo Science*, 66(4): 363–368.

Yoon, B.K., Jackman, J.A., Valle-González, E.R. & Cho, N.J. 2018. *Antibacterial free fatty acids and monoglycerides: Biological activities, experimental testing, and therapeutic applications*.

Yougbare, S., Chang, T.K., Tan, S.H., Kuo, J.C., Hsu, P.H., Su, C.Y. & Kuo, T.R. 2019. Antimicrobial gold nanoclusters: Recent developments and future perspectives. *International Journal of Molecular Sciences*, 20(12).

Zawadzki, J. & Kaczmarek, H. 2010. Thermal treatment of chitosan in various conditions. *Carbohydrate Polymers*, 80(2): 394–400. http://dx.doi.org/10.1016/j.carbpol.2009.11.037.

Zdybicka-Barabas, A., Bulak, P., Polakowski, C., Bieganowski, A., Waśko, A. & Cytryńska, M. 2017. Immune response in the larvae of the black soldier fly Hermetia illucens. *Invertebrate Survival Journal*, 14(January): 9–17.

Zhang, H., Wang, Z. & Liu, O. 2015. Development and validation of a GC-FID method for quantitative analysis of oleic acid and related fatty acids. *Journal of Pharmaceutical Analysis*, 5(4): 223–230. http://dx.doi.org/10.1016/j.jpha.2015.01.005.

Zhang, J., Huang, L., He, J., Tomberlin, J.K., Li, J., Lei, C., Sun, M., Liu, Z. & Yu, Z. 2010. An Artificial Light Source Influences Mating and Oviposition of Black Soldier Flies, Hermetia illucens . *Journal of Insect Science*, 10(202): 1–7.

Zhang, Q.W., Lin, L.G. & Ye, W.C. 2018. Techniques for extraction and isolation of natural products : a comprehensive review. *Chinese Medicine*: 1–26. https://doi.org/10.1186/s13020-018-0177-x.

Zhang, S. & Kawakami, K. 2010. One-step preparation of chitosan solid nanoparticles by electrospray deposition. *International Journal of Pharmaceutics*, 397(1–2): 211–217. http://dx.doi.org/10.1016/j.ijpharm.2010.07.007.

Zhao, Z. & Xu, Y. 2010. An extremely simple method for extraction of lysophospholipids and phospholipids from blood samples. *Journal of Lipid Research*, 51(3): 652–659. http://dx.doi.org/10.1194/jlr.D001503.

Zheng, L., Hou, Y., Li, W., Yang, S., Li, Q. & Yu, Z. 2012. Biodiesel production from rice straw and restaurant waste employing black soldier fly assisted by microbes. *Energy*, 47(1): 225–229.

Zhong, Y., Zhuang, C., Gu, W. & Zhao, Y. 2019. Effect of molecular weight on the properties of chitosan films prepared using electrostatic spraying technique. *Carbohydrate Polymers*, 212(February): 197–205. https://doi.org/10.1016/j.carbpol.2019.02.048.